Molecular machines constructed from multichromophore arrays

Daniel González Lucas

A thesis submitted in part fulfilment of the requirements for the degree of Doctor of Philosophy

Supervised by Prof Andrew N. Cammidge

School of Chemical Sciences

University of East Anglia, Norwich

May 2014

Declaration

The research described in this thesis is, to the best of my knowledge, original except where due reference is made.

Daniel González Lucas

Abstract

Our long-term ambitious goal is to construct molecular assemblies or machines of unprecedented complexity leading to unique function. Porphyrins and phthalocyanines have been selected as the building blocks for the construction of the targeted molecular machines. The synthesis of different porphyrin/phthalocyanine building blocks is introduced with particular emphasis on the introduction of central metal/metalloid elements such as ruthenium, indium and lanthanides.

The linking of porphyrins to give covalent assemblies suitable for elaboration into machine-like arrays is then described. The synthesis of an array in which four porphyrin units surround a central porphyrin core is described, alongside modifications to the strategy that permits differential metal substitution.

Strategies for face-to-face elaboration of machine-like structures from the previously described covalent multiporhyrin array are discussed. Although unsuccessful, a separate reaction pathway is described that leads to controlled formation of triple-decker structures. Model diporphyrins, linked through flexible spacers, are smoothly metallated with lanthanum. Complementary phthalocyanine macrocycles are then easily inserted, giving high yields of triple decker molecules. The synthesis and materials are discussed, and the novel structures are characterised by absorption spectroscopy, NMR spectroscopy and crystallography. The versatility and generality of the strategy are demonstrated by synthesis of analogues that incorporate more heavily functionalised central (phthalocyanine) macrocycles. Rotation is hindered (NMR) in these cases.

Finally, preliminary assessment of extension of this approach towards higher-order stacks is described, alongside variation of the linking lanthanides to include magnetic elements such as dysprosium.

Acknowledgements

I would like to thank my supervisor Prof Andrew N. Cammidge for all his support both personally and professionally. Also for this great opportunity and all the motivation that he has provided all the way.

I must also thank INTERREG program for funding this PhD thesis. Also the crystallography centre at Southampton for their help with X-ray crystallography and Colin Macdonald for his help with NMR spectroscopy.

A big thank to Dr Hemant Gopee for all the good moments in and out of the lab as well as teaching me how everything works in a lab. I am also very grateful to Dr Alejandro Diaz-Moscoso, for all the help, new ideas and of course a big friendship. Both of you have been a real support all these years and will always be good friends.

I want to mention both my parents for supporting me and listening to me in the good moments as well as the bad ones and especially for their unconditional love and support that made me the person I am. I wish to thank my grandparents and the rest of my family back at home for always believing in me and making me feel close to them even if we are hundreds of kilometres apart. I have to thank Maite and Ismael because they supported me all the way as if I was their own child.

I would also like to thank all my friends and colleagues at UEA for making an amazing environment to work in. The past and present members of the Cammidge group as well as all the friends I made during this journey that made it really enjoyable Hanae, Jay, César, Victor, Desi, Flavia and Paulina, you will always have a place for a visit wherever we are.

I cannot forget Apa and Tito, who could have imagined I would become a doctor after the first year I met you? Also Oscar, Miguel, Pablo, Pana and Cumpli back at home for always welcoming us back as if we have never left, that shows what real friendship is. A special support were Marta and Luis who felt more like part of the family than only friends. I cannot stop mentioning Raquel who is the best friend I have from our degree and will always be a very close one.

Most importantly I would like to specially thank Sonia because I could not have done any of this without her. Thanks for always being there for me and your love that make me a better person every day.

List of abbreviations

Ac	Acetate
acac	Acetylacetonate
ATP	Adenosine triphosphate
br	broad
B.p.	Boiling point
C_{10}	Decane
C_{12}	Dodecane
°C	Celsius
cm	Centimetre
COSY	Correlation spectroscopy
δ	Shift value
d	Doublet
d-	Deuterated
dd	Doublet of doublets
DBU	1,8-Diazabicycloundec-7-ene
DCM	Dichloromethane
DCTB	*trans*-2-[3-(4-t-butyl-phenyl)-2-methyl-2-propenylidene]malononitrile
DDQ	2,3-Dichloro-5,6-dicyano-1,4-benzoquinone
DMF	Dimethyl formamide
DMSO	Dimethyl sulfoxide
DNA	Deoxyribonucleic acid
dppf	diphenylphosphino ferrocene
dt	Doublet of triplets
ε	Extinction coefficient
e.g.	Exempli gratia
et al.	Et alii
etc	Et cetera
eq	Equivalent
Fig	Figure
FT-IR	Fourier transform infrared spectroscopy
g	Grams

h	Hours
HOMO	Highest occupied molecular orbital
Hz	Herzs
IR	Infrared
J	Coupling value
K	Kelvin
L	Ligand
Ln	Lanthanide
LUMO	Lowest unoccupied molecular orbital
m	Multiplet
M (in structures)	Metal(any)
M	Molarity
MALDI-tof	Matrix-assisted laser desorption/ionization (time of flight)
Me	Methyl
MEK	Methyl ethyl ketone
MHz	Megahertz
mi	*Meta*-inside
min	Minutes
mg	Milligrams
ml	Millilitres
mm	Millimetres
mmol	Millimol
mo	*Meta*-outside
m.p.	Melting point
MS	Mass spectrometry
Mw molec weight	Molecular weight
nm	Nanometres
NMR	Nuclear Magnetic Resonance
oi	*Ortho*-inside
oo	*Ortho*-outside
Pc	Phthalocyanine
Pet.	Petroleum
pm	Picometre
Por	Porphyrin

ppm	Parts per million
prep-TLC	Preparative-Thin Layer Chromatography
py	Pyridine
pyr	Pyrrole
q	Quadruplet
rt	Room temperature
s	Singlet
S	Solvent
SAT	Sitting atop
SMM	Single Molecule Magnets
t	Triplet
*t*Bu	*terc*-butyl
TD	Triple decker
Tc	Coalescence temperature
TCB	1,2,4-trichlorobencene
Tf	Triflate
THF	Tetrahydrofuran
TLC	Thin Layer Chromatography
TFA	Trifluoroacetic acid
TPP	Tetraphenylporphyrin
TPP-OH	5,10,15-tris-phenyl-20-(*p*-hydroxyphenyl)porphyrin
tt	Triplet of triplets
UV-vis	Ultraviolet-visible spectroscopy

1. SUMMARY INDEX, LIST OF CONTENTS

2. AIMS

Our long-term ambitious goal is to construct molecular assemblies or machines[1] of unprecedented complexity leading to unique function. Such molecular machines could form the basis of true molecular electronics with applications in a wide range of areas such as molecular computing,[2] single molecule magnets,[3] molecular machines…[4] The machines will be constructed using organic molecules as building blocks that will form nanomachines or nanocomponents. This selection of organic molecules as building blocks will allow the manipulation of the machine at a molecular level using the incredibly wide range of organic chemistry reactions available. It is known that functionality and structure are always linked in everyday machines and structures. This inspired us to design the targeted molecular machines having real-life machines or structures as models for the design of their molecular variants. This function will have consequences to the potential applications of the molecular counterpart. With this in mind the aim of this project is to construct molecular machines capable of collecting and transferring or concentrating energy to another component, surface, or structure. Solutions to harnessing more complex processes are much more complicated and could not be achieved in such a small time and require a higher level of manipulation. A key step towards developing such function is, however, part of the proposed objectives. It is clear that for such compounds to be eventually exploitable their assembly onto substrates and subsequent manipulation will be vital. Our approach recognises this and it is incorporated as an important element of the project. The targeted machines designed for this project are molecular variants of a familiar fairground attraction, the "Teacups ride" (Figure 1).

Figure 1 Teacups ride fairground attraction used as real-life model.

With this machine in mind as the final target for the project, the challenge addressed is to construct complex molecular assemblies using organic chemical structures as building blocks. This will allow us to design and construct molecular machines of unprecedented complexity. The design of the molecular variant of the teacups ride fairground attraction can be achieved by careful analysis of the structure and then mimicking the real life structure. Such analysis and breakdown of the structure in simple units is represented in figure 2.

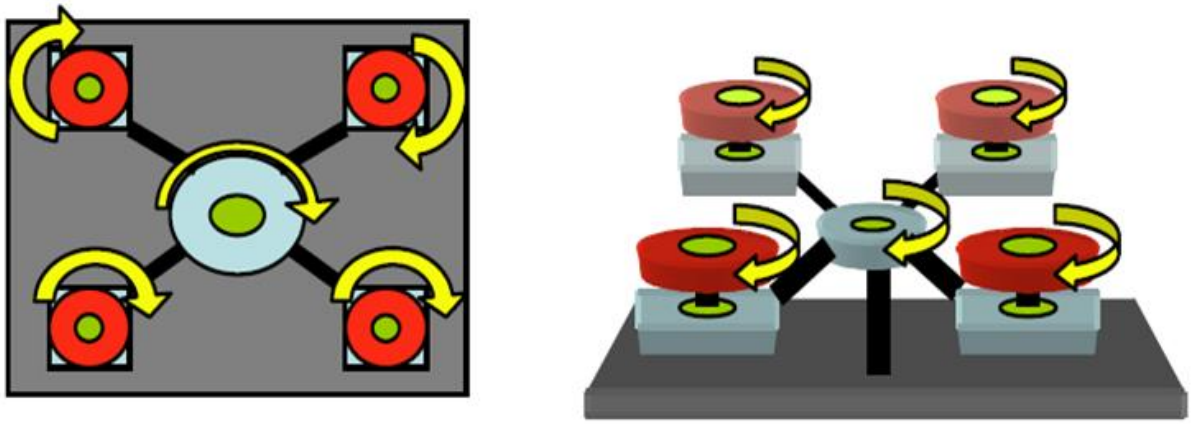

Figure 2. Proposed structure model for the target molecular machine.

This challenging molecular design can be broken down into different parts. This will help us to design the molecular machine by constructing the different parts/subunits of the machine and studying them separately. The subunits can be synthesised separately as well as linked together in many different ways. This wide range of methodologies allowed us to embark on such ambitious project as the methodology can be easily modified if different problems are encountered. Despite the fact that the designed machine can be broken down in many different subunits, the real life structure consists of different parts that will serve as a first model for the approach to be followed when constructing the molecular counterpart.

The teacups ride model structure is basically composed of a flat structure that is connected to the surface from the central position acting as fulcrum. This central position acts as the centre of the machine having the other different units attached to it. Therefore for the construction of the molecular version, we have to have in mind that this central unit is going to act as support for the rest of the molecular machine. In order to have suitable linking points between all the different units that make up the system, we have to differentiate between the connections that the central unit of the structure needs to have available: One in

the centre (to link the molecular machine to the surface) and another that needs to connect the rest of the units to it (to attach the free-rotating teacups).

A different part to take into account is the peripheral teacups themselves. These independent subunits need to be attached into the structure in very specific positions around the periphery of the molecular machine. This attachment needs to allow the units to have free rotation through the connection in order to mimic the real life machine. Interactions between the attached units and the flat structure will need to be possible to have the desired function.

The final challenge that needs to be studied is the way the different units that comprise the system are connected to each other. There are different parts of the machine that need to be connected differently and separately. According to this, the "teacups" subunits need to be connected onto the frame allowing interactions between the different subunits as well as free rotation of the teacups. Separately, the way the entire machine is connected onto the surface will be crucial. Finally, both ways to interconnect the system need to be independent to one another.

Therefore, we need to construct a molecular structure that will act as a frame with different subunits attached on top of it allowing free-rotation. The molecular machines could then be assembled onto a suitable surface in a controlled way. The entire machine requires unsymmetrical building blocks in order to provide link-points for the construction. The synthesis will be designed in a stepwise manner by interrogating different parts of the superstructure separately in order to leave the chemistry as simple as possible

3. GENERAL INTRODUCTION

A molecular machine can be defined as an assembly of a discrete number of molecular components (that is, a supramolecular structure) designed to perform mechanical-like movements (output) as a consequence of an appropriate external stimulus (input). This expression is often more generally applied to molecules that simply mimic functions that occur at the macroscopic level. Each molecular component performs a single function (structural or dynamic) whilst the entire assembly performs a more complex function leading to work. The extension of the concept of machine to the molecular level is important, not only for the sake of basic research, but also for the growth of nanoscience and the development of a bottom-up approach to nanotechnology. The miniaturization of components for the construction of useful devices is currently pursued by a reduction approach, that is, by creating smaller machines with the same function such as modern microchips for example. This approach, leads physicists and engineers to manipulate smaller pieces every time which have intrinsic limitations. As chemistry is already at the bottom, since it allows the manipulation of molecules, it is in the ideal position to develop a bottom-up strategy for the construction of nanoscale machines.

Scientists and engineers have learnt from the selectivity, specificity, precision and accuracy of biological processes and the ensembles formed on a cellular and sub-cellular level. Also they have been able to apply these concepts in the laboratory to create molecular devices and machines. Natural machines such as ATP-ase, DNA-polymerase, chlorophyll, ribosomes etc. are all complex and fascinating examples of Nature's approach to nanoscaled machines. The synthesis and assembly of molecular building blocks capable of functioning in a controlled way and in a wholly synthetic sense is an achievable goal and, to this end, prototypical machines that demonstrate specific tasks or design features are being reported in increasing amounts.

Our own body can be viewed then as a very complex ensemble of molecular machines. The idea of constructing artificial molecular machines, however is quite recent. This topic was briefly discussed for the first time by Richard P. Feynman,[5] in his address, "There's Plenty of Room at the Bottom", to the American Physical Society in 1959. Only in the past years have systematic studies been performed in this field.[4,6,7] Our choice of the molecular constructs is then a deliberate link between molecular construction and structures familiar in the macroscopic world.

The challenge addressed during this project is to construct, in a controlled manner, complex assemblies using different building blocks leading to unique functionality such as light absorption and energy transfer. The units that are going to be used for the construction of the previously designed molecular machines are chromophores. A chromophore is a part of an organic molecule that is responsible for its colour by absorbing energy from light over a certain range of wavelengths in the visible region. Transmission or reflection of the remaining light gives rise to the observed colour of the compound. Therefore, chromophores are the perfect molecules to build the machines as they already absorb light. There are many different chromophores in nature, such as food colourings, fabric dyes, pH indicators, etc. In order to select the best chromophore we need to look at biological systems with complex functionalities to act as models as they already have the light absorption properties we are looking for. Such common biological structures are photosynthetic plants and an example of it is chlorophyll (Figure 3).

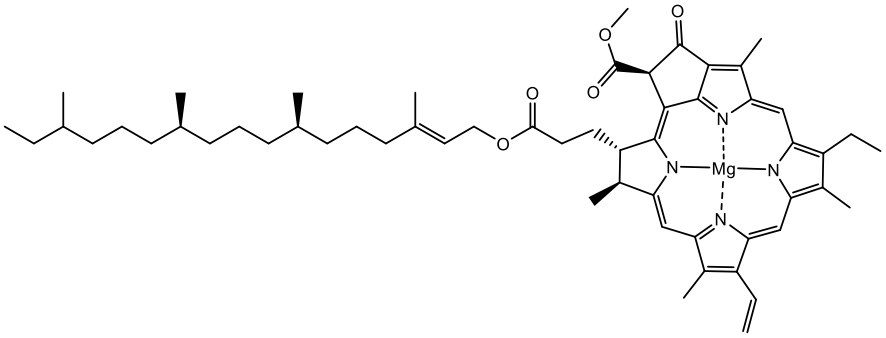

Figure 3. Structure of chlorophyll a.

Photosynthesis transforms the energy of the sun into a chemical form useful to the cell. Therefore, the photons to be absorbed come from the sun's emission radiation. Since the sun is essentially a black body at about 5000-6000 K, its quantum output is the broad band of Planck's radiation peaking near 600 nm (Figure 4).[8] Absorption in this visible region requires a large conjugated molecule such as chlorophyll (Figure 3). Increased conjugation brings the HOMO and LUMO orbitals closer together and the energy required to effect the electron promotion is therefore less, and the wavelength that provides this energy is increased correspondingly ($\Delta E = hc/\lambda$).[9]

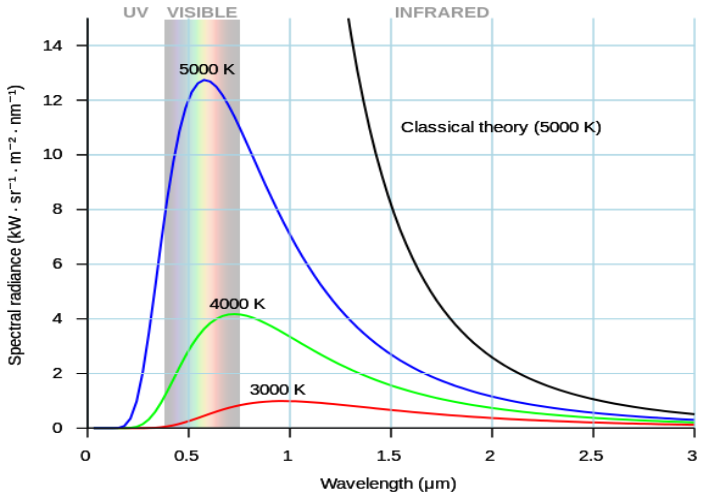

Figure 4. Planck's law electromagnetic radiations of black bodies at various temperatures.

This photosynthetic process requires the absorption of solar photons and chlorophyll plays a vital role for photosynthetic organisms, allowing the photons to be absorbed. Moreover, the nature of the molecular organization of the different chlorophylls in plants is of fundamental importance in the photoreaction processes.[10,11] Also, chlorophyll will be required to absorb light and transfer that energy by resonance energy transfer to another specific chlorophyll pair.[9] There are various different molecular types of chlorophyll: a, b, c_1, c_2, d and f.[12,13] Each one of them has a specific role in the photosynthesis process but with small structural changes.

Therefore, the function that this chromophore has in chlorophyll is the absorption of light required for the photosynthesis and the transference of that energy into other systems.[10,14] It is therefore logical to select related chromophore units, porphyrins and/or phthalocyanines as building blocks for our target molecular machines.[2,15-18]

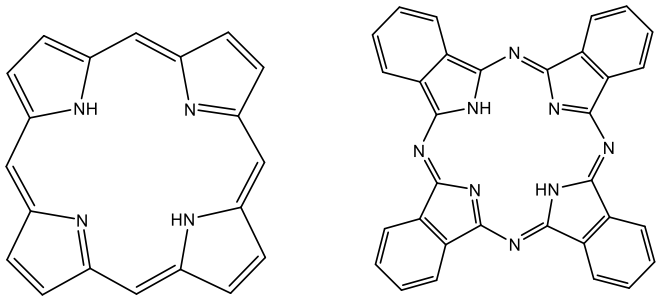

Figure 5. Parent structures for porphyrins (left) and phthalocyanines (right).

Porphyrins and phthalocyanines have been studied for a long period of time and their properties and chemistry are well known.[9,12,19] This vast knowledge of porphyrins can be observed as references to these compounds can be found from the early 19th century.[19-22] They are present in everyday life and their biological activities are the reason for the great interest over the past century. They hold some advantages in comparison to other types of electro- and photoactive compounds which arise from their 18 π-electron aromatic structure. These advantages are their high molar absorption coefficients and fast energy and/or electron transfer donor abilities to electron acceptor counterparts. Thus, porphyrins and phthalocyanines are widely used as molecular components in artificial photosynthetic systems,[23,24] both for energy-transfer and electron-transfer processes. Finally, porphyrins and phthalocyanines display complementary optical transitions.[25] In particular, the lowest energy absorption of phthalocyanines is red shifted and more intense than that of porphyrins, and the Soret band of the phthalocyanine is blue-shifted and weaker than that of the porphyrin.

On the other hand, the possibility of tailoring their redox potentials through peripheral functionalization represents an appealing feature for their use in the above mentioned energy-related areas and molecular machines. In this connection, both porphyrins and phthalocyanines have remarkable absorption in the visible region.[26-28] However, whereas regular porphyrins do not display significant absorption at energies higher than 550 nm, phthalocyanines show excellent light harvesting capabilities over a wide range of the solar light spectrum with a maximum at around 700 nm, close to where the maximum of the solar photon flux occurs.[29] Therefore a complex structure containing both chromophores will be optimal for the desired light harvesting properties of the molecular machines.[30]

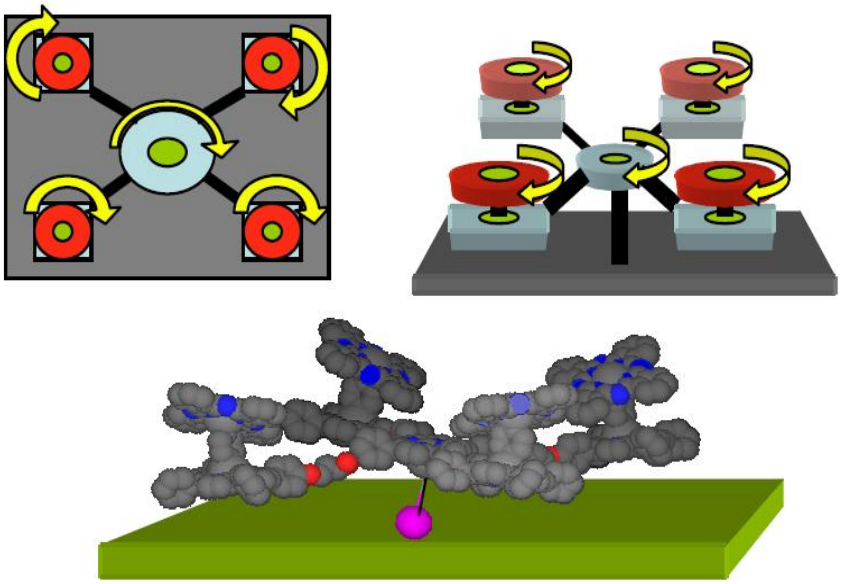

Figure 6. Proposed design for the molecular machine.

With this in mind, a molecular representation of the targeted light harvesting machine was designed using these chromophores as building blocks (figure 7). This molecular representation was designed using a porphyrin superstructure where different phthalocyanines were attached to resemble the teacups ride model.

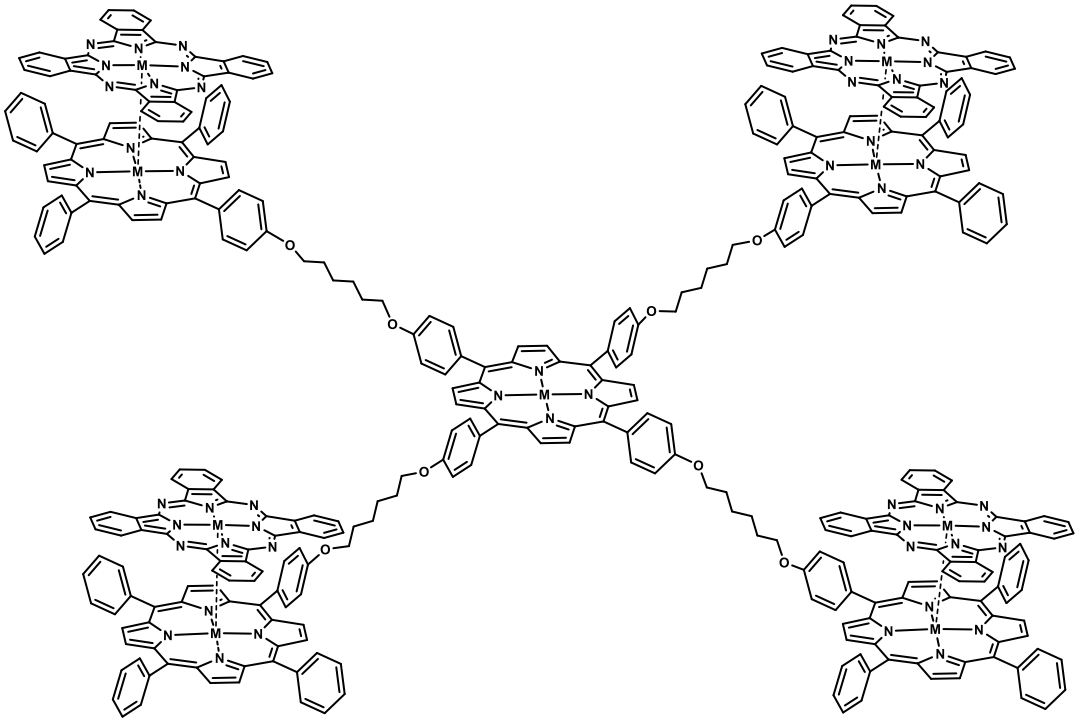

Figure 7. Proposed design for the molecular machine using porphyrins and porphyrins as building blocks.

The challenge for the synthesis can be broken down into two general areas: Construction of the molecular machines themselves and controlled assembly onto a suitable surface. Both structures require unsymmetrical building blocks in order to provide linking-points for construction of target molecules. The synthesis of the machines was planned to be achieved in a stepwise manner by interrogating different parts of the machine separately in order to leave the chemistry as simple as possible. For example, it was expected that the synthesis of useful unsymmetrical porphyrin derivatives would be relatively straightforward[18,20,31] and therefore employed first. Unsymmetrical phthalocyanines bearing one linking point can also be prepared but are generally more tedious.[32,33]

For the synthesis of the molecular machines, the first step is to identify the different subunits that form the system. In this case freely rotating units (phthalocyanines) are grafted onto a freely rotating superstructure (porphyrins). Also, the way that different units will be interconnected may play an important role for the future functionality of the molecular machine.[34-36] Many different approaches can be followed in order to have linkers of different rigidity, length and complexity. The order of machine assembly will also be crucial, along with selection of metal/metalloid elements to link the macrocycles (teacups) onto the frame, and to link the frame to the surface.

There are many possible applications including great potential for relevant multielectron processes for new generation energy capture systems. The transition from single to multiple electron processes remains one of the most significant and pressing challenges for harnessing solar energy. Single molecule processes could also be possible with most obvious application in molecular computing, data storage and security systems.

4.1 PORPHYRINS

4.1.1 Generalities

The porphyrins (Figure 8) are an important class of naturally occurring macrocyclic compounds found in biological systems that play a very important role in the metabolism of living organisms. They have a universal biological distribution and were involved in the oldest metabolic phenomena on earth. Some of the best examples are the iron-containing porphyrins found as heme (of haemoglobin) and the magnesium-containing reduced porphyrin (or chlorin) found in chlorophyll. Without porphyrins and their related compounds, life as we know it would be impossible and therefore the knowledge of these systems and their excited states is essential in understanding a wide variety of biological processes, including oxygen binding, electron transfer, catalysis, and the initial photochemical step in photosynthesis.[37,38]

The word porphyrin is derived from the Greek porphura meaning purple. They are in fact a large class of deeply coloured pigment, of natural or synthetic origin, having in common a substituted aromatic macrocycle ring that consists of four pyrrole rings linked by four methine bridges.[39] The porphyrin macrocycle is a highly-conjugated molecule containing 22 π-electrons, but only 18 of them are delocalized according to the Hückel's rule of aromaticity (4n+2 delocalized π-electrons, where n = 4).

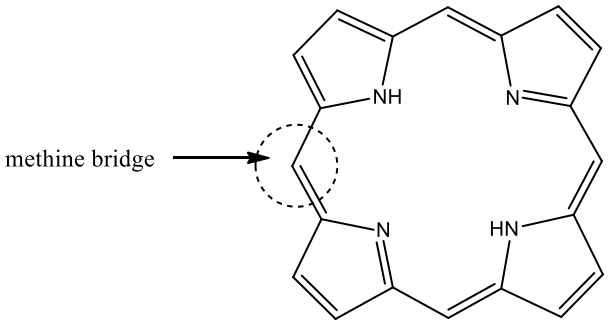

Figure 8. The structure of porphyrin.

The porphyrins have attracted considerable attention because they are ubiquitous in natural systems and have potential applications[2-4,16,25,39-41] in mimicking enzymes, catalytic reactions, photodynamic therapy, molecular electronic devices and conversion of solar energy. In particular, numerous porphyrin based artificial light-harvesting antennae, and

donor acceptor dyads and triads have been prepared and tested to improve our understanding of the photochemical aspect of natural photosynthesis.

4.1.2 Chemical characteristics of porphyrins

The synthetic world of porphyrins is extremely rich and its history began in the middle of 1930s. An enormous number of synthetic procedures have been reported until now, and the reason can be easily understood analysing the porphyrin skeleton.[31] In principle, there are many chemical strategies to synthesize porphyrins, involving different building blocks, like pyrroles, aldehydes, dipyrromethanes, tripyrranes and linear tetrapyrroles.

The most famous monopyrrole polymerization route to obtain porphyrins involves the synthesis of tetraphenyl porphyrins, from reaction between pyrrole and benzaldehyde. This procedure was first developed by Rothemund[20] and, after modification by Adler, Longo and colleagues,[42] was finally optimized by Lindsey's group.[43] In the Rothemund and Adler/Longo methodology the crude product contains between 5 and 10% of a by-product, discovered later to be the meso-tetraphenylchlorin, which is converted to the product under oxidative conditions (scheme 1).

Rothemund in 1935 set up the synthesis of porphyrins in one step by reaction of benzaldehyde and pyrrole in pyridine in a sealed flask at 150 °C for 24 h but the yields were low, and the experimental conditions so severe that few benzaldehydes could be converted to the corresponding substituted porphyrin.[20] The reason for the low yield is that the main (non-polymeric) by-product of reaction was meso-substituted chlorin **4** and in understanding the nature of its formation, Calvin and coworkers[21] discovered that the addition of metal salts to the reaction mixture, such as zinc acetate, increases the yield of porphyrin **3** from 4-5% for the free-base derivative, and decreases the amount of **4**. Other improvements were obtained by changing reactant, the reaction conditions and substituents on the benzaldehyde derivative.

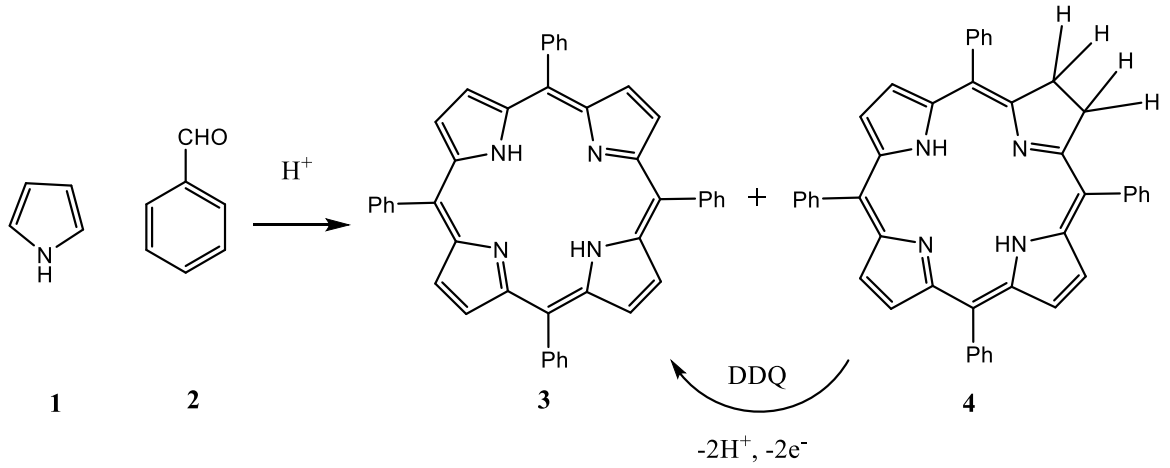

Scheme 1. Synthesis of 5,10,15,20-tetraphenyl porphyrin **3**.

Adler, Longo and coworkers, in 1967,[42] re-examined the synthesis of meso-substituted porphyrins and developed an alternative approach (Scheme 2) with a method that involves an acid catalysed pyrrole-aldehyde condensation in glassware open to the atmosphere in the presence of air. The reactions were carried out at high temperature, in different solvents and concentration range of reactants, with a yields of 30-40 %, and with chlorin contamination lower than that obtained with the Rothemund synthesis.

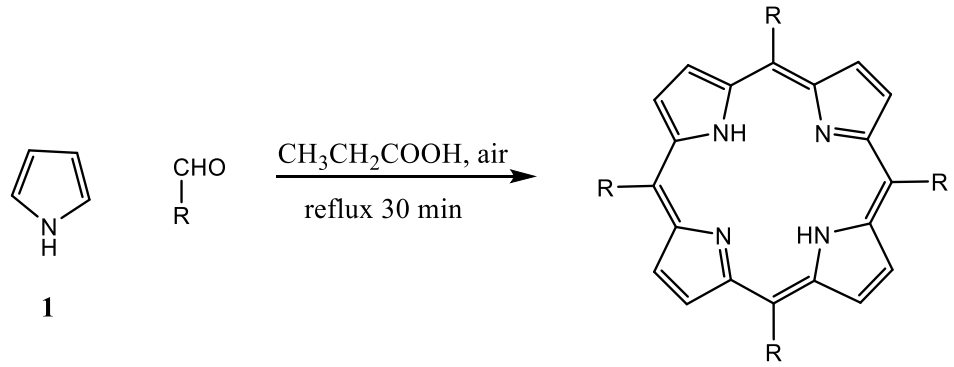

Scheme 2. Adler-Longo general method for preparing meso-substituted porphyrins.

Over the period 1979-1986, Lindsey developed a new and innovative two-step room temperature method to synthesise porphyrins. His work was motivated by the need for more gentle conditions for the condensation of aldehydes and pyrrole, in order to enlarge the number of the aldehydes utilizable and then the porphyrins available.[43] The method has been a new strategy for the synthesis of porphyrins, using a sequential process of condensation and oxidation steps. The reactions were carried out under mild conditions in an attempt to achieve equilibrium during condensation, and to avoid side reactions in all steps of the porphyrin-formation process (Scheme 3).

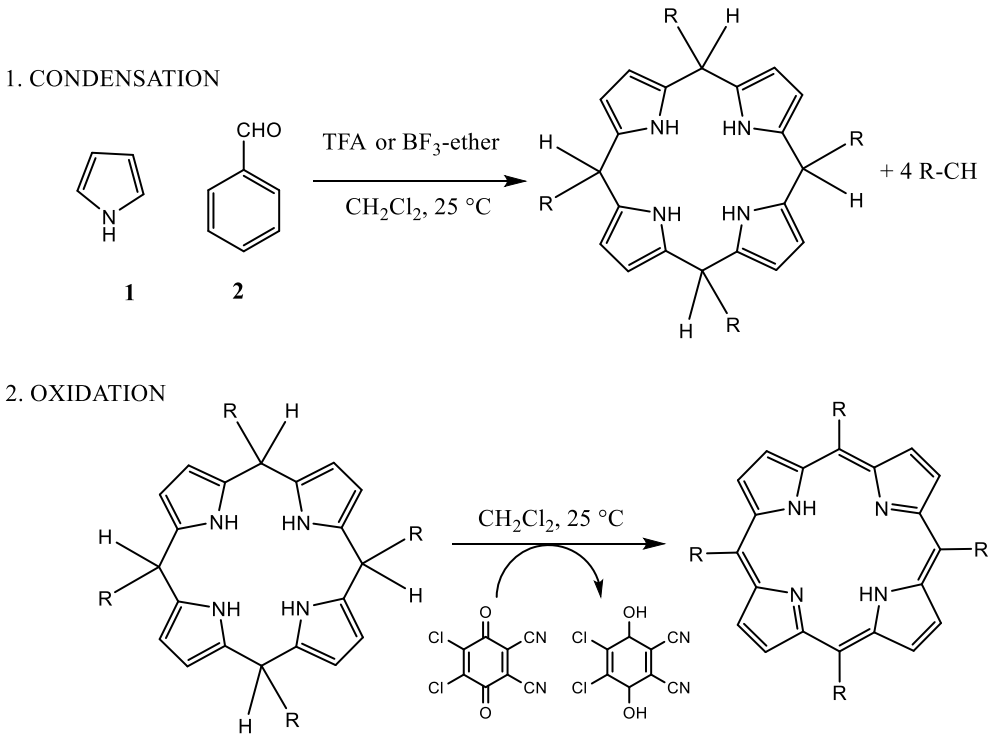

Scheme 3. Two-step one-flask room-temperature synthesis of porphyrins.

The porphyrin structure supports a highly stable configuration of single and double bonds with aromatic characteristics that permit the electrophilic substitution reactions typical of aromatic compounds such as halogenation, nitration, sulphonation, acylation, deuteration, formylation.

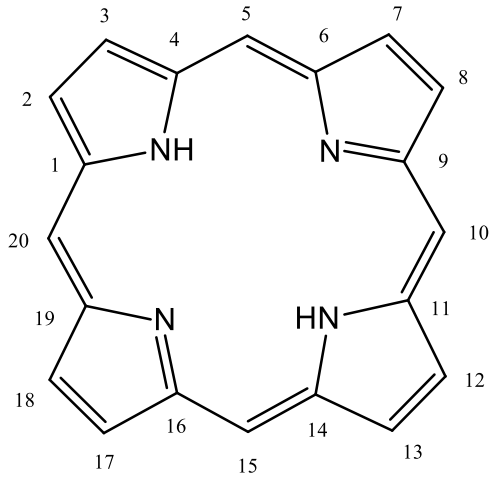

Figure 9. Porphyrin numeration.

There are two different sites on the macrocycle where electrophilic substitution can take place with different reactivity:[39] positions 5, 10, 15 and 20, called meso-positions and also 2, 3, 7, 8, 12, 13, 17 and 18, called β-pyrrole positions (figure 9). The β-substituted porphyrins are widely present in natural products, while the meso-substituted porphyrins have no counterpart in nature and were developed as functional artificial models. The activation of these sites depends of the porphyrin electronic character.

4.1.3 UV-vis spectroscopy of porphyrins

It was recognized early that the intensity and colour of porphyrins are derived from the highly conjugated π-electron systems and that is a feature of porphyrins that can be studied by their characteristic UV-vis spectra that consist of two distinct regions: one in the near ultraviolet and other in the visible (figure 10).

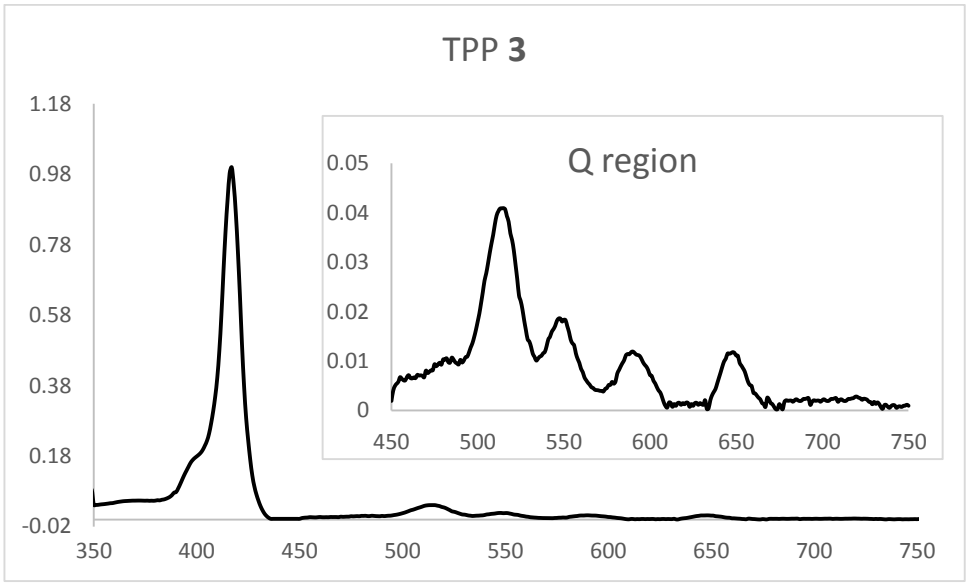

Fig 10. UV-vis spectra of porphyrin **3** and an expanded view of the Q-region.

It has been well documented that changes in the conjugation pathway and symmetry of a porphyrin can affect its UV-vis absorption spectrum.[27,28,44]

The absorption spectrum of porphyrins has long been understood in terms of the highly successful "four-orbital" (two highest occupied π orbitals and two lowest unoccupied π* orbitals) model first applied in 1959 by Gouterman[26] that has discussed the importance of charge localization on electronic spectroscopic properties.[27]

According to this theory, as reported in scheme 4, the absorption bands in porphyrin systems arise from transitions between two HOMOs and two LUMOs (scheme 4a), and it is the identities of the metal centre and the substituents on the ring that affect the relative energies of these transitions.

The electronic absorption spectrum of a typical porphyrin consists therefore of two distinct regions. The first involves the transition from the ground state to the second excited state (S0 → S2) and the corresponding band is called the Soret or B band. The range of absorption is between 380 and 500 nm depending on whether the porphyrin is β- or meso-substituted. The second region consists of a weak transition to the first excited state (S0 → S1) in the range between 500-750 nm (the Q bands). These favourable spectroscopic features of porphyrins are due to the conjugation of 18 π-electrons and provide the advantage of easy and precise monitoring of guest-binding processes by spectroscopic methods. Therefore, depending of the relative position of the substituents the spectra can be altered and the relative intensity of the Q bands will be therefore altered.

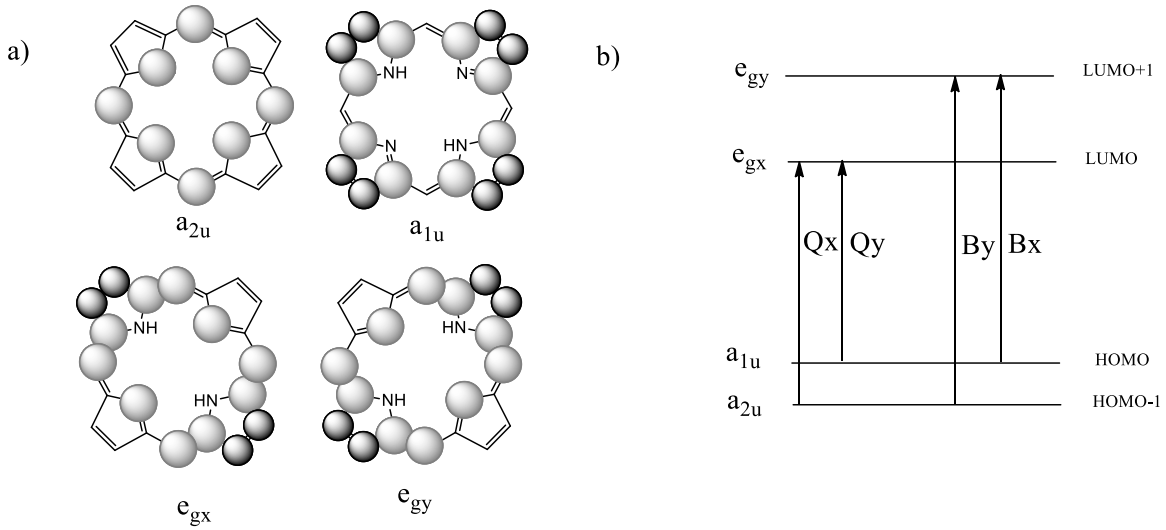

Scheme 4. Porphyrin HOMOs and LUMOs. a) Representation of the four Gouterman orbitals in porphyrins.[27] b) Drawing of the energy levels of the four Gouterman orbitals upon symmetry, lowering from D_{4h} to C_{2V}. The set of e_g orbitals gives rise to Q and B bands.

While variations of the peripheral substituents on the porphyrin ring often cause minor changes to the intensity and wavelength of the absorption features, protonation of two of the inner nitrogen atoms or the insertion/change of metal atoms into the macrocycle usually strongly change the visible absorption spectrum. When the porphyrin macrocycle is coordinated with any metal, there is a more symmetrical situation than in the free base porphyrin and this produces a simplification of the Q bands pattern and the formation of two Q bands.

4.1.4 Metallated porphyrins

Generally porphyrins are synthesised in a metal-free form and metal ions are separately inserted. When the metal ion M^{n+} is incorporated into the porphyrin $PorH_2$ to form $PorM^{(n-2)+}$, the two amine protons in $PorH_2$ are dissociated from the two pyrrole groups as reported in equation (1):

$$M^{n+} + PorH_2 \leftrightarrow MPor^{(n-2)+} + 2H^+ \quad (1)$$

The size of the porphyrin-macrocycle is perfectly suited to bind almost all metal ions and indeed a large number of metals can be inserted in the centre of the macrocycle forming metalloporphyrins that play key roles in several biochemical processes.[15,45,46] Depending on their size, metal ions (e.g. Zn, Cu, Ni, Co, etc.) can fit into the centre of the planar tetrapyrrolic ring system forming *regular* metalloporphyrins resulting in kinetically inert complexes.

When divalent metal ions (e.g. Co(II), Ni(II), Cu(II)) are chelated, the resulting tetracoordinate chelate has no residual charge. While Cu(II) and Ni(II) in their porphyrin complexes have generally low affinity for additional ligands, the chelates with Mg(II), Cd(II) and Zn(II) readily combine with one more ligand to form pentacoordinated complexes with square-pyramidal structure (figure 11a). Some metalloporphyrins (Ru(II), Fe(II), Co(II), Mn(II)) are able to form distorted octahedral geometries (figure 11b) with two extra ligands.[47,48]

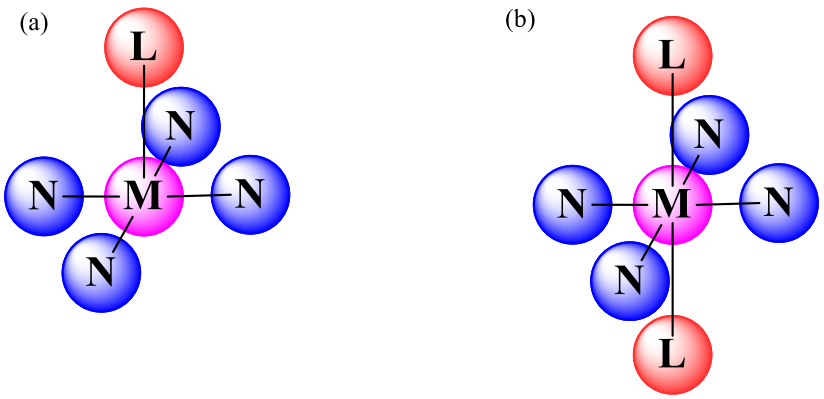

Figure 11. Schematic pictures of square-pyramidal (a) and octahedral structures (b) (only nitrogen N, metal M and extra ligands L).

Most of the natural metalloporphyrins are of regular type, i.e. their metal centres are located within the plane of the macrocyclic ligand as a consequence of their fitting size. The cationic radii are in the range of 55–80 pm corresponding to the sphere in the porphyrin core surrounded by the four pyrrolic nitrogens. While the symmetry group of the free-base porphyrins is D_{2h} due to the two hydrogen atoms on the diagonally located pyrrolic nitrogens, the coplanar (*regular*) metalloporphyrins (without these protons, figure 12a) are of higher symmetry (generally D_{4h}).

If, however, the ionic radius of the metal ions is too large (over 80-90 pm) to fit into the hole in the centre of the macrocycle, they are located out of the ligand plane, distorting it forming *sitting-atop* (SAT) metalloporphyrins (figure 12b) that are characterized by special properties[49-51] originating from the non-planar structure caused by, first of all, the size of the metal centre.

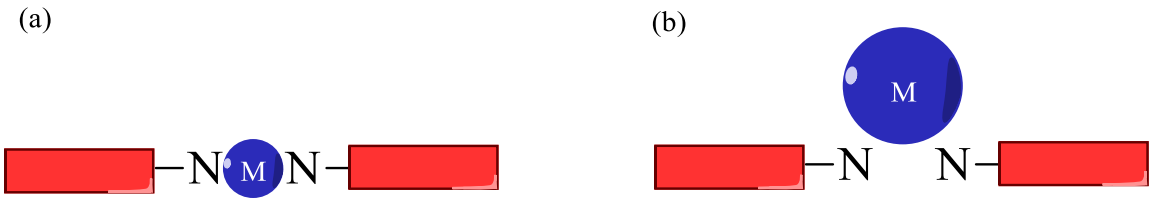

Figure 12. Schematic representation of (a) regular (M = Zn, Mg…) and (b) SAT metalloporphyrins (M = La, Eu…).

These complexes are kinetically labile and display characteristic structural and photoinduced properties that strongly deviate from those of the regular metalloporphyrins. The latter kind of structure induces special photophysical and photochemical features that are characteristic for all SAT complexes. For example, they allow the formation of stacked sandwich like complexes with other porphyrins/phthalocyanines that show intriguing intramolecular π-π interactions.[52-55] The symmetry of these structures is lower (generally C_{4v}-C_1) than that of both the free-base porphyrin (D_{2h}) and the regular, coplanar metalloporphyrins (D_{4h}), in which the metal centre fits into the ligand cavity.

Thus different metal insertions allow us to form links between porphyrins or attaching porphyrins into surfaces, by having different ligands in the apical positions (figure 11). These linking points allow us to have axial functionality perpendicular to the porphyrin plane by coordination with such metals. Such axially functionalized porphyrin could later on be further reacted in order to obtain porphyrin-porphyrin structures or

porphyrin-surface connections. Some examples of this type of functionalization have been achieved by the Cammidge group using in recent years silicon and germanium porphyrins.[17]

Other approaches can be observed using different metals such as In, Ru, La, etc. Some examples are shown below in figure 13, showing the formation of sandwich-like complexes through, for example, indium or ruthenium in **5**,[56,57] by having oxygen linkers with silicon porphyrins in **6**[30,58] or directly linked porphyrins with big metals such as lanthanides **7**.[1,59,60]

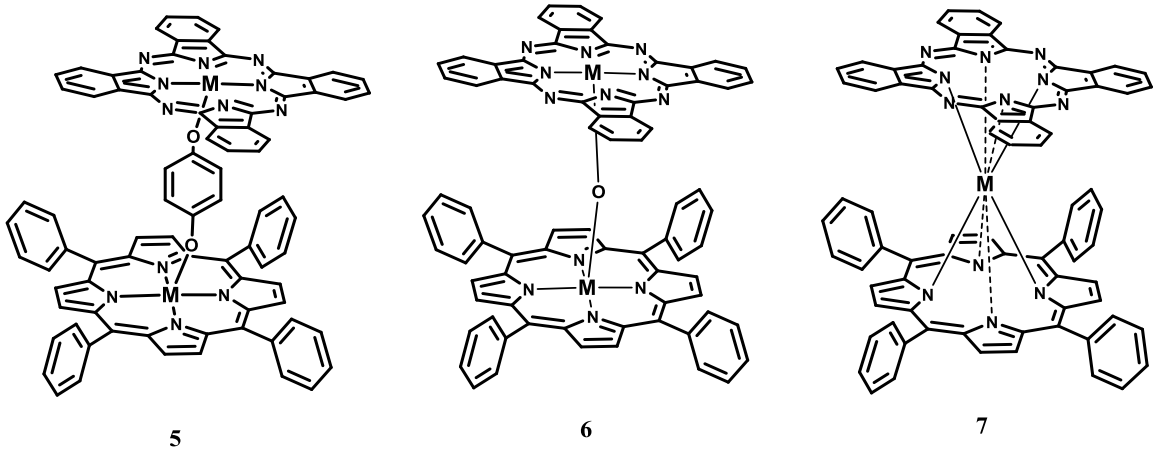

Figure 13. Different examples for the formation of porphyrin-phthalocyanine sandwiches using different metals or metal substitutions.

4.1.5 Synthesis of tetraphenylsubstituted porphyrins

The synthesis of symmetrical porphyrins is very well known and was previously described. During this work, various symmetrical porphyrins have been synthesised in order to have simple structures for the construction of the molecular machines. Also, simple structures such as TPP **3**, R=H allows the study of the reactivity of different metal complexes using them as models in test reactions. After studying the desired process using these simple models, we conceive using the same chemistry for construction of the molecular machines.

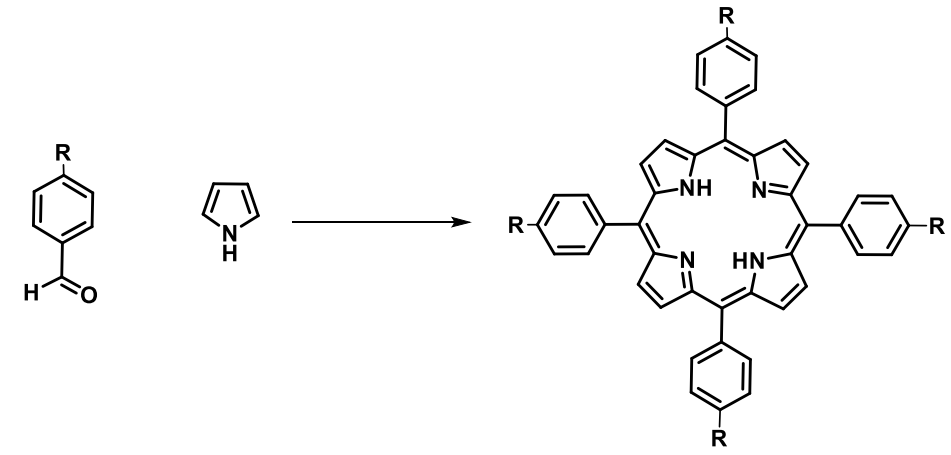

2 R=H
8 R = Br
9 R = MeO
10 R = $Br(CH_2)_6O$

1

3 R = H
11 R = Br
12 R = MeO
13 R = $Br(CH_2)_6O$

Scheme 5. General structure for tetra-*p*-phenylsubstituted porphyrins **11**-**13**.

For the synthesis of the symmetrical porphyrins used during this chapter and in general for this project, the method provided by Adler[42] was performed by reacting the corresponding aldehyde and freshly distilled pyrrole in propionic acid. This method allowed us to obtain a large range of symmetrical porphyrins with a very fast and easy procedure. Although the yield of the reaction is low (14–22 %), the very easy purification process and the very cheap and commonly available starting materials, makes this method the most convenient choice for the synthesis of tetra-substituted porphyrins. Several porphyrins have been synthesised using this method in gram scale, using either commercial aldehydes (**2**, **8** and **9**) or derivatives prepared using standard chemistry (e.g **10**).

The only porphyrin that has failed to be synthesised efficiently using this method is porphyrin **15** (R = OH) from *p*-hydroxybenzaldehyde **14**. This porphyrin **15** is one of the key porphyrin intermediates for the construction of the molecular machines. This particular porphyrin offers the perfect functionality and symmetry to be the central unit of the machine. Because of its high solubility, this porphyrin **15** could not be selectively precipitated from the reaction mixture (≈ 90 % impurities). Some attempts to purify this compound from the reaction mixture have been performed but all of them have proven to be unsuccessful or inefficient.

Therefore, the easiest way for the synthesis of **15** involved the synthesis of a protected precursor **12**. Once this protected porphyrin **12** was synthesised and purified, following the standard procedure by Adler,[42] it could be deprotected using boron tribromide or a mixture of HBr/AcOH to obtain the desired porphyrin **15** as represented in scheme 6.

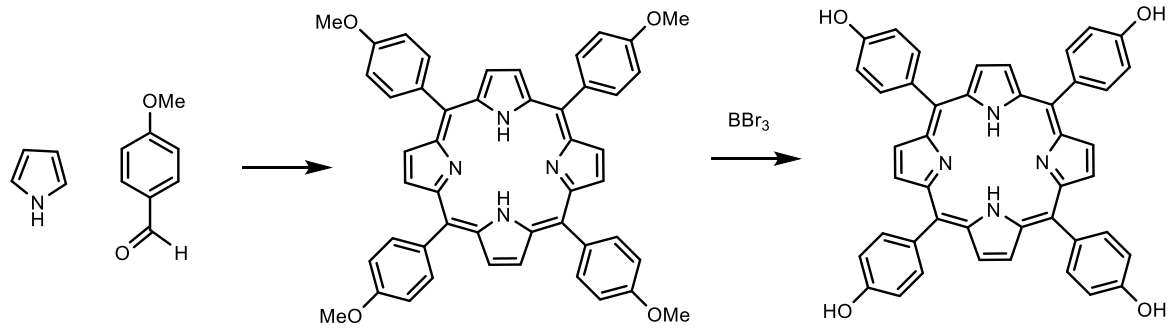

Scheme 6. Method for the synthesis of T(OH)PP **15.**

The desired porphyrin **15** could be obtained after column chromatography and recrystallisation. The previously described reactions could be performed in gram scale with a good overall yield allowing the synthesis of the desired porphyrin **15** in reasonable amounts for the construction of the target molecular machines.

4.1.6 Indium as linking point between porphyrins or porphyrins and surfaces.

The first choice for linking porphyrins was inserting indium (III) in the porphyrin cavity. It is know that indium forms highly stable covalent bonds with carbon and can also be inserted in tetrapyrrolic macrocycles.[61-63] This stability will generate highly stable links between rings or as fulcrum for building the molecular machines from the ground up and also, allows us to further react this monomer using various different reaction conditions with less chance of decomposition. This functional group will also allow the system to freely rotate through the In-C bond.

Indium chloride porphyrins can be easily obtained by metalating the free base porphyrin using indium(III) chloride.[64] This process yields the corresponding indium porphyrin derivative with a chlorine atom in the apical position. This could then be exchanged with any other aromatic group allowing it to have the desired 90° to the plane of the porphyrin and therefore allow as well free rotation through this linking point. Few attempts to exchange the chlorine for other organic groups have been reported in the literature[40,61] giving us a starting point for the reaction conditions to be tried. During this work, the substitution of the chlorine for different aromatic rings and a screening for reaction conditions were tried.

4.1.6.1 Metallation of porphyrins using $InCl_3$ as indium source

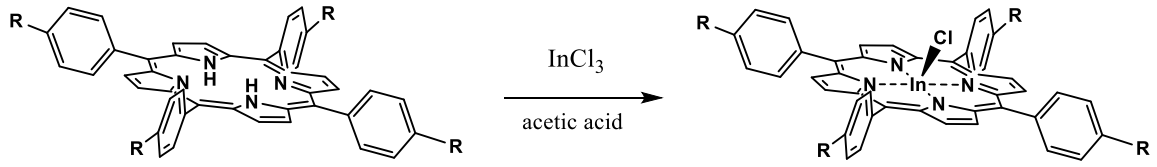

3 R = H
11 R = Br
15 R = OH

16 R = H
17 R = Br
18 R = OH

Scheme 7. Structure of InTPPCl **16.**

The preparation of indium porphyrin complexes was based on the "acetate method" reported by Buchler.[65] This method consisted of the reflux of a solution of the desired metal-free porphyrin and indium chloride in acetic acid for 24 h. After the reaction, the porphyrin product was precipitated with MeOH and purified by column chromatography over silica gel. The desired indium chloride porphyrins **16-18** were obtained in high yields, between 16 - 86 % depending on the porphyrin substituents.

Synthesis of phenylindium porphyrins

Before trying to introduce functionalized aromatic groups in the apical position of the porphyrin by substitution of the chlorine atom for other phenyl derivatives, the reactivity of the system was interrogated. The first reaction performed was between the indium chloride porphyrin complex and phenylmagnesium bromide (Grignard reagent) that is easy to make and even commercially available in solution. This is a straightforward reaction that allowed the reactivity of the system to be checked. If this reaction is successful, other reactions using different phenyl reagents for the synthesis of the desired target molecular machines can be designed.

The first trials were attempted using porphyrin **17** as starting material as represented in scheme **8**. This particular porphyrin was chosen because there is no other hydroxyl groups in the compound that might interfere in the reaction. The target porphyrin **20** has bromide functionality on the meso-phenyl gripus that could then be further reacted using Sonogashira or Suzuki coupling reactions for the construction of the target molecular machines.

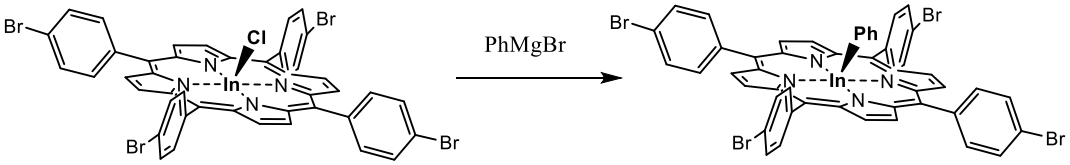

17 **20**

Scheme 8. Reaction attempted for the formation of **20.**

In the initial reaction, chloroindiumporphyrin **17** was treated with an excess of phenylmagnesium bromide in toluene at room temperature for 48 h as previously reported by Tabard for β-substituted porphyrins.[61] Workup and analysis of the crude product revealed that it contained mostly unreacted starting material **17** plus traces of the metal free porphyrin complex **11**. The product could not be obtained using this method.

The reaction solvent was changed from toluene to benzene as described in the reaction conditions given by Tabard[61] for β-substituted porphyrins or Stuzhin[63] for tetraazaporphyrinates. The rest of the conditions such us temperature, reagents and concentrations remained the same. In this case, the same outcome was observed, only demetallation of some of the starting material occurred but no product was observed in any case.

Synthesis phenoxyindium porphyrins

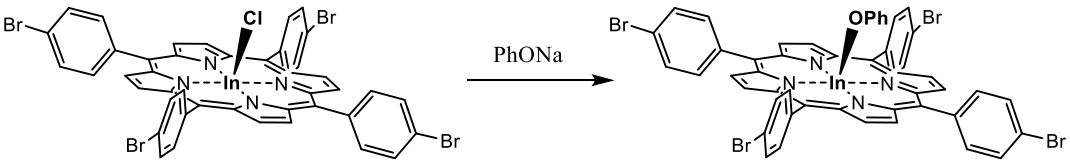

17 **21**

Scheme 9. Reaction attempted for the formation **21**.

As no straightforward conditions could be found for arylation reaction of indium porphyrins, the reaction between indium porphyrin **17** and sodium phenoxide (synthesised in situ from phenol and sodium hydride) in ether was then explored. Aliquots were taken from the reaction and checked using MALDI-tof MS every 30 min (expected molecular

weight of **21** of 1135 g/mol). After 1 h of stirring, a peak corresponding to 1158 g/mol was observed. The reaction was left stirring for another hour and stopped. After working up, the crude mixture was checked by MALDI-tof MS and TLC, observing only unreacted porphyrin **17** (molecular weight of 1078 g/mol).

Further reaction conditions were tested with chloroindiumporphyrin **16** as starting material. This porphyrin was selected for the test reactions because it is much easier to synthesize and it is the simplest aryl substituted porphyrin possible. Therefore, it is less likely to give other side reactions as long as the only possible reactivity point is the apical chlorinated position.

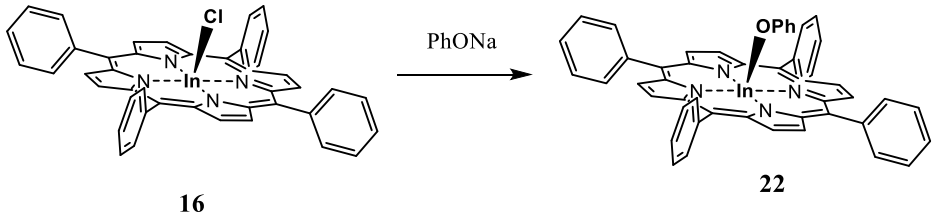

16 **22**

Scheme 10. Reaction attempted for the formation of **22.**

For the first attempt, a solution of sodium phenoxide was prepared by reacting phenol and sodium hydride in THF. To this solution, indiumporphyrin **16** dissolved in the minimum amount of THF was slowly added and the resultant mixture was left stirring under Ar. Then, aliquots were taken to monitor the reaction by TLC. After 8 h with no observed changes, the reaction was left stirring overnight. After 18 h stirring, no product was observed and the starting material **16** remained unreacted in the reaction mixture. Consequently, the reaction temperature was increased to reflux for 24 h. After analysis of the reaction mixture by TLC and MALDI-tof MS, only the unreacted starting material **16** was observed as a single spot on TLC as well as single signal peak in MALDI-tof MS.

To the same unreacted material **16**, hydrolysis of the porphyrin was attempted for the formation of hydroxyindiumporphyrin **23** as shown below on scheme 11. To do so, an excess of concentrated NaOH was added to the reaction mixture. After heating the reaction mixture at reflux for 24 h, the reaction was checked by TLC and a small spot appeared on the baseline. The crude was then checked by MALDI-tof MS but no peaks were observed for any indium porphyrin derivative expected. The reaction was stopped and the products

separated by column chromatography, collecting a major fraction of the unreacted starting material **16** and two other small fractions were obtained that could not be characterised.

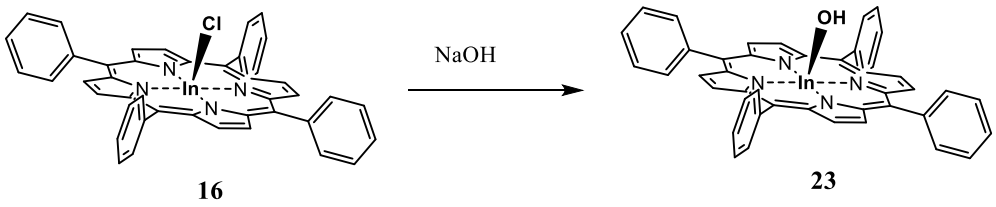

16 **23**

Scheme 11. Hydroxylation of **16**.

The observation of different compounds after the reaction was a promising result. Another reaction was then attempted by adding a few drops of concentrated NaOH in a solution of **16** in toluene. After the overnight reflux, the reaction was checked by TLC and MALDI-tof MS appearing only to be unreacted starting material **16**. No product **23** was observed. Another methodology need to be then explored and, following the literature,[62] tetrabutylammonium hydroxide instead of sodium hydroxide was used for introduction of the OH group into bromoindiumphthalocyanines. A 25 % solution of tetrabutylammonium hydroxide in MeOH was added to another solution of the corresponding chloroindium porphyrin **16** in THF and the mixture set to reflux. Aliquots from the reaction were checked by TLC after 1 h, 4 h, 24 h and 48 h without observation of formation of any products. Then the solvent was removed and the starting material **16** recovered unreacted.

A final attempt for the formation of the target complex **22** was followed by introduction of the metal into the porphyrin in the presence of sodium phenoxide in one step (scheme 12). Doing this we expected some of the indium chloride to react with the phenoxide before or during the insertion of the metal into the porphyrin.

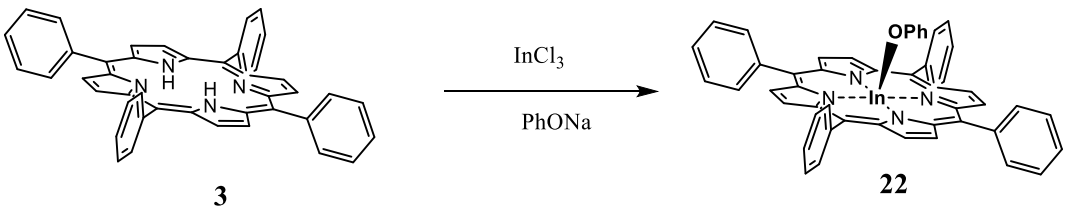

3 **22**

Scheme 12. Attempted one step synthesis of **22**.

To do so, two different reactions were prepared. In the first one, indium chloride and sodium phenoxide were reacted separately (refluxing for 2 h) followed by addition of the metal free porphyrin **3**. In the other one, the porphyrin **3**, indium salt and sodium phenoxide were all reacted together in a one pot one step reaction. Both reactions were left refluxing for 72 h under an inert atmosphere. After workup and analysis of the reaction products, only unreacted starting material was recovered in both cases.

Another final experiment was then attempted using solvent-free conditions by mixing porphyrin **16** and an excess of phenol in a sealed tube leaving the mixture reacting at 200 °C overnight. The reaction was checked by MALDI-tof MS and after 24 h a small peak in the MALDI-tof MS corresponding to 820 m/z was observed by increasing the laser power. The reaction was stopped and checked by TLC but only starting material was observed.

4.1.6.2 Metallation of porphyrins using In_2O_3 as indium source

In this case, a different indium insertion into porphyrins was attempted as reported by Yu-yi Lee and coworkers.[66] It is reported that indium (III) oxide could be used as indium source for the metallation of the porphyrin in the presence of acetic acid to form the corresponding indium porphyrin. We decided to modify this procedure by replacing acetic acid with phenol. This way, the desired indium complex **22** is expected to be obtained as product of the same metallation step (scheme 13).

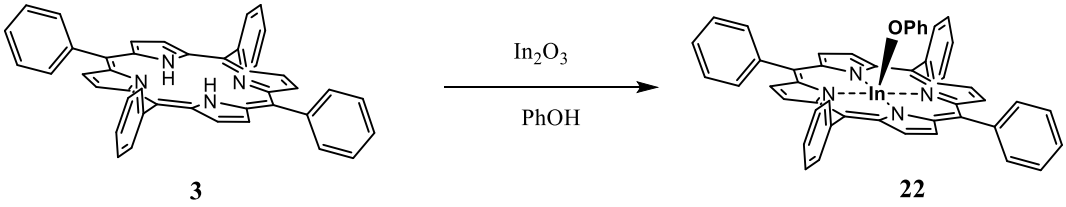

Scheme 13. Formation of **22** using In_2O_3 as indium source.

In order to study the formation of the desired porphyrin complex **22** from indium oxide, a one pot one step reaction was performed first. Toluene was chosen as solvent because its boiling point (110 °C) is very similar to that of acetic acid (118 °C) and therefore allows the reaction to reflux at a similar temperature. After refluxing the mixture for 24 h,

the reaction was checked by TLC and only unreacted porphyrin **3** was observed. It was then noted that indium oxide was not dissolved in toluene as it remained precipitated as white solids in the reaction mixture. Therefore, the solvent for the reaction was changed to dioxane (boiling point 101 °C). In this case, after 72 h refluxing in dioxane, no reaction was observed and the reaction solvent was substituted for DMSO and the temperature increased to 250 °C. Again, no product was observed after the reaction.

Consequently, a solvent-free reaction between phenol and indium oxide followed by addition of **3** was attempted. Indium oxide was mixed with an excess of phenol in a sealed tube filled with Ar and heated to 150 °C. After 4 h, **3** was added and the mixture left at 150 °C for 48 h. At this stage, no product was observed so the crude mixture was further reacted at 170 °C for 24h. Again, only unreacted starting material **3** was recovered.

After all these failed attempts of exchanging the chlorine atom from the indium porphirin derivatives, the idea of using indium porphyrins for the construction of the molecular machines was abandoned.

4.1.7 Ruthenium as linking point between porphyrins or porphyrins and surfaces.

Ruthenium porphyrins have been extensively studied for a long time. The first ruthenium porphyrin complex was described in 1969.[67] It was a ruthenium-porphyrin chloride complex, although two years later a corrected formulation of the complex, Ru(TPP)(CO)(EtOH) **24**, was published.[56] The chemistry, however, has been restricted primarily to studies of ligand exchange at the sixth coordination site.[68] Fortunately, previous research in our group reported successful double and single ligand exchanges from the carbonyl complexes in porphyrins and/or phthalocyanines.[47] This allowed us to accept the challenge of applying this chemistry into more complex structures. As expected, phosphines, thiols and amine donors bind particularly strongly to the metal centre, and once bound, exchange of the ligands can be very slow.[31] Also, this leads to highly stable complexes as ruthenium porphyrins cannot be easily demetallated, even in the presence of concentrated sulphuric acid.

There are different methodologies for inserting ruthenium into the porphyrin cavity,[47,69,70] normally forming intermediates like **24** first, using ruthenium dodecacarbonyl as ruthenium source, and then reacting it further to exchange the solvent molecule (S) on the opposite plane to the carbon monoxide, as shown in scheme 14.

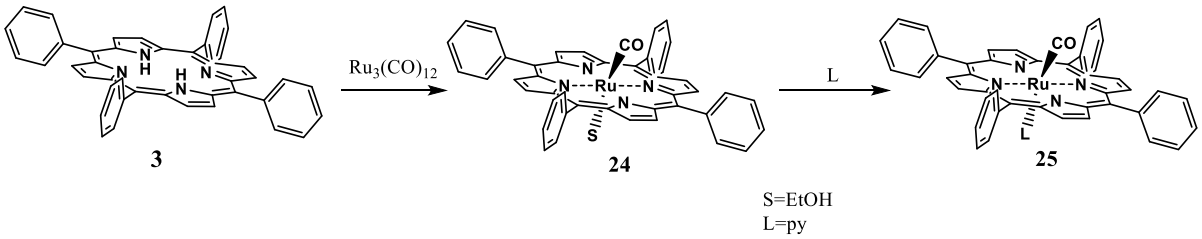

Scheme 14: Synthetic pathway for the formation of ruthenium substituted porphyrins.

These standard conditions were therefore followed.[70] A mixture of ruthenium dodecacarbonyl and TPP **3** in toluene was refluxed overnight under an inert atmosphere. Then, the reaction was cooled down and precipitated with EtOH overnight. The resultant crude solids were further purified by column chromatography on neutral alumina followed by recrystallisation of the desired ruthenium porphyrin **24** in good yield.

Ruthenium porphyrin **24** was further reacted by stirring with pyridine for 30 min. When the reaction was completed, the mixture was evaporated under reduced pressure and dried under high vacuum overnight to obtain the pure ruthenium porphyrin complex **25** TPPRu(CO)(py) in a 57 % overall yield. The substitution of ethanol for pyridine was straightforward and it could be achieved under very mild conditions. Ruthenium porphyrins could therefore provide a suitable linking point for attachment of a superstructure to a surface, most reasonably using a surface functionalised with tethered pyridine ligands as represented in scheme 15.

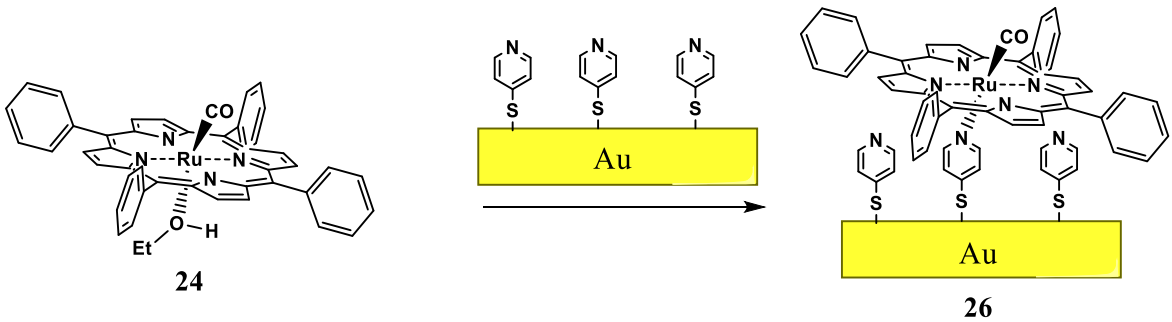

Scheme. 15. Proposed surface attachment of porphyrins into surfaces **26** using ruthenium porphyrin **24**.

Using this approach, the molecular machine could be constructed containing a ruthenium porphyrin unit in the central core position and different porphyrin-phthalocyanine complexes in the peripheral positions. Then, the entire molecular machine could be selectively attached to, for example, a gold surface. This central connection using ruthenium chemistry could act as fulcrum.

Different chemistry is however required for construction of the face-to-face chromophore arrays at the peripheral positions of the molecular machine to form the molecular variations of the "teacups" from the model.

4.1.8 Lanthanides as linking points between chromophores

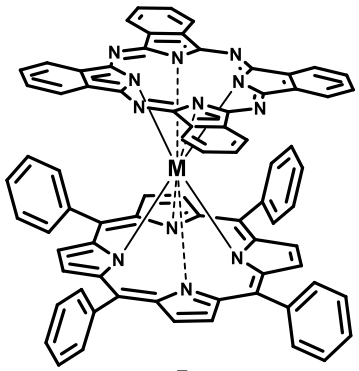

7

Figure 14. General structure for porphyrinate phthalocyanate lanthanide double deckers **7**.

In our case, for the construction of the desired molecular machines, incorporation of freely rotating phthalocyanines in the peripheral positions of the multiporphyrin array needed to be achieved. Our early work indicated that the originally proposed face-to-face construction of Por/Pc chromophores through In-C or In-O links would be difficult to achieve. We therefore turned our attention to the formation of sandwich-like structures linked via lanthanides.

Different multidecker complexes with large central metal ions including rare earth, actinide, early transition, and main group metals, have been fascinating chemists for several decades owing to their potential applications as versatile materials in various disciplines such as molecular machines,[1,71] single molecule magnets[3] or molecular electronics.[4] The first

known double decker was made by Lindstead *et al.* in 1936 from $Sn(Pc)Cl_2$ and $Na_2(Pc)$[19] where they deduced the constitution $Sn(Pc)_2$ from elemental analysis but did not give hints to the structure. The sandwich nature of this compound was proven by X-ray crystallography after the discovery by Lux *et al*. of the actinoid phthalocyanines.[72] Since then, considerable efforts have been devoted to the synthesis and investigations of electronic and optical properties of these complexes. Due to the intra- and inter-molecular π-π interactions and the intrinsic nature of the metal centres, these complexes have shown extraordinary optical, electrical, thermodynamic and magnetic properties.[16,41,55,73] They are expected to have applications in molecular electronic, photonic, and magnetic devices. Moreover, their unique electronic and optical properties make these complexes promising for photovoltaic applications.

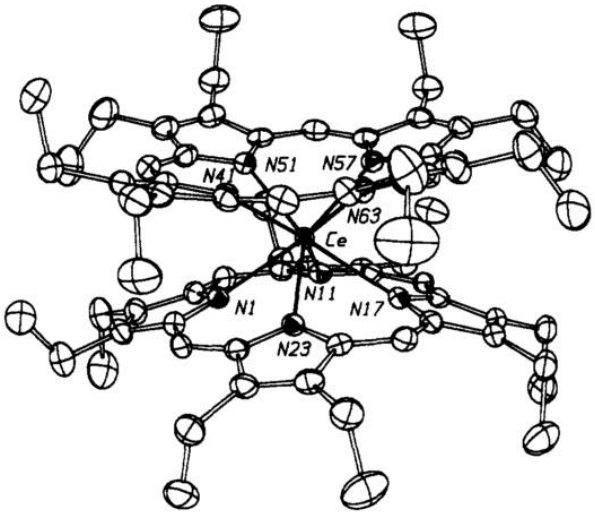

Fig 15. Representation of the first christallographically identified porphyrin sandwich.[74]

This type of sandwich structure of Por/Pc shows interesting optical properties and they have been studied extensively.[52,54,75] One of the obvious properties that can be observed are their UV-vis absorption spectra. As it can be expected this heteroleptic complexes, display those bands of the individual chromophores. For example, [LaH(Pc)(TPP)][53] (see figure 16) shows bands at 621 and 421 nm that corresponds to the $(Pc)^{2-}$ and $(Por)^{2-}$ ions respectively. The same common spectral properties can be observed in other heteroleptic double deckers $[M^{III}(Pc)Por)]^{-}$.[76,77] Therefore, UV-vis should be an important tool for the analysis of this type of sandwich structures.

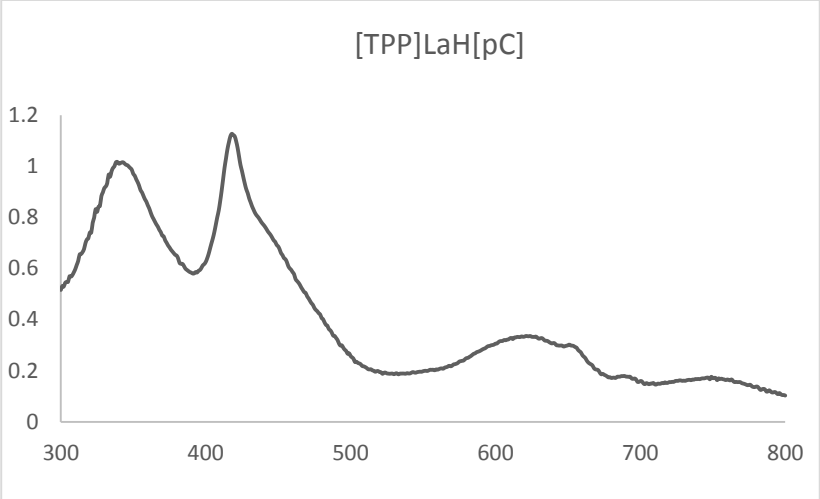

Fig 16. UV-vis spectra of [LaH(TPP)(Pc)].[53]

Different approaches for the selective synthesis of Por/Pc lanthanide heteroleptic double decker structures **7** have been published.[68,75,78] Almost all previously described methods are multistep synthetic procedures which apply one-by-one deck construction of the target molecules starting by metallation of the porphyrin forming a SAT complex ([TPP]Ln(acac)) **27** in a high boiling point solvent. For example, it was shown that the double-decker **7** with M = Eu could be selectively synthesised in a pseudo one-step procedure.[60] This synthetic protocol includes the generation of the SAT precursor **27** with Ln=Eu ([Por]Eu(acac)), which is used without purification to interact with phthalonitrile to form the desired double-decker complex by formation of the phthalocyanine in situ around the metal. This procedure was used as the starting point for the formation of the double decker complexes during the present work.

Stability of the macrocycle, test reaction

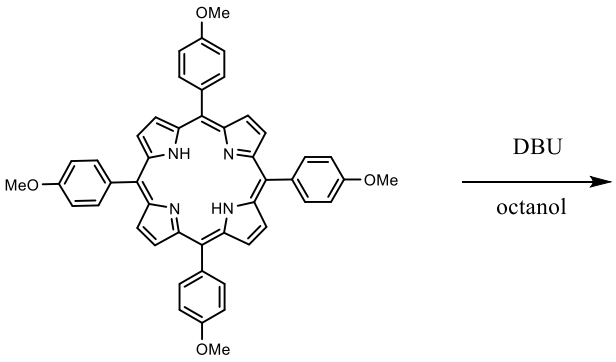

12

Scheme 16. Proposed stability check reaction.

For the synthesis of the desired complex superstructures bearing double deckers, the stability of the multicromophore array was tested under the conditions needed for the formation of the double deckers. We therefore performed a test reaction by refluxing porphyrin **12** under the presence of DBU in octanol (scheme 16) to see if some decomposition or side reaction is observed and therefore, check the stability of the ether bond under these conditions. To do so, 20 mg of **12** was subjected to the standard procedure. After 24 h under reflux, the crude mixture was then checked by MALDI-tof MS observing a single sharp signal corresponding to the starting material (734.44 m/z). Then after precipitating the crude with MeOH, 18 mg of the porphyrin **12** were recovered unreacted. There was no evidence of exchange between the methoxy group and octanol.

Almost a quantitative amount of starting material could be recovered after the reaction time. This result allowed us to think that the future multicromophore array should then be stable enough under the harsh conditions needed for the formation of the double deckers directly over the superstructure. Once the stability of the array was tested, the synthesis of double deckers can be explored.

4.1.8.1. General synthesis of double deckers via phthalonitrile 29

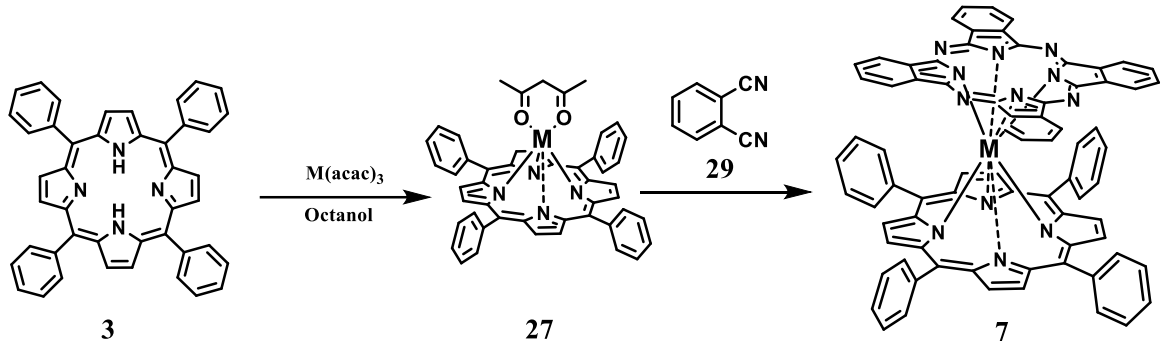

Scheme 17. Representation of the procedure for the synthesis of heteroleptic double deckers **7.**

In a modified procedure[60] for the formation of double deckers **7**, a mixture of free porphyrin **3** and $[M(acac)_3]\cdot nH_2O$ in n-octanol was refluxed under a slow stream of nitrogen. The progress of the reaction was monitored by analysing aliquots from the reaction by UV-vis spectroscopy and the reaction stopped when no more changes were observed in the Q-region of the spectra (500 - 750 nm). After 4–6 h, depending on the metal salt, the transformation to the SAT complex **27** was essentially completed. Then phthalonitrile **29** and DBU were added to the reaction and the mixture left refluxing overnight. Then, the reaction was cooled down and the crude mixture precipitated with MeOH. The resultant crude solids were purified by column chromatography on neutral alumina and recrystallisation to obtain analytically pure double deckers **7**, in 17 % yield (M=Dy) and 70 % yield (M=La).

4.1.8.2. General synthesis of double deckers via phthalocyanine 19

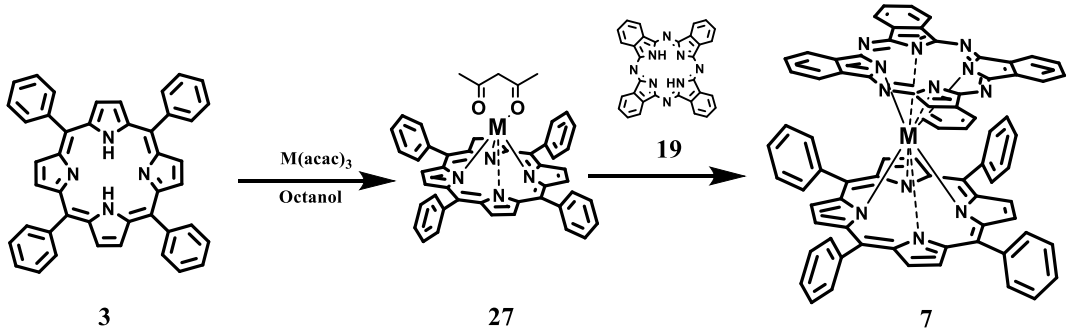

Scheme 18. Representation of the procedure for the synthesis of **7** via Pc **19.**

A different procedure was then attempted to try to improve the yield for the formation of the desired double deckers. The main impurity observed during the formation of double deckers via the phthalonitrile was phthalocyanine homoleptic double decker. An attempt to decrease the formation of this side product was performed by using previously synthesised Pc **19** instead of phthalonitrile **29**. The rest of the reaction conditions remained the same. When the reaction was completed in the same two steps one pot conditions, the crude mixture was precipitated with MeOH and the crude solids obtained were purified by column chromatography. In this case, the desired double decker was also obtained and the yield increased slightly but only traces of phthalocyanine double decker were observed.

Both methodologies afforded the desired double deckers **7** in high yields and the reactions could be performed in gram scale. In the case of the reaction via phthalonitrile **29**, homoleptic double decker was obtained as side product from the reaction while in the reaction via the previously synthesised phthalocyanine **19,** this side product was only observed as traces making the purification process slightly easier. Also, a slightly higher yield was observed for the formation of double deckers via phthalocyanine. On the other hand, the second method requires the synthesis of the phthalocyanine **19** from phthalonitrile **29** which results in a lower overall yield for the desired products. The reaction via the phthalonitrile was therefore preferred from now on for the formation of double deckers **7**.

4.1.8.3. NMR analysis of double deckers

Due to the magnetic properties of the metal, NMR spectrum of the dysprosium double decker complex could not be obtained. On the other hand, UV-vis and MALDI-tof MS were in fully accordance with the literature. In the case of lanthanum, previous studies on the analysis of double deckers by NMR spectroscopy were previously reported.[75,79,80] Therefore, only lanthanum double deckers could be analysed by ^{1}H NMR spectroscopy.

The presence of Pc **19** as π-radical anion ($Pc^{\cdot -}$) in these type of complexes are well known.[75,81] Due to the presence of this unpaired electron, these complexes, like other analogues, are usually NMR silent or broad. We employed the strategy developed by L'Her[81] using hydrazine hydrate as the reducing agent to generate the monoanionic $([TPP]La[Pc])^{-}$ or protonated ([TPP]LaH[Pc]) species (figure 17), in which both macrocycles become diamagnetic. We were able to obtain satisfactory ^{1}H NMR spectroscopic data for the reduced form of the lanthanum double deckers. The NMR spectrums were produced by dissolving complex **32** in d-DMSO and then adding 1 drop of hydrazine hydrate to the NMR tube to form the reduced diamagnetic complex and therefore obtaining a clean ^{1}H-NMR spectrum as shown in figure 17 for the same NMR tube before and after the treatment with hydrazine.

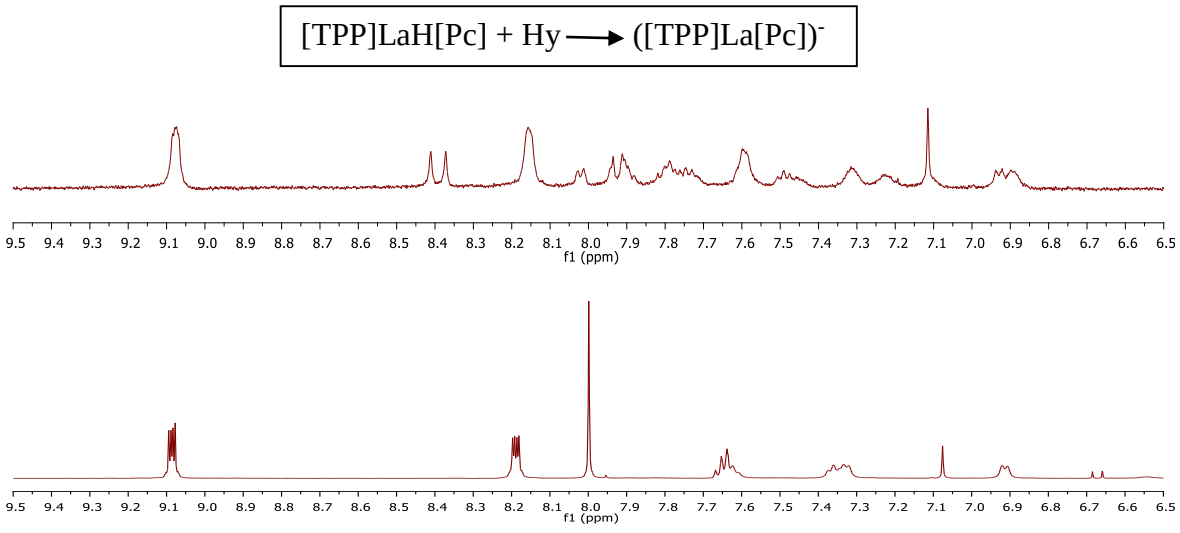

Figure 17. NMR analysis of La[TPP][Pc] **32** before (above) and after (below) the addition of hydrazine hydrate.

As can be seen in the ^{1}H NMR spectra, the phthalocyanine peaks can be observed at 9.1 and 8.2 ppm. The porphyrin peaks can be observed at 7.65, 7.35 and 6.9 ppm

corresponding to the phenyl aromatic protons and a singlet at 8.0 ppm corresponding to the 8 pyrrolic protons.

4.2 Multiporphyrin arrays

There are some examples of different multichromophore arrays where porphyrins or phthalocyanines have been used for constructing molecular devices.[34-36,82] For example, Anderson's group from Oxford developed a controlled synthesis of several multiporphyrin nano-rings using a Vernier template-driven synthesis.[36] In this case, a synthetic template is used for the controlled synthesis of a 12-porphyrin nano-ring using porphyrin metal to template interactions (figure 18).

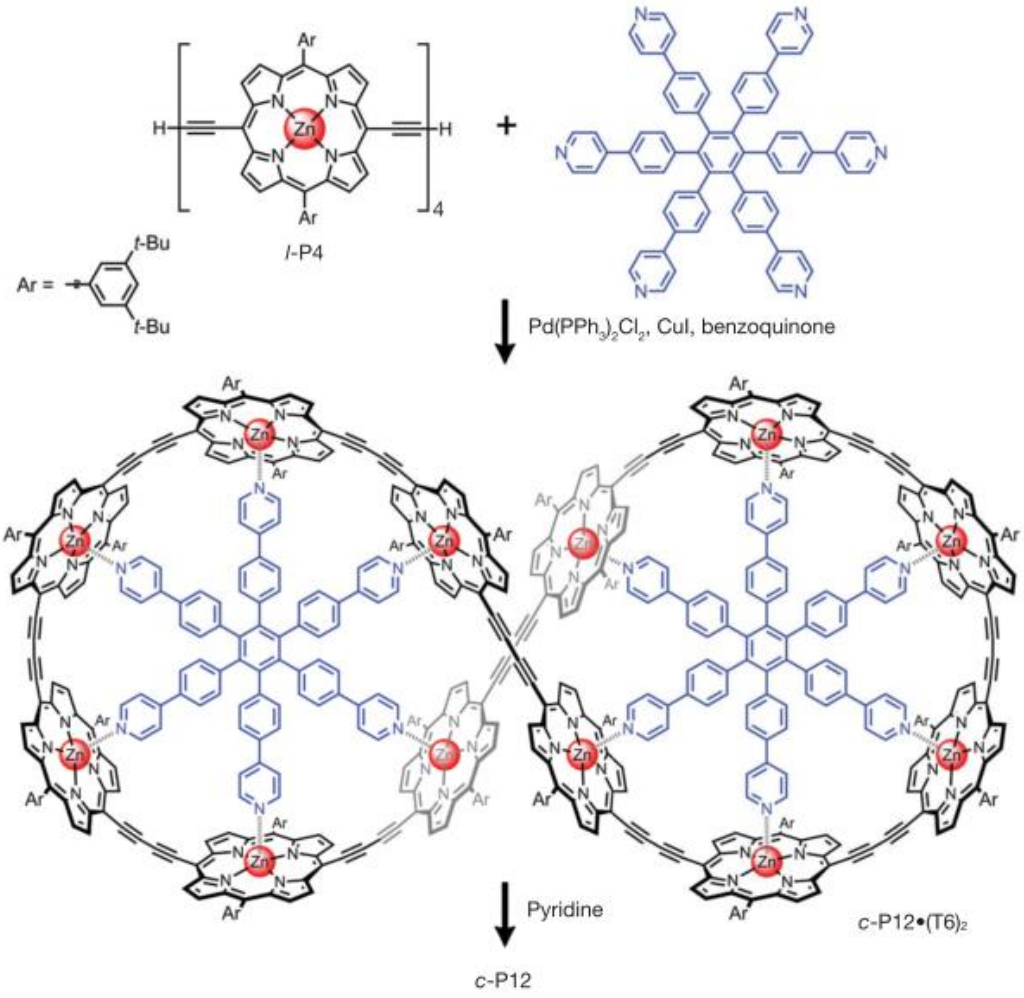

Figure 18. Vernier template- synthesis of a porphyrin nano-ring.[36]

Another good example is the approach developed by Lindsey where phenylacetylene groups are used as linkers for the construction of various multichromophore arrays using porphyrins and phthalocyanines (figure 19) for application in photodynamic processes.[35] Here, it is worth noticing that differentiation is achieved between the peripheral and central units, each having metal-free or metallated chromophores. This was achieved by the use of metallation processes early in the synthesis. Then, the different metal or metal-free units were coupled together to construct the array with metal and metal/free sites selectively. All remaining metal-free units were then metallated identically in the last step of the synthesis.

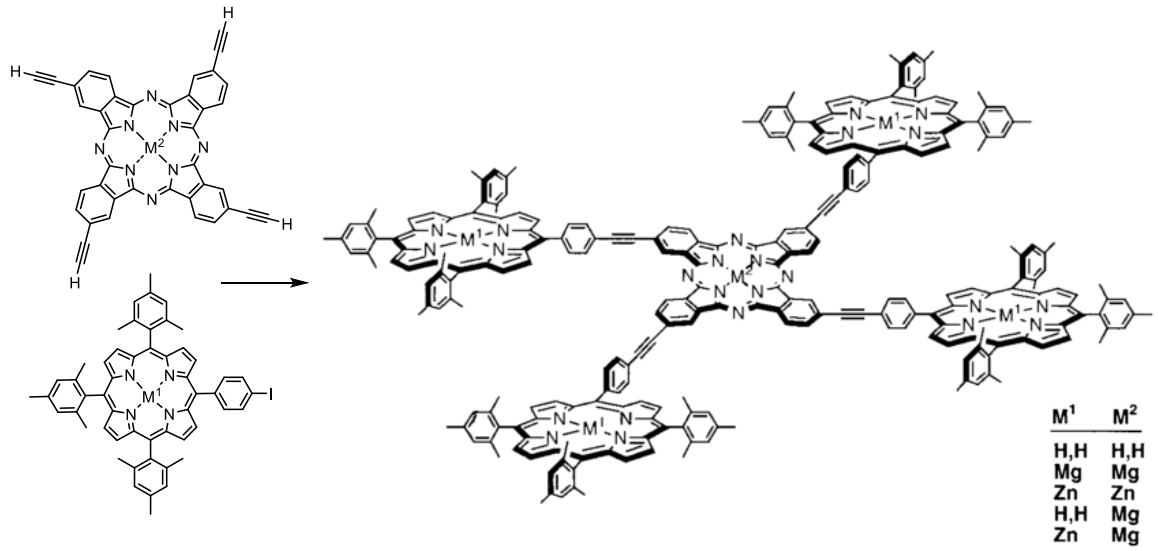

Figure 19. Multiporphyrin arrays using phenylacetylene bridges.[35]

Another example is the work developed by S. Ogi[1] where two different molecular rotors were interlocked into a bevel-gear-shaped rotor (figure 20). This structure consists of a lanthanum double decker (red) and a porphyrinatorhodium(III)-based rotor (blue). This provided two different rotational activities in the system.

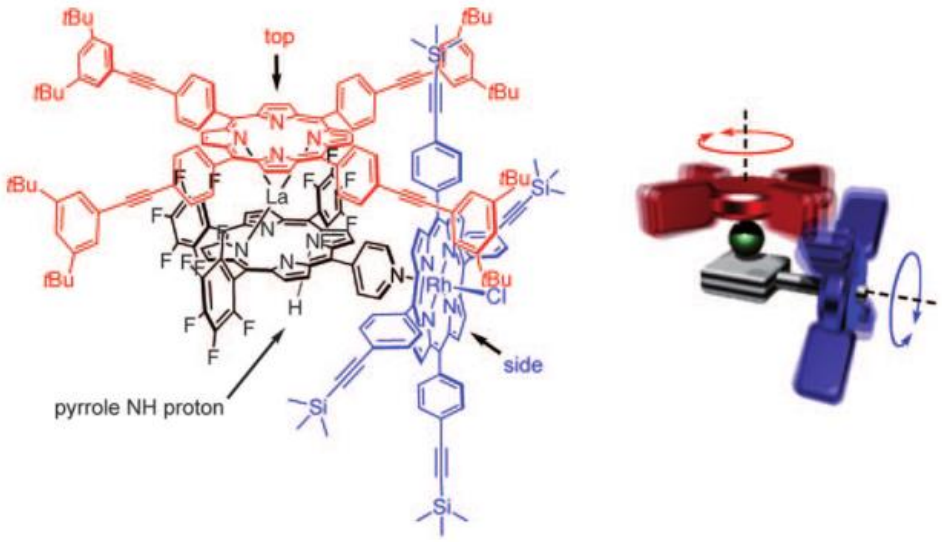

Figure 20. Bevel-gear-shaped rotor developed by S. Ogi et al.[1]

In order to achieve the overall goal, a straightforward synthesis of substructures comprising porphyrins/phthalocyanines around a complementary central unit was required. Porphyrin building blocks were selected, and the key challenge was therefore to devise a strategy that enabled control over the different metal (or metal-free) centres of the core and/or peripheral units. A representative target, **33**, is shown in figure 21. This structure would form the core of a molecular machine. The peripheral units will be elaborated with the face-to-face assemblies, while the central metalloporphyrin will be used for binding to a surface.

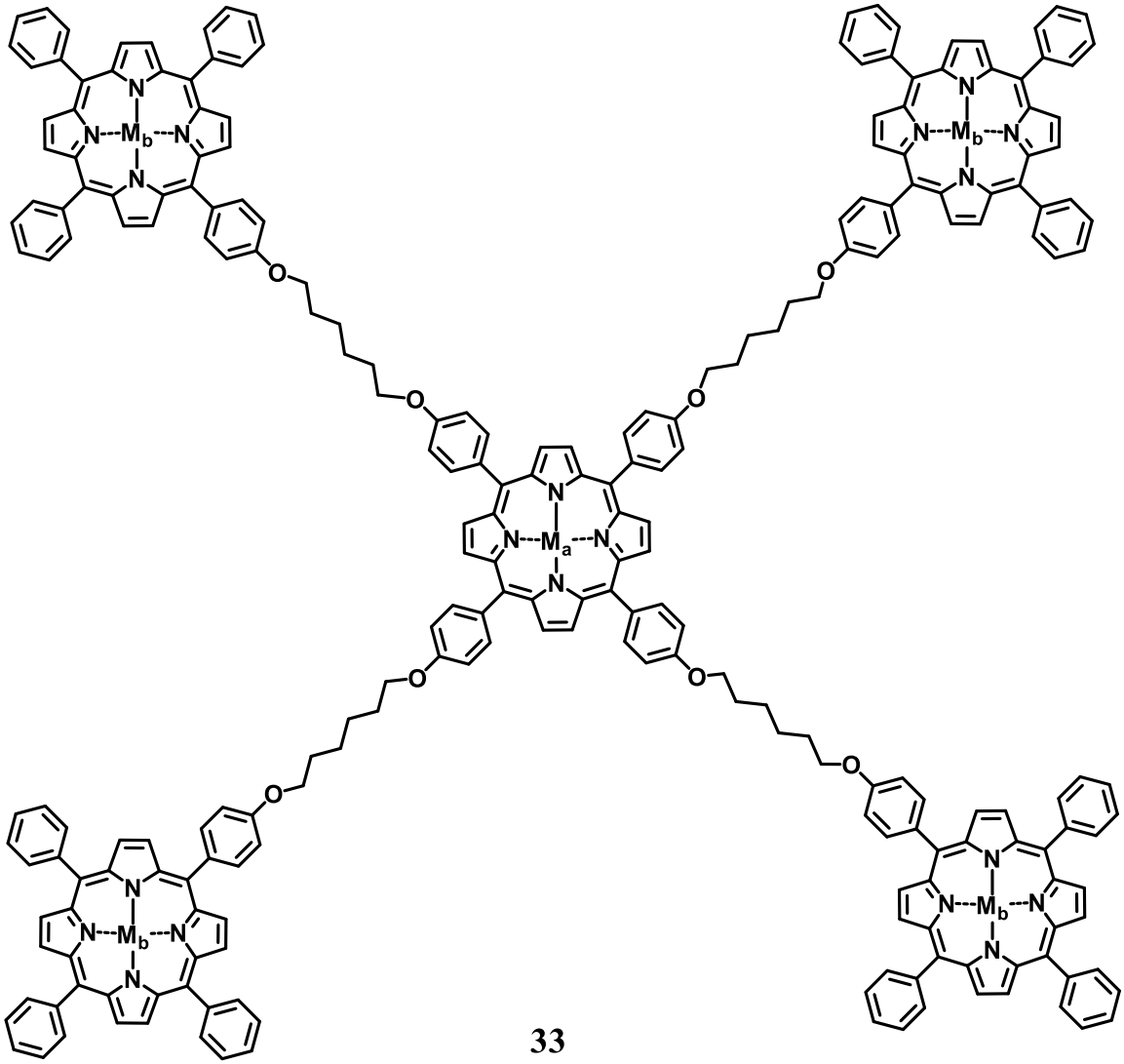

33

Figure 21. Designed array **33** bearing different metals in the peripheral (M_b) and central (M_a) positions.

Multiporphyrin **33** shows the peripheral porphyrin units linked to the central core via flexible spacers. These spacers were planned to be aliphatic chains (between 5-10 carbons long). They allow free movement and are expected to combine ease of synthesis with good solubility of the products. Intermediate hexane chains were initially selected.

For the first synthetic optimisations, metal-free porphyrins were used in conjunction with zinc metallated porphyrins. This allowed us to optimise the methodology for the synthesis of the multiporphyrin arrays **33**, where M_a or M_b were Zn or H_2 respectively. Zinc was chosen for this analysis because of its high affinity with porphyrins as well as lack of reactivity when inserted into porphyrins. [22,31,34-36] This way it can not only be proven that

different metals can be successfully inserted into the structure but some further reactions could be explored without having other possible reactive positions.

4.2.1. Synthesis of porphyrin building blocks

Analysing synthetic strategies, the main structure can be broken down into two different porphyrin precursors as represented in scheme 21. The peripheral porphyrin units are unsymmetrically substituted and the central are symmetrical. Therefore, the first challenge identified was the preparation, in reasonable quantity, of unsymmetrically substituted metal-free and zinc metallated porphyrin building blocks. Our ideal target would be easy to synthesise and isolate, leading to selection of monohydroxyporphyrins **35** or **40**. We reasoned that this peripheral unit would offer various approaches to attachment to the core, most simply through alkyl linkers (ethers).

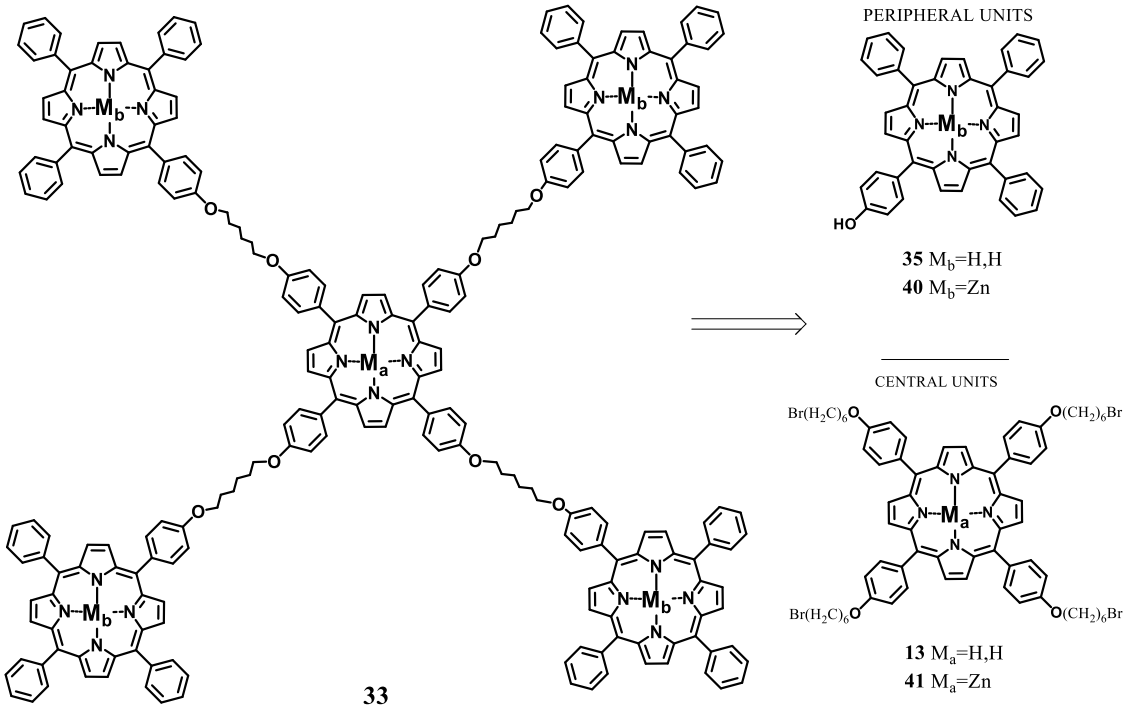

Scheme 19. Designed array **33** bearing different metals in the peripheral (M_b) and central (M_a) positions.

This peripheral porphyrin unit was synthesised using a modified version of Adler's methodology[42] using a statistical mixture of benzaldehydes as reported by Little et al.[83] In

our case, the multigram scale synthesis (scheme 20) employed a mixture of benzaldehyde **2** and 4-hydroxybenzaldehyde **14**. The mixture of aldehydes was refluxed in propionic acid and freshly distilled pyrrole was added dropwise to the refluxing mixture. After 30 min, the mixture was cooled down and the porphyrin mixture precipitated with methanol. The mixture of porphyrin products were filtered off, leaving the majority of side products in solution. Column chromatography of the porphyrin mixture gave monohydroxyporphyrin **34,** TPP-OH, in around 5 % yield after a recrystallisation from DCM/Methanol.

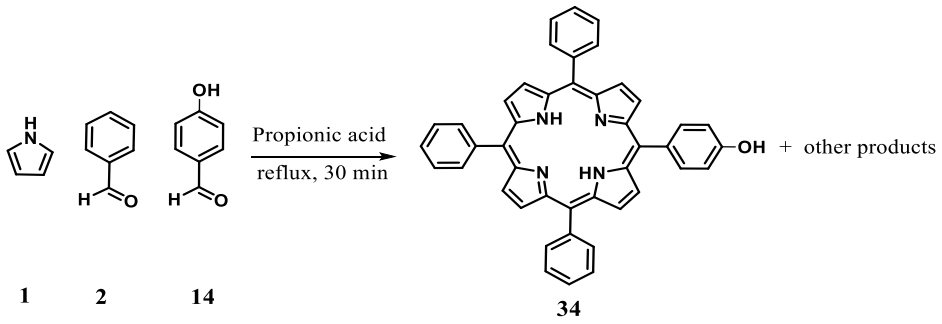

Scheme. 20. Synthesis of unsymmetrically substituted porphyrin **34**.

With the straightforward synthesis of TPP-OH in hand, attention was turned to the core porphyrin **13**. This porphyrin **13** consists of a TPP derivative functionalised with bromoalkyloxy groups on each of the phenyl *para*-positions. This porphyrin could be easily synthesised by alkylation of tetrakis-*p*-hydroxyphenylporphyrin **15**. In theory, this porphyrin **15** can be prepared simply by reaction between 4-hydroxybenzaldehyde **14** and pyrrole. However, in practice this approach is not convenient because the porphyrin does not precipitate from the reaction mixture and it is therefore isolated after workup alongside polypyrrole tars. Separation is difficult and tedious. Alternative routes were investigated:

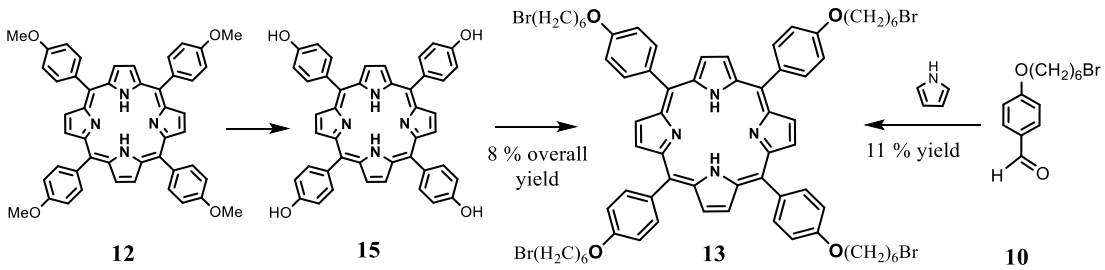

Scheme 21. Different methodologies followed for the synthesis of central tetraalkylated porphyrin **13**.

In the first route, 4-methoxybenzaldehyde **9** was condensated with pyrrole in refluxing propionic acid using previously described conditions. The symmetrical tetrakis-(4-methoxyphenyl)porphyrin **12** is easily isolated. Hydrolysis of the methyl ethers was achieved using a refluxing mixture of HBr/acetic acid or BBr_3.[84] Realkylation using an excess of dibromoalkane (1,6-dibromohexane was used in the first instance) gave the desired core porphyrin **13** with an overall yield of 8 %. Subsequently an alternative approach was preferred. 4-hydroxybenzaldehyde **9** was alkylated with an excess of dibromohexane to give the substituted benzaldehyde **10**. Condensation of **10** with pyrrole under standard conditions again yielded porphyrin **13** in 11 % yield. This second route afforded the desired porphyrin in a better yield and more convenient way therefore this was the preferred route for the synthesis of porphyrin **13**.

The prepared peripheral and central porphyrins were then metallated separately prior to coupling.

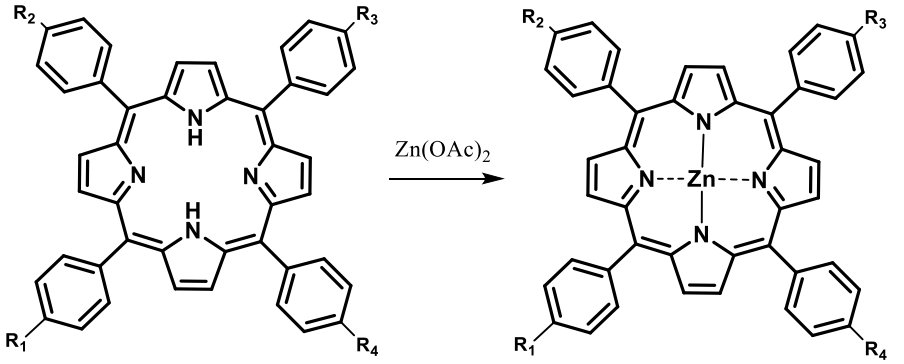

34 $R_1 = R_2 = R_3 = H$, $R_4 = OH$
13 $R_1 = R_2 = R_3 = R_4 = O(CH_2)_6Br$
15 $R_1 = R_2 = R_3 = R_4 = OH$

39 $R_1 = R_2 = R_3 = H$, $R_4 = OH$
40 $R_1 = R_2 = R_3 = R_4 = O(CH_2)_6Br$
41 $R_1 = R_2 = R_3 = R_4 = OH$

Scheme. 22. Zinc metallated tetraphenyl substituted porphyrin structures **39**-**41**.

Following typical metallation procedures[85] porphyrins **13**, **15** or **34** were heated in refluxing acetone in the presence of zinc acetate ($Zn(OAc)_2$) for 30 to 60 min. After completion, the solvent was evaporated and the crude solid extracted with DCM/H_2O, dried over $MgSO_4$ and concentrated to collect the pure product. Using this procedure, zinc hydroxyphenylporphyrin **39** ZnTPP-OH and zinc tetraalkoxyphenylporphyrin **40** $ZnT(OC_6Br)PP$ were obtained in near quantitative yield. On the other hand, zinc tetrakis(4-hydroxyphenyl)porphyrin **41** was isolated in 71 % yield.

4.2.2. Synthesis of multi-porphyrin arrays 35 (M_a=H,H M_b=Zn) and 36 (M_a=Zn, M_b=H,H)

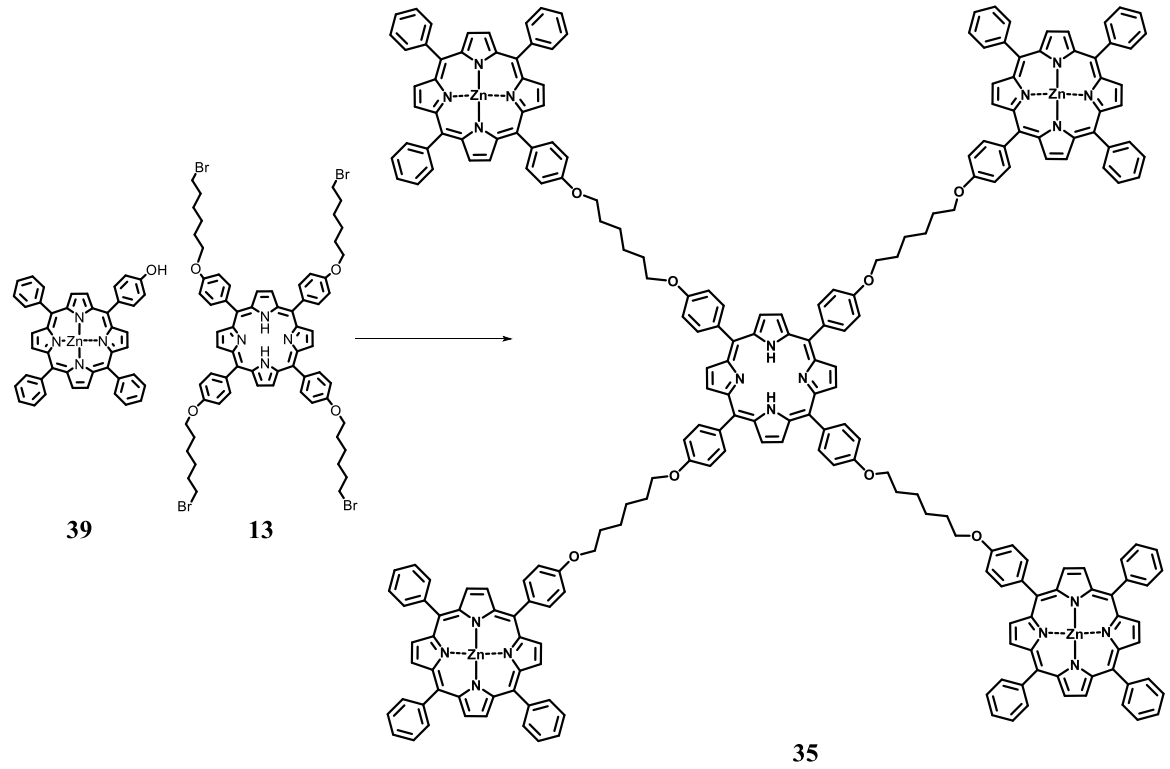

Scheme 23. Proposed starting materials **13** and **39** for the formation of multi-porphyrin array **35** having the peripheral porphyrin units protected with Zn.

Array **35** has zinc porphyrins on the periphery of a metal-free central porphyrin. In the first attempt, porphyrin **13** and the monohydroxylated porphyrin **39** were reacted in refluxing MEK with an excess of potassium carbonate. The reaction was followed by TLC and MALDI-tof MS but even after 7 days, no product formation was observed.

Monohydroxylated porphyrin **39** was reacted with tetrabromo porphyrin **13** using the same conditions as before but changing the solvent to DMF. After reacting at 100 °C for 4 days, the crude mixture was poured into water. The resultant purple solid was subjected to column chromatography followed by recrystallization to recover the desired multiporphyrin array **35** in a yield of 26 %.

Array **36**, on the other hand, has the reverse arrangement. A zinc porphyrin core surrounded by metal-free peripheral units. It was prepared following a similar procedure than that developed for the synthesis of analogue **35** employing TPP-OH **34** and zinc porphyrin **40**. In this case the yield of array **36** was 44 %.

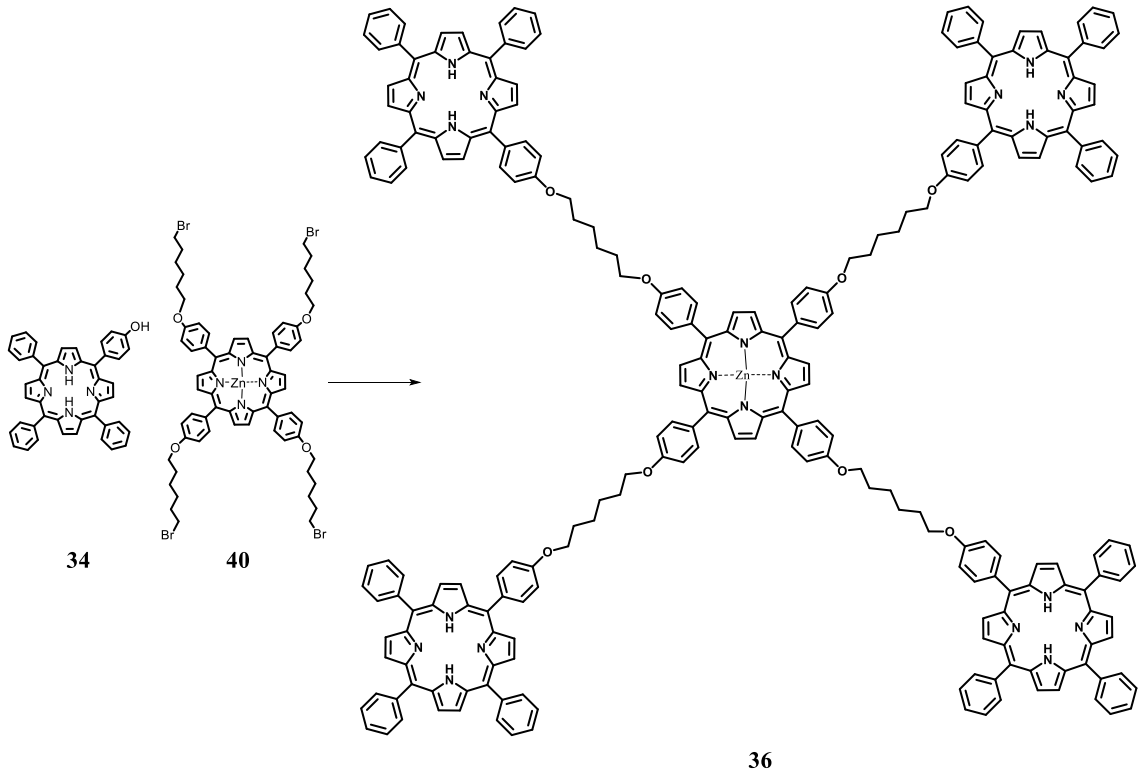

Scheme 24. Synthesis of multi-porphyrin array **36**.

Both multiporphyrin arrays were fully characterised by MALDI-tof MS, UV-vis and ^{1}H-NMR spectroscopies.

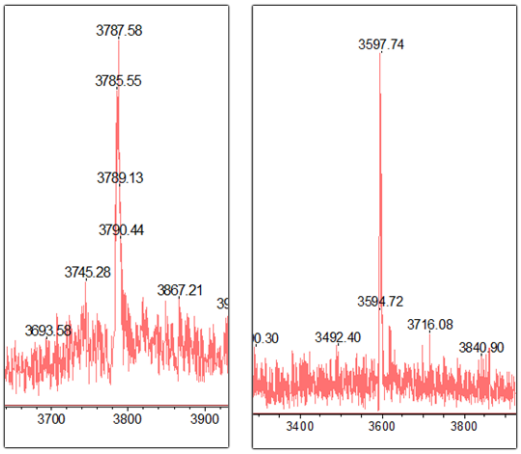

Figure 22. MALDI-tof MS of array **35** (m/z = 3787) and **36** (m/z = 3597).

UV-vis spectrum were obtained for both analogues (Figure 23). The Soret bands appear slightly shifted, at 415 cm^{-1} for array **35** and at 420 cm^{-1} for array **36**. Special attention can be put in the Q-region of the spectrum between 450 and 700 cm^{-1}. In this region, array **35** absorption pattern, resembles those of metallated porphyrins whereas array **36**, resembles those of metal-free porphyrins.

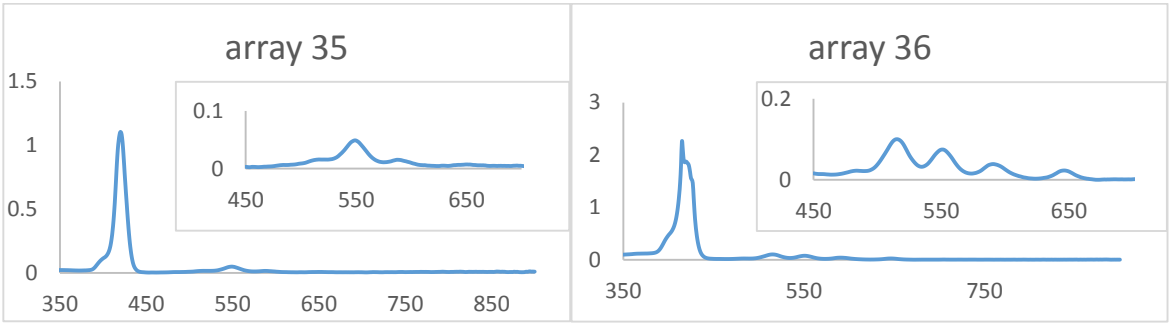

Figure 23. UV-vis spectrum obtained for arrays **35** and **36**.

Finally, ^{1}H NMR spectra were recorded for both arrays (figure 24). The region corresponding to the linking chains appears to be mostly symmetrical and gives similar signals for both compounds at around 4.3, 2.1 and 1.7 ppm. The very characteristic N*H* singlet at -2.7 ppm corresponding to the metal-free porphyrins is present in both analogues integrating for two protons in array **35** (metal-free central porphyrin) or for eight protons in array **36** (metal-free peripheral units). Finally, in array **35**, a singlet can be observed at 3.25 ppm corresponding to 12 protons that corresponds to a molecule of methanol (used as recrystallisation solvent) bonded to each one of the four zinc metals present.

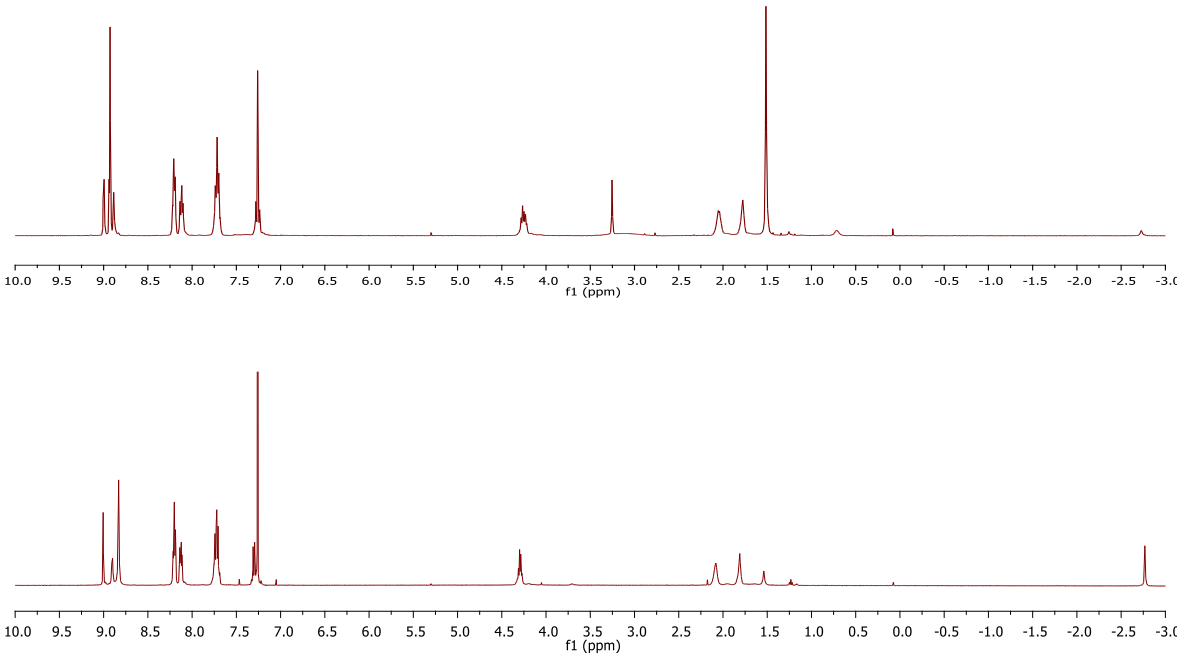

Figure 24. ^{1}H NMR spectrum of complex **35** (above) and **36** (below).

4.2.3. Synthesis of multi-porphyrin arrays for studies in surface attachment and/or multidecker formation

For the surface attachment of the molecular machines into surfaces, the possibility of using previously studied ruthenium chemistry[57,68] to act as fulcrum looks promising. Also, formation of sandwich-like structures in the peripheral porphyrins using ruthenium chemistry could be explored. With this in mind, previously synthesised arrays **35** and **36**, were further metallated using previously developed ruthenium chemistry.[35] By using this approach, multiporphyrin arrays with ruthenium/zinc in the peripheral or central positions could be selectively achieved in a straightforward manner. The aim was then to design a synthetic pathway two obtain the desired fully metallated analogues in the selected positions.

4.2.3.1. Synthesis of ruthenium multi-porphyrin array 37

The first analogue, metallated multi-porphyrin array **37**, (M_b=Zn, M_a=Ru) had zinc in the peripheral positions and ruthenium in the central position. It was synthesised by refluxing multiporphyrin array **35** in toluene in the presence of 1 equivalent of ruthenium dodecacarbonyl for 18 h. Then, the solvent was evaporated to dryness and the residue stirred in pyridine for 30 min. pyridine was then removed under vacuum to collect a dark purple solid containing the product **37**.

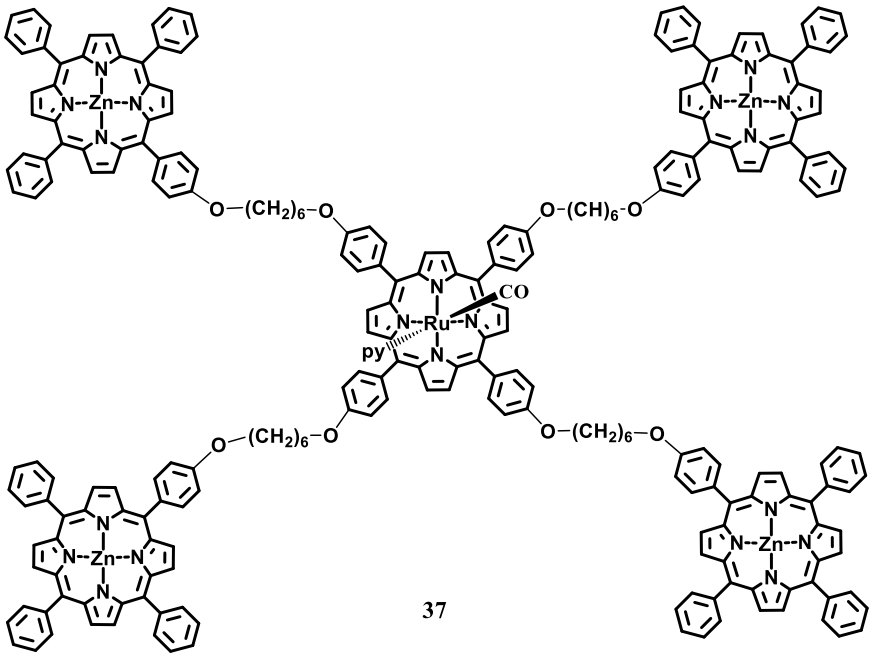

Figure 25. Structure of metallated multiporphyrin array **37** (linking chains omitted for clarity).

The resulting complex was then analysed by ^{1}H NMR spectroscopy and compared with the spectrum obtained for the starting material (figure 26).

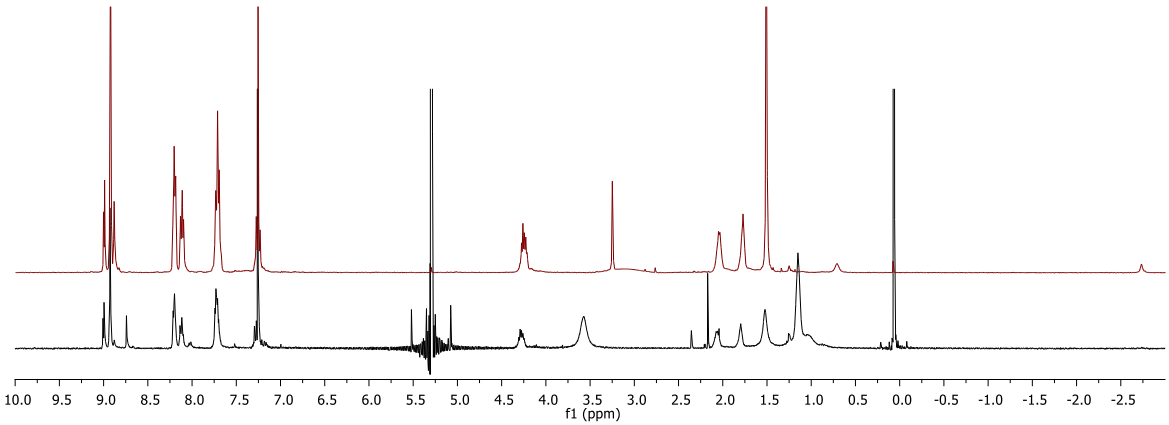

Figure 26. Comparison between starting material array **35** (red, top) and the ruthenium array **37** (black, below).

In this comparison, it can be seen that the signal at -2.7 ppm corresponding to the central metal-free N*H* porphyrin peaks is no longer present. This is proof that there was a metal insertion in the central position and no more free-porphyrin is present in the system. Finally, the presence of the ruthenium metal can also be observed in the IR spectrum, where the very characteristic signal for the CO group attached to the ruthenium appears at 1941 cm^{-1}. This signal is also in the same region as previously reported ruthenium complexes.[56,67,68] These results, proved that the chemistry developed for a simple model porphyrin can also be applied to more complex structures.

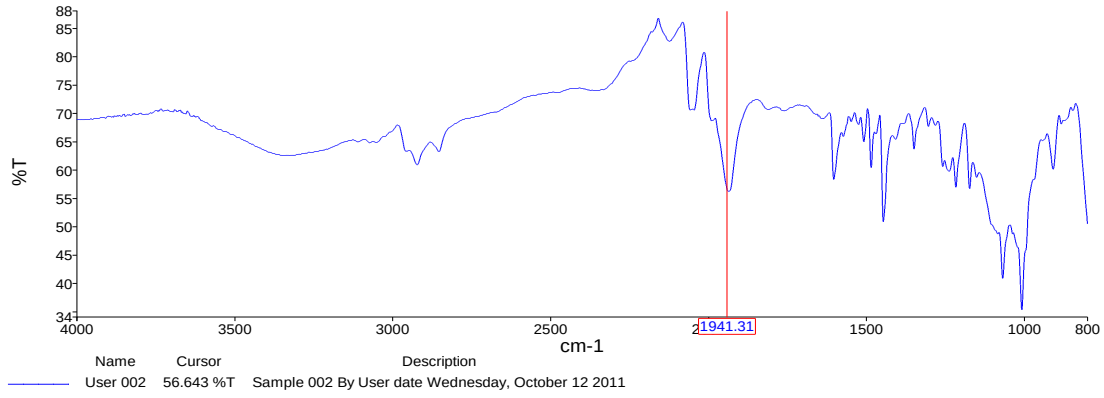

Figure 27. IR spectrum obtained for ruthenium array **37**.

4.2.3.2. Synthesis of ruthenium metallated multi-porphyrin array 38

The second analogue, metallated multi-porphyrin array **38**, (M_b=Ru, M_a=Zn) had ruthenium in the peripheral positions and zinc in the central position.

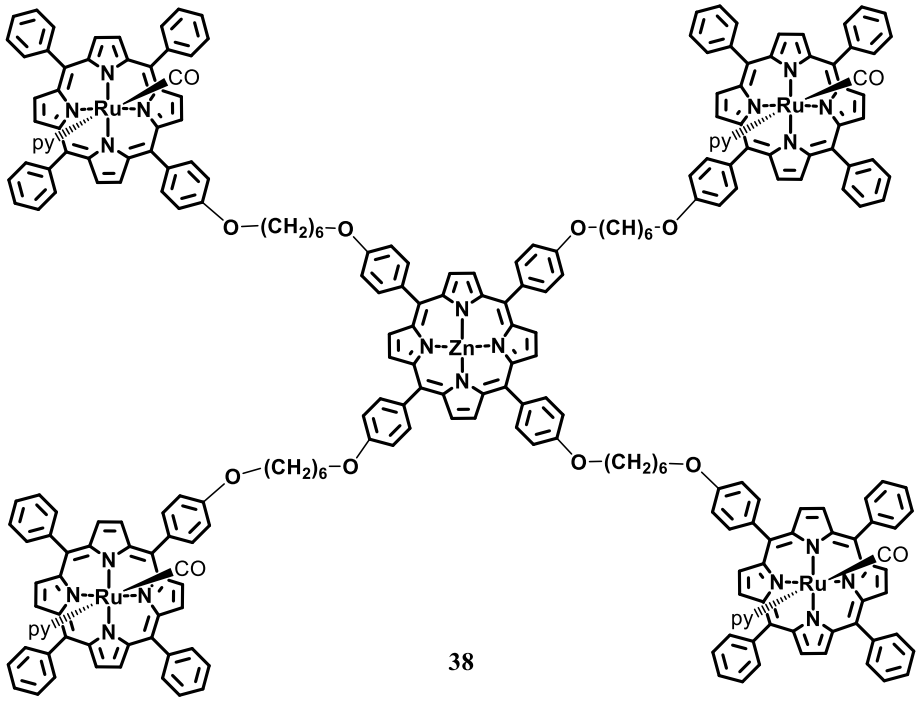

Figure 28. Proposed structure of metallated multiporphyrin array **38** (linking chains omitted for clarity).

Array **36** was refluxed in toluene with an excess of ruthenium to obtain the four desired additions. When the addition was completed, the crude mixture was stirred in pyridine for 30 min to attach the pyridine to the metallated system. After the reaction and purification, the mixture was checked first by ^{1}H NMR spectroscopy and the N*H* peak corresponding to the free porphyrin at -2.7 ppm was not observed in any case proving the absence of metal-free porphyrins in the product. Also, IR spectra of the product was obtained (figure 29), observing the characteristic peak at 1949.75 cm^{-1} similar to analogue **37**. However, in this case, other peaks at 2061.84 and 1996.20 cm^{-1} were also observed.

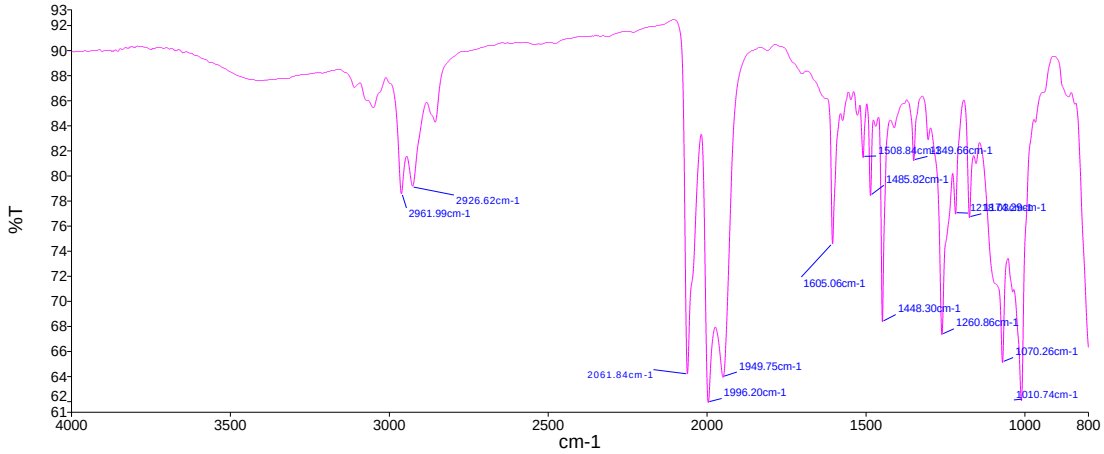

Figure 29. IR spectrum obtained for the ruthenium array **38**.

The complex was dissolved in DCM and attached to a balloon of CO and stirred overnight in order to ensure complete CO complexation. However, after this treatment, no sharp signals were observed on the ^{1}H NMR spectrum. MALDI-tof MS, gave a signal at m/z = 4585.06 that matches the addition of two pyridine ions to the targeted array $[M(py)_2]^+$.

Although it was then clear that selective metallation could be achieved in these multiporphyrin arrays, the multiple introduction of ruthenium was unsatisfactory. Therefore, we turned our attention to alternative synthesis of multideckers.

4.2.4 Synthesis of multidecker porphyrin arrays using lanthanides

The next set of experiments that were studied involved the possible formation of multiporphyrin arrays using functionalized lanthanide double deckers as building blocks for the construction of the desired molecular machines.

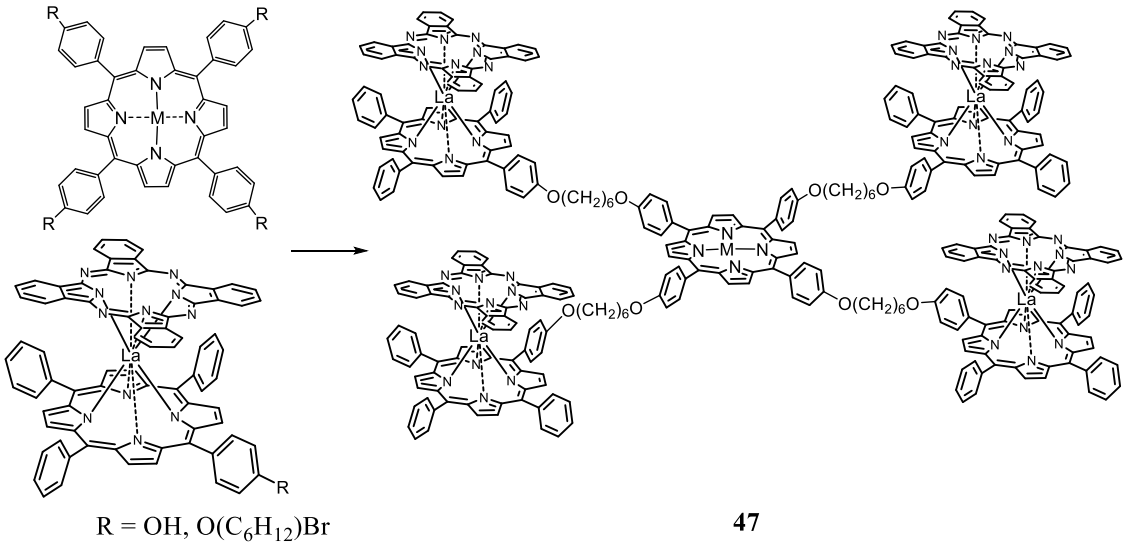

Scheme 25. Designed synthesis of molecular machine **43**.

We reasoned that use of pre-synthesised double deckers as starting materials should be an easy way of introducing the desired free rotating units into the molecular machines. Phthalocyanine **19** was chosen as the complementary unit to be attached to the peripheral positions of the arrays. These positions therefore comprises a heteroleptic sandwich complex.

4.2.4.1 Synthesis of multi-porphyrin double decker array via functionalised heteroleptic double deckers

The first, most straightforward approach to assemblies like **43** involved the reaction between hydroxylated lanthanide double decker **42** with symmetrically substituted porphyrin **40**.

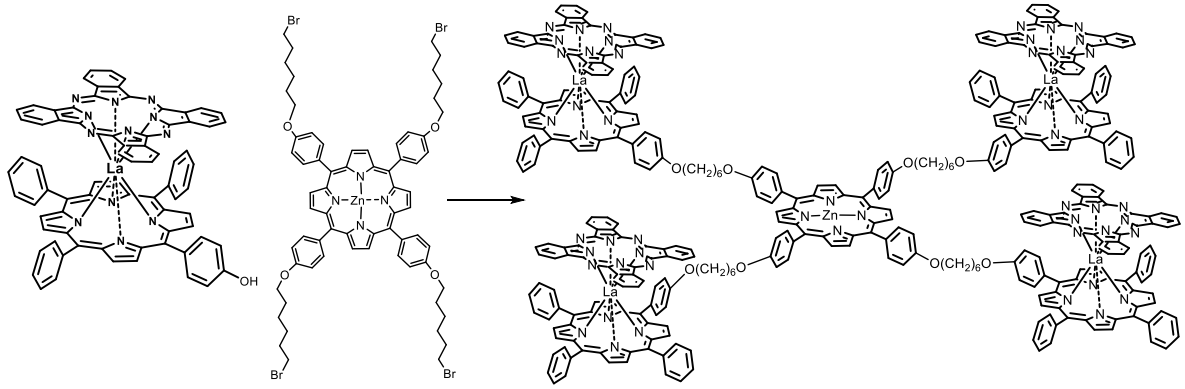

Scheme 26. Proposed general synthesis for the formation of **43**.

The synthesis of this double decker complex **40** was achieved using the general method for the formation of porphyrin-phthalocyanine heteroleptic double decker via phthalonitrile using porphyrin **34** as starting material (scheme 27).[60] TPP-OH **34** and lanthanum acetylacetonate were refluxed in octanol for 6 h followed by addition of phthalonitrile and a catalytic amount of DBU. The resultant mixture was then refluxed overnight and then, the reaction was cooled down and precipitated with MeOH. The resultant crude solids were purified by column chromatography in neutral alumina and recrystallisation to obtain analytically pure double decker **42** in 72 % yield.

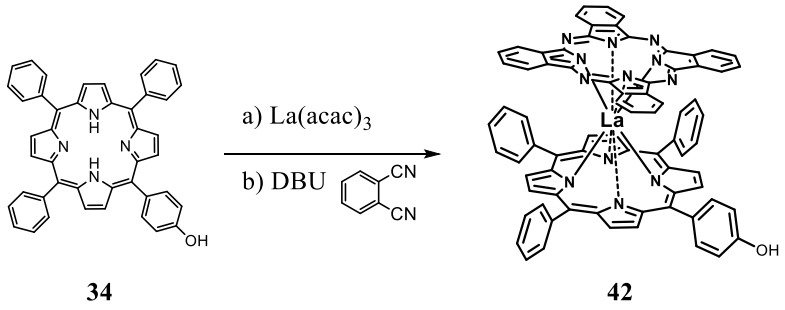

Scheme 27. Synthesis of hydroxylated double decker **42**.

This functionalized double decker **42** was then mixed with zinc porphyrin **40** and potassium carbonate and left stirring at 60 ˚C in DMF following the same conditions as previously optimized for the formation of the multiporphyrin arrays **35** and **36**. After five days reacting, the mixture was precipitated with distilled water and the crude solids obtained were checked by MALDI-tof MS. No peaks corresponding to the desired product were observed. The only peaks observed corresponded to unreacted starting materials double decker **42** (1281.97 m/z) and zinc porphyrin **40** (1394.04 m/z) that remained unreacted. From this result, it could be concluded that there was no reaction occurring under this conditions. Then, the reactivity of the double decker **42** was examined under a simple reaction by refluxing it with 1,10-dibromodecane in MEK as test reaction (scheme 28) in order to obtain the alkylated double decker **44**.

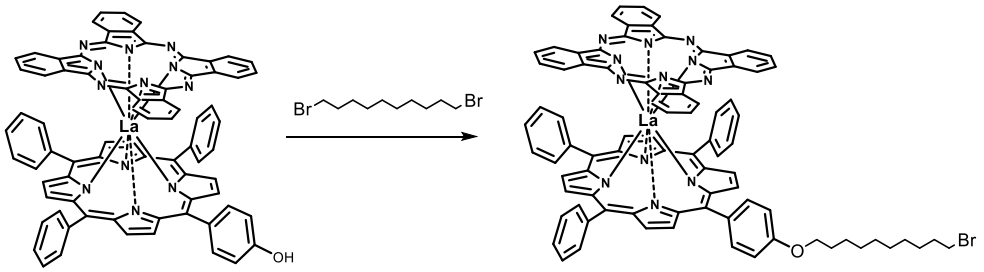

42 **44**

Scheme 28. Test reaction.

The solids obtained after the overnight reflux of the double decker **42** and 1,10-dibromodecane obtained after precipitation with methanol were checked by MALDI-tof MS to observe only a peak corresponding to the unreacted double decker **42** (1280.87 m/z) and a very small peak (12% relative intensity) at 1346.53 m/z that correspond to the addition of a molecule of solvent (MEK) to the starting material. The reaction was then purified by column chromatography over silica gel to obtain a single fraction containing the unreacted starting material **42** and traces of another small fraction that by MALDI-tof MS shows peaks corresponding to double decker **42** 1280.93 m/z (100%) and 1346.53m/z (45%). NMR spectrum was obtained for the mixture but no pure material could be observed even after the addition of hydrazine hydrate to the NMR tube. With this results in mind, it could be then concluded that the double decker **42** is not reactive against alkylation as around 95 % of the material was recovered after the test reaction.

Other reactions were tested in different solvents but any encouraging results were obtained so far, as using DMF instead of MEK leaded to decomposition of the double decker **42** after 3 days without any formation of product **44**. A final trial was attempted using toluene as solvent but also decomposition of the double decker was observed. Therefore, the pathway for the construction of molecular machines from functionalised double deckers was abandoned.

4.2.4.2 Synthesis of multi-porphyrin double decker array via double decker in situ formation

A new methodology was the formation of the double deckers in situ on the metal-free peripheral units of the previously synthesised multiporphyrin array **36** (scheme 29). In this case, the central core porphyrin was protected with zinc to avoid reactions on this position.

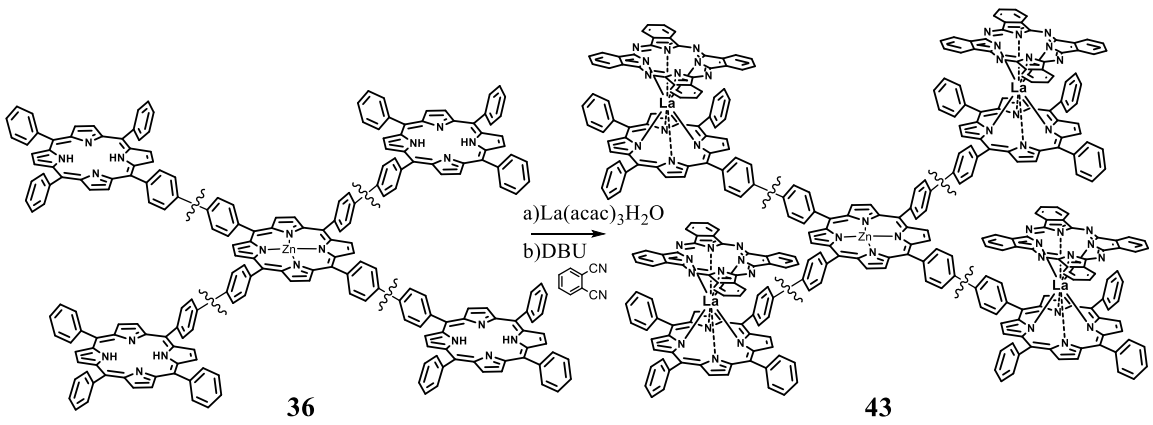

Scheme 29. Proposed synthesis of molecular double decker array **43** (linking units omitted for clarity.

Previously synthesised multi-porphyrin array **36** was refluxed in octanol with the lanthanide complex $[La(acac)_3]\cdot nH_2O$ followed by addition of phthalonitrile and DBU. When the reaction was completed, it was cooled down and solvent removed under vacuum to obtain a purple solid. This solid was then checked by TLC and MALDI-tof MS observing a very complicated outcome of multiple spots on TLC and high mass peaks by MALDI-tof MS. None of the peaks observed corresponded to the desired product **43** of mass 6191.26 m/z. Some possible side reactions were the formation of Pc double deckers (observed in MALDI-tof MS) leading to less metal ions being available for the formation of the product

leading to partially metallated compounds. The reaction was then repeated with more lanthanum metal equivalents (8 eq) to try to avoid the lack of metallation centres in the porphyrin due to possible side reactions. Unfortunately, the same outcome was observed being the analysis and purifications very difficult.

Another test reaction was attempted by reaction of the multi-porphyrin array **36** with Pc **19** and the same lanthanum complex to try to avoid side reactions formed during the formation of the Pc under this conditions. Array **36** was refluxed in octanol in the presence of 8 eq of lanthanum acetyl acetonate. Then, Pc **19** was added and everything left refluxing overnight. Then, the octanol was removed by distillation and the resultant solids analysed by MALDI-tof MS observing a very complicated MALDI-tof MS (figure 30). No expected products were observed but also, no starting material remained in the crude mixture after the reaction. Finally, the formation of various unidentified higher mass structures were observed (corresponding molecular weights higher than 3500 m/z) but could not be purified or analysed by other spectroscopic techniques.

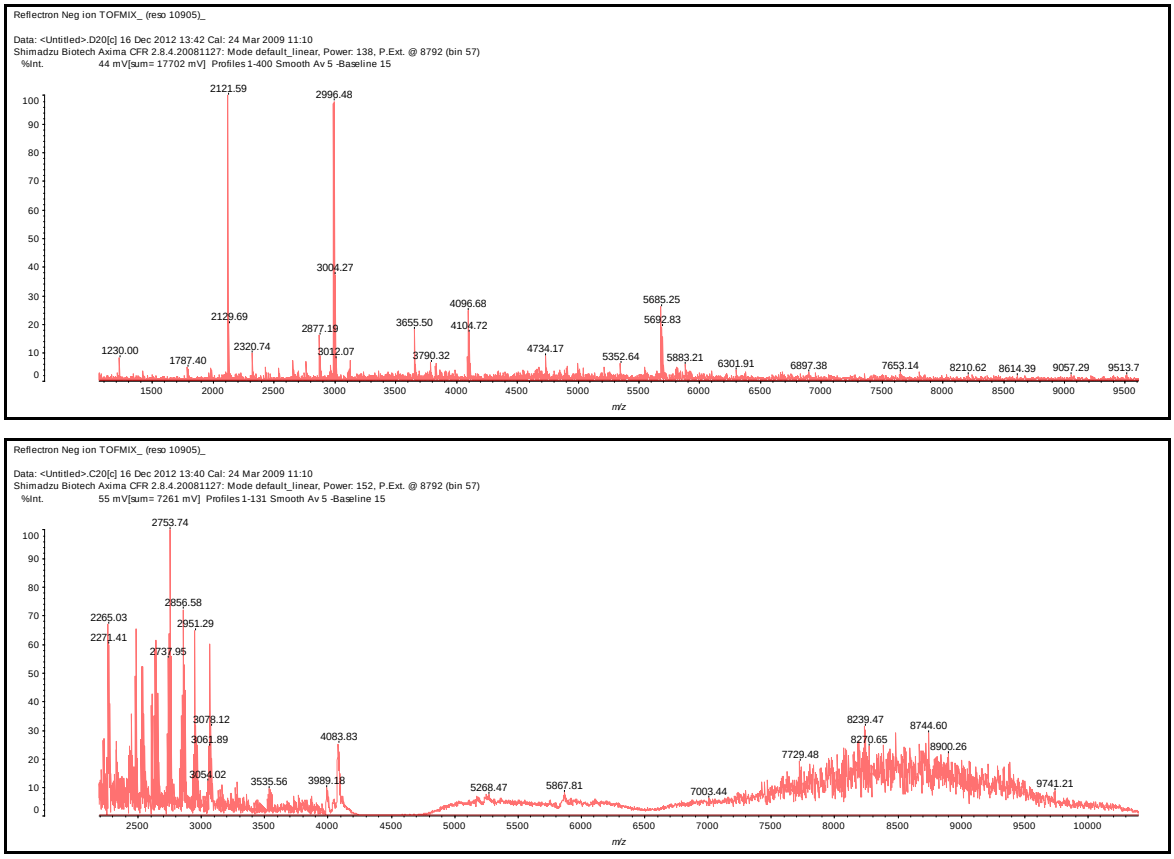

Figure 30: MALDI-tof MS spectrum of the outcome for the formation of **43** with low and high laser power.

Clearly, no product was obtained using this methodology. Also, the analysis of all the different sub-products was proven difficult as there were many side products and intermediates that could be obtained such as half sandwich complexes, multiple deckers, etc.

4.2.5. Conclusions

Different multichromophore arrays having different metals in the peripheral and central positions have been successfully synthesised. By using previously metallated porphyrins for the construction of the arrays, several analogues could be synthesised following an optimised general methodology. This process allowed the formation of arrays with different metal and or metal-free selected positions that could be easily designed depending on the needs.

On the other hand, the desired sandwich complexes with lanthanides could not be obtained during this chapter. This was due to lack of reactivity of functionalised double deckers.

The chromophore arrays with metal-free positions **35** and **36** shows favourable reactivity for further metal insertion. This process was also proven by the insertion of ruthenium in both peripheral and central positions separately and selectively. Equally important, this ruthenium complexes shows great affinity for pyridine derivatives. This affinity could be used for the future formation of high complexity molecular machines for example using pyrazine derivatives as linkers between different chromophores. Finally, further surface studies could be attempted with multiporphyrin array **37** where ruthenium metal was inserted in the central position using pyridine-functionalised surfaces.

4.3. Porphyrin dyads, reaction models

For the study of the formation of double deckers on multi-porphyrin arrays, simplified porphyrin dyads were selected to act as simple models of the components present in our multiporphyrin array **36** (scheme 30). This dyads consists of two porphyrins linked together by long alkyl chains. This will allow us to understand the behaviour of the porphyrin framework in a more controlled manner.

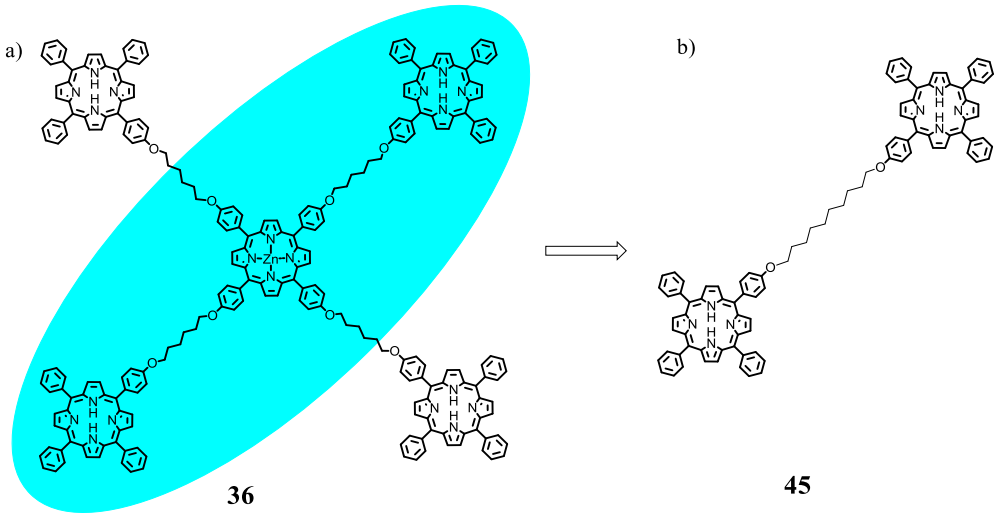

Scheme 30. Representation of the region in **36** (light blue highlighted) that served as model for the design of the porphyrin dyad **45** to be used as model.

Once the porphyrin dyads are synthesised, the next step will be to form double deckers on each side of them following the optimised conditions for the formation of double deckers that were developed in previous chapters (scheme 31). Depending on the observations, we reasoned that the same principles could then be applied to the formation of double decker complexes on the peripheral positions of the previously synthesised multi-porphyrin array **36** (scheme 30a) to form the desired molecular machines.

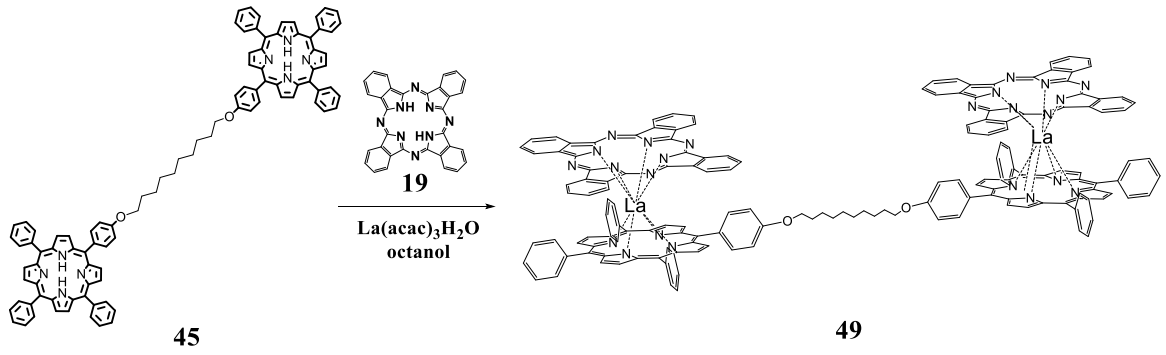

Scheme 31. Proposed model **49** synthesis.

4.3.1. Formation of model porphyrin dyads

In order to keep the synthesis of porphyrin dyads as straightforward as possible, previously synthesised porphyrin **34** was synthesised following the same known procedures[86,87] previously developed for the synthesis of multiporphyrin arrays. Different dyads with different chain lengths were synthesised to study the possible influence of the distance between the porphyrins on reaction outcome and reactivity. In the first approach, 1-*n*-dibromoalkanes (n=10 and 12) were used as linkers for the formation of the dyads using the reaction conditions shown below:

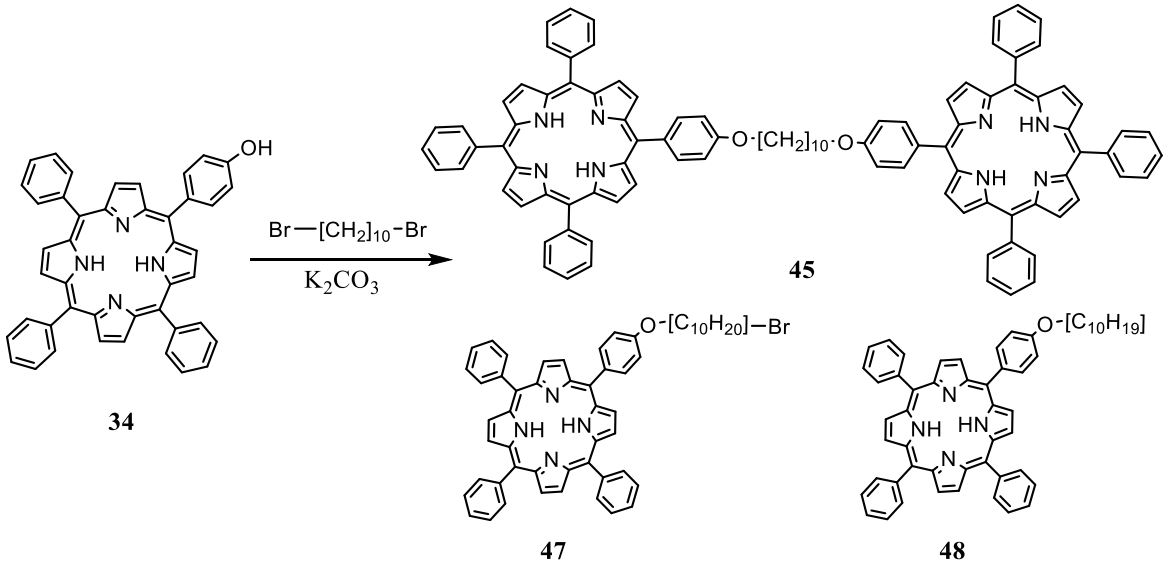

Scheme 32. Proposed synthetic pathway example for the formation of porphyrin dyad **45** using dibromodecane with expected side products **47** and **48**.

TPP-OH **34** and the appropriate dibromoalkane were reacted in DMF at 60 ˚C in the presence of potassium carbonate. After elimination of the solvent and column chromatography, the desired porphyrin dyad was obtained albeit in low yield. The production of large amounts of monosubstituted starting material **47** (TPP-$OC_{10}Br$) and its elimination side product **48** (TPP-$OC_{10}H_{19}$) as well as unreacted starting material **34** (TPP-OH) were observed.

Due to this low product yield, the tedious elimination of the DMF and the significant amounts of side products obtained, the reaction was then optimised by a small screening of the most commonly used solvents, inorganic salts, catalysts and purification procedures found in the literature for this particular type of reaction.

4.3.1.1. Optimisation of the reaction conditions for the formation of C_{10} porphyrin dyad 45

Porphyrin **34** and 1,10-dibromodecane were reacted in DMF at 60 ˚C with an excess of potassium carbonate. The reaction times were checked by taking aliquots from the reaction until completion. Full consumption of starting material was not observed even after 7 days reaction and only the elimination side product **48** (TPP-$OC_{10}H_{19}$) was increasing with time. It can be concluded that longer reaction times only lead to the higher formation of side products so it is not a convenient parameter to be changed.

The next change was the use of MEK instead of DMF as reaction solvent. Also, the use of a catalytic amount of KI (10 % mol) was added to the reaction mixture in order to try to avoid the side reaction of elimination in the intermediate as reported in equation (2) as this will add iodide ions to the reaction mixture which can be exchanged with some of the bromide ions in the alkyl chain increasing the reactivity of the system and therefore favouring the formation of products:

$$(\text{TPP-OC}_{10}\text{H}_{20}\text{-Br} \longrightarrow \text{TPP-OC}_{10}\text{H}_{19} + \text{HBr}) \qquad (2)$$

47 **48**

An increment of yield with higher consumption of TPP-OH **34** was observed after a longer reaction time of 48 hours**.** On the other hand, an increment of the elimination product **48** obtained was also observed in the same manner.

These conditions were promising as the starting material was mostly consumed so the reaction was carried out in different scales from 200 mg to 1 g but for the high scale reactions, large amounts of unreacted starting material were recovered unreacted. In this case, the yield of the reaction decreased when the scale of the reaction was increased and also elimination side product was a major side product of the reaction in all cases.

It seems that the elimination side product always appeared during the reaction. In order to avoid this side reaction, the temperature was reduced. The solvent was changed to acetone keeping the rest of the conditions the same. The reaction was checked by TLC over the course of two days to observe completion of the reaction without any elimination side product after 48 h of reflux with high conversion to the desired porphyrin dyad **45**.

Due to the lack of elimination side product using acetone as solvent system, the need of KI as catalyst might not be longer necessary so two reactions were prepared with and without KI using acetone as solvent. In both cases the same results and yields were observed in the same reaction times so we can conclude that the presence of KI was no longer necessary to complete the reaction when using acetone as solvent as the elimination process was no longer occurring.

Solvent	Temperature (°C)	Base	Catalyst	Time (h)	Product **45**	Elimination
DMF	100	K_2CO_3	-	20	8 %	>80%
MEK	reflux	K_2CO_3	-	48	31%	26%
MEK	70	K_2CO_3	KI(10%)	18	-	-
MEK	80	K_2CO_3	KI(10%)	24	-	-
MEK	reflux	K_2CO_3	KI(10%)	24	40%	30%
MEK	reflux	K_2CO_3	KI(10%)	48	36%	31%
MEK	reflux	K_2CO_3	KI(10%)	72	38%	33%
acetone	reflux	K_2CO_3	-	72	57%	-
acetone	reflux	K_2CO_3	KI(10%)	72	55%	-

Table 1: Representation of the different reaction conditions screened.

4.3.1.2. Optimisation of the purification procedure for the formation of C_{10} porphyrin dyad 45

For the treatment of the crude reaction and for all the conditions used, the solvent had to be removed under vacuum, the residue redissolved in DCM and extracted several times with water to remove the excess base. In the particular case of using acetone as solvent, the crude reaction was only precipitated with water and filtered to obtain a purple solid of the crude reaction that needed to be further purified.

The first attempts of purifying the crude purple solid were by using silica gel column chromatography and 3:7 THF:pet ether as eluent, but big amounts of purple solids containing the product were stacked in the baseline and could not be recovered with any other more polar solvent, even with MeOH. Only between 60 % and 80 % of the starting crude mixture could be recovered after the column. To try to avoid the loss of material using silica gel, the same column chromatography was performed in alumina but no improvement was observed. Instead, more aggregation of the porphyrins was observed leading to product mixtures in the column fractions having to repeat the column in silica to recover the pure product.

In all cases that the product was purified by column chromatography, the fractions containing the product needed to be further recrystallised from the mixture of DCM:MeOH to obtain analytically pure material. During this precipitation process, a very low solubility of the product dyad was observed in the presence of small amounts of MeOH. Due to this observation, the crude solids from the reaction mixture obtained after the elimination of the solvent were subjected to direct recrystallisation without any previous purification by column chromatography. Using two careful recrystallisations it was possible to obtain analytically pure dyad **45** without any chromatography.

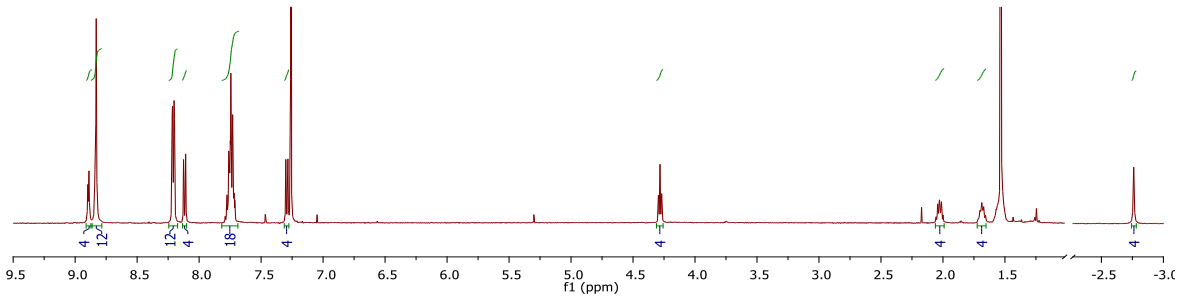

Figure 31. ^{1}H NMR spectrum obtained for porphyrin dyad **45** without column chromatography.

In summary, the best conditions obtained for the reaction were the reflux in acetone for 72 h, addition of water and filtration of the precipitate followed by careful recrystallisations to collect the product **45** as a purple solid (57 % yield).

4.3.2. First model double decker formations

Once the methodology for the synthesis of the porphyrin dyads was optimised, a study of the formation of double deckers with them was possible. Initially, the modified method of two step, one pot procedure developed by Birin[88] was followed (scheme 33). Metallation of the porphyrin dyad with lanthanum acetylacetonate was followed by addition of Pc **19** to the reaction mixture to form the double deckers.

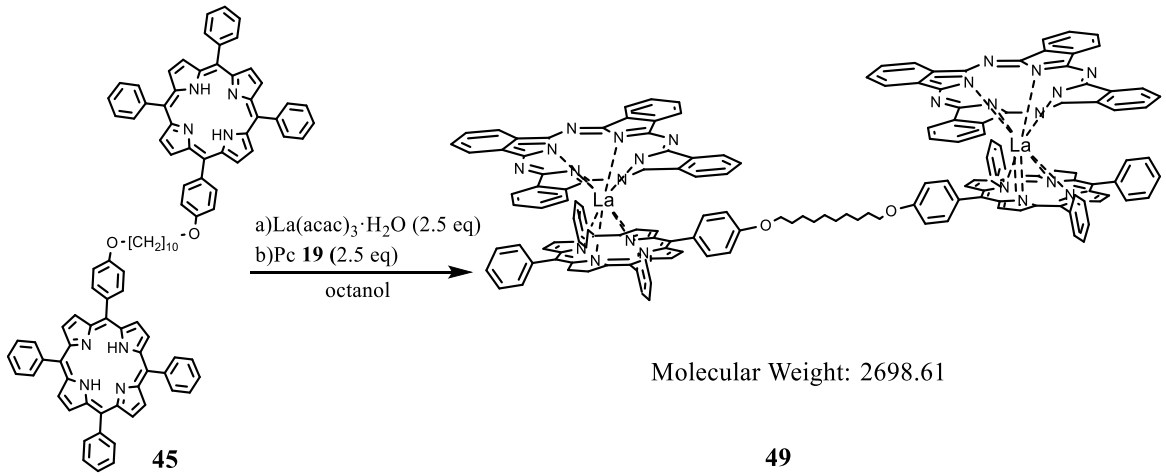

Scheme 33. Proposed reaction scheme for the formation of the dyad double decker **49**.

In the first attempt, the reaction was performed on a small scale by reacting porphyrin dyad **45** and lanthanum acetylacetonate in refluxing octanol for 6 h. At this stage, UV-vis spectroscopy indicated full metallation of the porphyrins. This step was followed by addition of phthalocyanine **19** and reflux overnight. When the reaction was completed, the solvent was distilled off and the residue recrystallized from a DCM/MeOH mixture to recover green solids that were analysed by TLC. Two spots were observed and the mixture was then checked by MALDI-tof MS (figure 32). Only two main peaks were observed corresponding to 2185.5 m/z and 4002 m/z. The expected mass for the product containing two double deckers was 2698.55 m/z but that peak could not be observed in the reaction mixture.

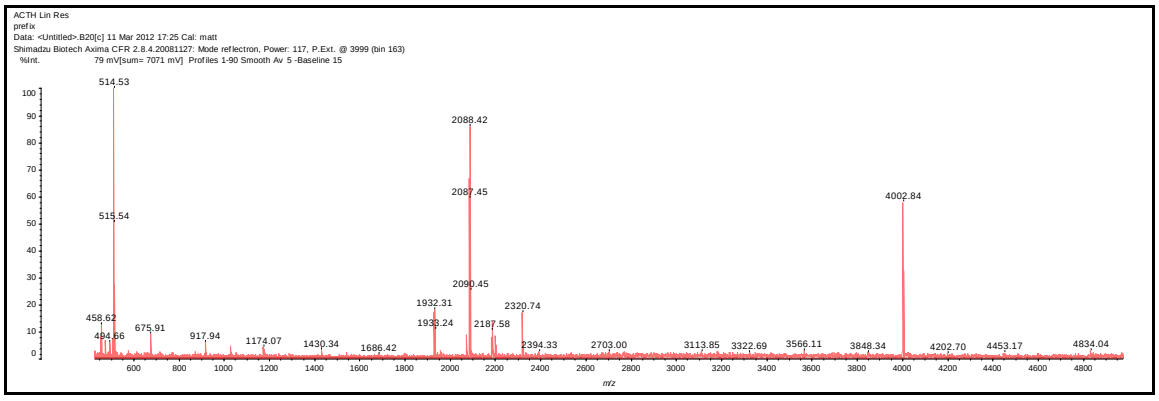

Figure 32. MALDI-tof MS obtained from the reaction mixture.

The reaction was repeated at larger scale using 50 mg of porphyrin dyad **45** following the same procedure. The isolated green solids where subjected to flash column chromatography in THF:Pet ether to obtain two different fractions (first brown and second green fractions). Both fractions were analysed separately by MALDI-tof MS and ^{1}H-NMR spectroscopy.

4.3.2.1. Analysis of the brown fraction

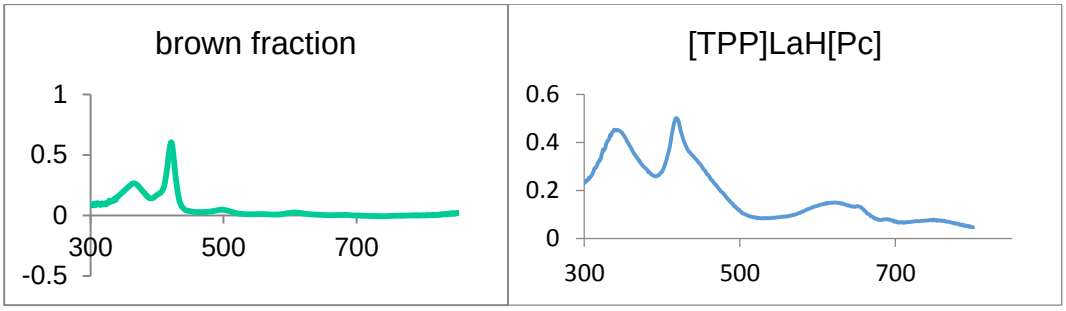

Figure 33. UV-vis spectrum obtained for the first brown fraction compared with the UV-vis obtained for [TPP]LaH[Pc] **32**.

First of all, the UV-vis spectrum that was obtained for the pure brown fraction (figure 33) does not look like a typical UV-vis spectrum of a double decker as the typical absorption on the Pc region at around 700 cm^{-1} is not present in this case which mean the complex is not a double decker but there is a new absorption at around 360 cm^{-1} that tell us that we are not looking to a simple porphyrin or metallated porphyrin complex either where

this absorption should not be present. On the other hand a sharp absorption can be observed at around 420 cm^{-1} that can correspond to the Soret band typical for porphyrins.

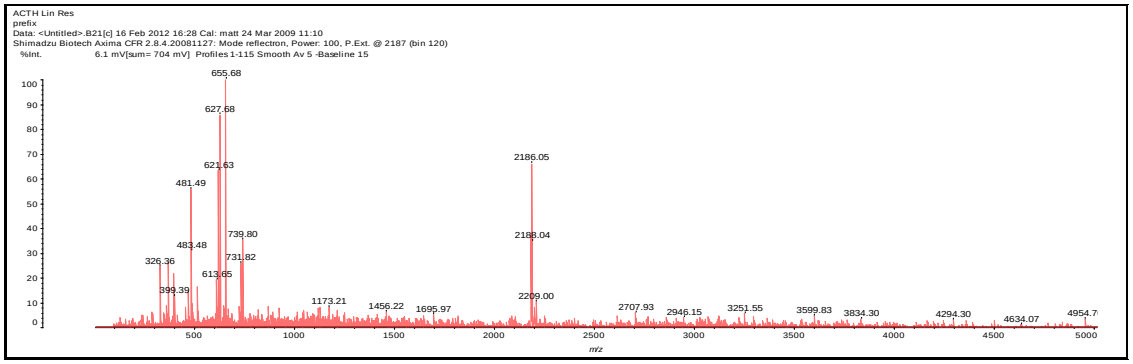

Figure 34. MALDI-tof MS obtained for the brown fraction.

Then, with this in mind, by a simple observation of the molecular mass observed on the MALDI, the difference in mass from the expected product corresponds to a difference of 512 m/z to the expected product, which fits exactly with the molecular mass of the deprotonated **19** Pc^{2-}. In other words, the mass corresponds to a triple decker structure. There are many possible arrangements that fit with the observed mass (figure 35).

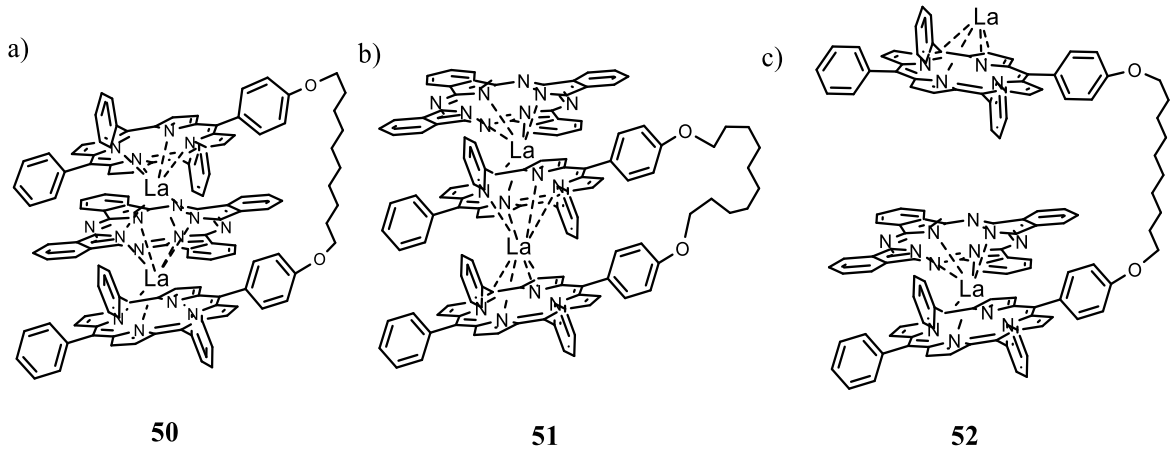

50 **51** **52**

Figure 35. Proposed structures **50**-**52** for the first brown fraction of the reaction.

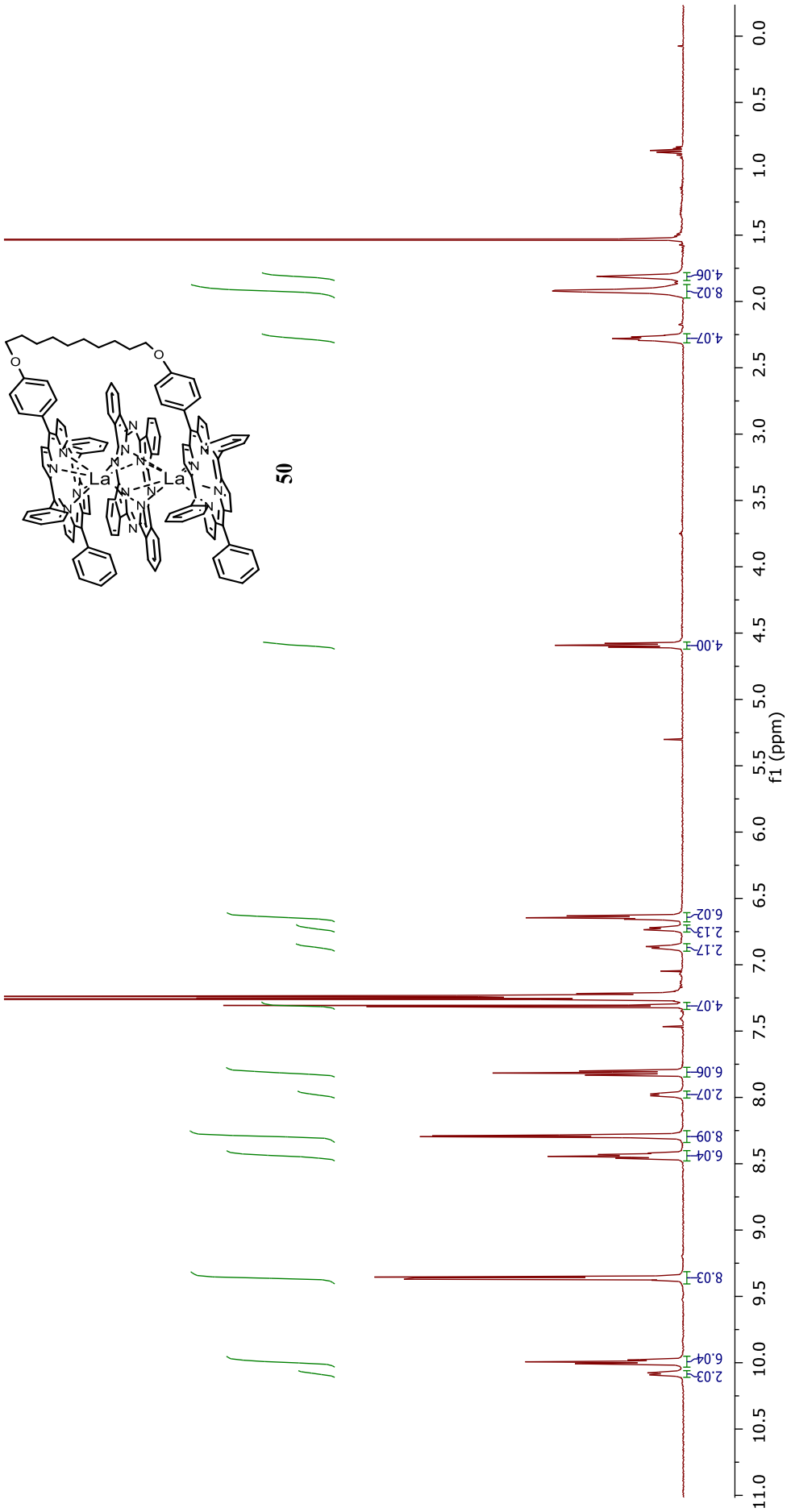

Figure 36. ^{1}H NMR spectrum obtained for the brown fraction.

In order to differentiate from the possible structures, the NMR spectrum was examined. It could be noted that there is no metal-free porphyrin because the characteristic peak at -2.7 ppm was not present on the spectrum. To distinguish between the possible structures, attention was focused in the very characteristic alkoxide signal (-O-C$\underline{H_2}$-) that appears as a triplet at around 4.6 ppm in the ^{1}H NMR spectrum. As long as there was only one signal in this region, it could be concluded that both ends of the aliphatic chain must be in identical environments (symmetrical molecule). The only proposed structure that meets this condition was the first closed triple decker **50**, composed of a triple decker structure with the Pc in between the porphyrins with the aliphatic chain interconnecting both porphyrins.

Finally, the structure was then characterised with an X-Ray analysis (figure 37).

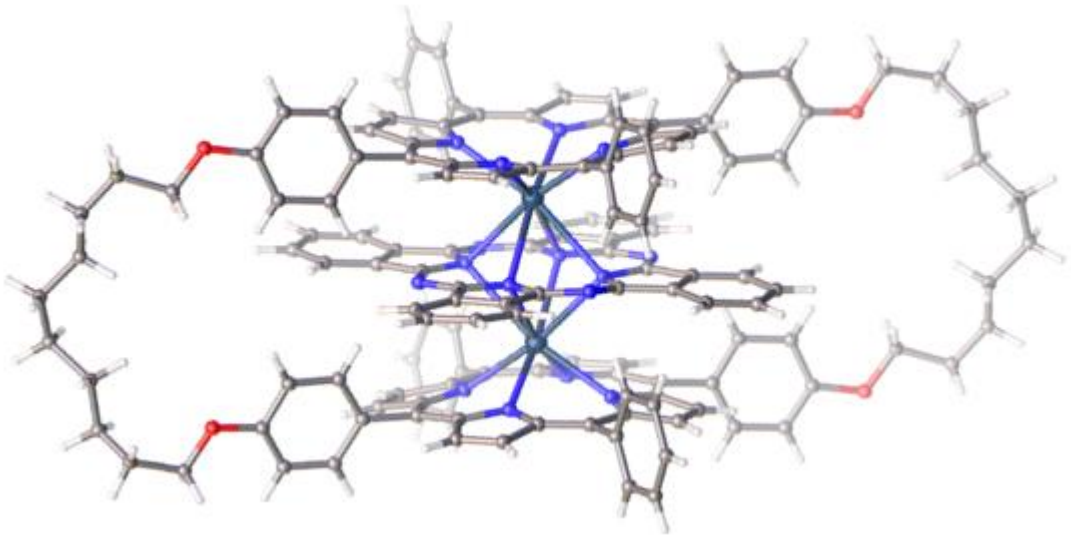

Figure 37. X-ray analysis obtained of **50**. Note that most of disorder components are not shown for clarity except for the linker chain which is exactly 50:50 disordered over both sites.

This proposed closed triple decker **50** ^{1}H NMR spectrum could then be compared with the small number of (not interconnected) triple deckers reported (figure 38).[79,80] During this work, the complicated ^{1}H NMR spectra signal splitting are totally analysed.

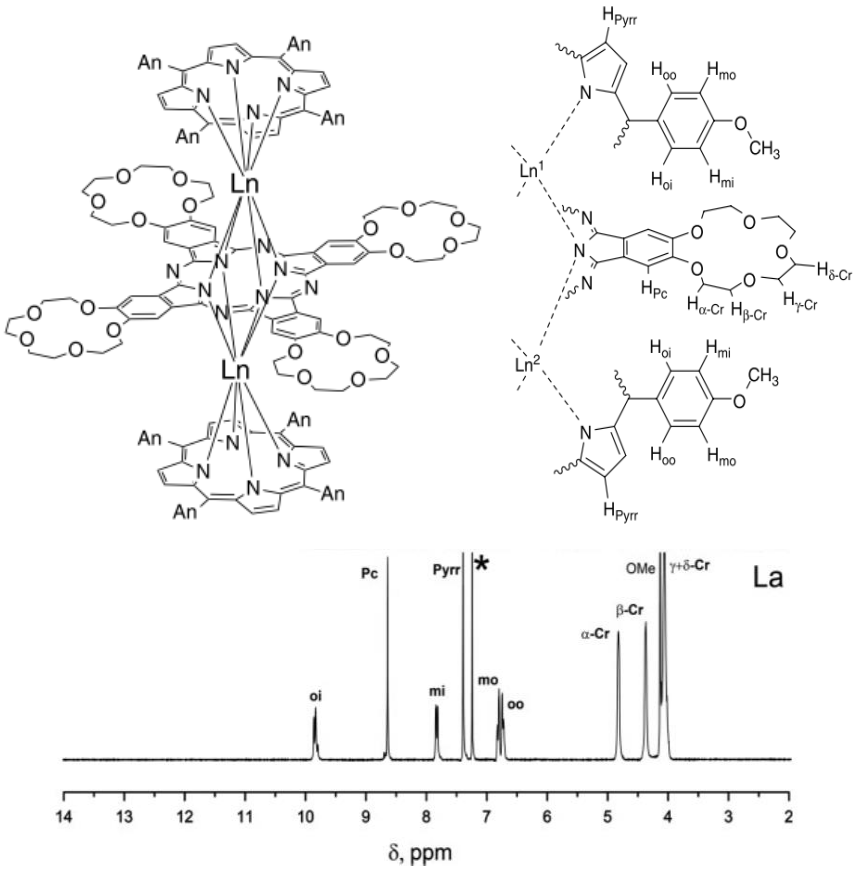

Figure 38. ^{1}H NMR spectrum studies of La triple deckers reported by Birin.[80]

In our case, our structures were very similar to those reported in Birin's work but further splitting of the phenyl signals was expected due to the lower symmetry of the complex because of the aliphatic chain interconnecting the porphyrins. This structure was then analysed in detail in the same way (figure 39). Note that the signals corresponding to the substituted phenyl protons are differentiated with apostrophe.

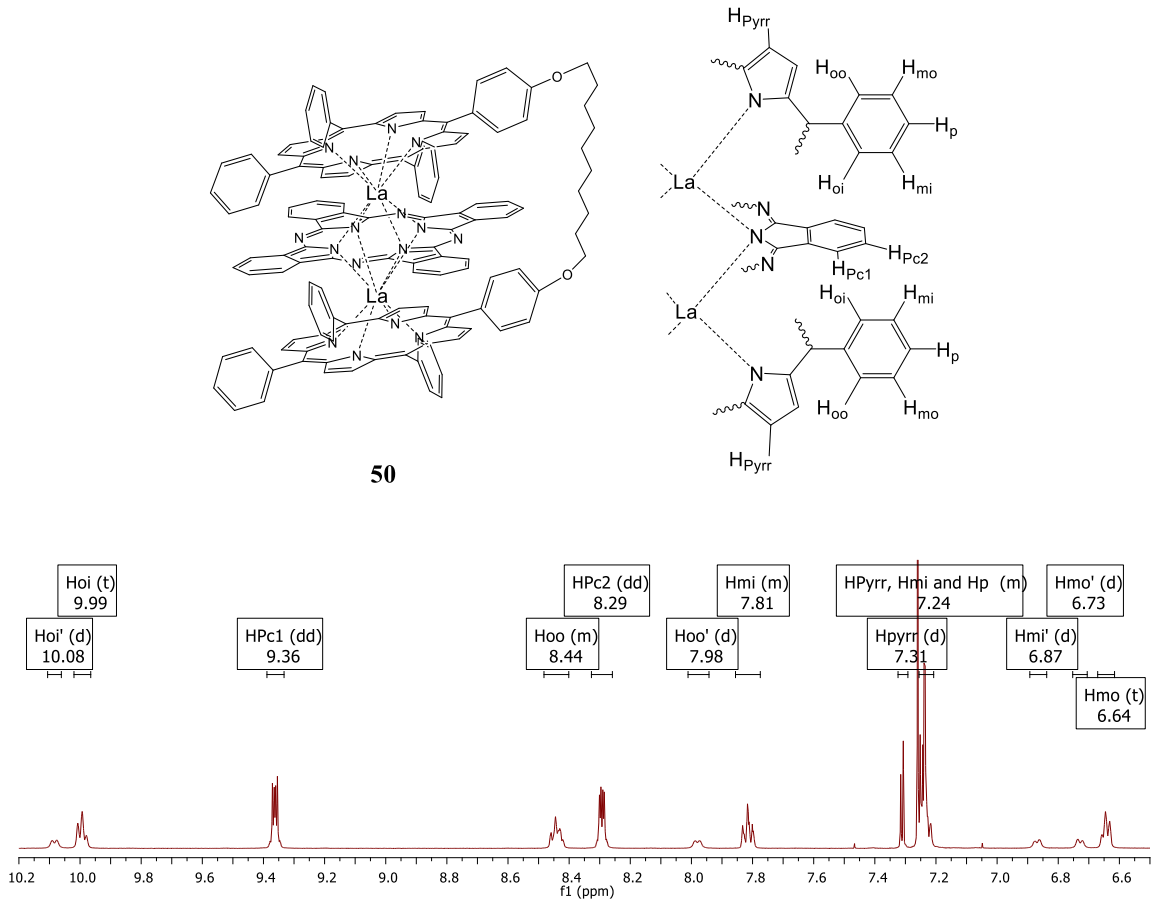

Figure 39. Analysis of ^{1}H NMR spectrum of complex **50**.

According to the structure of the compound, we should expect the Pc peaks H_{Pc1} (non-peripheral protons) and H_{Pc2} (peripheral protons) to be split as proposed in figure 40a where we should have eight different signals as we have 8 pairs of magnetically non-equivalent protons due to the plane of symmetry, represented as a dotted line that crosses the structure trough the aliphatic chain of the side of the triple decker to connect the two porphyrins. On the other hand, we can easily observe two signals (H_{Pc1} and H_{Pc2} on figure 39) that closely resembles a completely symmetrical Pc as represented in fig 40b. It therefore appears that there is fast rotation of the Pc inside of the triple decker in the NMR time scale that make all protons of the Pc indistinguishable.

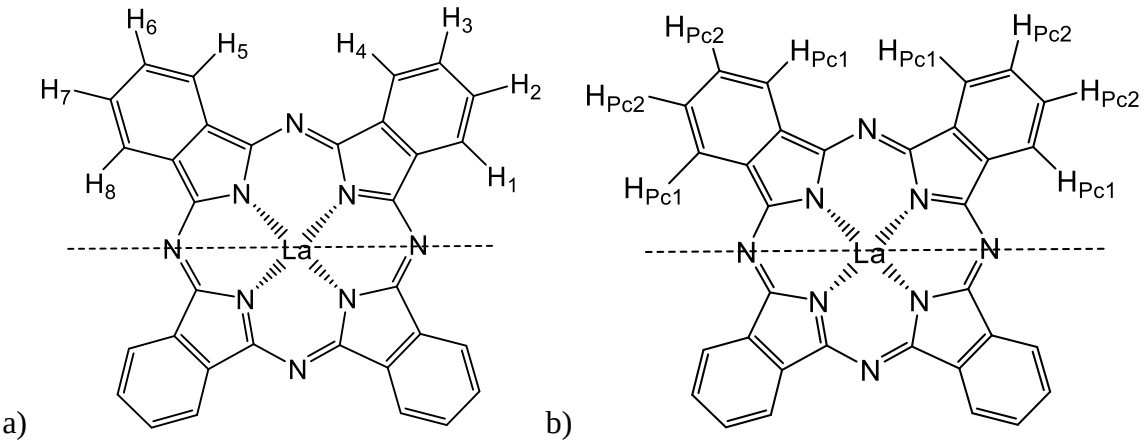

Figure 40. Representation of the Pc in triple decker **50** view from above, with the porphyrins omitted for clarity. The dotted line represents a plane of symmetry.

4.3.2.2. Analysis of the green fraction

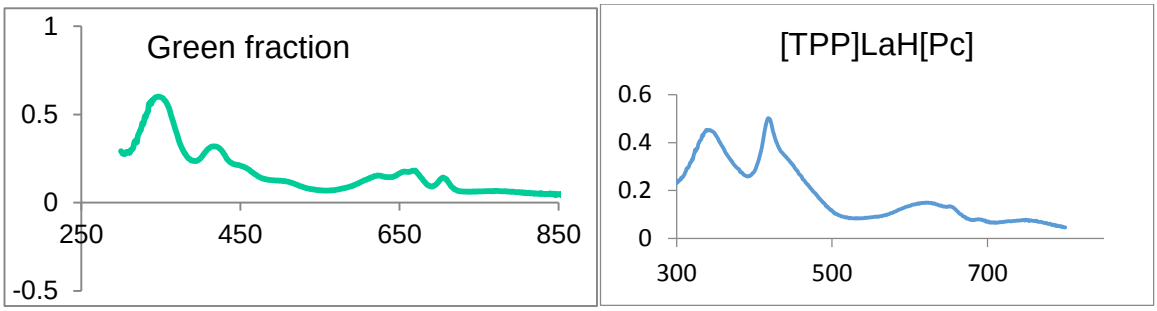

Figure 41. UV-vis spectrum obtained for the green fraction compared with the one of a double decker.

Again, the first characterisation to look at was the UV-vis spectrum obtained for the pure second green fraction (figure 41). It did not look like the previous brown fraction and more closely to the typical UV-vis spectrum of double deckers with a few differences. First of all, it shows an absorption at 700 cm^{-1} on the Pc region that was not present in the previous brown fraction. Therefore it had then a different arrangement of porphyrins and Pcs. Also, the absorption at around 360 cm^{-1} was also present in the complex, typical for sandwich-like structures. On the other hand it can be observed that the sharp absorption at around 420 cm^{-1} is much weaker than in any other complex. All that together, might give us an idea of the structure where the UV-vis of this fraction was the opposite of the other fraction, very likely to be the porphyrins sandwiched in between Pcs.

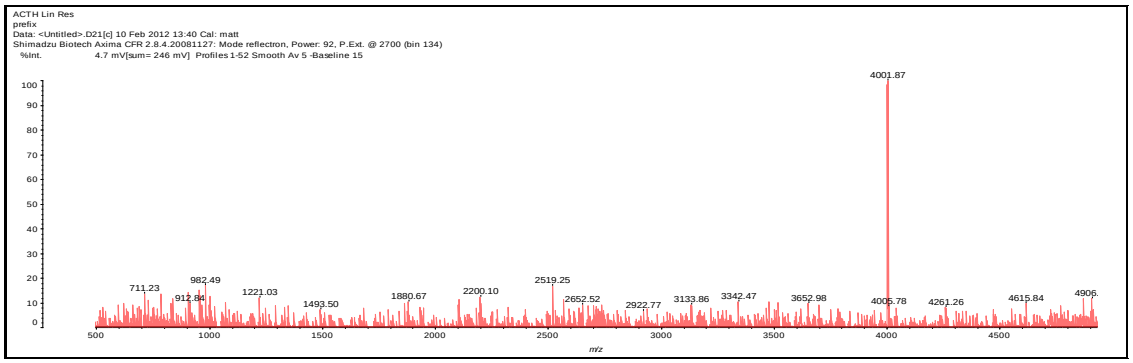

Figure 42. MALDI-tof MS spectrum obtained for the green fraction.

In this case, by MALDI-tof MS, a molecular ion of 4000 m/z was observed that can fit with the addition of four metals and four Pcs to the starting porphyrin dyad. There were two possible triple deckers that could have been formed fitting the corresponding molecular weight: **53** and **54** as shown in figure 43. These are basically the formation of triple deckers where the Pcs are at each side of the porphyrin (**53**) or one Pc on top of the other (**54**).

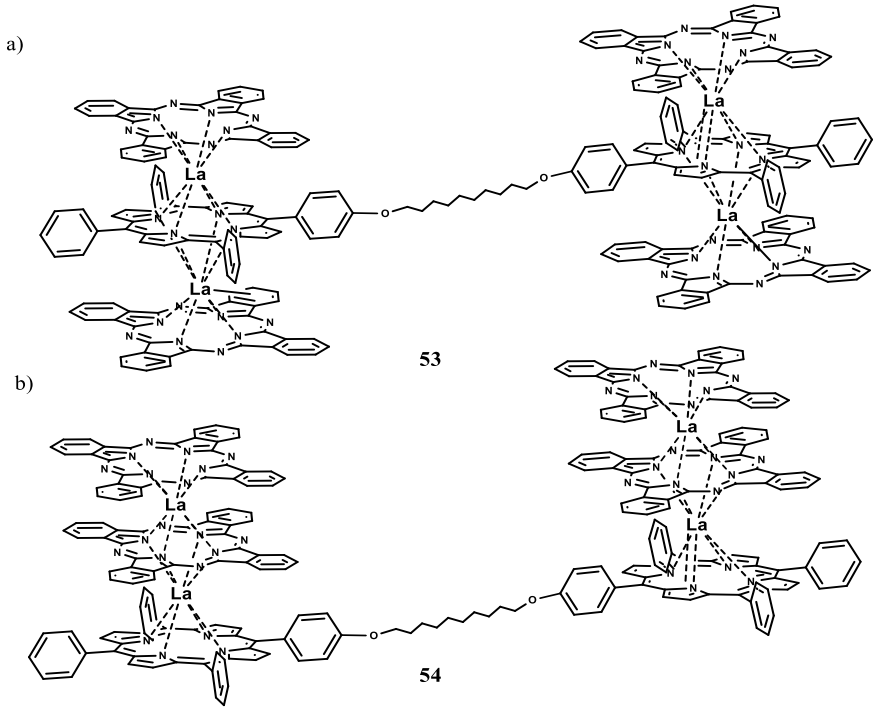

Figure 43. Proposed structures **53** and **54** for the green fraction of the reaction.

Again, the possible structures could be differentiated by analysing the ^{1}H NMR spectrum obtained for the fraction. In this case, the aliphatic protons should be the same in both cases so we focused on the aromatic region (Fig 44). The obtained spectrum in this case

appear to be much more complicated due to the major splitting of porphyrin signals but the same Pc proton splitting can be observed. This splitting means that all phthalocyanines are equivalent and the only way that this is possible is by the double addition to both sides of each porphyrin as proposed in structure **53**. Also, the integral value for the peaks (32 protons each at 8.74 ppm and 7.77 ppm) mean that effectively, four Pcs have been added symmetrically to the dyad **45**. In the other proposed structure **57**, there are two phthalocyanine environments, one in between the top Pc and the porphyrin and there are only two phthalocyanine peaks on the NMR spectrum.

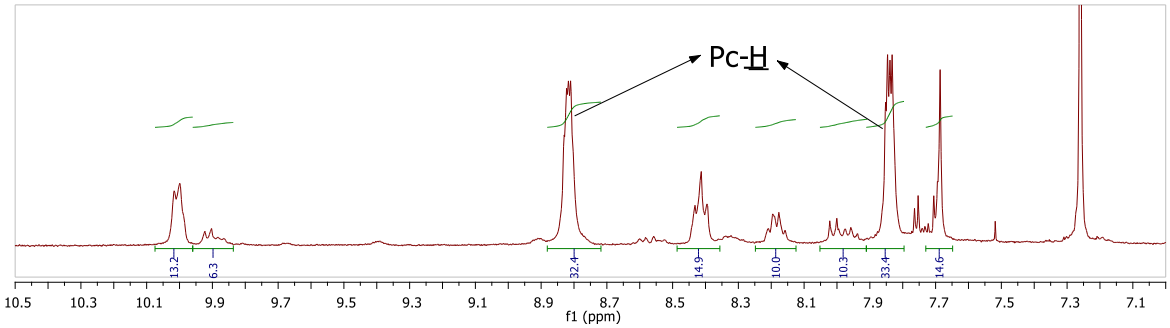

Figure 44. Aromatic region expansion of the ^{1}H NMR spectrum obtained for bis(tripledecker) **53**.

4.3.3. Selective synthesis of triple deckers

The first bis(phthalocyanate)-metal complex [SnIV(Pc)$_2$] was reported as early as in 1936.[19] The bis(phthalocyaninato)-rare earth sandwich analogues have been known since the mid-1960's,[89] while the studies of bis(porphyrinato) counterparts were started in the 1980s.[90,91] Heteroleptic sandwich compounds with different porphyrinato or phthalocyaninato ligands were not reported until 1986.[92] The first porphyrin triple decker complexes appeared a bit later, in 1986s.[74]

Different approaches for the selective synthesis of heteroleptic (porphyrinato)(phthalocyaninato) lanthanides have been published earlier.[52,60,75,88,93] All previously described methods are multistep synthetic procedures which apply one-by-one deck construction of the target complexes (scheme 34).

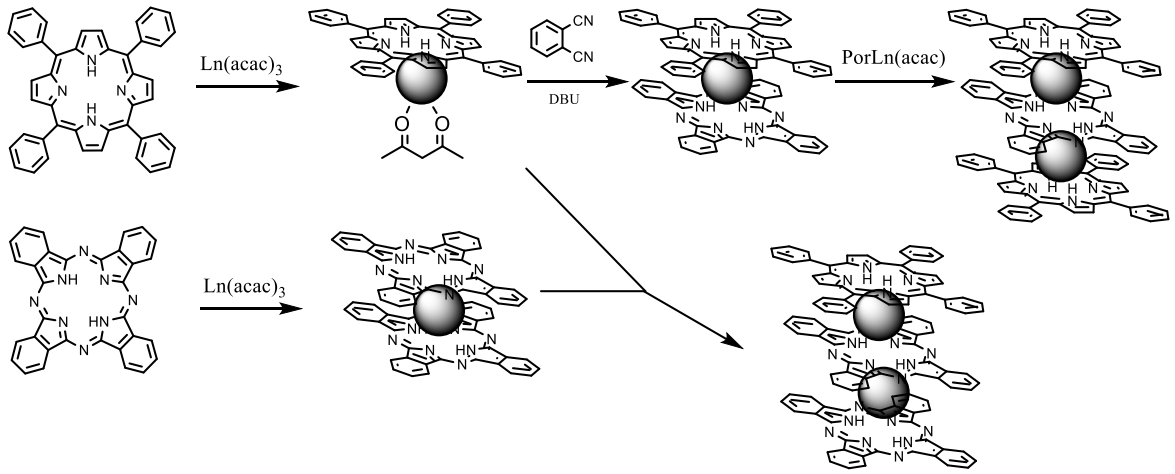

Scheme 34. One-by-one deck construction of triple deckers.[88]

Most of the published work operate with the late lanthanide series because of the higher stability of the half sandwich species. This synthetic procedure includes the generation of the [Por]Ln(acac) precursor, which is used without further purification to interact with phthalonitrile to form the desired double-decker complexes. Also, mixtures of triple-decker complexes $[Por]_2[Pc]Ln_2$ and $[Por][Pc]_2Ln_2$ were directly prepared using the corresponding double deckers and the [Por]Ln(acac) precursor.[92]

A recent publication describes an alternative one-pot procedure that allows the synthesis of heteroleptic double- and triple-decker (porphyrinato)(phthalocyaninates) of various lanthanides (La, Eu, Nd) starting from porphyrin, phthalonitrile and lanthanide acetylacetonate using a high-boiling point alcohol as solvent.[80,88] The difference between all previously described protocols and this one-pot procedure is that the triple-decker complexes [Por]Ln[Pc]Ln[Por] can be obtained in a one-step procedure of prolonged reflux of porphyrin, phthalonitrile and $Ln(acac)_3$ without any additional treatment of the reaction mixture. This method does not need generation of monoporphyrinates and avoids rise-by-one-story formation of triple-decker complexes. The corresponding double-decker complexes and other triple decker structures are also present in the reaction mixture, but the yields of the triple-decker compounds are comparable to, and in several cases higher than that of double-decker ones that range from 4 % up to 65 %[88,93-95] but most yields are more generally around 10-30 % with a few exceptions. This final methodology looks promising to be used for the study of the synthesis of the desired interconnected triple deckers that are the base of this chapter.

4.3.3.1. Selective synthesise of closed triple decker dyad 50

To synthesise the closed triple decker dyad **50**, porphyrin dyad **45** and two equivalents of metal were refluxed in octanol under inert atmosphere followed by addition of one equivalent of the Pc as shown in scheme 35:

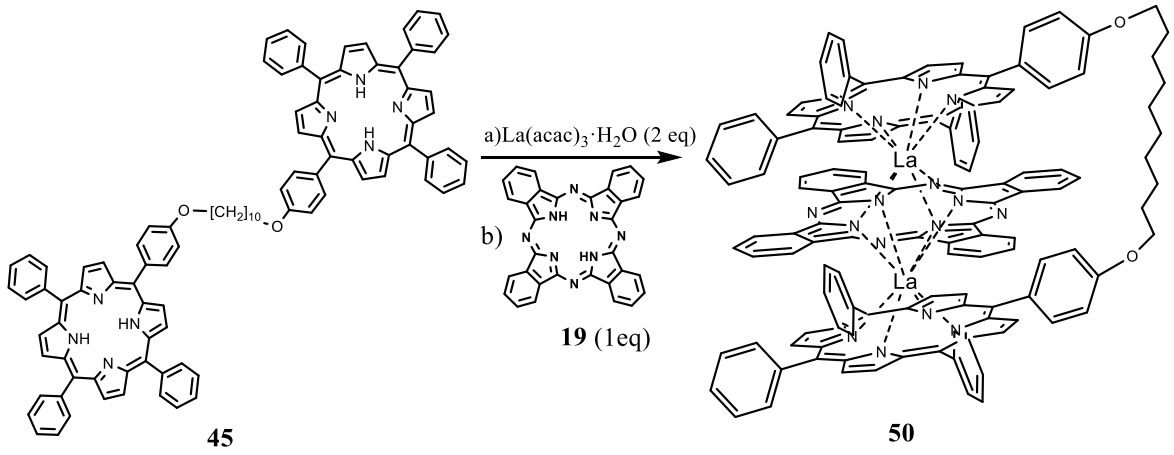

Scheme 35. Proposed reaction procedure for the formation of closed triple decker **50**.

After completion of the reaction, the crude product mixture was concentrated under vacuum and then recrystallised from DCM:MeOH. The resulting dark solids were analysed by MALDI-tof MS (figure 45). Formation of only the closed triple decker **50** was observed without any formation of the open triple decker **53** (4002 m/z). Only peaks corresponding to 1399 and 2186 m/z were observed in the crude solid mixture.

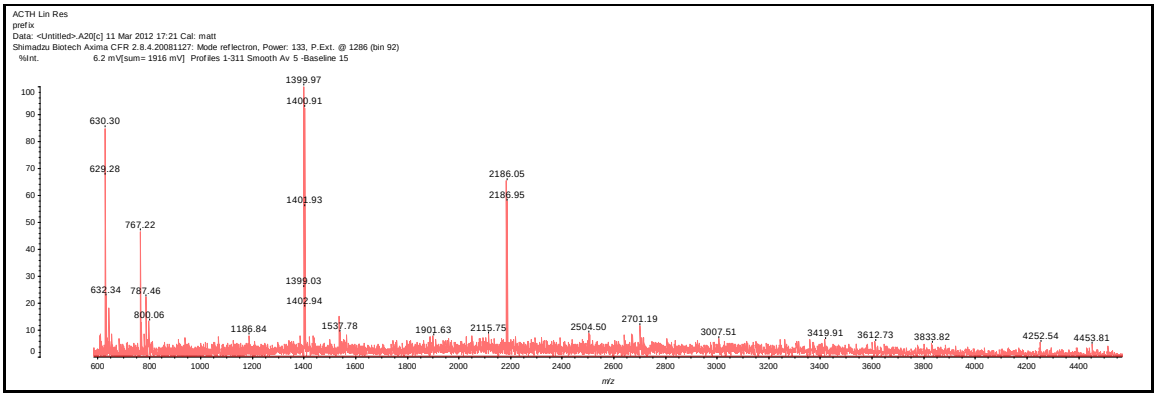

Figure 45. Crude MALDI-tof MS of the reaction.

Therefore, the selective synthesis of closed triple decker dyads can be successfully achieved by careful stoichiometric reaction of the porphyrin dyad with two equivalents of $La(acac)_3 \cdot H_2O$ followed by addition of one equivalent of previously synthesised Pc **19**. Analytically pure closed triple decker **50** was obtained in 86 % yield by this method. This yield is very high, specially comparing it with previous triple decker synthesis reported where the previously reported yields for the formation of this structures are between 4-63 %.[59,88,92,93,96]

4.3.3.2. Selective synthesis of open bis triple decker 53

To selectively synthesise the open bis triple decker **53**, porphyrin dyad **45** and 4.2 equivalents of metal were refluxed in octanol under an inert atmosphere followed by addition of an excess (10 eq) of Pc **19** as shown in scheme 44:

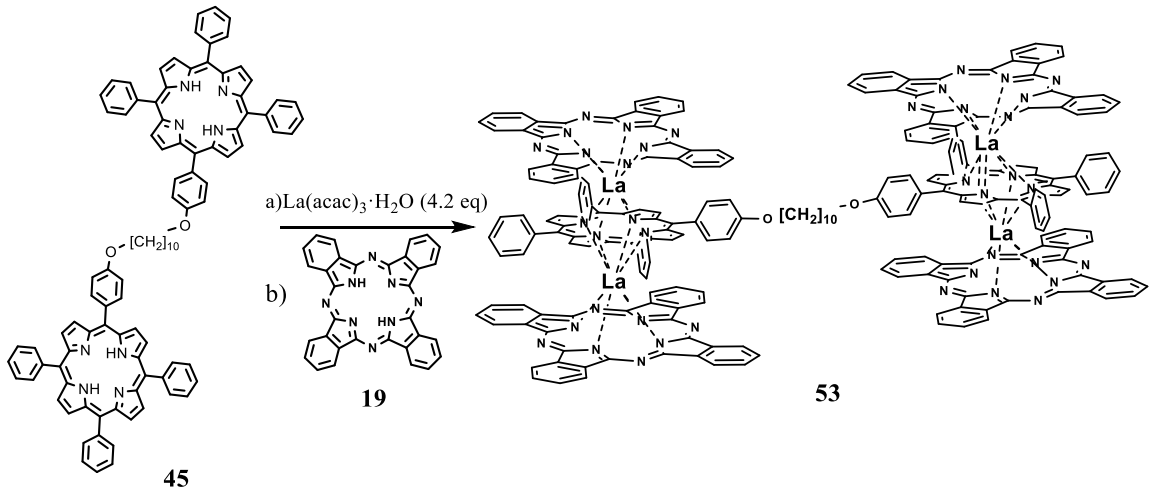

Scheme 44: Proposed reaction procedure for the formation of the open triple decker **53**.

When the reaction was completed, it was cooled down and precipitated with pet ether to collect green solids that where then checked by MALDI-tof MS.

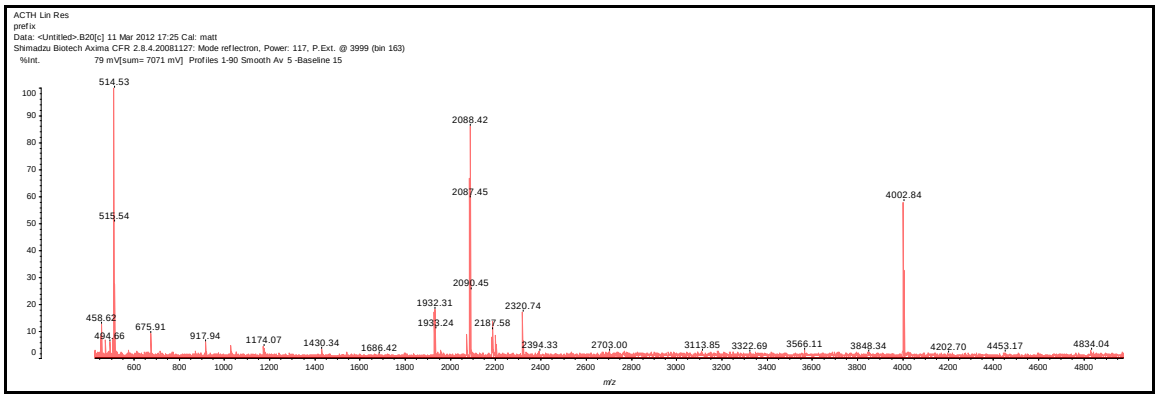

Figure 47. MALDI-tof MS of the crude reaction.

The liquids from the filtration (pet. ether/octanol) were also checked by MALDI-tof MS and a small amount of closed triple decker **50** was observed in the remaining octanol (2185 m/z). In this case, no unreacted starting material **45** (1399 m/z) was observed in the crude spectrum. The pure material **53** could be obtained pure after column chromatography in 34 % yield. This yield was lower than that obtained for the formation of triple decker **50** due to the formation of other products, primarily the closed triple decker **50** analogue (2186 m/z) that was also formed during the reaction conditions. On the other hand it is still higher than that obtained in previously reported methods.

4.3.3.3. Synthesis of closed triple decker analogues 57, 58 and 64.

It can be concluded that both open and closed triple decker dyads **50** and **53** could be synthesised selectively by using the right amount of metal and Pc **19** equivalents for the reaction. To check the reproducibility of the methodology, closed triple decker **72** was also synthesised from C_{12} porphyrin dyad **46** synthesised from 1,12-dibromoundecane using the same conditions previously optimised for porphyrin dyad **45**.

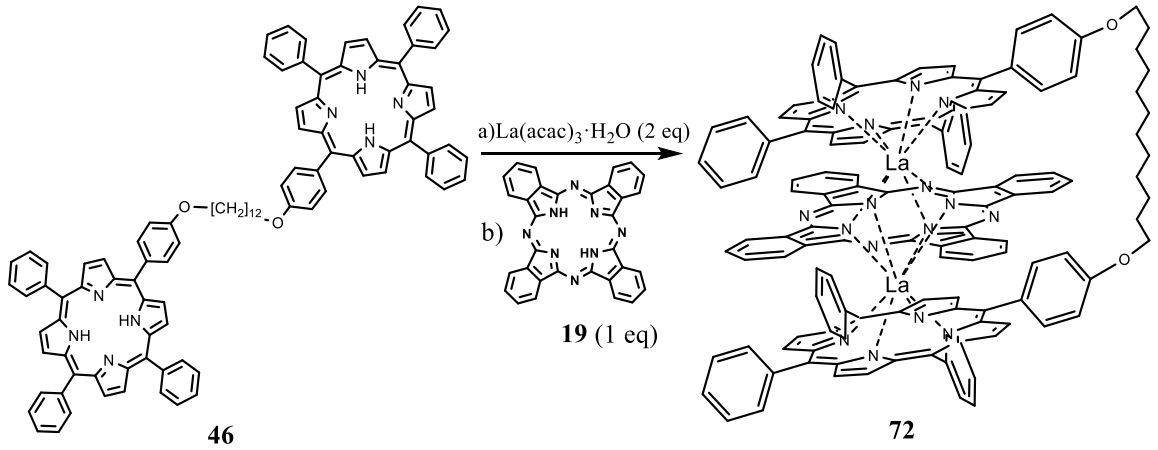

Scheme 37. Selective synthesis of closed triple decker **72**.

The same method was followed by refluxing porphyrin dyad **46** and lanthanum acetylacetonate in octanol for 6 h until metallation was completed (checked by UV-vis spectroscopy). Then, Pc **19** was added and the mixture refluxed for another 18 h. When the reaction was completed, the solvent was distilled off and the crude residue obtained recrystallised from DCM/MeOH. The resulting dark solids were purified by column chromatography followed by recrystallisation to obtain the pure triple decker **72** in 62 % yield.

Synthesis of analogues with substituted phthalocyanines

As the method was reproducible, a series of analogues were obtained by using different Pcs for the formation of closed decker triple deckers. Phthalocyanines can generally be substituted in the peripheral positions (2,3,6,7,10,11,14,15) as well as the non-peripheral positions (1,4,5,8,9,12,13,16).[97] By using these Pcs, simpler aromatic regions in the NMR spectrum were expected as either the peripheral or the non-peripheral protons were

eliminated and therefore the couplings between them. With this in mind, the possibility of the Pc to be rotating rapidly on the NMR time scale was studied by introducing bulky groups in the Pc and therefore, blocking the rotation by interaction between the Pc substituents and the porphyrin chain linker.

To prepare the analogues, the first choice was to introduce an alkylated Pc in the triple decker. Peripherally and non-peripherally substituted Pcs **55** and **56** were selected to synthesise the corresponding triple deckers **57** and **58** using the same previously developed methodology[88] from C_{10} porphyrin dyad **45** as shown in scheme 38:

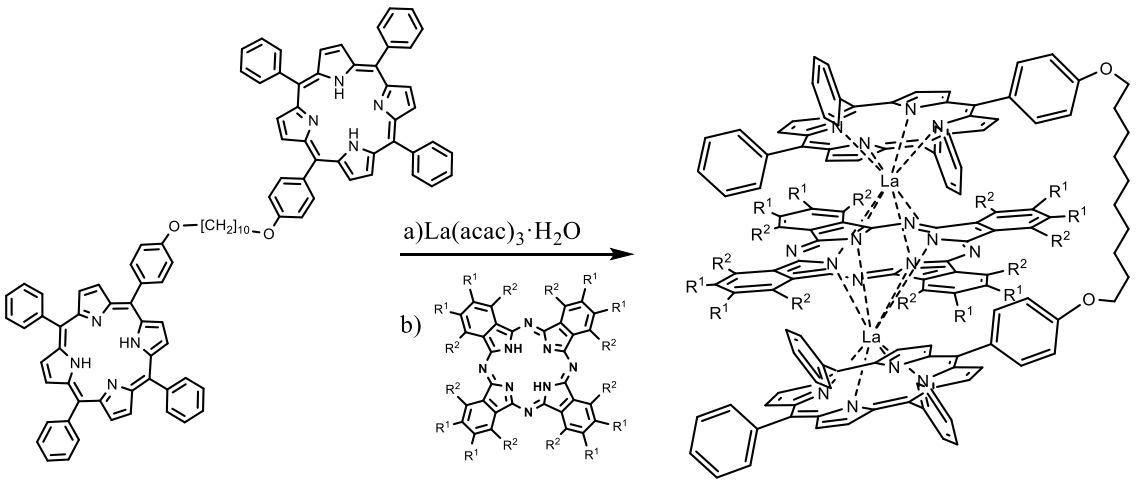

45 **55** **57** Peripherally substituted: R^1=C_8H_{17}; R^2=H
56 **58** non-Peripherally substituted: R^1=H; R^2=C_8H_{17}

Scheme 38. Proposed synthesis of substituted triple deckers **57** and **58**.

Both Pcs were synthesised separately from the corresponding phthalonitriles using previously optimised methodologies in our group[98,99] and then used for the formation of the corresponding triple decker derivatives.

Several problems were observed during these studies due to the difficulties trying to obtain good NMR spectra for the first reaction attempts. Impure NMR spectra were obtained even after two consecutive purifications by column chromatography followed by recrystallisations. These impurities appeared despite single spot TLC and single peak MALDI-tof MS spectrum were obtained for the products. The first attempt to obtain pure samples was by optimisation of the purification process using various solvent systems for the column chromatography (in silica or alumina) after the reaction but the same results were observed in all cases. Slow decomposition of the material was then observed in the

recrystallisation vials for the substituted triple deckers when chloroform was used as solvent. It was then concluded that the triple deckers with substituted Pc **56** were not stable enough in the used NMR solvents ($CDCl_3$). To obtain good NMR spectrum of the compounds, the use of deuterated dichloromethane treated before with molecular sieves was necessary. Under this conditions, NMR spectrums of the triple deckers could be successfully obtained after purification of the crude mixtures by column chromatography in silica gel followed by recrystallisation.

Synthesis of closed triple decker 57

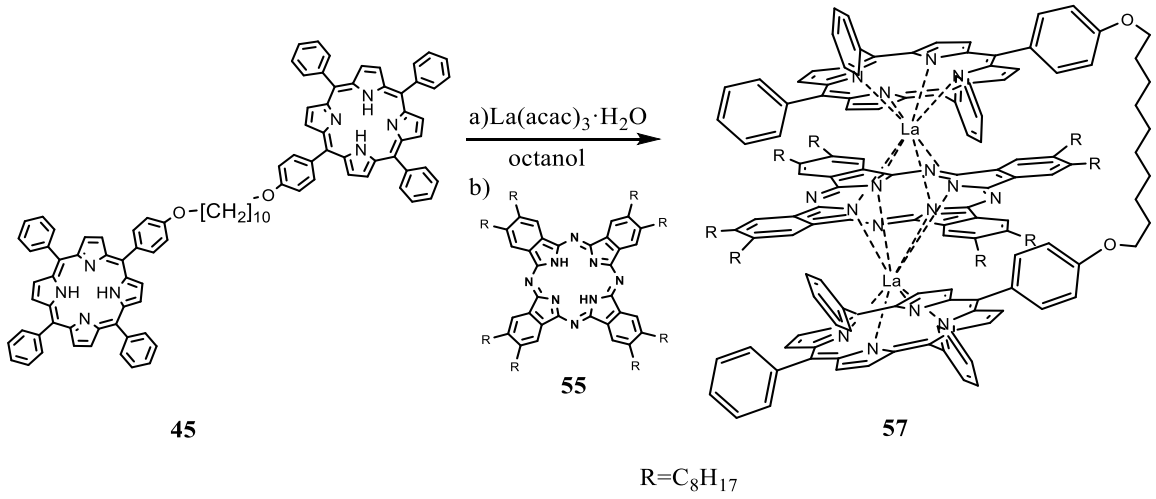

Scheme 39. Synthesis of peripheral octaoctylsubstituted triple decker **57**.

The closed triple decker **57** was obtained after the standard one pot two step procedure for the formation of triple deckers. Then, the completion of the reaction was checked by MALDI-tof MS analysis of the crude and the expected peak for the product was observed at 3085.4 m/z. In this case, ^{1}H NMR spectrum could be obtained using CD_2Cl_2 as solvent (figure 48).

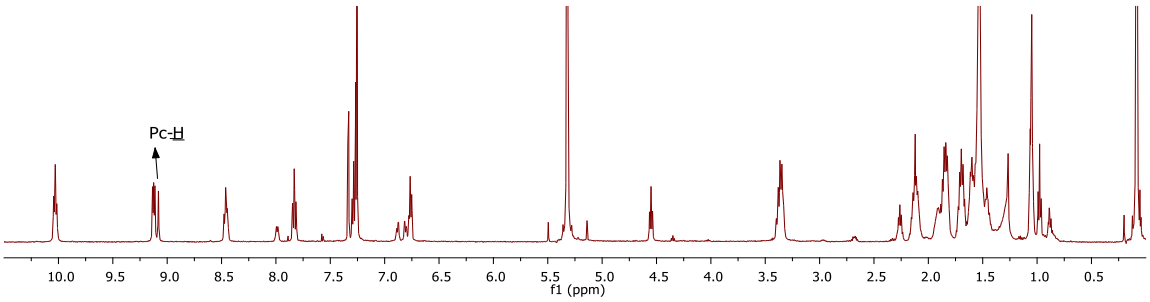

Figure 48. ^{1}H NMR spectrum obtained for closed decker triple decker **57**.

In the case of triple decker **57**, the phthalocyanine was peripherally substituted and therefore only one set of signals for the phthalocyanine aromatic protons was observed at 9.1 ppm. On the other hand, the splitting of the porphyrin aromatic protons are on the same regions which is in accordance with the formation of the closed triple decker analogue. This obtained ^{1}H NMR spectrum was then compared with the one obtained for the previous triple decker **50** where the Pc was not substituted.

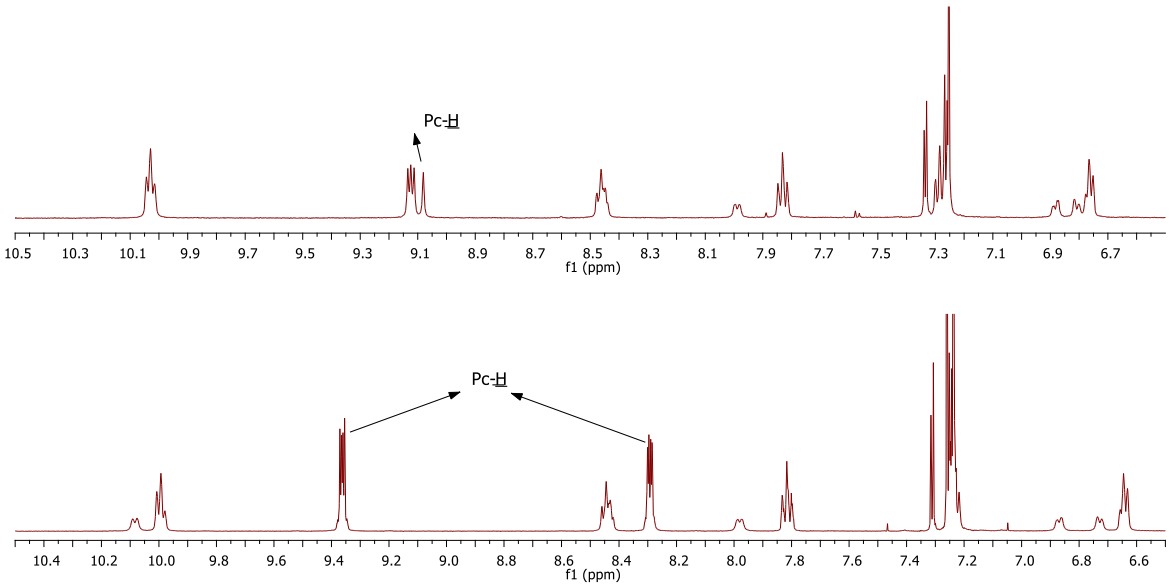

Figure 49. ^{1}H NMR spectrum obtained for closed decker triple decker **57** (above) compared with that of closed triple decker **50** (below).

For this substituted analogue, all the Pc aromatic peaks are expected to be singlets as the peripheral positions are functionalized with alkyl chains. If phthalocyanine is rapidly rotating, only a singlet would appear as all the aromatic positions (Ha) should be equivalent in the NMR time scale as represented in figure 50a. However, that is not what was observed in the spectrum for the aromatic protons of the Pc around 9.1 ppm. What can be observed on the other hand is a group of four singlets, as could be expected for a fixed Pc not rotating rapidly on the NMR time scale ($H_{1\text{-}4}$ in Fig 50b). Therefore in the case of triple decker **57**, the phthalocyanine is not rotating in the NMR time scale.

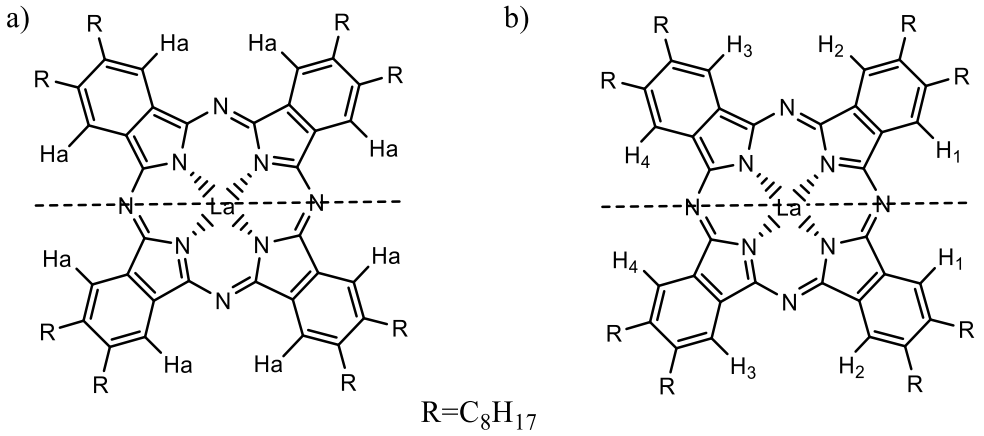

Figure 50. Representation of the peripherally substituted Pc in triple decker **57** view from above with the porphyrins omitted for clarity. The dotted line represents a plane of symmetry.

Synthesis of closed triple decker 58

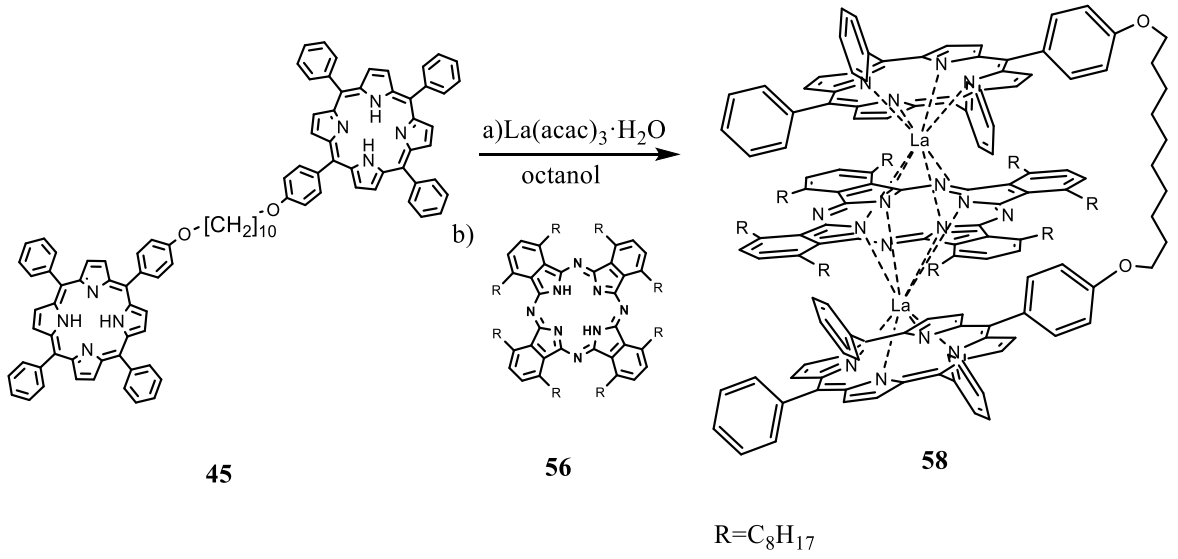

Scheme 40. Proposed synthesis of triple decker **58**.

The same methodology of one pot, two step reflux in octanol was followed using pre-synthesised Pc **56**.[98] To do so, the porphyrin dyad and lanthanum acetylacetonate were refluxed in octanol followed by addition of Pc **56**. MALDI-tof MS was checked after the reaction and the expected peak at 3085.40 m/z was observed. The solvent was distilled off and the crude recrystallised from DCM/MeOH. The resulting solid was purified by column chromatography and recrystallisation to recover a dark-green fraction containing the product as checked by MALDI-tof MS (3085.4 m/z) as well as single spot in the TLC. Then, the NMR spectrum of the sample was performed but it was significantly different from the previous triple deckers **50** or **57** (figure 51).

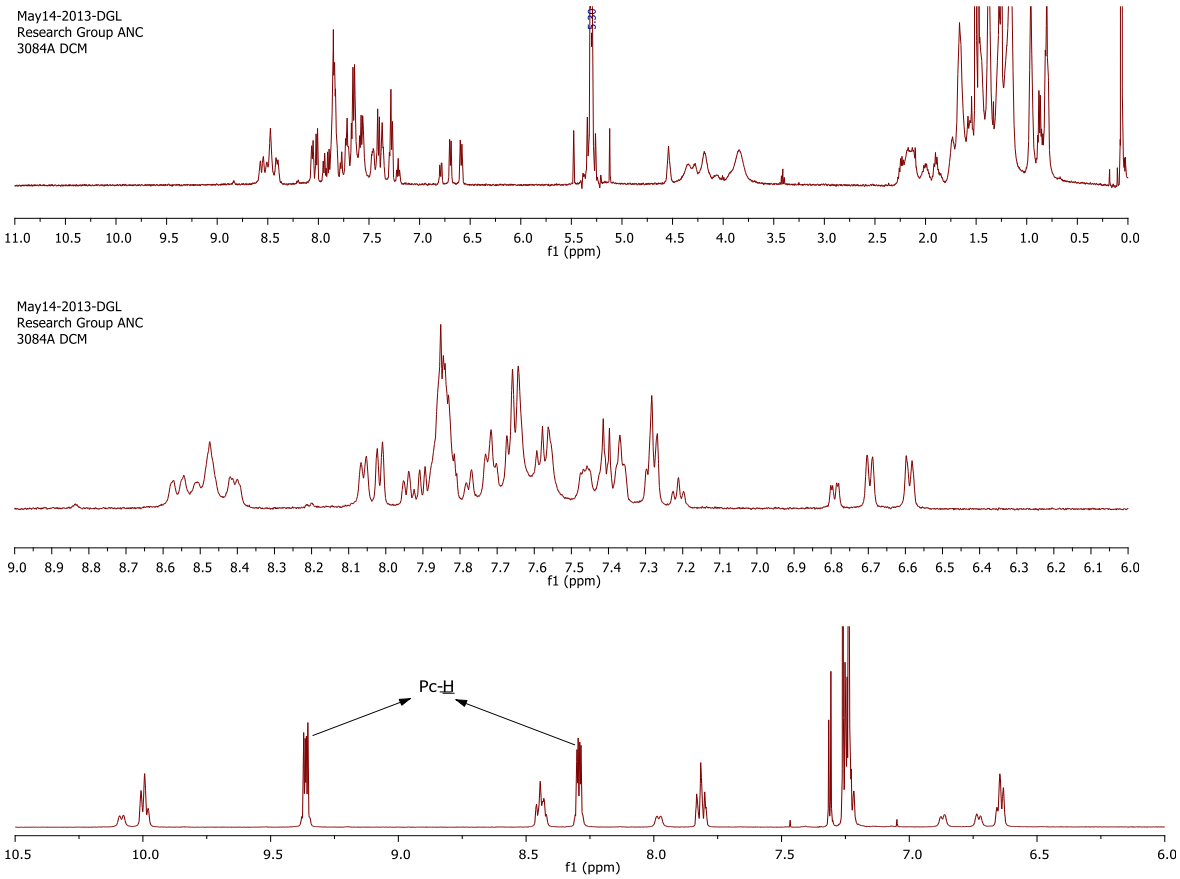

Figure 51. ^{1}H NMR spectrum obtained for the closed decker triple decker **58** (top) and expansion of the aromatic region (middle) and previous triple decker **50** (bottom).

As it can be observed in the spectrum, the typical signals for the porphyrin peaks that were observed previously for other closed triple deckers at around 10 ppm from the $_{oi}$Ph*H* were no longer present in the spectrum for this analogue **58**. However, some of the other signals typical of closed triple deckers were present, like the signals at around 6.5 - 7.0 ppm that corresponds to the $_{m}$Ph*H* in the triple decker **50**. This observations made us think that we were looking to some other analogue or processes happening with this particular porphyrin-Pc complex and it needed to be analysed deeply.

Analysis and comparison of closed triple deckers 57 and 58

Further information on the structure of **58** can be obtained by comparing the UV-vis spectra for the obtained complexes. If the UV-vis spectrum for porphyrins and Pcs are compared (figure 52), it can be concluded that each of them absorbs in very different regions of the UV-vis as shown in figure 52.

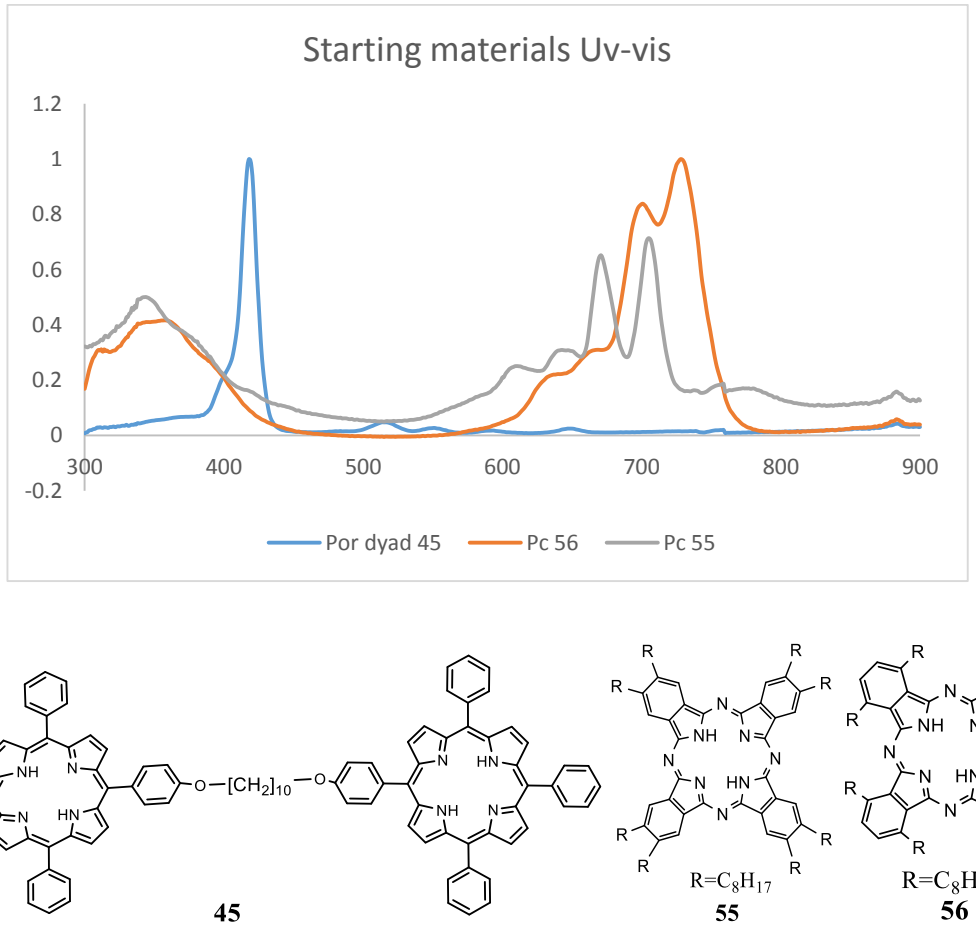

Figure 52. UV-vis of porphyrin dyad **45** and Pcs **55** and **56**.

Therefore, it can be expected that in double decker complexes, for example, both absorptions should be present in the complex. This can be observed for [TPP]La[Pc] double decker **32** (figure 53) where a sharp absorption at around 400 cm^{-1} is present along with another at around 600-700 cm^{-1} and a final absorption at around 300 cm^{-1}, typical for this kind of double decker complexes.[53,100]

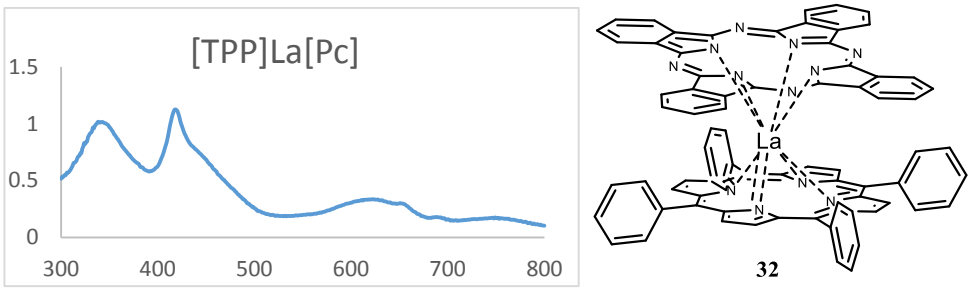

Figure 53. UV-vis of porphyrin heteroleptic double decker **32**.

With this in mind, the spectrum obtained for the multidecker structures **50**, **53**, **57** and **58** can be further interrogated. Then, when looking at the UV-vis spectra of unsubstituted closed triple decker **50** (figure 54), a sharp absorption at the porphyrin region of 400 cm^{-1} can be observed along with another broad absorption at around 300 cm^{-1} typical for sandwich-like complexes. In this case, no absorption was observed in the phthalocyanine region between 600 and 700 cm^{-1}. This data also fitted with the expected spectrum observed for other structures of this kind where the Pc is located between two porphyrins ([Por]M[Pc]M[Por]).[75,93] The same type of spectrum was obtained for the triple decker analogue **57** (figure 54). In this spectrum, the sharp porphyrin absorption is present at around 400 cm^{-1} as well as the absorption typical for sandwich-like structures at 350 cm^{-1} indicating that the structure is also a closed triple decker.

Finally, the non-peripherally substituted closed triple decker analogue **58** (Fig 54) showed a particular spectrum. The main absorption was still at around 400 cm^{-1}, typical for porphyrins as well as triple deckers and also the absorption at around 300 cm^{-1} corresponding to sandwich-like structures but there was also the typical absorption of Pcs at around 600-700 cm^{-1} that is also present in double deckers.[75,101] It can be concluded that the absorption spectrum of **58** doesn't correspond to a closed triple decker and is more alike to those of double deckers (figure 53).

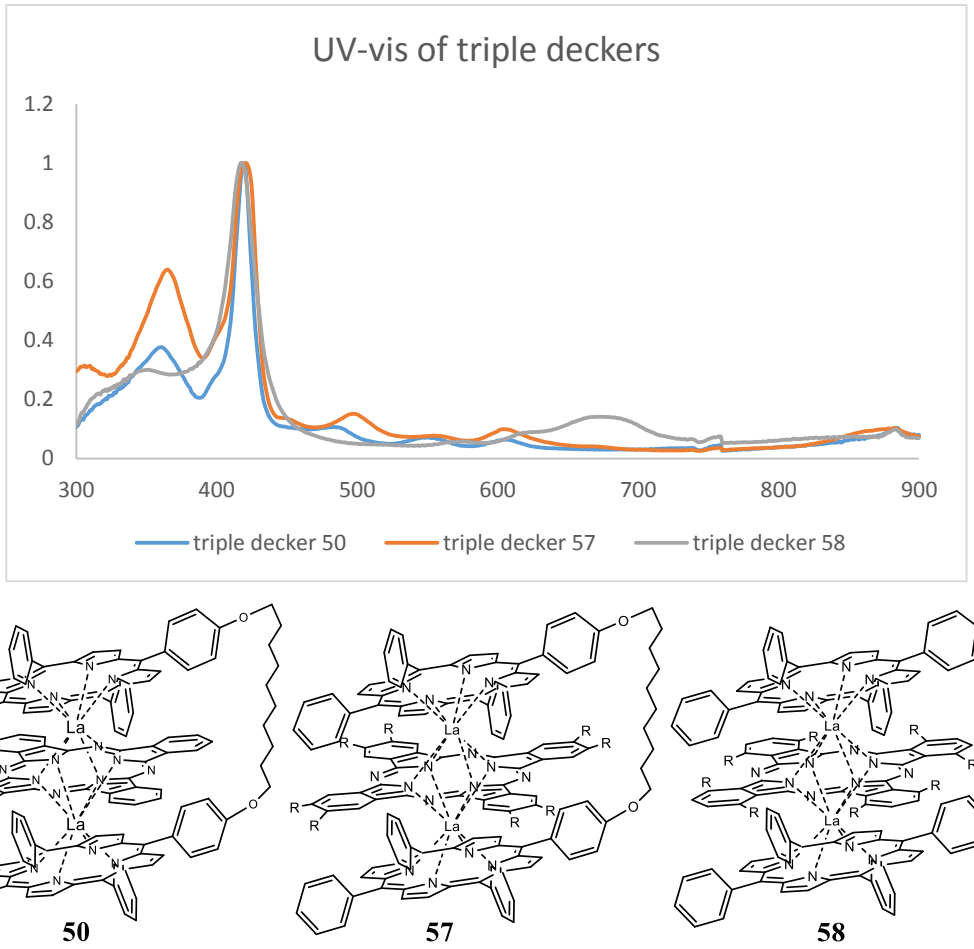

Figure 54. UV-vis of triple deckers **50**, **57** and **58**.

That observations for compound **58** (single spot on TLC as well as single and sharp MALDI-tof MS signal), could be explained if the compound had various structure arrangements and what is observed is the average of absorption of those arrangements. If the compound switch from one arrangement to another fast enough in the NMR time scale, that might explain why the NMR spectrum signals were not as expected for closed triple deckers or double deckers. That process could be the Pc switching from one of the porphyrins to the other to form an equilibrium between two different double deckers like it is proposed on the next scheme for structure of **58**.

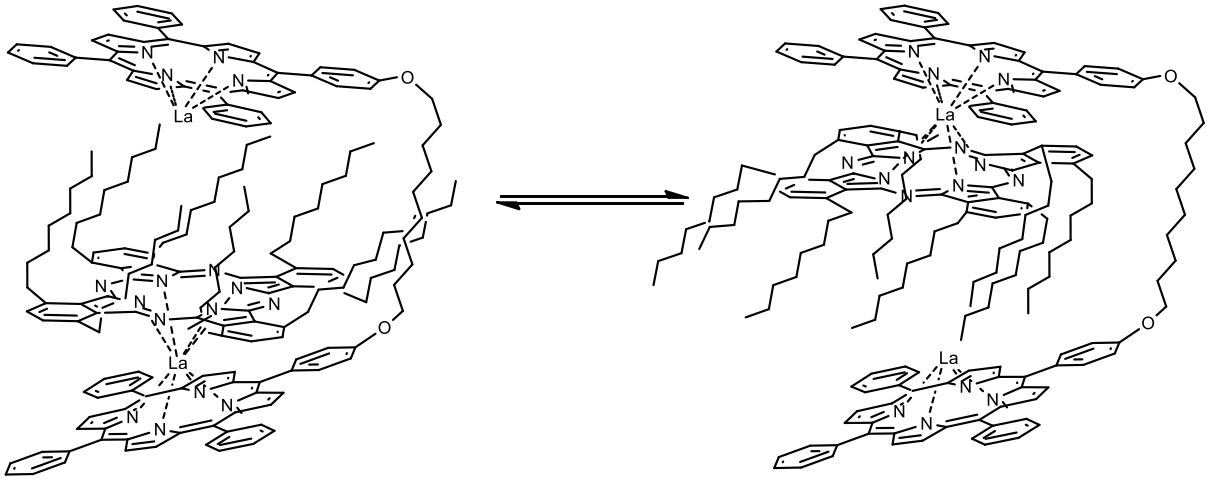

58 **58**

Scheme 41. Representation of the opening/closing process. Bond lengths and angles not representative for clarity.

This process could be supported due to the steric effects that this particular Pc has.[102] It can be observed in the X-Ray analysis for a similar metallated phthalocyanine[98] (figure 55), that the chains cannot fit the same plane of the Pc and therefore some of the side chains appear to be perpendicular to the Pc plane. This observed steric repulsion might be responsible or at least have some effect in how difficult it is for the triple decker to be formed.

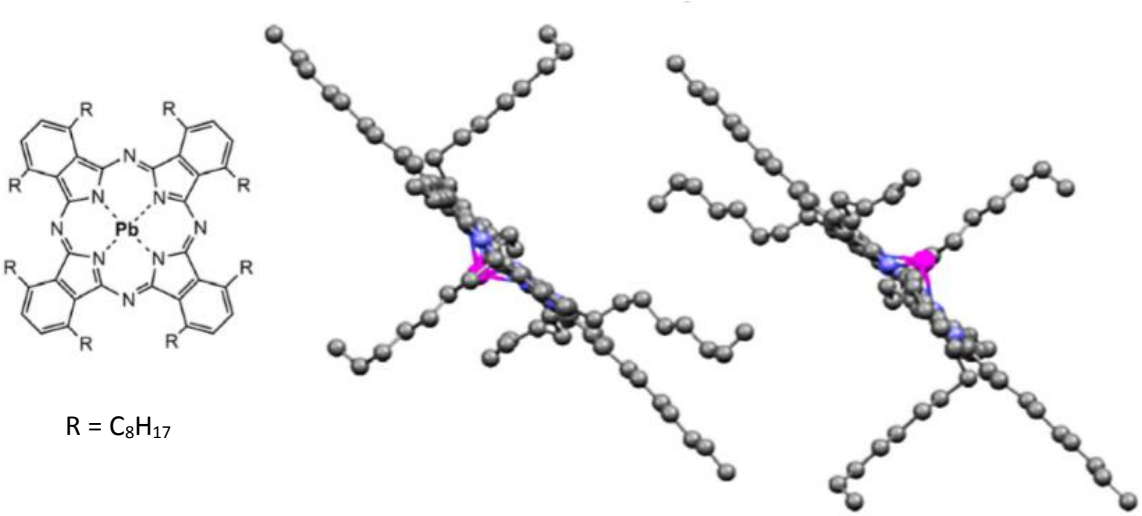

Figure 55. Previously reported X-ray structure for a metallated non-peripherally substituted phthalocyanine.[98]

This theory could be interrogated by the study of the formation of a non-peripherally substituted heteroleptic phthalocyanine porphyrin double decker **60** [C_8Pc]La[TPP] (scheme 42). The synthesis of this complex was attempted using both previously studied methods, addition of the already formed Pc **56** over the freshly metallated porphyrin and/or formation of the Pc in situ over the metallated porphyrin **31** using phthalonitrile **61** and DBU as catalyst as represented in the next scheme.

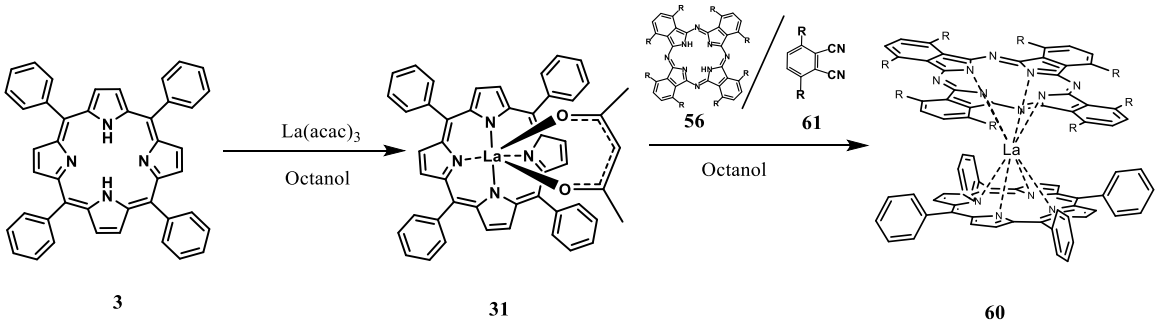

Scheme 42. Reaction pathway for the formation of **60** [C_8pC]La[TPP] complex via Pc **56** or phthalonitrile **61**.

In both cases the heteroleptic double decker **60** formation was checked by MALDI-tof MS (figure 56) after completion and work-up. The same results were obtained in all cases and formation of the double decker (m/z = 2161) was not observed in any case.

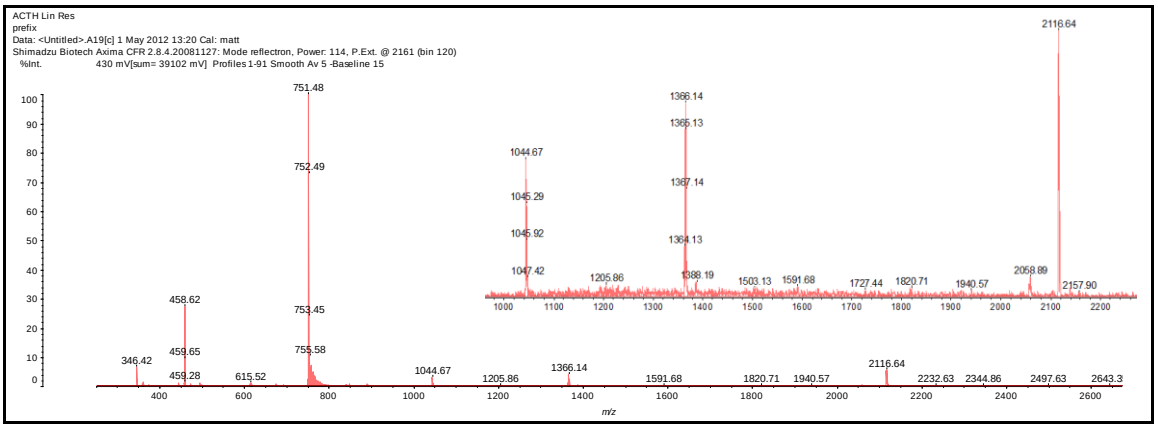

Figure 56. MALDI-tof MS of the crude reaction for the formation of double decker **60** via Pc **56**.

In this spectrum different compounds were observed with relative masses corresponding to: TPP **3** (615.5 m/z), La[TPP] **31** (751 m/z), La[TPP]$_2$ **62** (1366 m/z), La$_2$[TPP]$_3$ **63** (2116 m/z) and other peak with a relative mass of 1044 m/z that could not be assigned. No peak corresponding to the desired heteroleptic double decker **60** of 2161 m/z could be observed.

This result demonstrated that the non-peripherally substituted Pc **56** was not a good precursor for the formation of double deckers or triple deckers as after subjecting the metallated porphyrin to the double decker formation methods, the only sandwich-like structures that could be observed at the end were only porphyrin multideckers and formation of heteroleptic/homoleptic deckers containing the phthalocyanine were not observed.

Synthesis of closed triple decker 64

Another closed triple decker analogue was synthesised in order to see if the same results could be obtained with a different peripherally functionalised phthalocyanine. The triple decker was designed to have a peripherally substituted functionality that should help us further interrogate the ability of the internal porphyrin to rotate inside of the system. This Pc was then required to have bulky substituents in the peripheral positions with relative size between the non-substituted Pc **19** and the octaoctyl substituted Pc **55**. The selected phthalocyanine was dimethyldioxolane Pc **65**. This phthalocyanine has the perfect size and also, the dimethyldioxolane groups are suitable for a ^{1}H NMR study of the possible complex formed.

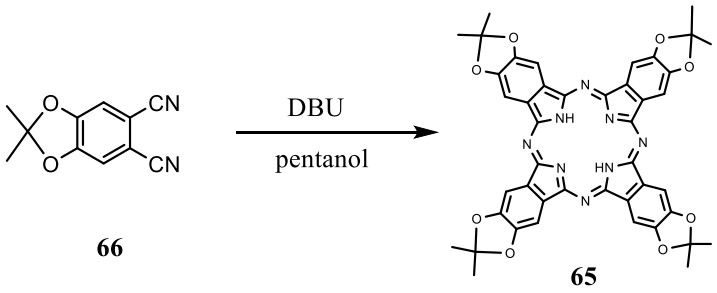

66 **65**

Scheme 43. Synthesis of phthalocyanine **65**.

Phthalocyanine **65** was obtained by heating phthalonitrile **66** and a catalytic amount of DBU in refluxing pentanol. When the reaction was completed, the phthalocyanine was selectively precipitated with MeOH and recrystallised from the THF/MeOH mixture. It was then used for the formation of the correspondent triple decker **64** as shown in the next scheme:

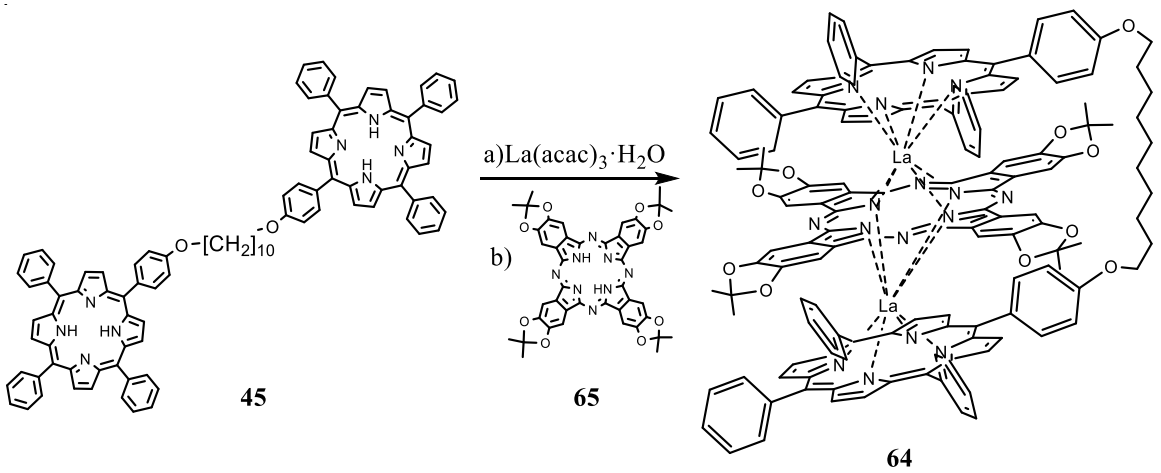

Scheme 44. Synthesis of triple decker **64**.

The same standard procedure of one pot, two steps of reflux in octanol was followed and after distillation of the solvent and precipitation of the crude residue with MeOH, the obtained solid was checked by MALDI-tof MS (figure 57). The desired peak corresponding to triple decker **64** at 2476.39 m/z was observed. Then, the crude solids were separated using silica gel chromatography followed by recrystallisation to collect the pure product as a brown solid in a 76 % yield.

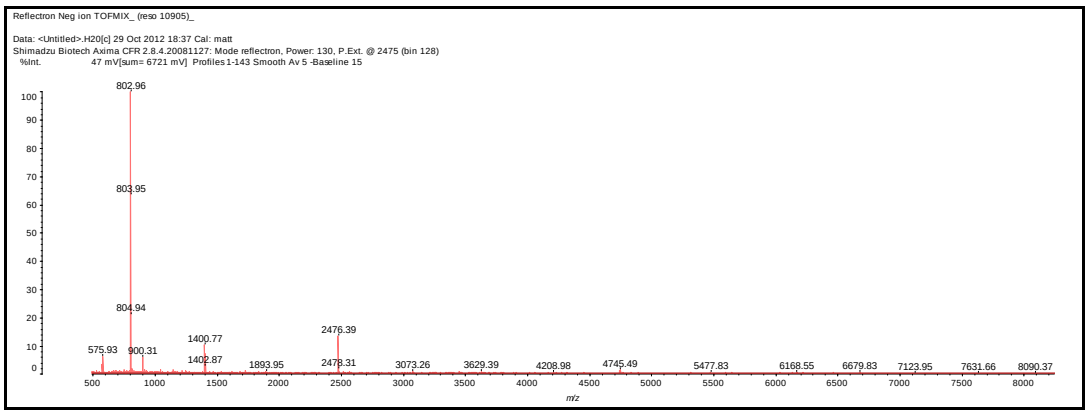

Fig 57. MALDI-tof MS of the crude mixture of **64** after concentration.

NMR spectrum of the pure product was successfully obtained in CD_2Cl_2 (figure 58) and the expected signals were observed, as compared with previous triple deckers. We observe the peaks corresponding to the Pc at around 8.6 ppm for the aromatic phthalocyanine protons as well as the signals corresponding to the dimethyldioxolane groups that are no longer symmetrical at around 2.14 ppm. This observed pattern matched with a blocked rotation of the Pc inside of the triple decker.

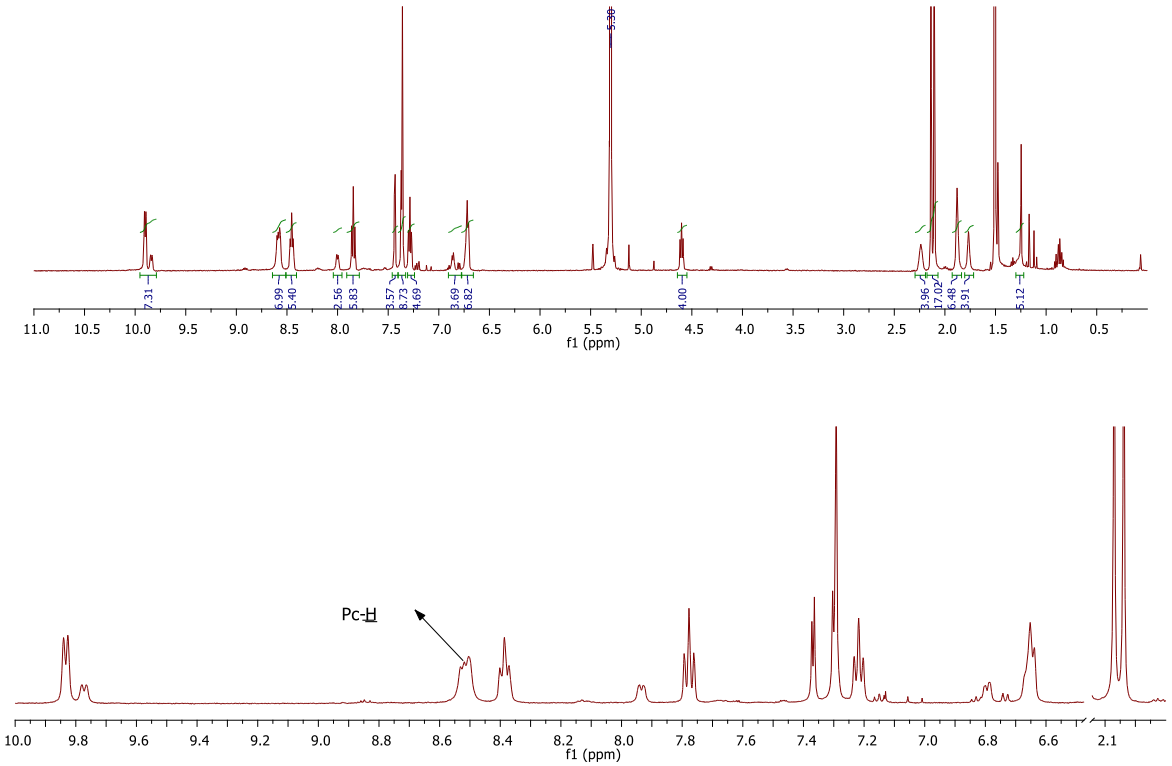

Fig 58. NMR spectrum obtained for **64** in d-DCM and expansion of the aromatic region and methyl peaks at around 2.14 ppm.

4.3.3.4. Rotation studies

Using the new optimised methodology, various closed triple deckers were synthesised (figure 59). This triple deckers, have different rotation properties as observed in the NMR spectra for the Pc aromatic peaks.

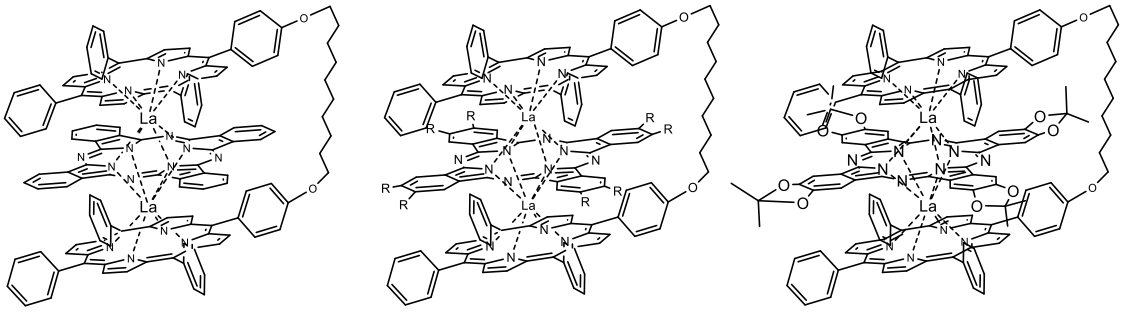

50 **57** **64**

R = C_8H_{17}

Figure 59. Different closed triple deckers synthesised.

We assume the central Pc can be observed rotating in unsubstituted triple decker **50** and that rotation to be completely blocked in peripherally substituted triple decker **57**. Finally triple decker **64** shows blocked rotation of the phthalocyanine and the aromatic signals appeared to be four broad singlets. This intermediate compound was then used to study if temperature changes can be used in order to modify the rotation of the complex. It could be expected that the rotation could be faster at high temperatures and slower at lower temperatures. According to this, the aromatic signals of the Pc could be expected to sharpen-up at lower temperatures as the system stops or slows down the rotation and to broaden as the temperature increase causing the rotation to be faster (figure 60). The coalesce temperature is defined as the temperature at which the appearance of the spectrum changes from that of two separate peaks to that of a single, flat topped peak.[103] Therefore by performing this study the coalescence temperature for the rotation of the Pc in the system was expected to be determined.

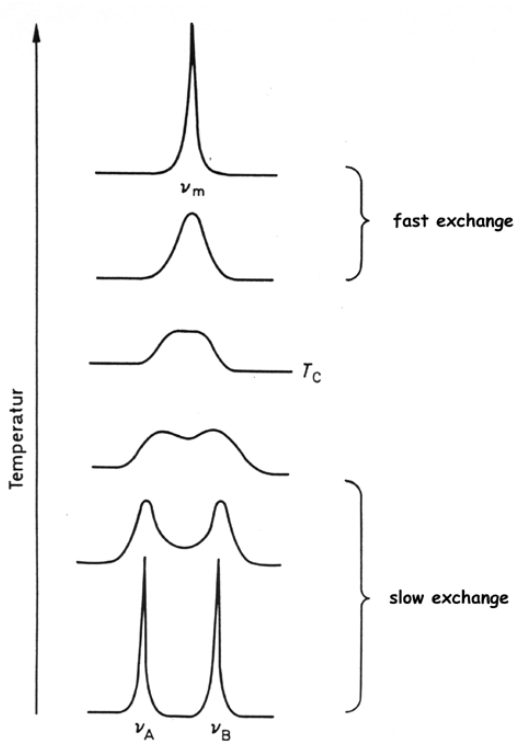

Figure 60. Proton resonance as a function of temperature.[103]

The first studies increased the temperature of the NMR experiments.[104] The boiling point of dichloromethane is relatively low so the solvent was exchanged to d-toluene and various ^{1}H NMR spectrums were collected at temperatures ranging from 300 K to 375 K (figure 63). By increasing the temperature, it was expected that the Pc rotation would be faster and then, the aromatic protons for the Pc should become a broad singlet at the coalescence temperature. The same process should then be expected for the dimethyldioxolane protons (the two singlets would coalesce).

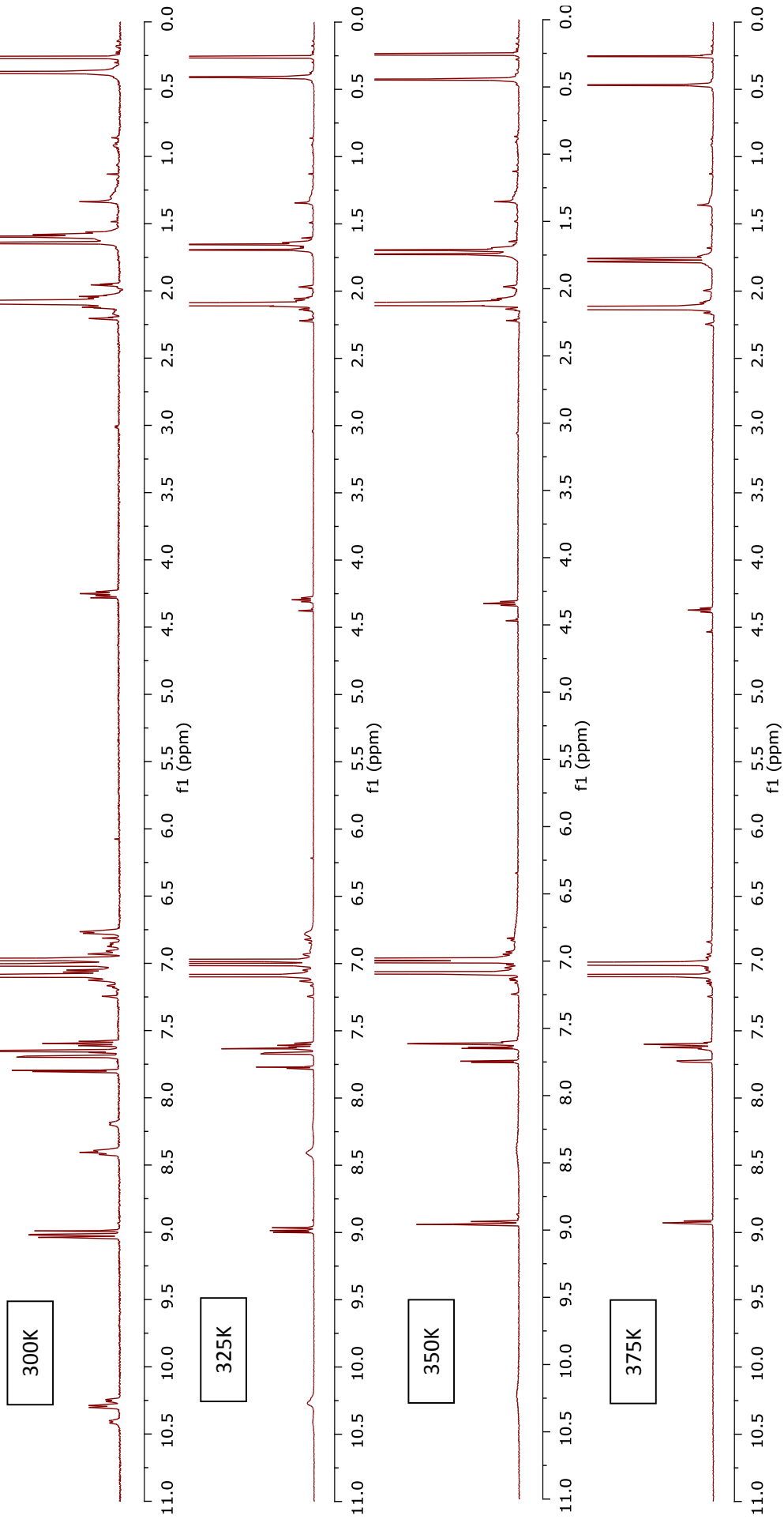

Fig 61. ^{1}H NMR spectrums of **64** in d-toluene at various temperatures.

In fact, when the temperature is increased, the signals for the phthalocyanine aromatic protons and the dioxolane methyl protons remains sharp. Temperature-related processes were observed but those changes did not occur in the Pc region of the spectrum as seen in the expansion of the aromatic region of the spectrum (figure 64). It was observed that the aromatic Pc peaks that appeared at around 9.0 ppm remained sharp at 300 K and 375 K. No coalescence was observed for the given peaks, only slight shifting regarding to temperature changes. On the other hand, beginning of coalescence procedures were observed for the phenyl protons of the porphyrin rings at around 10.2, 8.4, 7.6 and 6.7 ppm ($_{oi}$Ph*H*, $_{oo}$Ph*H*, $_{mi}$Ph*H* and $_{mo}$Ph*H* respectively) as they became broad signals. Unfortunately the coalescence temperature could not be reached as it was above the boiling point of the solvent used in the NMR spectrum (383.83 K).

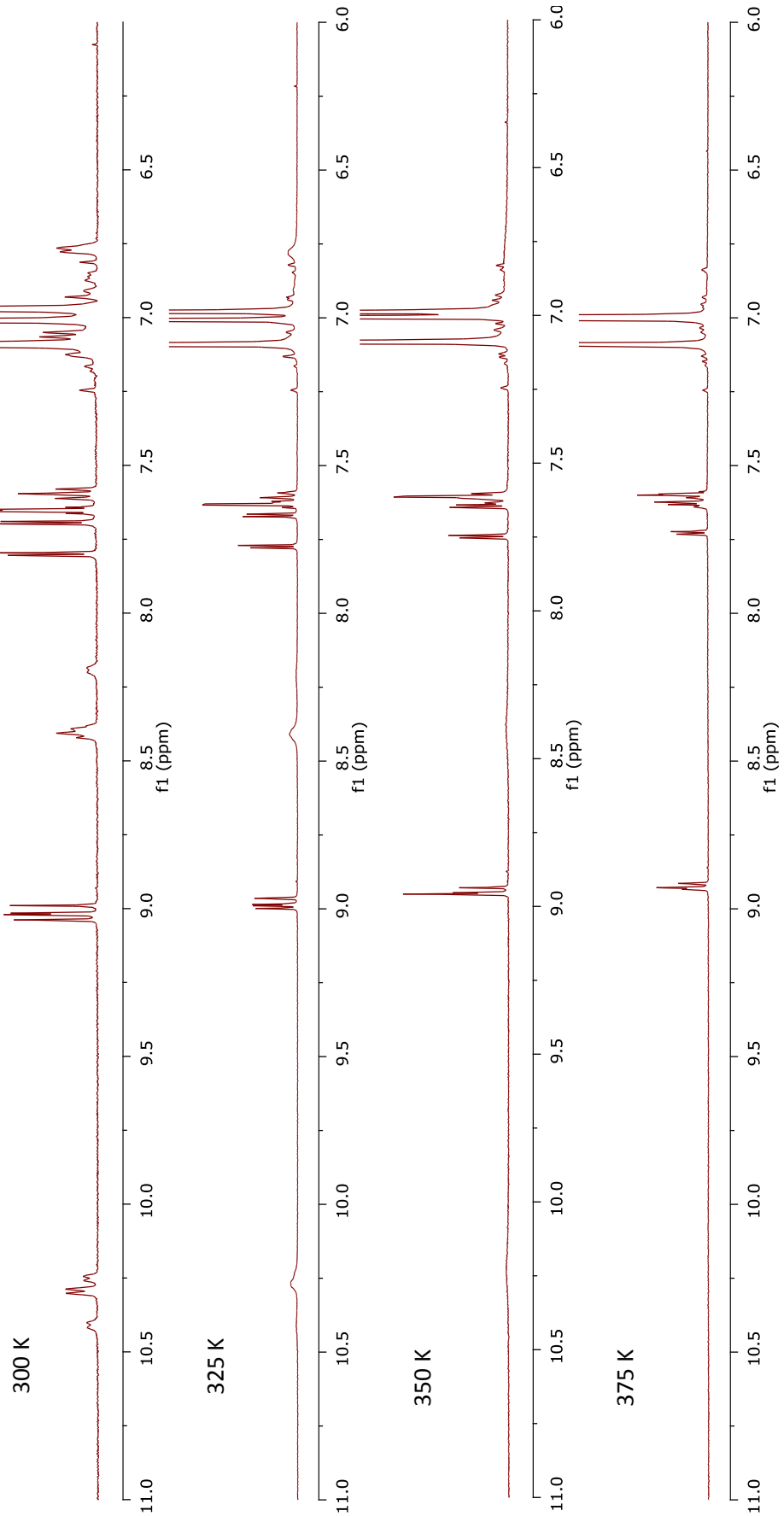

Fig 62. Optimised aromatic region expansions of the ^{1}H NMR spectrum of triple decker **64** in d-toluene in various temperatures.

4.3.4. Conclusions

The synthesis of porphyrin dyad double decker **49** was not possible using the simple analogues due to the preferable formation of triple deckers **50** and **53** instead. This process, explain the high complexity of the reactions that where performed with the multiporphyrin arrays during the previous chapter as other different complex triple deckers could have been formed instead using the same reaction conditions. On the other hand, the triple deckers formed under this chapter were of high interest as they are molecular machines by themselves and therefore were studied in more depth. Synthesis of various analogues of the closed triple decker **50**, **53**, **57** and **64** were possible by the refinement of the methodology for synthesizing the triple deckers. This method allowed the synthesis of triple deckers selectively without formation of other side products, as occurred in previously developed methodologies.[88,94] This lack of side products also produced the triple deckers in unprecedented high yields that are in the range of 76-96 % yield, allowing us to design different triple decker analogues selectively and in reasonable amounts for future analysis.

The rotation properties of closed triple deckers was studied further by the design and careful analysis of various triple decker analogues with different steric hindrance. The analogues could be synthesised with different substituted Pcs. The analogues where the Pcs are substituted in the non-peripheral positions seem to behave differently to the peripherically substituted ones and the characterisation was much more complicated. Substituted triple decker analogues allowed us to have some different Pcs embedded in between porphyrins. Some phthalocyanines shown rotation properties which could be blocked by the substitution of the Pc for another one with bulkier substituents on the peripheral positions, allowing us to have different triple deckers with and without rotating units allowing us to have some control by design. The modification of the rotation of the Pc with variations of temperature seems tricky and more analogues need to be designed to find the limits between rotation and no-rotation in the NMR time scale.

Indeed, although a single compound was isolated which has a mass corresponding to the triple decker, spectroscopic evidence suggests a rapidly equilibrating structure exists.

4.4. Synthesis of magnetic closed triple deckers

Lanthanides are metals with lots of electrons and the first row containing occupied f orbitals. The magnetic properties of lanthanides are currently of great interest.[105-107] In particular, metals with high magnetic properties are being extensively studied because of their possible applications in the field of single molecule magnets (SMMs).[105] This provides the metals with high magnetic susceptibilities which are the origin of their magnetic behaviour. Several experimental values of magnetic susceptibilities have been obtained for lanthanides.[108-110] Some theoretical models for the simple calculation of magnetic susceptibilities have been also reported.[106] All this information shows that the middle-late lanthanides, dysprosium to erbium, are the lanthanides with the highest magnetic susceptibilities (figure 65).[106]

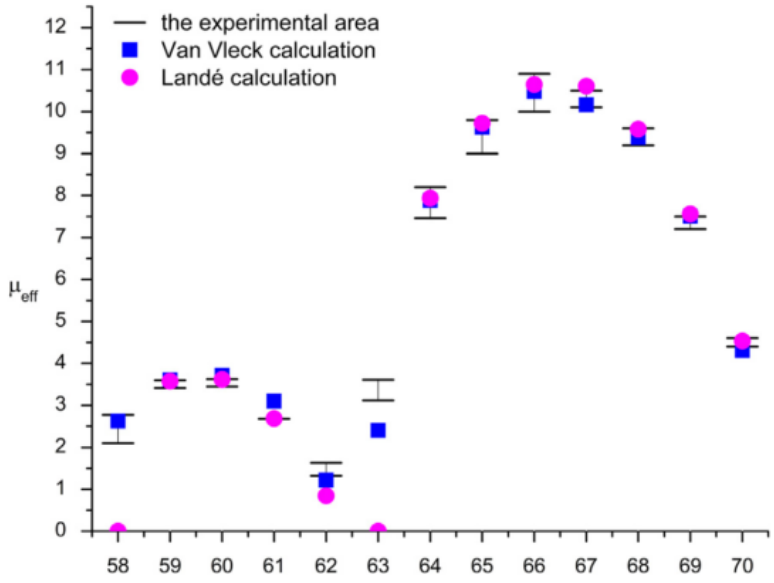

Figure 65. Magnetic susceptibility of Ln^{3+} ions (with the atomic numbers) at room temperature.[106]

In particular, triple decker structures with magnetic metals such as Dy or Y, show the most interesting magnetic properties as reported by J. Jiang (see figure 66).[105] During their work, some triple deckers were synthesised and their structure fully analysed by X-Ray crystallography.[59,95] Also their magnetic properties appear to be angle-dependant which is a very interesting characteristic as the previously synthesised closed triple deckers developed during this thesis appear to be completely overlapped, having a different angle θ. This

overlapping is a really unique structure observed for triple deckers which could lead to unique characteristics.

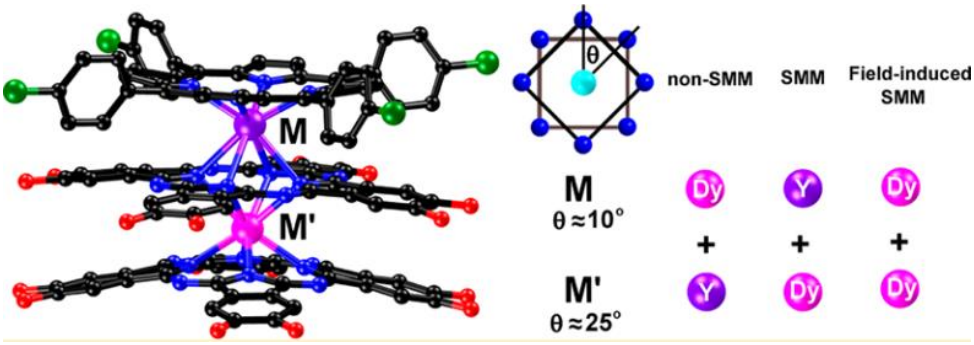

Figure 66. Molecular structure of magnetic triple deckers reported by J. Jiang.[105]

During this work, different closed triple deckers containing highly magnetic lanthanides were studied. The synthesis of triple deckers were performed from previously linked porphyrin dyads as developed in previous chapters. Because of availability, high magnetic susceptibility and previously optimised synthesis, closed triple deckers of dysprosium **67** were selected as targets during this work.

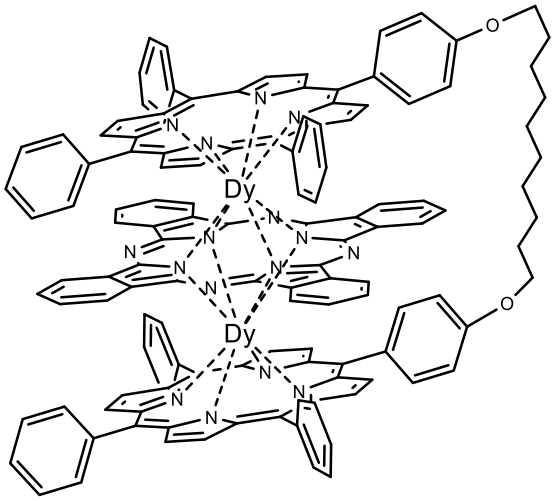

67

Figure 67. Targeted Dy triple decker **67**.

Characterisation of this complex was expected to be challenging as its magnetic properties make the ^{1}H-NMR spectra analysis difficult due to the lanthanide induced shifts.[107] This effect was firstly reported by Hinckley in 1969.[111] It appears as a substantial chemical shift caused by lewis acid complexation of lanthanide atoms with other molecules. The effects are consistent with the presence of large shielding and deshielding cones around the lanthanide atom caused by unpaired electrons in the f shell of the lanthanide.[112] For example, europium complexes produce downfield shifts while praseodymium complexes produce upfield shifts.[112] Such metals were widely used as shift reagents for the determination of enantiomeric purity during the 1970s and 1980s.[113]

A few ^{1}H-NMR spectrums of triple decker structures of dysprosium were previously reported in the range between 10 ppm to -70 ppm (figure 68) and same characteristics should therefore be expected for structure **67**. It can be observed in the spectra that there are some highly upfield shifted phthalocyanine peaks (i and ii) due to the effect of the magnetic metals.

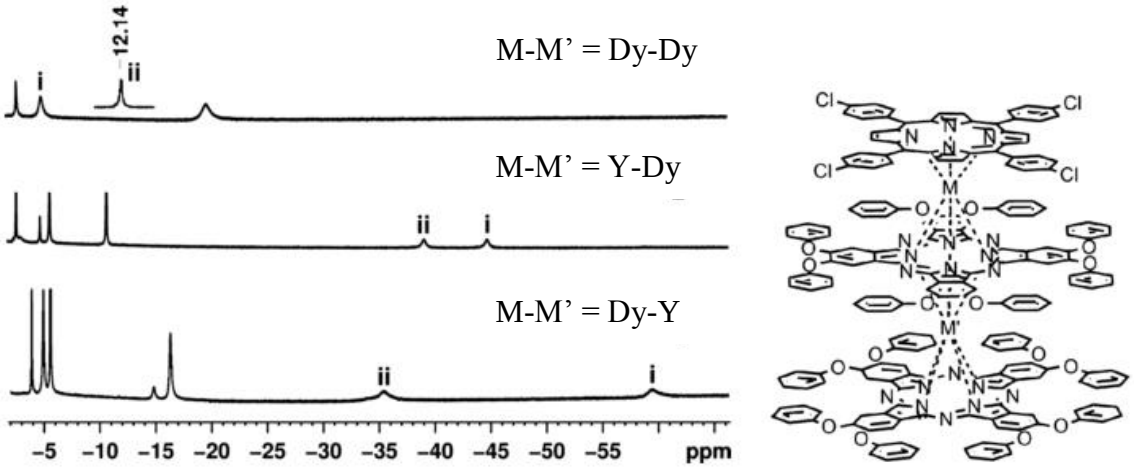

Figure 68. Various ^{1}H NMR spectrum expansions of various triple deckers.[105]

4.4.1 Synthesis of dysprosium closed triple decker

Following the general procedure for the synthesis of closed triple deckers described in the previous chapter, the synthesis of dysprosium closed triple decker **67** was attempted using C_{10} porphyrin dyad **45** as starting material as represented below.

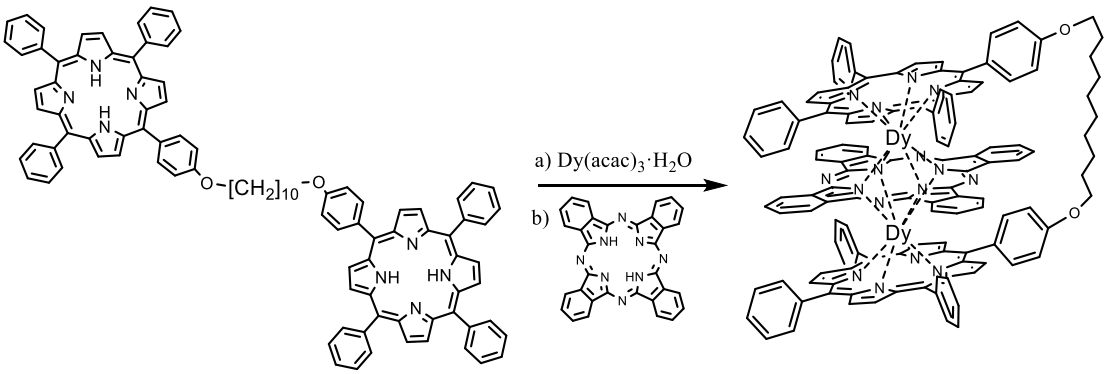

45 **19** **67**

Scheme 45. Proposed synthesis of dysprosium closed triple decker **67**.

The reaction was performed by refluxing porphyrin dyad **45** and $Dy(acac)_3 \cdot H_2O$ for 6 h in octanol. After the metallation was completed, Pc **19** was added and the mixture refluxed overnight. Then, the solvent was eliminated by distillation and the resulting crude solid analysed by MALDI-tof MS observing the formation of various high mass structures on the expected range.

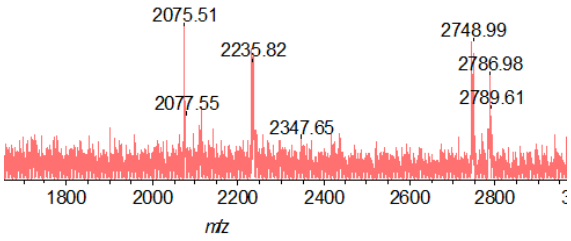

Figure 69. Expansion of the MALDI-tof MS obtained.

The relative masses observed corresponded to the addition of one dysprosium metal and one phthalocyanine (2075.51 m/z), two dysprosium metals and one phthalocyanine (2235.82 m/z) and finally two dysprosium metals and two phthalocyanines (2748.99 m/z). These additions could match different arrangements with the same relative masses.

The crude mixture was then separated by silica gel column chromatography using THF/Pet ether as eluent. Two different fractions were collected but neither appeared to be pure by TLC analysis, so both were mixed together and separated on neutral alumina column chromatography. After successful separation of both fractions, they were analysed by MALDI-tof MS and ^{1}H NMR spectroscopy. The first fraction corresponded to a relative mass of 2074.29 m/z and the second fraction corresponded to a relative mass of 2235.85 m/z. No other compound could be collected from the column. The fractions matched with the addition of one metal and one phthalocyanine to the starting material and two metals and one phthalocyanine respectively. The NMR spectra obtained for this first fraction appeared to be an extremely complicated NMR spectrum on the range of 10 to -75 ppm as shown on the next figure.

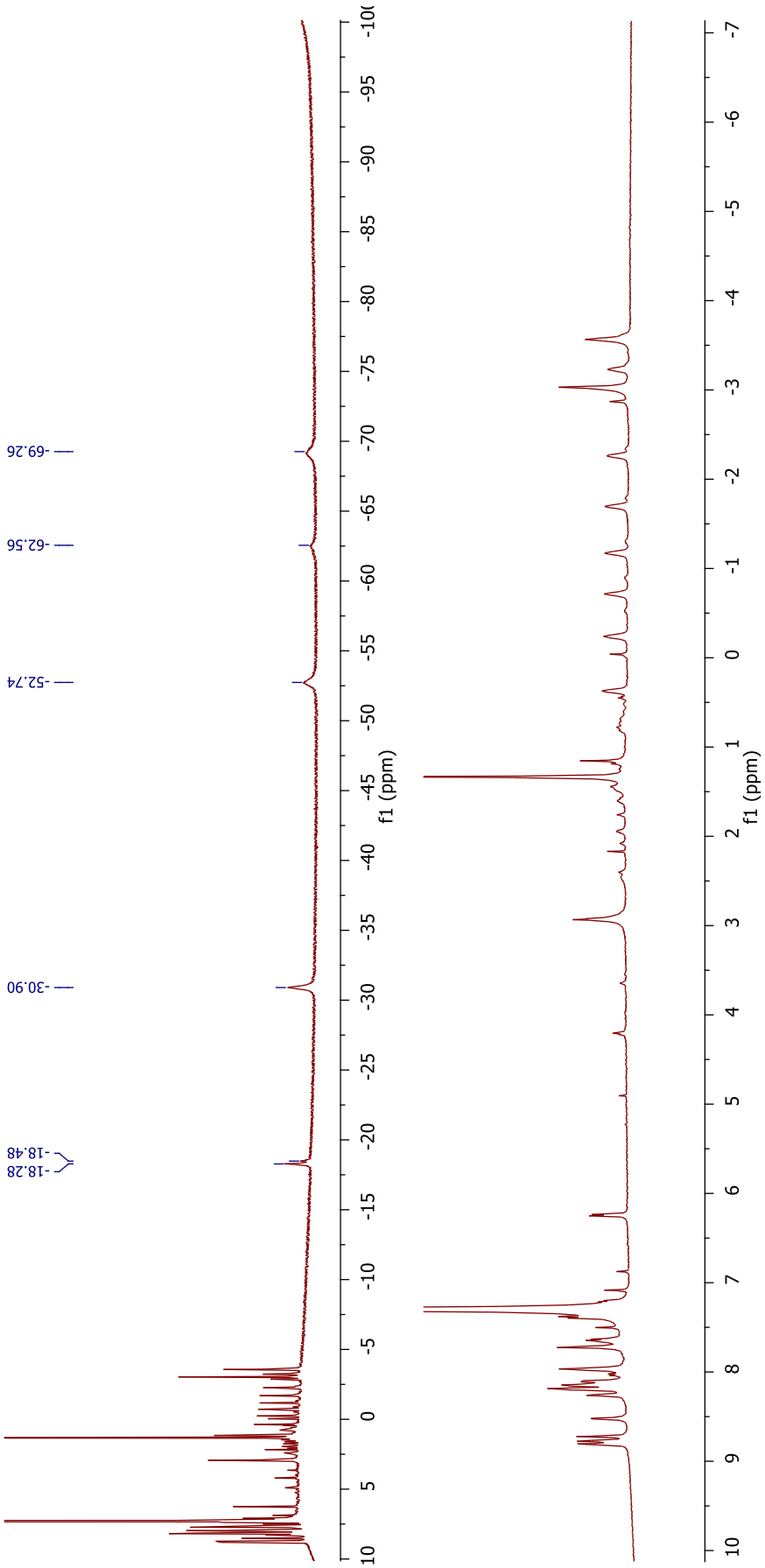

Figure 70. ^{1}H NMR spectrum and expansions of the fraction of relative mass 2074.29 m/z.

The highly upfield shifted ^{1}H NMR spectra obtained was in agreement with previous reports of porphyrin/phthalocyanine dysprosium complexes (see figure 68).[105] This could indicate that a sandwich-like structure of dysprosium was formed. The decker structure could be a double or a triple decker but, according to the relative mass obtained (2074.29 m/z), it can be concluded that only one metal and one phthalocyanine were added to the porphyrin dyad. Therefore, only a double decker structure was formed and the obtained product must be extended double decker **68**.

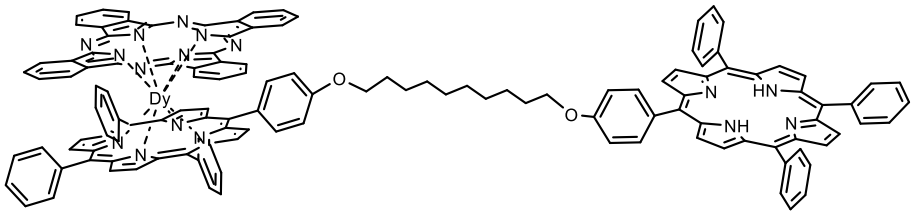

68

Figure 71. Proposed structure for extended double decker **68**.

In the ^{1}H NMR spectrum, the region between 9 and 7 ppm of the spectrum corresponds to the free porphyrin part of the molecule, the same region as the highly shifted peaks corresponding to the double decker which makes the peak assignment difficult. Another region to be interrogated are the aliphatic protons interconnecting the porphyrins. These peaks were seen between 4.5 and -4.0 ppm also in accordance with the formation of the double decker in one side of the system. It should be expected that the C$\underline{H_2}$ protons are all different and highly shifted the closer they are to the double decker.

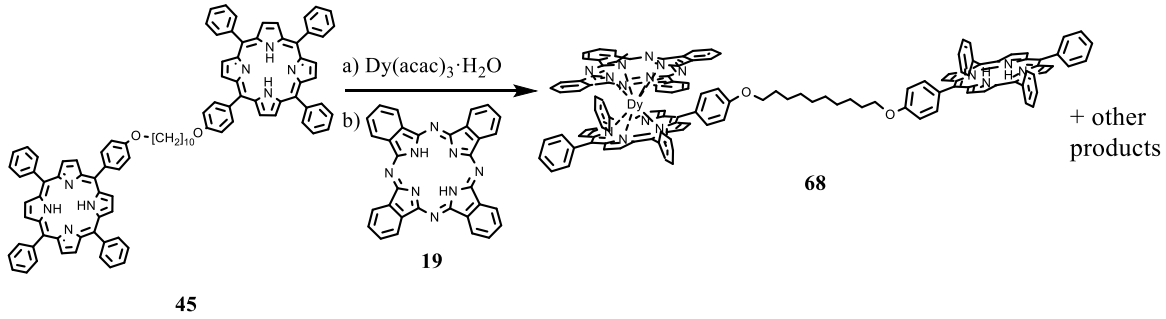

45 **19** **68**

Scheme 46. Proposed reaction scheme.

On the other hand, the second fraction from the reaction of relative mass 2235.82 m/z, corresponded to the desired dysprosium triple decker **67**. This triple decker **67** was further purified by column chromatography but an analytically pure sample could not

be obtained. In all attempts, traces of porphyrin dyad **45** and extended double decker **68** were observed as fractions, even when they were not observed in the TLC analysis before the separation process. This observation could prove the relative instability of this dysprosium triple decker as it could not be obtained as a pure material by column chromatography.

4.4.2 Selective synthesis of mixed metal triple deckers

This dysprosium double decker complex **68** is the perfect starting material for the selective synthesis of triple deckers with mixed metallic centres. This, allows the development of a synthesis by design were the second metal can be selectively inserted. The proposed synthetic strategy involves the formation of the open double decker dyad **68** followed by a second metal insertion forming the desired mixed triple decker **69** selectively, as represented on the next scheme.

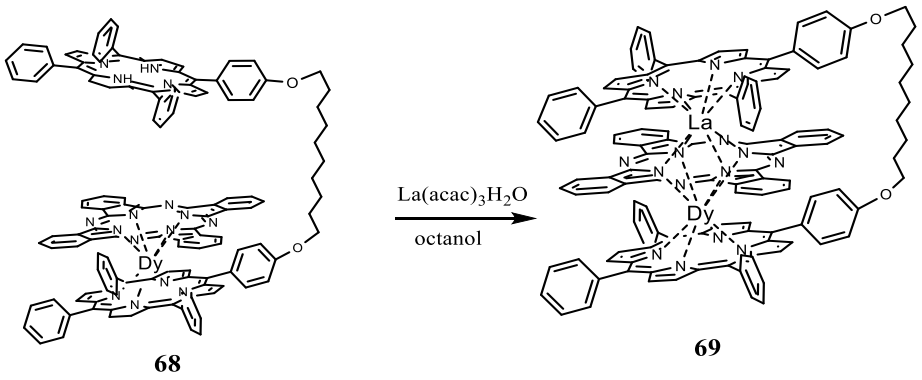

68 **69**

Scheme 47. General procedure for the selective synthesis of mixed metal triple decker **69**.

A test reaction was performed by refluxing the previously synthesised double decker dyad **68** and lanthanum acetylacetonate hydrate for 24 h. Then, the solvent was distilled and the crude solid recrystallized from DCM/MeOH. The recovered brown solids were checked by MALDI-tof MS (figure 72).

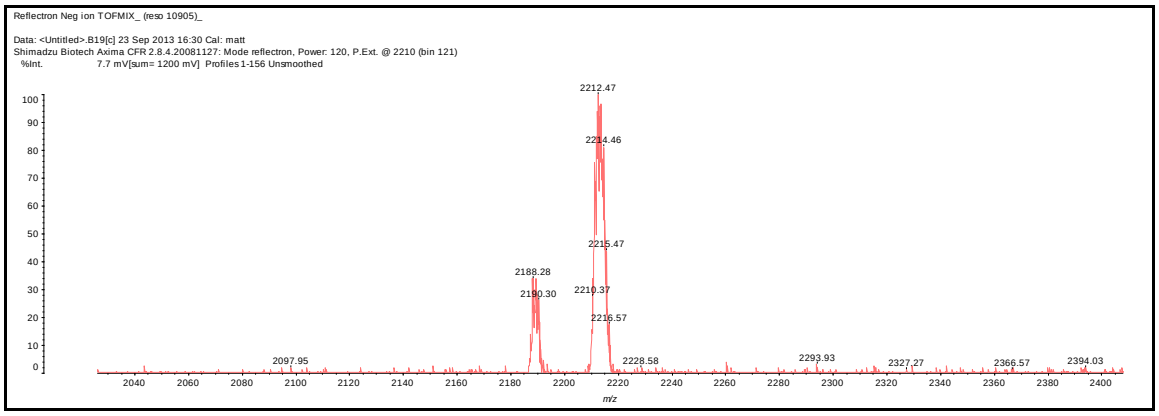

Fig 72. MALDI-tof MS for the crude mixture for the formation of mixed triple decker **69**.

By analysis of the obtained spectrum, it could be concluded that the desired triple decker (Exact mass = 2210.58 g/mol expected, and m/z = 2212.47 observed) was successfully formed. It can also be observed the formation of another compound of 2188.28 m/z that matched with the bislanthanide triple decker **50**. After passing the crude solids through a silica gel pad using DCM as eluent, the main brown fraction was collected and TLC analysis showed a single spot. The same MALDI-tof MS was then obtained for this fraction and ^{1}H NMR spectrum (figure 73) was then processed observing a mixture of both triple deckers LaDyTD **69** and LaLaTD **50**.

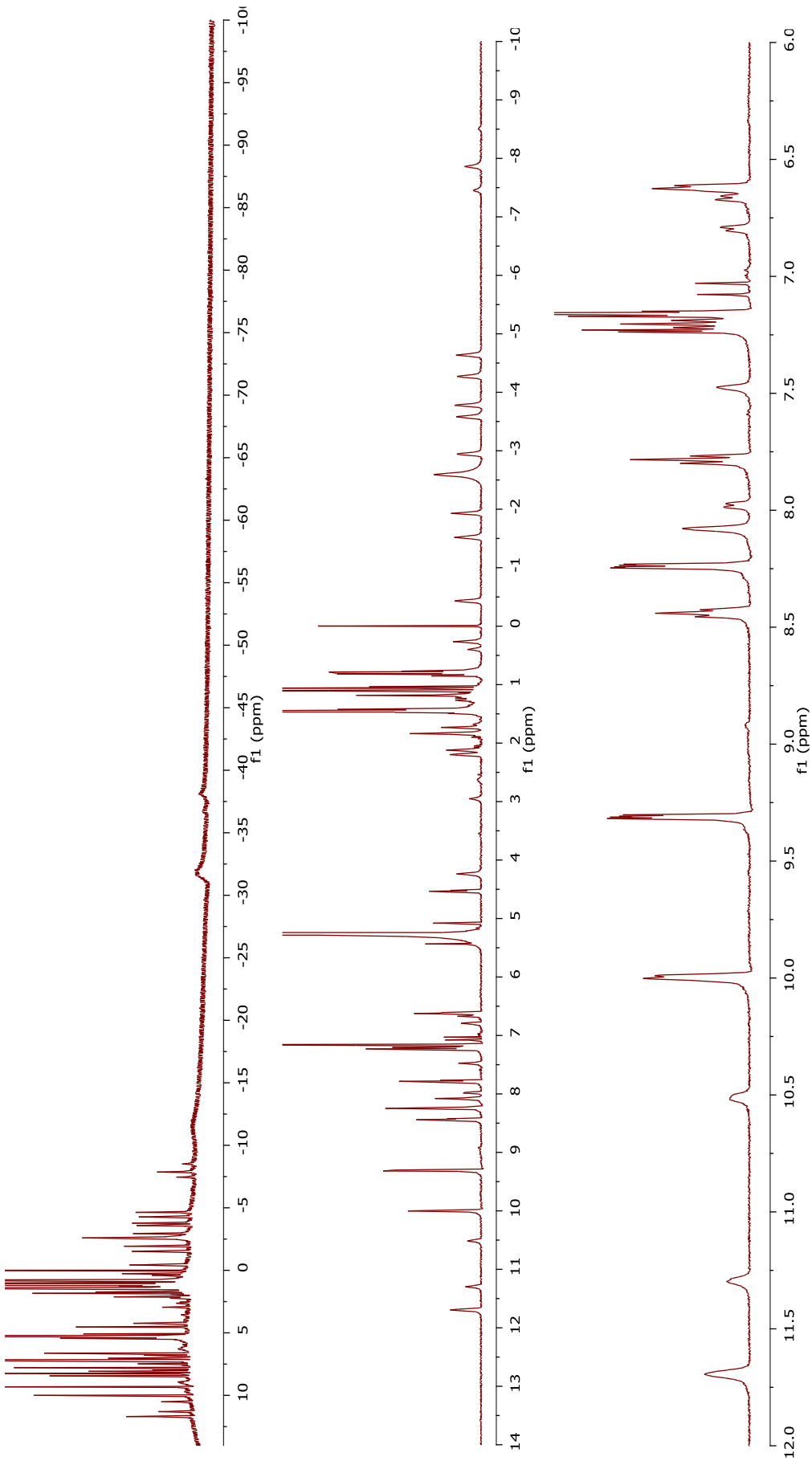

Figure 73. ^{1}H NMR spectrum and expansions obtained for the mixed triple decker test reaction brown fraction.

Further purification attempts by column chromatography or recrystallizations were unsuccessful and both triple deckers could not be separated. The reaction was then tried in a bigger scale to try to separate the mixture of triple deckers by recrystallisation or prep-TLC but all attempts were unsuccessful.

The next attempt tried was the one pot two steps reaction for the selective formation of mixed triple decker **69** to check if the purification of the intermediate extended dysprosium double decker **68** is avoidable and also to check if the synthesis of the mixed triple deckers can be reproduced.

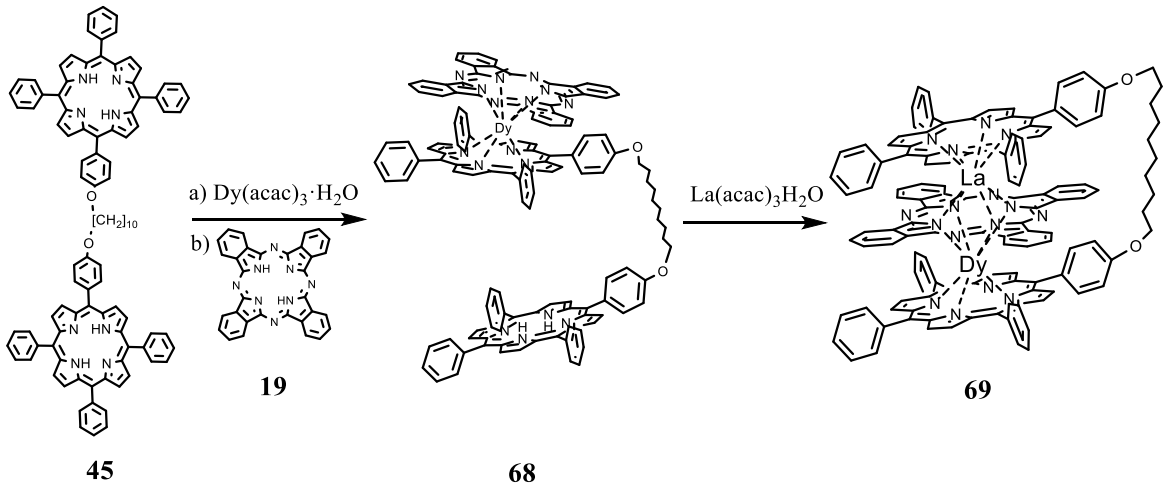

Scheme 48. Proposed one pot two step synthesis of mixed triple decker **69**.

In this case, porphyrin dyad **45** was subjected to metallation with 1 eq of dysprosium acetylacetonate in refluxing octanol for 6 h. Then, Pc **19** was added to the mixture and the mixture refluxed overnight to form the intermediate **68** in situ. After the overnight reaction, lanthanum acetylacetonate was added to the reaction and everything refluxed for further 24 h. When the reaction was completed, the solvent was distilled and the resultant solids recrystallised. MALDI-tof MS of the obtained brown solids was analysed and a complex mixture was observed, the LaLaTD **50** being the main peak. A complex mixture was also observed by TLC analysis so this approach is not useful as it resulted in a more complex mixture than the step-by-step procedure previously developed.

During this reaction, formation of lanthanum triple decker **50** was observed in all cases, even when starting from the pure intermediate dysprosium extended double decker **68**. This result showed that the dysprosium metal might be exchanged by a lanthanum metal during the reaction process. This observation can be tested by a simple reaction in which the

obtained mixture of triple deckers **50** and **69** obtained previously will be treated with lanthanum acetylacetonate metal under the standard reaction conditions of refluxing octanol. During this process, dysprosium metal is expected to be exchanged by lanthanum, the disappearance of the peak corresponding to DyLaTD **69** in the MALDI-tof MS analysis should disappear and mainly the peak corresponding to LaLaTD **50** should be observed as represented in the next scheme.

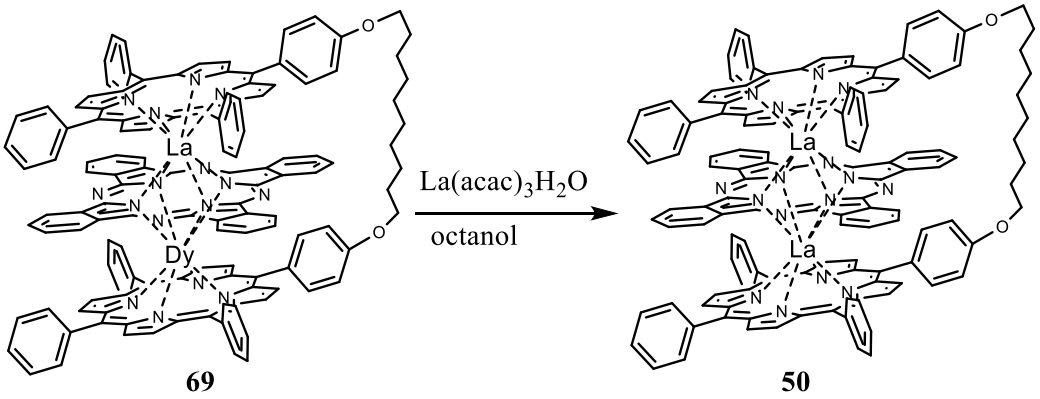

Scheme. 49. Possible side reaction of substitution of dysprosium for lanthanum.

A mixture of triple deckers **69** and **50** was refluxed with an excess of lanthanum acetylacetonate in octanol. A reference of the mixture of triple deckers was checked by taking an aliquot from the reaction mixture before the addition of the lanthanum metal complex. Another aliquot of the same volume was taken after 24 h reflux. This way, all the parameters were maintained constant during the MALDI-tof MS analysis.

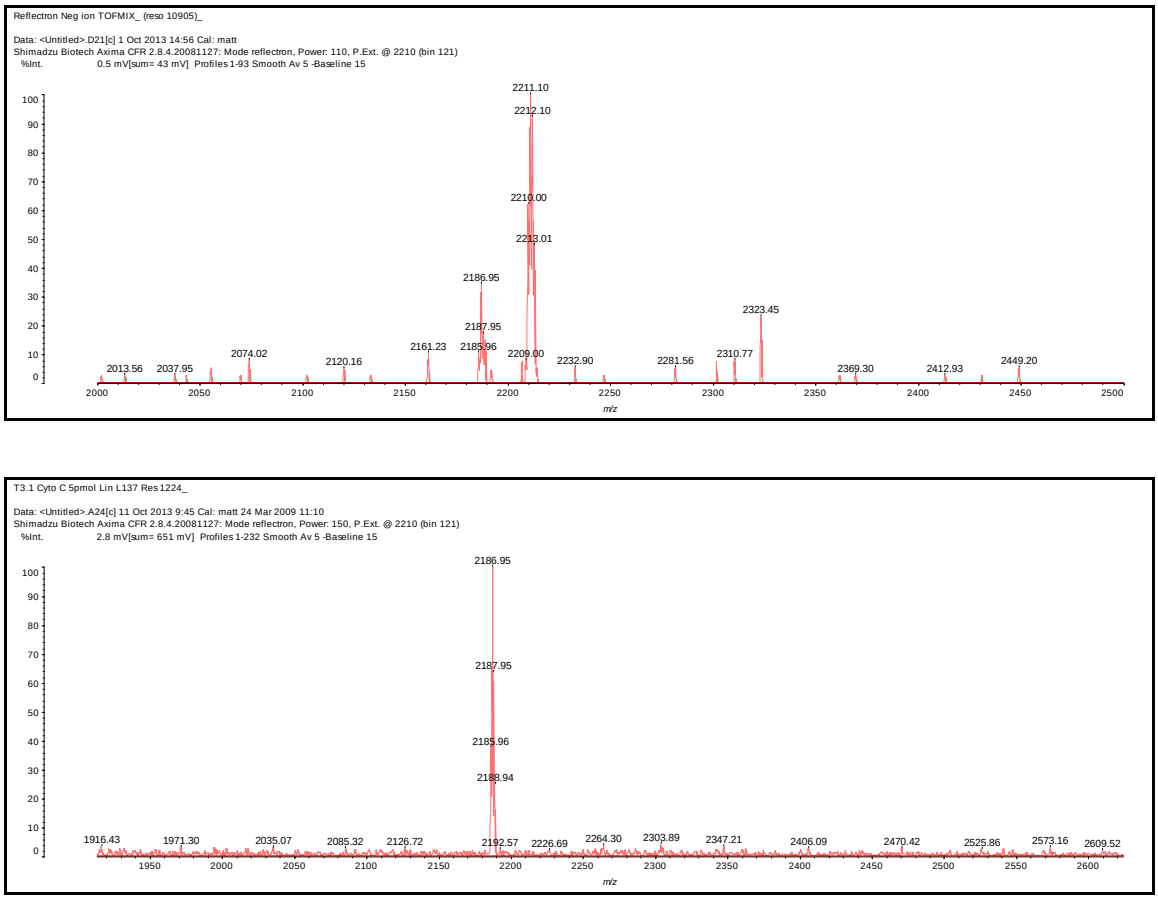

Figure 74. MALDI-tof MS of the aliquots before (above) and after (below) 24 h reflux.

With this simple test, it could be observed that the peak corresponding to the mixed TD **69** of 2211.10 m/z was no longer present and only the peak corresponding to the TD **50** of 2186.95 m/z was observed in the crude MALDI-tof MS after the reaction. This result indicated that the dysprosium ion was displaced by lanthanum ions under the standard reaction conditions. Therefore, selective synthesis could not be achieved in a stepwise manner for this particular set of triple deckers.

Synthesis of mixed metal triple deckers from C_{12} porphyrin dyad 71

The next study regards the dependence of the chain length interconnecting the porphyrins in the formation of mixed metal triple decker complexes. This feature was tested by performing the same reaction conditions previously developed but using a longer C_{12} porphyrin dyad **46** as starting material. Dysprosium double decker extended dyad **70** was

first synthesised followed by reaction with the corresponding lanthanum metal to form the desired triple decker as represented in the next scheme.

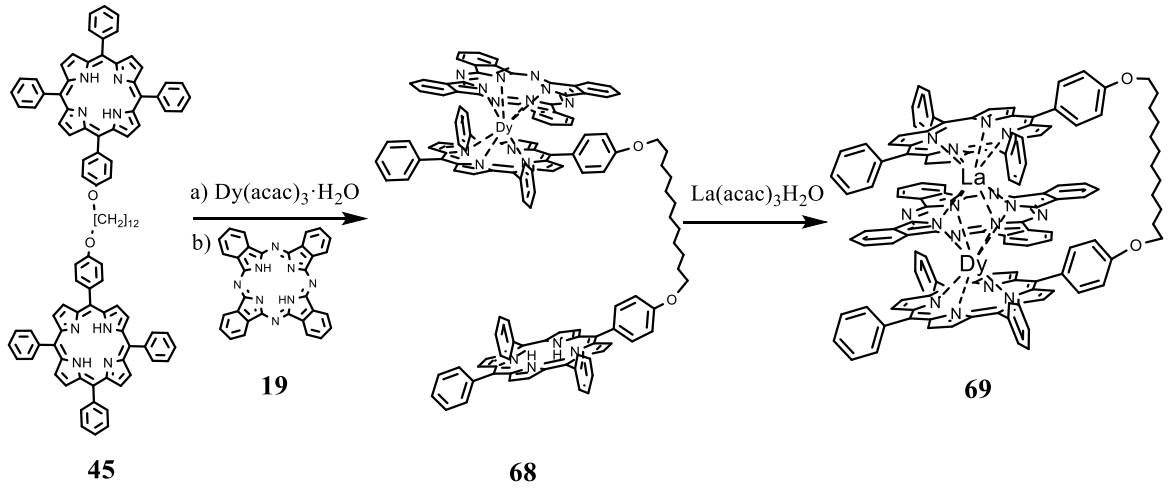

45 **19** **68** **69**

Scheme 50. Proposed synthesis of mixed triple decker **71** from the C_{12} dyad **46**.

The first step consisted in metallation of C_{12} porphyrin dyad **46** using dysprosium acetylacetonate metal in 6 h of refluxing octanol. Then, phthalocyanine **19** was added and everything refluxed for 18 h. After the reaction, the crude mixture was concentrated to dryness and recrystallised from DCM/hexane. The filtered dark solids containing the desired double decker **70** were purified by several column chromatography and recrystallizations but analytically pure material could not be obtained. It was then used without further purifications for the next step (single spot in TLC).

Then, partially purified **70** was mixed with ≈1 eq of lanthanum acetylacetonate and refluxed in octanol for 18 h. After precipitation of the crude mixture and purification by column chromatography, the product was analysed by TLC to appear as a single brown spot. After performing a MALDI-tof MS of the product (figure 75), it appeared again as a mixture of two triple deckers, one of them with two lanthanum metals **72** (m/z = 2215. 47) and the other one with mixed metals **71 (**m/z = 2239.68), one dysprosium and one lanthanum as it appeared for the C_{10} analogues.

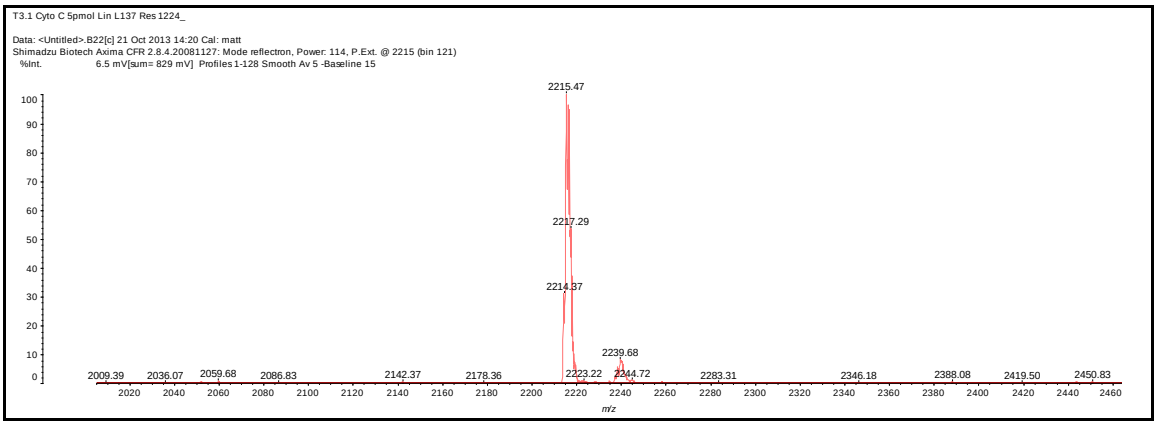

Figure 75. MALDI-tof MS of the crude mixture of formation of triple decker **71**.

Then, the mixture of triple deckers **71** (La, Dy) and **72** (La, La) was treated with an excess of lanthanum acetylacetonate and refluxed for 24 h. The reaction crude obtained was checked by MALDI-tof MS to check if the dysprosium metal was exchanged for lanthanum.

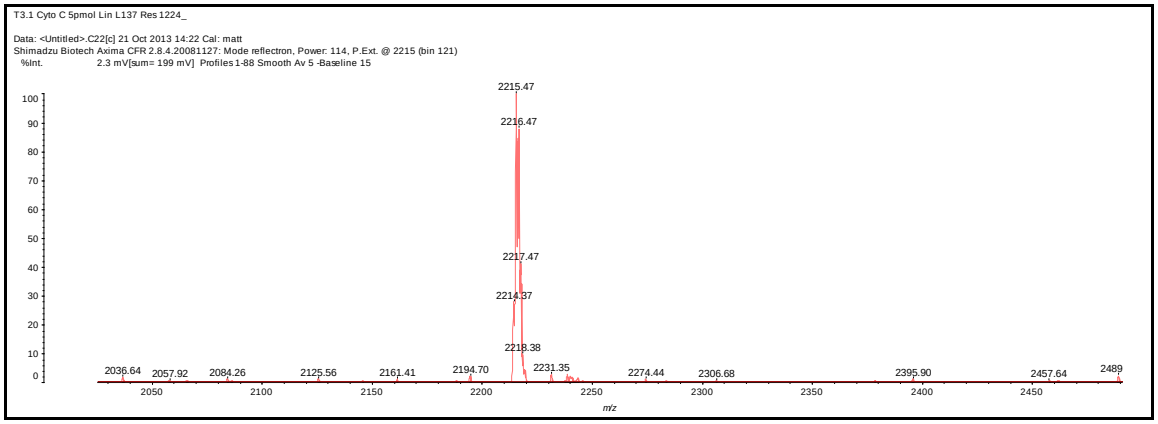

Figure 76. MALDI-tof MS of the crude mixture of metal exchange test.

In this case, the dysprosium was also exchanged for a lanthanum ion in the mixed metal triple decker complex **71** as it can be observed by the MALDI-tof MS analysis as the peak corresponding to 2239.68 m/z could not be observed anymore in the spectrum.

4.4.3 Conclusions

Triple deckers of dysprosium could not be synthesised using the developed procedure for the selective formation of linked closed triple deckers. Instead, extended double decker **70** was obtained. This extended double decker, was tested as a starting material for the selective synthesis of triple deckers containing two different lanthanides. The mixed metal triple deckers can be synthesised from the extended double deckers but metal exchange was then observed leading to preferred formation of lanthanum triple deckers.

The same selective synthesis of different metal triple deckers was then attempted using porphyrin dyads with a longer linker leading to exactly the same results. Even though the selective synthesis of mixed metal triple deckers was proven to be possible and reproducible, the metal exchange process could not be eliminated by expansion of the length of the linking chain.

4.5. Synthesis of multidecker structures

Expansion of the triple decker system was attempted for the formation of more complex structures. Only a few multidecker structures based on porphyrins and/or phthalocyanines with more than three stacked chromophores are known to date, mostly reported by J. Jianzhuang (figure 77).[114-116]

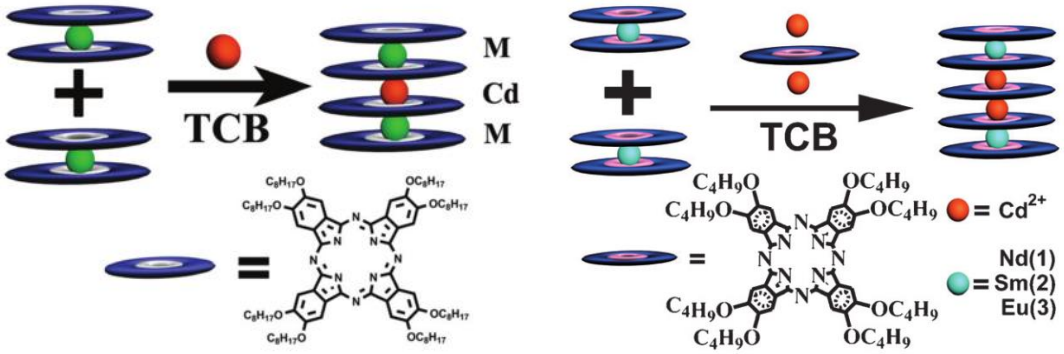

Figure 77. Phthalocyanine quadruple and quintuple deckers structure reported by J. Jianzhuang.[115,117]

During their work, a series of quadruple[117] and quintuple[115] deckers were synthesised by combining phthalocyanine lanthanide double deckers and cadmium. These complexes were obtained using a one pot reaction procedure to obtain the desired quadruple and quintuple deckers in yields from 14 % to 63 %. In both cases, neutral complexes were obtained using a combination of Ln^{3+} and Cd^{2+} ions.

During previous work, several linked triple deckers were reported. The next step forward consists in extending the stack of chromophores in order to obtain higher linked structures such as pentadecker **74**, represented in scheme **51**. Unlike the derivatives developed by J. Jianzhuang our high order stacks are expected to be robust and stable.

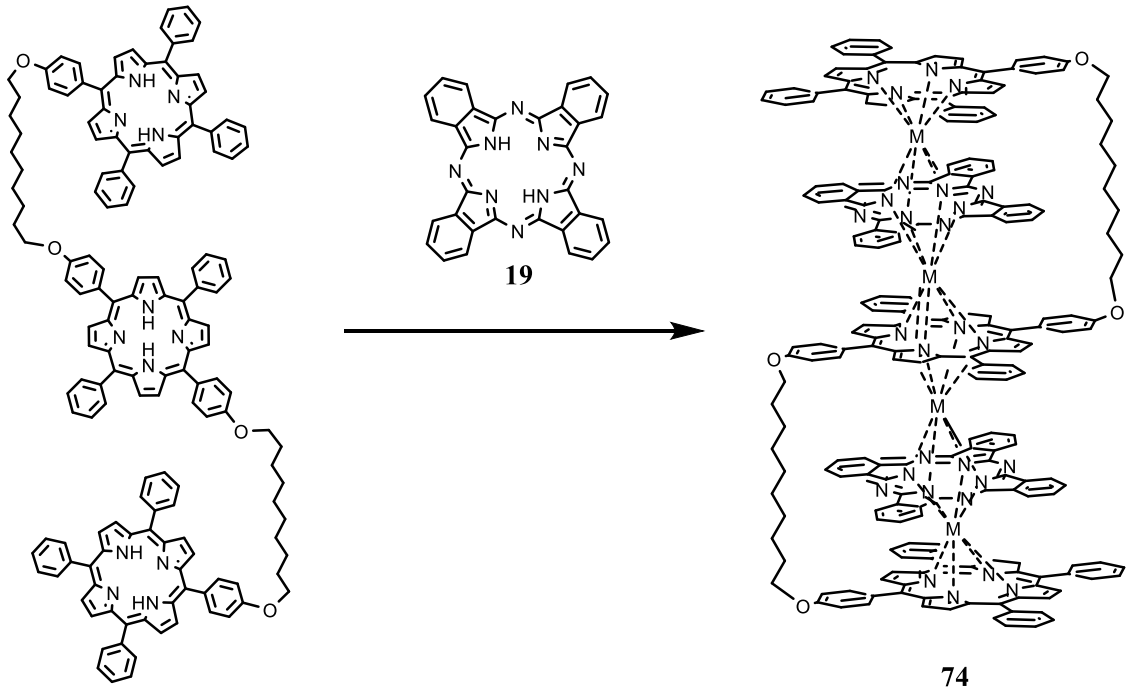

Scheme. 51 General scheme showing the formation of pentadecker **74**.

Synthesising such complex structures is not expected to be straightforward but the same step by step synthesis was performed as used for the formation of triple deckers with appropriate modifications. For the triple decker formation, the starting material used was a porphyrin dyad (C_{10} dyad **45** and C_{12} dyad **46)** and, therefore, for the formation of pentadeckers, a *trans*-porphyrin triad **73** was selected as starting material.

The first selected synthesis was to subject the porphyrin triads to the previously developed procedure for the formation of triple deckers to try to observe if such compounds are as suitable for the formation of deckers as porphyrin dyads are. With this synthesis in mind, a series of triple deckers should be expected as the most likely outcome for the reaction (Scheme 52). Analysis of the outcome from this known methodology should give some insight in the reactivity of these extended deckers as well as the type of complexes that are preferred.

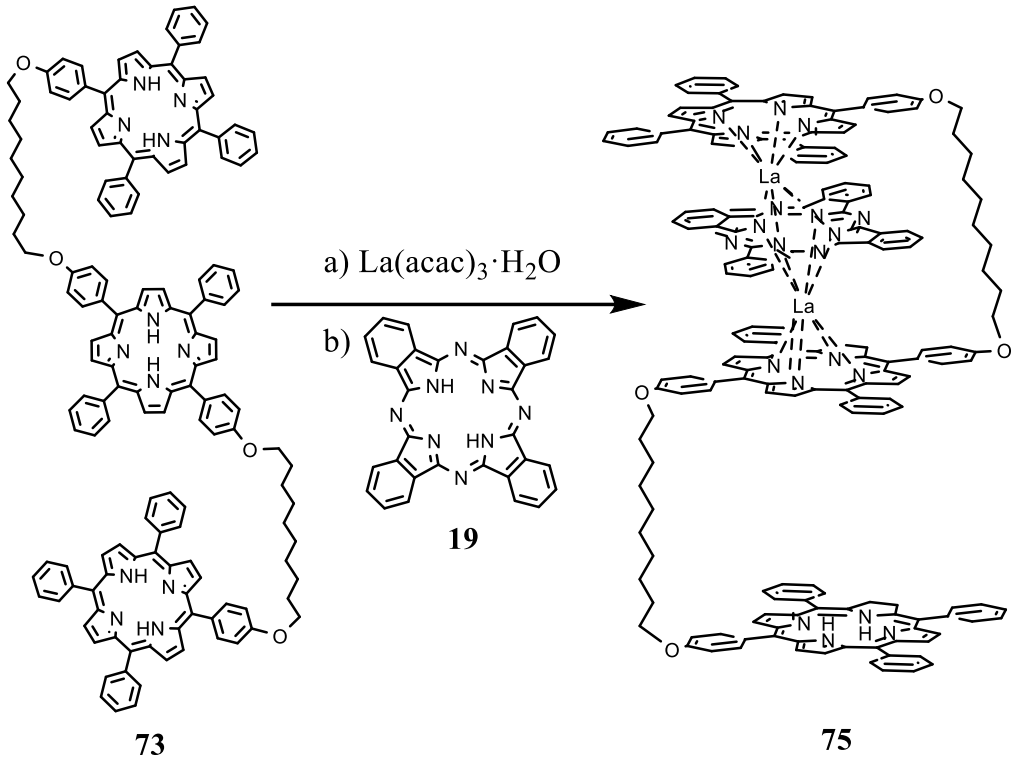

Scheme. 52. Expected synthesis of expanded decker **75** from porphyrin triad **73**.

4.5.1. Synthesis of porphyrin triad 73

There are many possible synthetic routes that can be followed in order to synthesise *trans*-porphyrin triad **73.** The selected synthesis involves the same reaction conditions used for the synthesis of porphyrin dyads using unsymmetrical *trans*-porphyrin **80** as starting material (Scheme 53). This is a straightforward procedure that should allow the synthesis of porphyrin triads in large scale for the synthesis of multidecker structures.

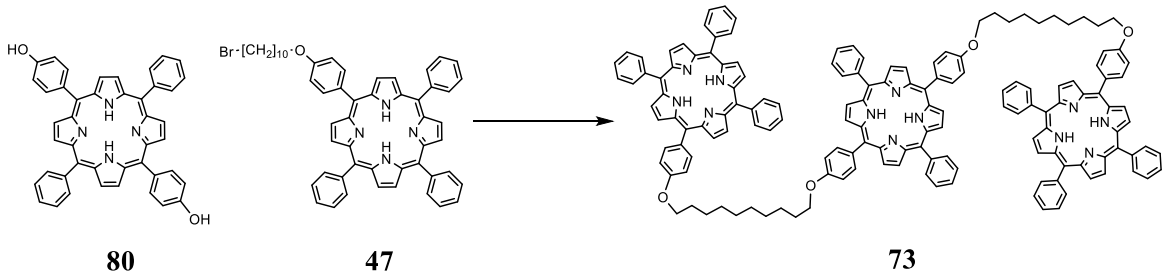

Scheme 53. Proposed synthetic pathway for the synthesis of porphyrin triad **73**.

Obtaining *trans*-porphyrin **73** in reasonable scale will be crucial for the synthesis of porphyrin triads. *Trans*-porphyrins cannot be efficiently obtained by the statistical synthesis of porphyrins reported by Adler[42] due to the difficulty in the purification of the isomers that are formed under these conditions. Therefore, the synthesis of these starting materials was performed following previously published methodologies by Lindsey.[43,118,119] Two different starting materials and routes can be selected for the formation of the desired 5,15-*p*-hydroxyphenyl-10,20-phenylporphyrin **80** (*trans*-TPP(OH)$_2$) as represented in scheme 54.

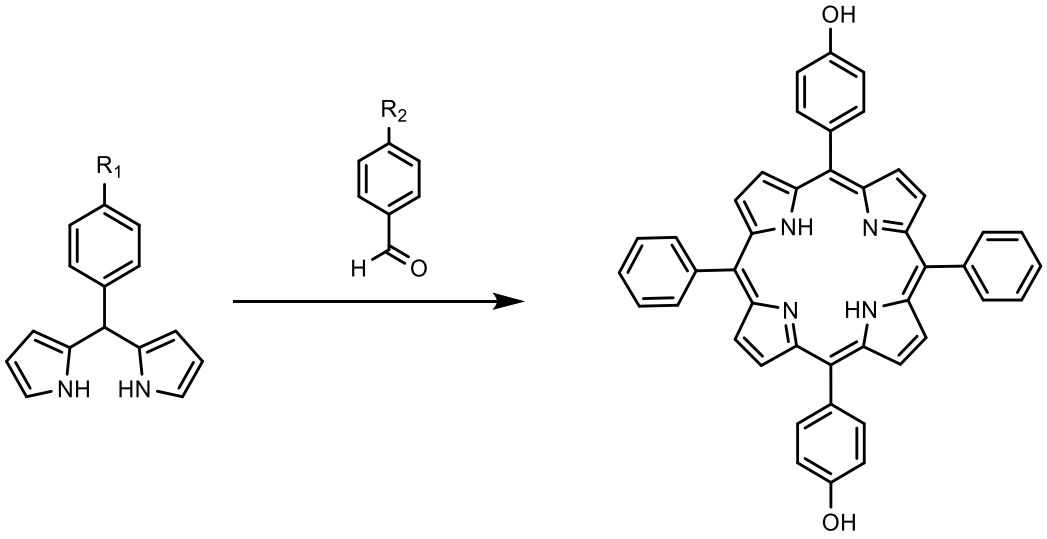

76: R_1=H
78: R_1=OH

14: R_2 = OH,
2: R_2 = H

80

Scheme 54. Proposed synthesis of *trans*-porphyrin **80**.

This *trans*-hydroxyporphyrin **80** provides the substitution pattern that can be used for the construction of the desired porphyrin triad **73**.

4.5.1.1. Synthesis of dipyrromethanes

Trans-Substituted porphyrins are key structural components found in a wide range of model systems in biomimetic and materials chemistry.[4,34,36] Synthetic *trans*-patterned porphyrins offer significant attractions compared to that of β-substituted porphyrins. This is due to the rectilinear arrangement of substituents and potential to be formed from pyrrole and simple aldehydes. For this reasons, there have been many previous different attempts to provide a general, rational approach for the formation of porphyrins with up to four different meso-substituents.[43,120-124] During the past 20 years, Lindsey's group have achieved some very important advances into the rational synthesis of dipyrromethanes and *trans*-porphyrins that has relied on a number of advances including:

- Development of simple yet efficient routes to dipyrromethanes, and other related derivatives.
- Development of mild reaction conditions for the synthesis of porphyrins allowing the use of a broad scope of substituents.
- Identification of acid catalysts and reaction conditions for condensations of pyrromethane species without accompanying acidolysis (which underlies scrambling and formation of a mixture of porphyrin products (scheme 55).
- Selection and refinement of synthetic methods to increase yields and to limit or avoid use of chromatography, thereby achieving scalability to multigram levels.

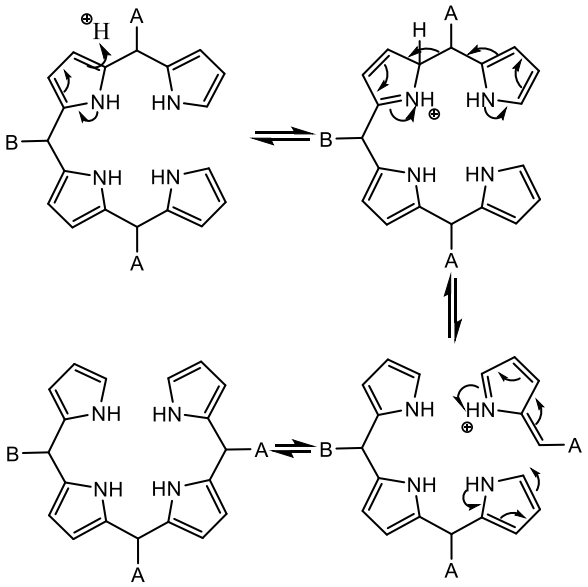

Scheme 55. Representation of a general scrambling process.[118]

5-Substituted dipyrromethanes **76** and **78** were the selected precursors for the synthesis of *trans*-substituted porphyrin **80**. Several one-flask methods were reported for the synthesis of 5-substituted dipyrromethanes by the condensation of an aldehyde and pyrrole using various combinations of acids and solvents.[120,121,123-126] More importantly, Lindsey previously reported an optimised one-flask synthesis of dipyrromethanes in which an aldehyde is dissolved in a 40-fold excess of pyrrole with a catalytic amount of acid at room temperature in the absence of any other solvent (see scheme 57).[119,126] This method afforded good yields of several 5-substituted dipyrromethanes with many types of functional groups.

During the following studies, synthesis of various dipyrromethanes and methodologies were approached. Two routes were selected, the first one reacting dipyrromethane **76** and *p*-hydroxybenzaldehyde **14** and the second one, using dipyrromethane **78** and benzaldehyde **2**. Finally, if any problem is encountered, methoxy protected *trans*-porphyrin **79** can be synthesised via condensation of benzaldehydes **2** or **9** and dipyrromethanes **77** or **76** respectively followed by standard deprotection with BBr_3 to obtain *trans*-porphyrin **80** as represented in the next scheme.

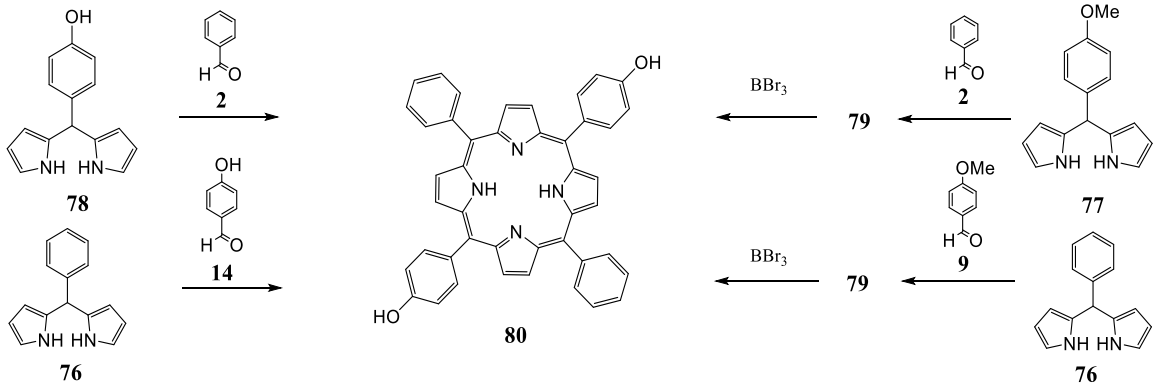

Scheme 56. Possible synthetic routes for the synthesis of *trans*-porphyrin **80**.

For the synthesis of dipyrromethanes **76-78**, a modified version of the procedure developed by Lindsey[126] was performed by stirring a mixture of previously distilled and degassed pyrrole (40-fold excess) and the desired 4-substituted benzaldehyde with a 10 % TFA as a catalyst at room temperature for 10 min (scheme 57).

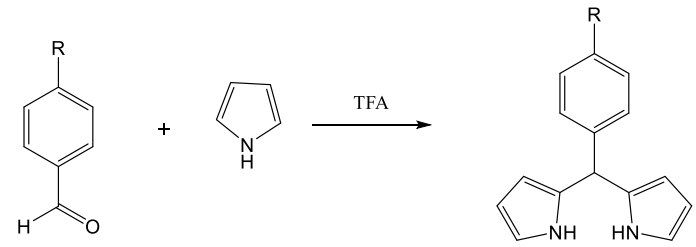

2: R = H
9: R = MeO
14: R = OH

1

76: R = H
77: R = MeO
78: R = OH

Scheme 57: general synthesis of phenyldipyrromethanes **76**-**78**.

In our case, direct distillation of the crude mixture could not be performed in multigram scales due to the lack of necessary equipment needed according to literature (kugelrohr distillation system for bulky samples, figure 78a). Therefore, only small scale reactions could be purified by direct distillation using the kugelrohr system pictured in figure 78b.

a)  b) 

Figure 78. Kugelrohr distillation systems: a) for bulky samples b) for small samples.

As a general procedure, when the 10 min reaction was completed, it was quenched with NaOH and ethyl acetate was added. The organics were washed with water and dried (Na_2SO_4), and the solvent removed under vacuum to afford an oil. This oil could be purified by direct distillation or column chromatography followed by recrystallisations depending on the amount obtained. The desired dipyrromethanes **77** and **78** could be easily synthesised using this methodology and were obtained as crystalline solids with spectroscopic data in full accordance with literature.

In the case of 5-phenyldipyrromethane **76**, analytically pure samples could not be obtained in any case due to its high instability. In this particular case, the dipyrromethane

was partially purified by column chromatography followed by distillation and used without further purification for the synthesis of *trans*-porphyrins.

4.5.1.2. Synthesis of *trans*-porphyrins from dipyrromethanes

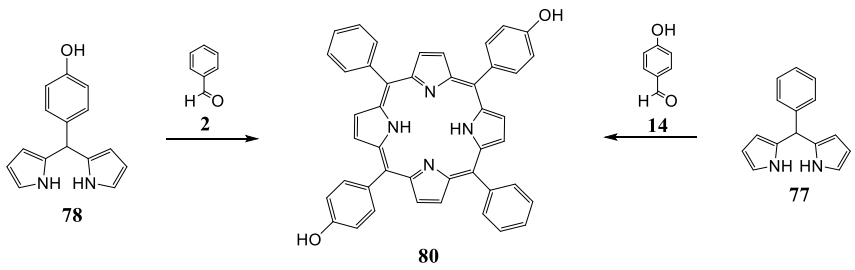

Scheme 58: Selected synthetic routes for the synthesis of *trans*-porphyrin **80**.

The first synthesis attempted for synthesising *trans*-porphyrin **80** was a modified version of the procedure of porphyrin formation from dipyrromethanes at room temperature developed by Lindsey *et al*.[118] Pre-synthesised dipyrromethane **78** and benzaldehyde were dissolved in DCM. To this, TFA (10 % mol) was slowly added and the mixture stirred for 10 min. When the reaction was completed, DDQ was added and the mixture stirred for further 2 h. Then, water was added to the mixture to precipitate the porphyrin but no solids were obtained. The crude was distilled under reduced pressure to leave black solids that could not be dissolved in organic solvents. Due to this insolubility, it could be concluded that no porphyrin was obtained from the reaction.

Dipyrromethane **78** did not form any porphyrin so the same methodology was tried by reacting 5-phenyldipyrromethane **76** and 4-hydroxybenzaldehyde **14** in the presence of a catalytic amount of TFA (scheme 58). As analytically pure dipyrromethane **76** could not be obtained using standard methodologies due to its high instability, it was freshly synthesised before the reaction and used without further purification after column chromatography.

Partially purified dipyrromethane **76** (1 spot on TLC and similar melting point to that reported in literature[119]) and benzaldehyde **14** were stirred in DCM for 30 min in the presence of TFA, followed by oxidation with DDQ. When the reaction was completed, it was extracted with NaOH, then H_2O and dried over $MgSO_4$. Finally, MeOH was added but no precipitate was formed and no product was detected in any case. This particular procedure

did not seem promising due to the impossibility to obtain analytically pure samples of dipyrromethane **76**. Therefore, it could not be proven that the lack of product at the end of the reaction was caused by the interference of impurities, decomposition of the starting materials or any other factor.

Then, the synthesis of protected *trans*-porphyrin **79** from methoxy-functionalized dipyrromethanes/aldehydes was attempted. The same low scrambling methodology was followed reacting dipyrromethane **77** and benzaldehyde with a catalytic amount of TFA. The reaction crude was then purified using different procedures (column chromatography, recrystallisations) but no product was observed in any of the attempts.

Formation of 5,15-bis-(*p*-methoxyphenyl)-10,20-diphenylporphyrin magnesium 83:

As *trans*-porphyrin **80** could not be obtained using standard methods, another approach was followed by formation of *trans*-methoxyphenylporphyrinato magnesium **83**. This metallated porphyrin could be easily demetallated following standard procedures if synthesis is successful. The methodology used for the formation of magnesium porphyrin **83** was the procedure reported by Lindsey[43] as represented in the next scheme.

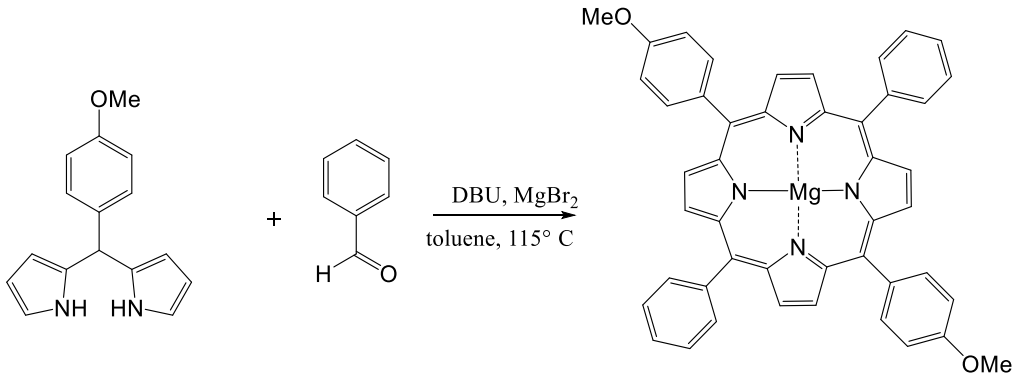

77 **2** **83**

Scheme 59: Procedure for the formation of magnesium porphyrin **83**.

Benzaldehyde and dipyrromethane **77** were heated in refluxing toluene in the presence of magnesium dibromide using DBU as catalyst. The crude mixture was

precipitated using MeOH to obtain a purple solid. The solids were filtered off and checked by MALDI-tof MS but, unfortunately, scrambling was observed using this methodology (figure 79).

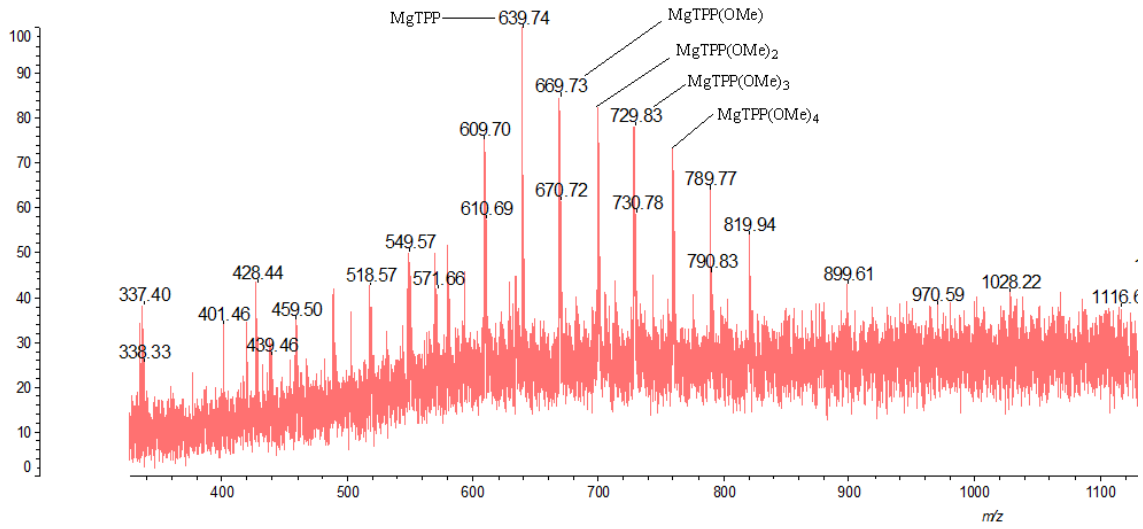

Figure 79. MALDI-tof MS obtained for the crude reaction of the formation of *trans*-magnesium porphyrins.

The exact same reaction conditions were followed using previously synthesised *p*-hydroxyphenyldipyrromethane **79** instead of *p*-methoxyphenyldipyrromethane **77** but the same scrambling process was observed from the crude solids obtained (figure 80). Using these conditions porphyrins were formed but an inseparable mixture of isomers was obtained. Therefore, this method was not appropriate for the selective formation of *trans*-porphyrins and a different strategy needed to be explored.

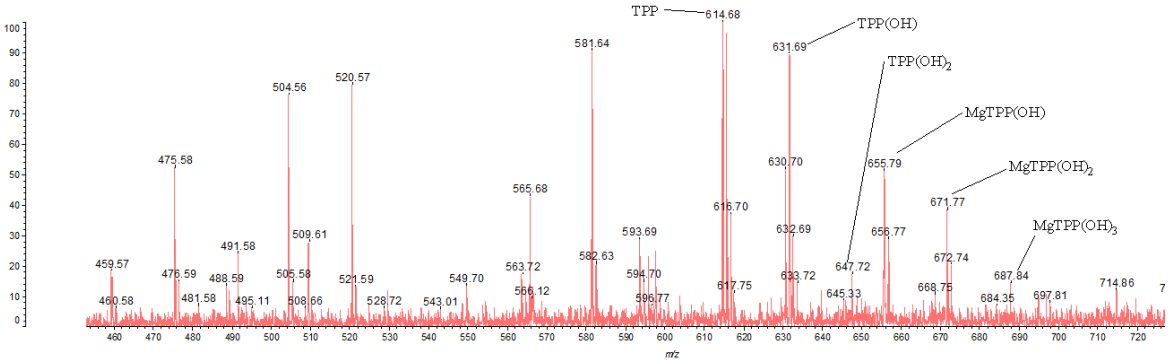

Figure 80. MALDI-tof MS obtained for the crude reaction of the formation of *trans*-magnesium porphyrins.

Formation of *trans*-alkylated porphyrin 82:

The next attempted method for the synthesis of *trans*-porphyrin **82** involves alkylation of *p*-hydroxybenzaldehyde **14** prior to the formation of the porphyrin in order to obtain directly *trans*-alkylated porphyrin **82** (scheme 60).

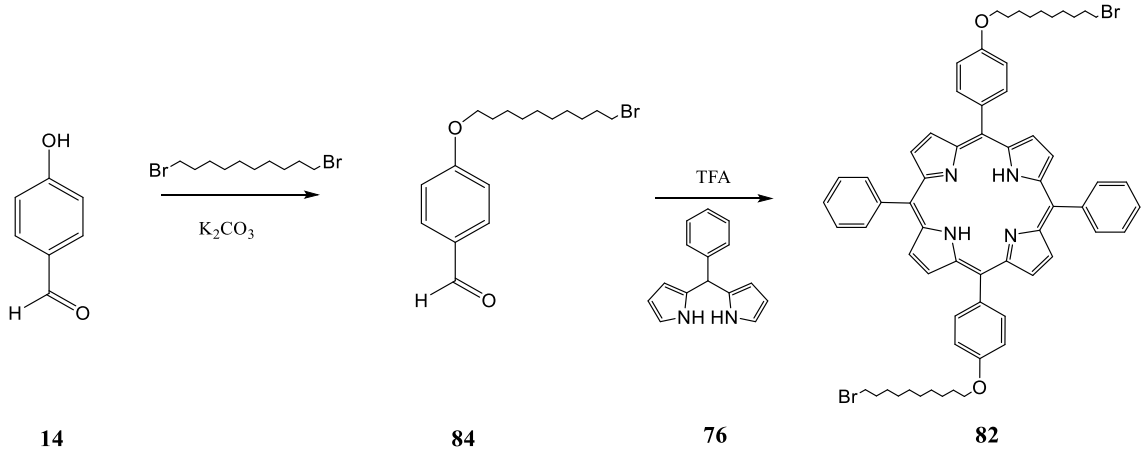

14 **84** **76** **82**

Scheme 60: Direct synthesis of *trans*-alkylated porphyrin **82** from previously alkylated benzaldehyde **84**.

Benzaldehyde **14** was refluxed with 1,10-dibromodecane and potassium carbonate in acetone to obtain pure benzaldehyde **84** as a crystalline solid after column chromatography on silica gel. Then, dipyrromethane **76** was synthesised by the standard Lindsey[118] method of stirring benzaldehyde in freshly distilled pyrrole using TFA as catalyst followed by purification by column chromatography. Finally, both aldehyde **84** and partially purified dipyrromethane **76** were stirred in DCM and TFA was added to the reaction. After stirring the mixture for 10 min, the crude was extracted with NaOH, water and dried over $MgSO_4$. Then, MeOH was added to the mixture and the purple precipitate obtained was filtered and checked by MALDI-tof MS (figure 81).

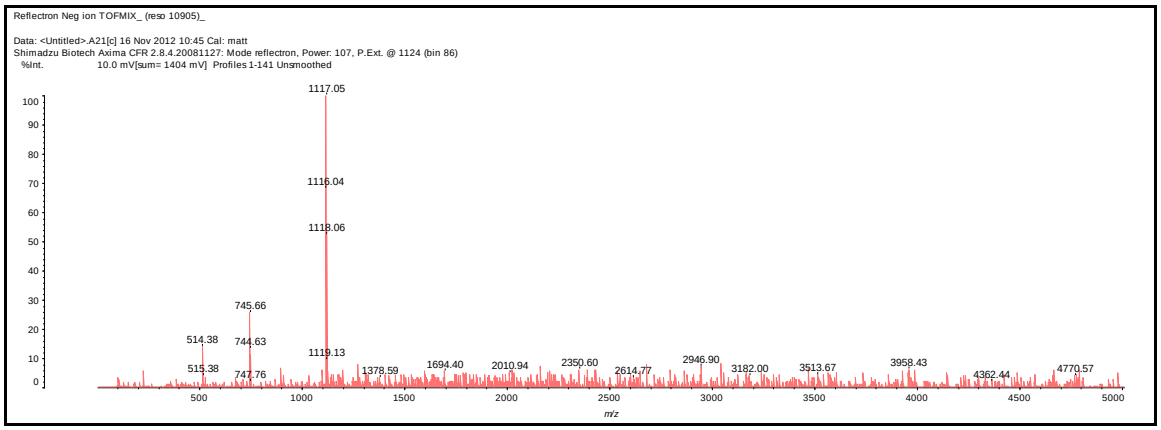

Figure 81. MALDI-tof MS spectra of the reaction crude.

The observed peak did not match with the mass of 1084.37 m/z expected for the porphyrin product **82** but it does match the substitution of one molecule of TFA for one of the bromine atoms instead forming *trans*-porphyrin **85** (figure 82).

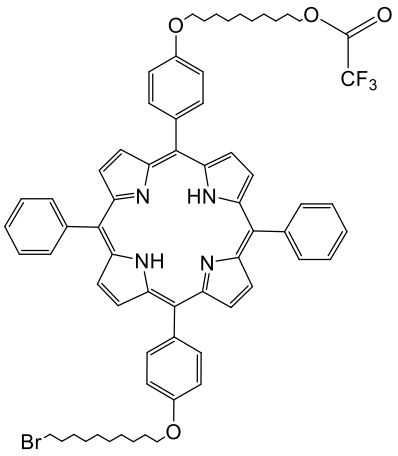

Molecular Weight: 1118.19

85

Figure 82. Obtained side reaction product after the addition of TFA.

To try to overcome the formation of **85**, the same reaction was performed using another Lewis acid as catalyst. The study from Lindsey *et al.* showed that boron trifluoride diethyl etherate ($BF_3 \cdot Et_2O$) can also be used for the formation of *trans*-porphyrins.[126] This other catalyst has lower nucleophilicity, therefore it is less likely to give this side reaction. In this case, the same reaction conditions were followed with the only change of the catalyst and after the same work-up, the MALDI-tof MS was checked for the crude solid obtained. Unfortunately, scrambling was observed.

As the dipyrromethanes appear to be unstable or give scrambling during the formation of *trans*-porphyrins, other synthetic pathways for obtaining *trans*-porphyrins were explored. The selected route was the statistical reaction of aldehydes for the formation of hydroxyphenylporphyrins (scheme 61).[42] The statistical reaction between freshly distilled pyrrole and the corresponding benzaldehydes **2** and **14** in refluxing propionic acid was performed. The resultant crude was then precipitated with MeOH to obtain the mixture of porphyrins. After the selective precipitation, the mixture of isomers **80** and **87** was separated by column chromatography from the rest of the porphyrins that were produced during the reaction.

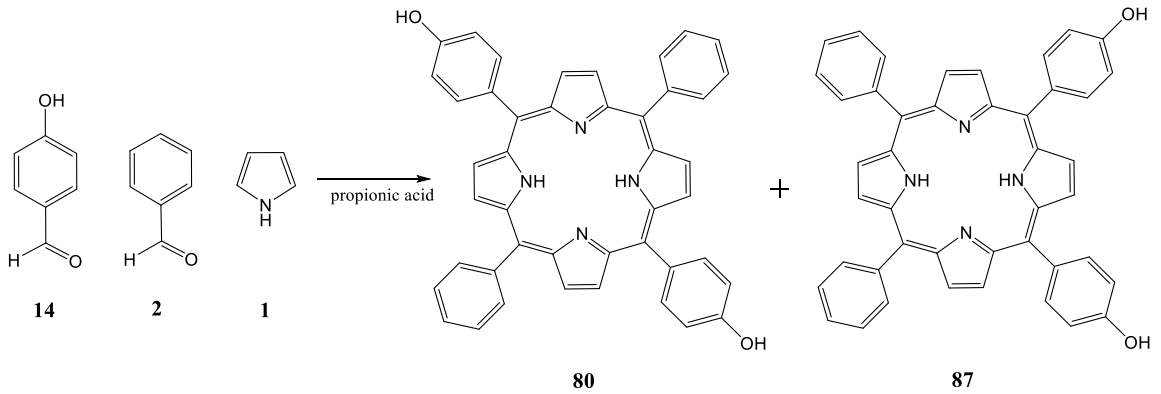

Scheme 61: Formation of *trans*- and *cis*- porphyrins **80** and **87** (amongst other porphyrins).

The previously separated isomers of TPP-$(OH)_2$ **80** and **87** were then further purified. In order to separate both on silica gel, THF:toluene:Pet. ether (1:2:2 v/v) mixture was selected as eluent as it allowed separation of spots by TLC analysis. By this purification method, the isomers could be partially separated. Both where isolated and analysed by NMR spectroscopy allowing the characterization of both structures. Unfortunately this method is not optimal for the synthesis of the desired *trans*-porphyrin **80** in big scale due to the tedious purification process and low yielding methodology.

Synthesis of porphyrin triads via pentafluorophenyldipyrromethane 90:

Due to the instability of the dipyrromethane **76** as well as the scrambling process observed during the formation of the corresponding *trans*-porphyrins, pentafluorophenyldipyrromethane **90** was selected for the synthesis of *trans*-porphyrins (scheme 62). This dipyrromethane **90** was chosen due to its known synthesis as well as stability. This, allowed us to synthesise it on large scale and test various scrambling-free procedures for the synthesis of *trans*-porphyrins.[118,126] Using **90** as starting material would lead to triads having the central porphyrin substituted with pentafluorophenyl groups. This characteristic will help us to analyse the target multidecker structures by NMR due to the elimination of some of the ^{1}H signals as well as allowing us to interrogate the designed compounds using ^{19}F-NMR.

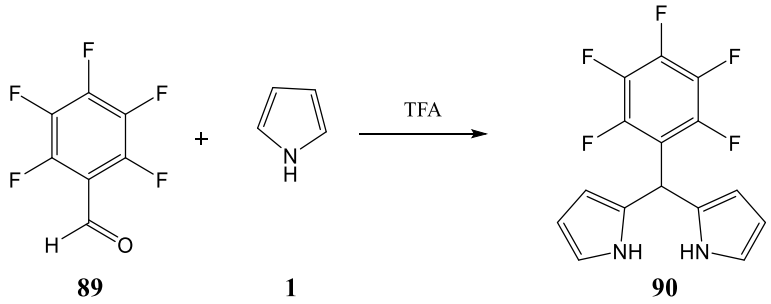

Scheme 62: Formation of pentafluorophenyldipyrromethane **90**.

For the synthesis of pentafluorophenyldipyrromethane **90**, pentafluorobenzaldehyde **89** was stirred with freshly distilled pyrrole using TFA as catalyst using Lindsey's method.[119] When the reaction was completed, the reaction was quenched with NaOH and ethyl acetate added. The organic phase was washed with water and dried over $MgSO_4$, the solvent was then evaporated to obtain a green oil that was further purified by column chromatography to obtain the pure dipyrromethane as an orange oil that crystallized over time.

The obtained dipyrromethane **90** was then used for the formation of different *trans*-porphyrins. These porphyrins should then act as starting materials for the formation of porphyrin triad **94**. This triad can be synthesised from two different central porphyrins as represented in scheme 63. One method consisted in coupling complementary *trans*-functionalized porphyrin **92** or **93** and single functionalized porphyrin **34** or **47** respectively. These two complementary functional groups can be hydroxyl (porphyrins **34** or **92**) or

bromoalkoxyl (porphyrins **47** or **93**) to be able to couple them together using previous methodologies.

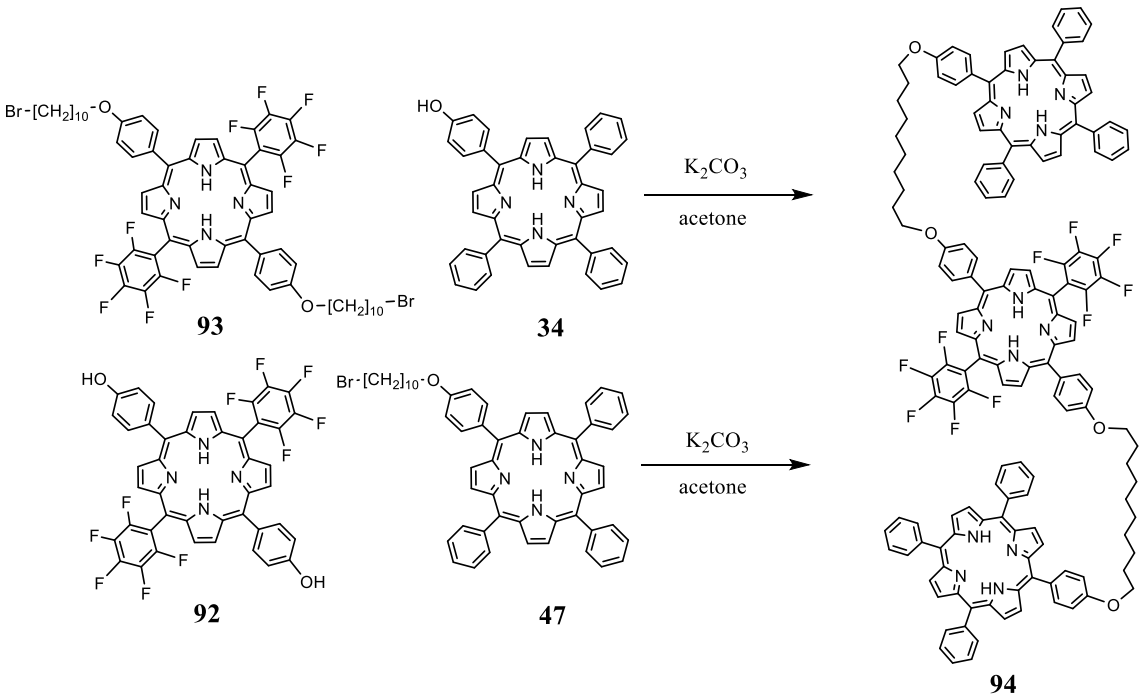

Scheme 63: proposed synthesis of porphyrin triad **94** from *trans*-porphyrins.

Synthesis of *trans*-porphyrin 92:

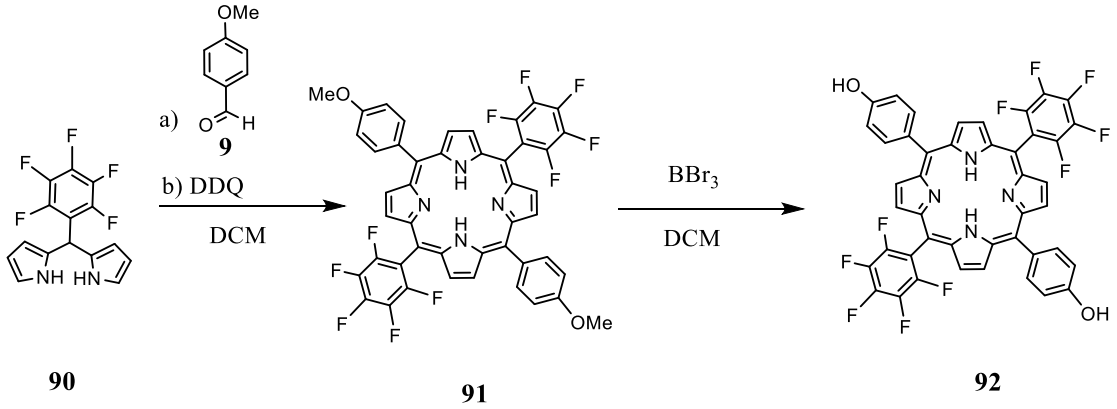

Scheme 64: deprotection of porphyrin **91** to obtain porphyrin **92**.

In this particular case, due to the expected high solubility of targeted porphyrin **92**, it was synthesised from the protected *trans*-porphyrin analogue **91**. After stirring aldehyde

9 with dipyrromethane **90** in DCM for 30 min at rt., DDQ was added and the mixture stirred for 1 h. The complete reaction mixture was then poured onto a pad of alumina and eluted with DCM until the eluting solution was pale brown. The solvent was removed under vacuum to give a black solid which was dissolved in toluene and heated under reflux for 1 h in the presence of DDQ to oxidize any remaining chlorin. After cooling to room temperature, the entire reaction mixture was passed through a short pad of alumina and eluted with DCM until the purple material had completely eluted. After removal of the solvent and recrystallisation, analytically pure *trans*-porphyrin **91** was obtained.

In this case, very encouraging results were obtained as no scrambling was observed and the porphyrin could be synthesised in big scale. Then, the methoxyl groups were deprotected by stirring porphyrin **91** in the presence of BBr_3 overnight and the obtained porphyrin **92** was obtained pure after recrystallisation. With these conditions, the desired porphyrin **92** could be obtained analytically pure in big scale and good yields.

Synthesis of *trans*-porphyrin 93:

Due to the success on the synthesis of this *trans*-porphyrin **92**, the same procedure was followed for the synthesis of *trans*-porphyrin **93** in only one step using previously alkylated benzaldehyde **84** and dipyrromethane **90** as shown in scheme 65:

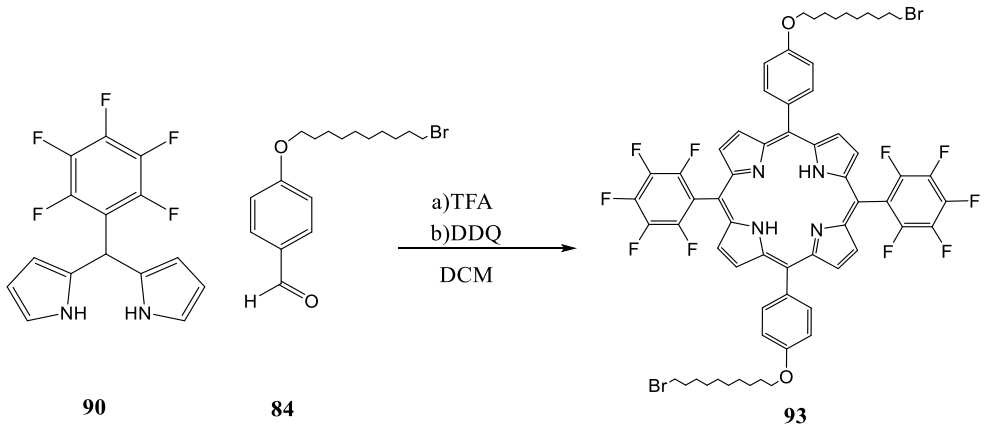

90 **84** **93**

Scheme 65: One step synthesis of alkylated *trans*-porphyrin **93**.

Dipyrromethane **90** and aldehyde **84** were stirred for 30 min in DCM in the presence of a catalytic amount of TFA. Then, DDQ was added and everything stirred for 1 h. When

the reaction was completed, the crude mixture was passed through an alumina pad and the resultant solution was partially concentrated and MeOH was added. The purple precipitate formed was filtered off and checked by MALDI-tof MS to observe scrambling leading to a mixture of porphyrins. The different porphyrins obtained could be separated by column chromatography but the mixture of isomers could not be further separated by any of the methods tried.

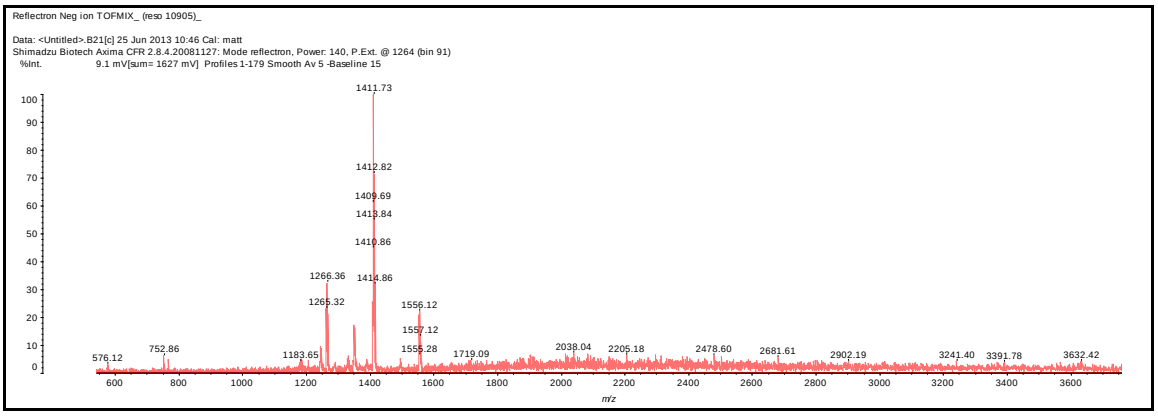

Figure 83. MALDI-tof MS obtained for the synthesis of *trans*-porphyrin **93**.

Due to the successful reaction of formation of *trans*-protected porphyrin **91,** and its similarity with **93**, another reaction was tested in order to try to eliminate the scrambling process observed in this particular case. The same reaction procedure was followed but in this case, the reaction was performed at 0 °C instead of rt. maintaining the rest of the conditions the same. In this case, product **93** was obtained with no scrambling as observed by MALDI-tof MS (figure 84) and TLC analysis. Analytically pure *trans*-porphyrin **93** was obtained after a short column chromatography over silica gel with a 17 % yield.

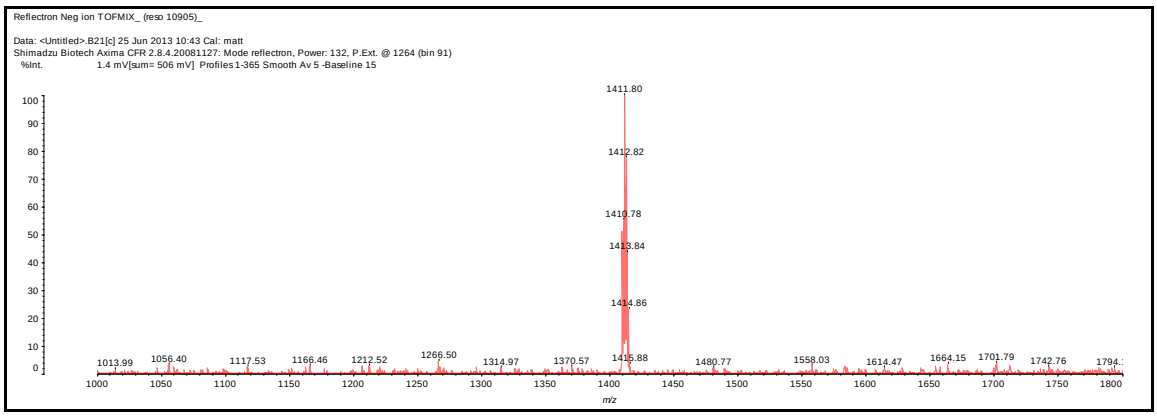

Figure 84. Scrambling-free MALDI-tof MS obtained for *trans*-porphyrin **93**.

4.5.1.3. Synthesis of porphyrin triads

The synthesis of *trans*-porphyrins **92** and **93** in reasonable scale was successfully performed in scrambling-free conditions. Therefore, the synthesis of porphyrin triad **94** could be attempted. For the desired synthesis, two different pathways could be followed as previously stated (scheme 63). One of them using the *trans*-alkylated porphyrin **93** and the other *trans*-hydroxylated porphyrin **92** as starting materials. Both pathways should lead to the same porphyrin triad **94**.

Synthesis of porphyrin triad 94 via alkylated central porphyrin 93:

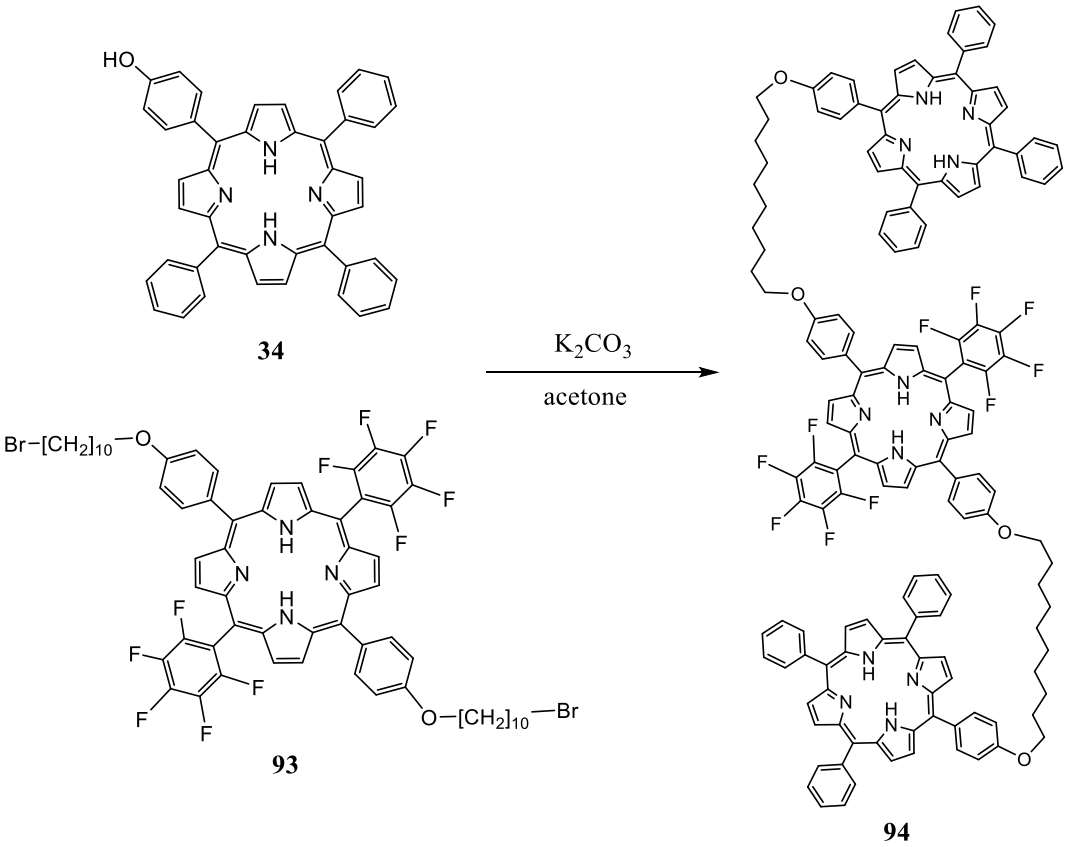

Scheme 66. Proposed synthesis of **94** using *trans*-porphyrin **93**.

The first reaction tried was refluxing *trans*-porphyrin **93** and an excess of porphyrin **34** in acetone with an excess of K_2CO_3 to form porphyrin triad **94**. The reaction was followed by TLC and stopped when no more changes were observed. After purification of all fractions by column chromatography, the desired porphyrin triad relative mass could

not be observed in any of the fractions by MALDI-tof MS analysis. On the other hand, by ^{1}H-NMR analysis of the different purified fractions obtained (figure 85), a very complicated pattern in the aromatic region of the NMR spectrum could be observed in all fractions even when they appear as a single spot on TLC. The desired product was not present in any of them.

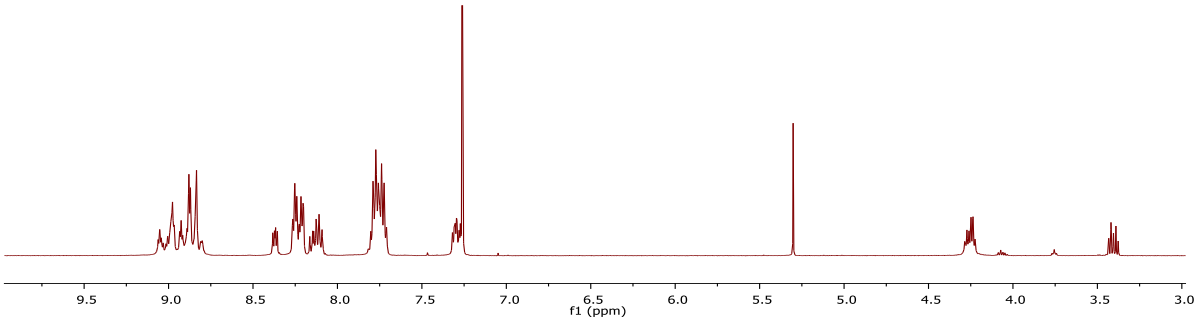

Figure 85. Expansion of the ^{1}H NMR spectra one of the main fractions obtained from the reaction.

Observing this NMR, it can be concluded that the aromatic region as well as the signals around 3.4 and 4.25 ppm of the spectra became highly unymmetrical. Also, the MALDI-tof MS analysis of the fractions didn't show any peak corresponding to any expected side products of the reaction or intermediates. However, some additions were taking place, but not forming the expected product. This could be explained if other side reactions were taking place, leading to different products. This possibility was explored a little bit further and some examples of nucleophilic substitution reactions between pentafluorophenyl derivatives and different nucleophiles were observed in the literature (scheme 67).[127-130] Some of the reported reactions occurred even without the use of catalysts. This findings allowed us to think that the excess of hydroxylated porphyrin **7** and base in the reaction mixture are very favourable conditions for this process to occur.

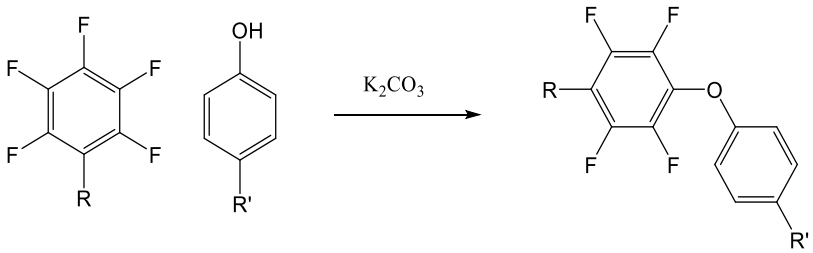

Scheme 67. Proposed side reaction occurring under the coupling conditions.

To try to overcome this process, the same reaction was tested adding a catalytic amount of KI to the reaction mixture. Unfortunately, it produced no changes to the reaction outcome and the same side reactions were observed. A final test was then performed by changing the solvent system to DMF with presence of a catalytic amount of KI in the reaction mixture. The reaction was performed stirring at 60 °C over 3 days but the same undesired processes were observed in all cases, and therefore, the product could not be obtained following this method.

Synthesis of porphyrin triad 94 via hydroxylated central porphyrin 92:

The next attempt was the reaction of *trans*-dihydroxylated porphyrin **92** with previously alkylated porphyrin **47**.

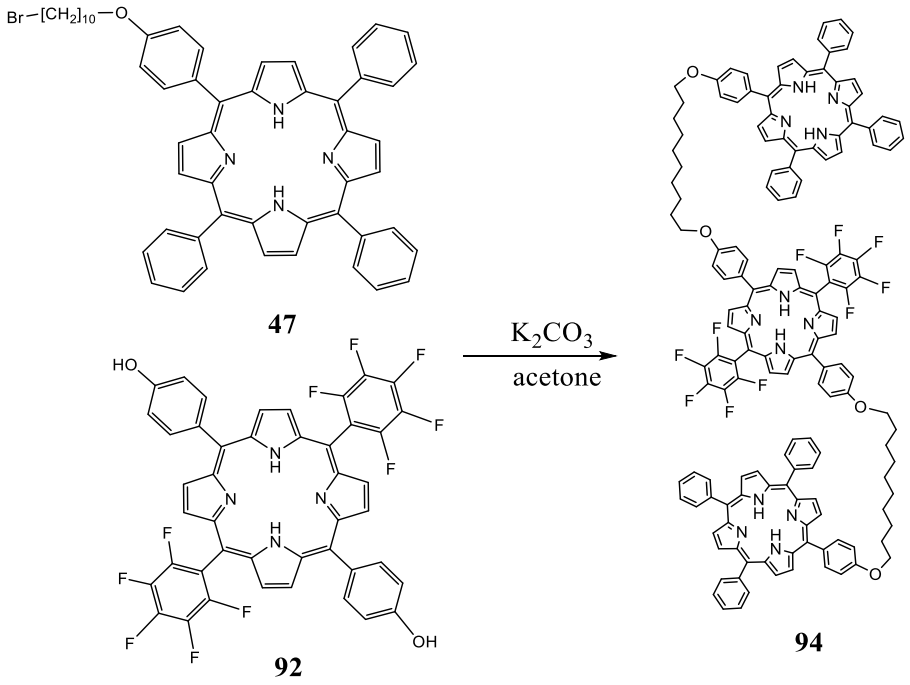

Scheme 68. Proposed synthesis of porphyrin triad **94** using *trans*-porphyrin **92**.

The same reaction conditions used previously were followed by refluxing the mixture of porphyrins **47** and **92** in acetone with an excess of K_2CO_3 for 3 days. Then, the crude mixture was concentrated and purified by column chromatography. The fractions obtained were checked by MALDI-tof MS and the desired product observed with expected mass of 2367.4 m/z. After recrystallisation of the fraction containing the product, only traces of

porphyrin triad **94** could be obtained. Another reaction was prepared changing the solvent to DMF.

The exact same reaction was performed in DMF for 3 days at 60 °C. Then the crude was precipitated with water and the purple solid obtained was purified by column chromatography and recrystallisation. In this case, the fraction containing the product (checked by MALDI-tof MS) was analysed by ^{1}H-NMR appearing to be the product with only a trace impurity as shown on figure 86. Recrystallisation did not improve the purity.

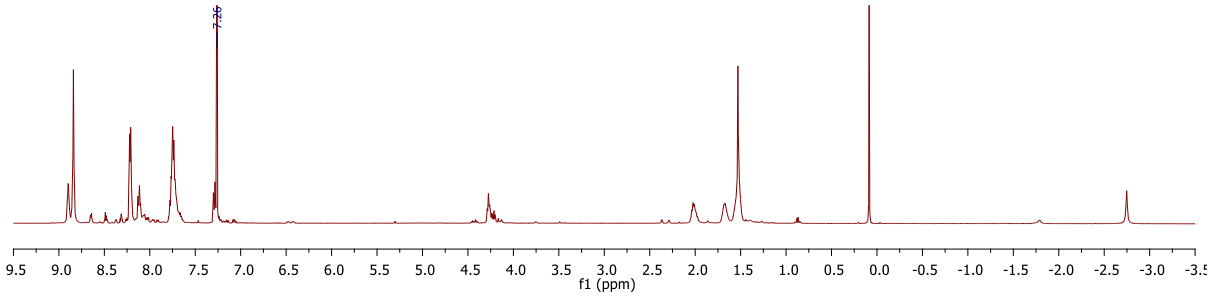

Figure 86. Obtained spectra obtained for the porphyrin triad following the above procedure.

Synthesis of porphyrin triad 73 via *trans*-alkylated porphyrin 82

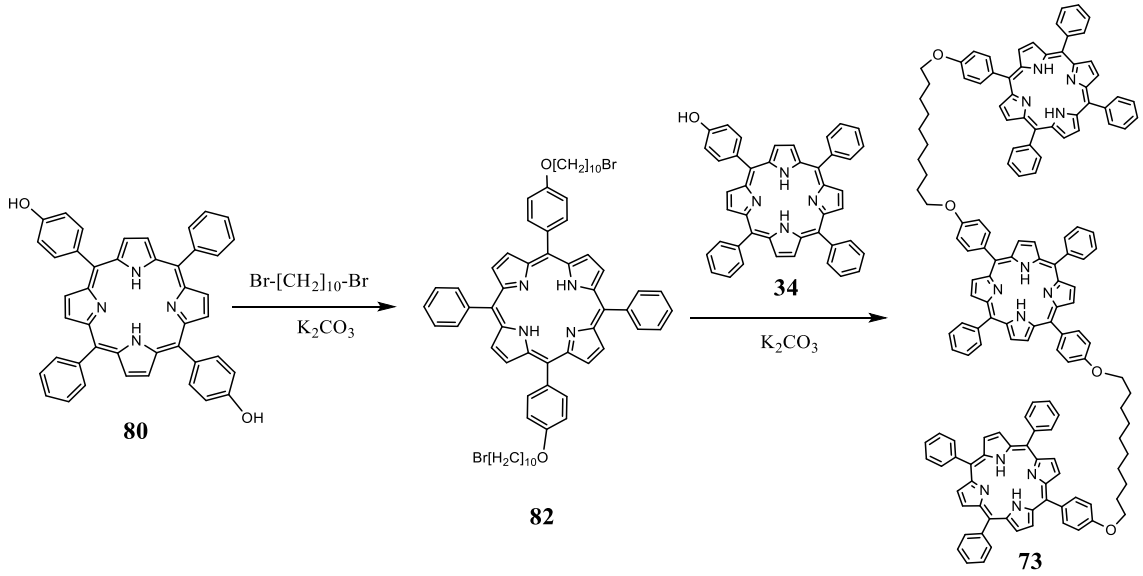

Scheme 69: Proposed synthesis of porphyrin triad **73** using *trans*-alkylated porphyrin **82**.

Trans-porphyrin **82** was obtained by alkylating *trans*-porphyrin **80** with 1,10-dibromodecane and potassium carbonate in acetone and obtained pure after column chromatography. Then, *trans*-porphyrin **82** was reacted with porphyrin **34** in refluxing acetone in the presence of potassium carbonate. After several recrystallisations, the desired porphyrin triad **73** was obtained. This method of synthesis of porphyrin triad **73** involves a low yielding step of alkylation of *trans*-porphyrin **80**. This porphyrin synthesis and purification is tedious which makes this approach not optimal as the overall yield is very low and could not be done in high scale.

Synthesis of porphyrin triad 73 via *trans*-hydroxylated porphyrin 80

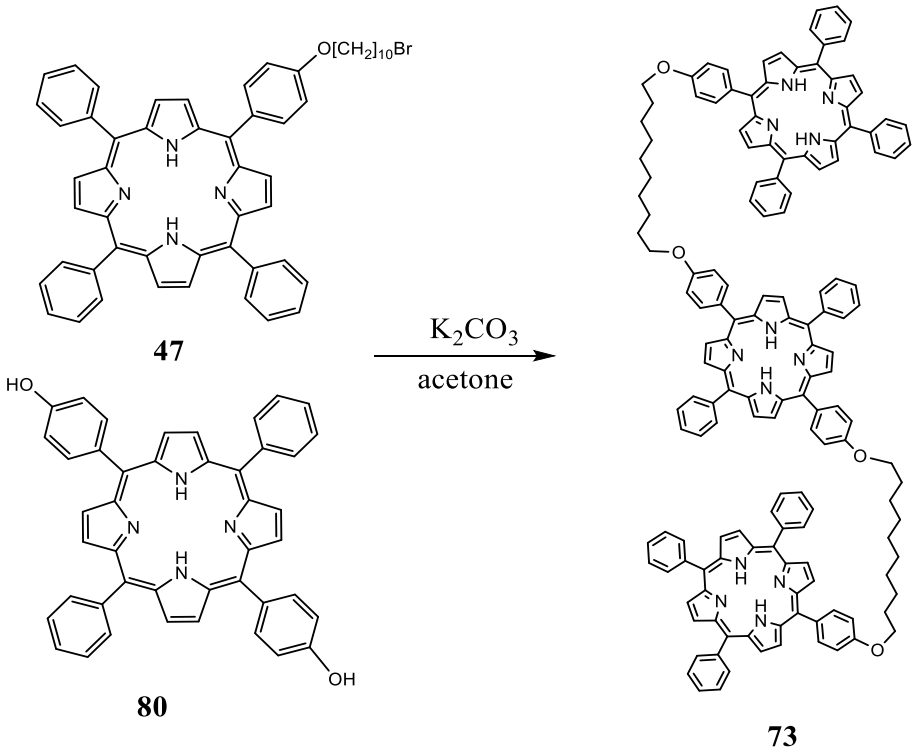

Scheme 70: synthesis of porphyrin triad **73** via *trans*-porphyrin **80**.

The complementary methodology involves the reaction of *trans*-porphyrin **80** with previously alkylated porphyrin **47**. This synthetic route was attempted in order to obtain *trans*-porphyrin triad in reasonable scale. This way, the need of alkylating *trans*-porphyrin **80** was avoided. Porphyrins **80** and **47** were refluxed in acetone with an excess of K_2CO_3. When the reaction was completed, the crude mixture was purified by column chromatography followed by recrystallisation. The desired porphyrin triad **73** was obtained in low yield and analytically pure product could not be obtained. With these results, another methodology was performed using DMF as solvent to try to improve the solubility of all materials. Then, the same procedure was performed in DMF and analytically pure porphyrin triad **73** was obtained after two recrystallisations in 53 % yield.

4.5.1.4. Synthesis of extended triple deckers

There are many different multidecker structures that can be formed from the synthesised porphyrin triads **73** or **94**. The first attempts involved the use of porphyrin **94** as starting material as it could be obtained in reasonable scale and more material was available. These tests consisted of subjecting the triads to the methodology of triple decker formation. In order to do so, the porphyrin triads were metallated followed by addition of phthalocyanine **19** into the reaction system. With this methodology, an extended triple decker **95** was expected as represented in the next scheme:

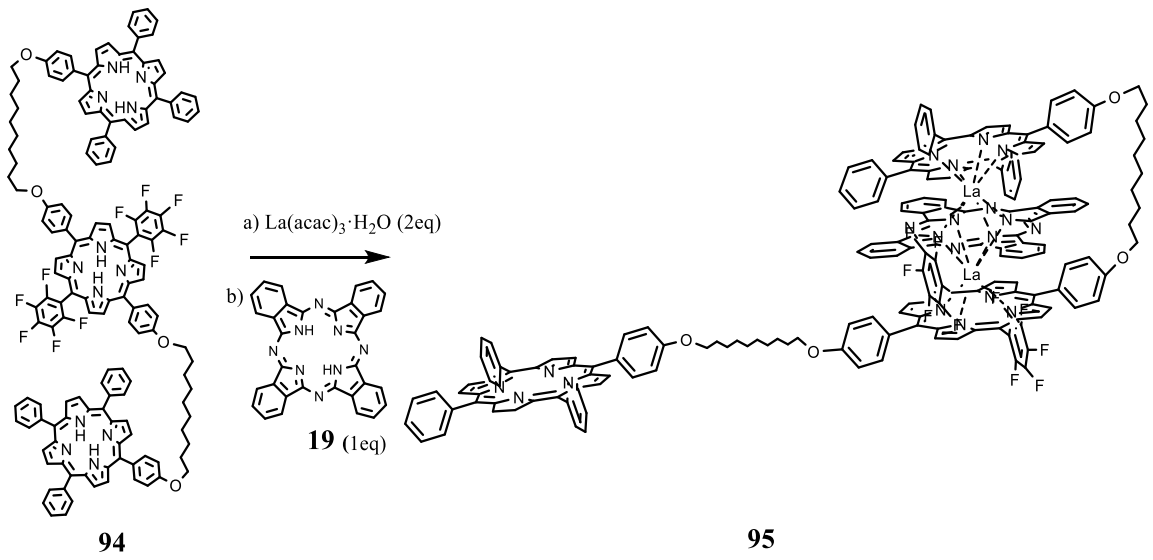

Scheme 71: Proposed synthesis of extended triple decker **95**.

The synthesis of **95** was attempted by reacting a stoichiometric amount of porphyrin triad **94** and lanthanum acetylacetonate hydrate (2 eq) in octanol for 18 h followed by addition of phthalocyanine **19** (1 eq) and further 15 h reflux. The solvent was then reduced by distillation and the crude precipitated with MeOH to recover a purple solid that were purified by column chromatography over silica gel. Analysis of the fractions obtained by MALDI-tof MS indicated two different products. The expected mass for the extended triple decker **95** represented in scheme 71 corresponded to 3148.9 m/z but it could not be observed in any of the fractions.

The main fraction obtained did not give any signal under any conditions used in the MALDI-tof MS. The sample was then sent to a high resolution mass spectrometry facility and the spectra obtained appeared to be a very complicated polymeric mixture of compounds with peaks at 2585, 3241, 4027, 5056, 5956 and 6743 m/z respectively. None of them

corresponded to any of the products expected. ^{1}H-NMR spectra was recorded for this fraction but due to the high complexity of the splitting observed as well as the broad signals observed in the spectra, it could not be analysed. The broad signals and the relative masses obtained pointed towards the formation of polymeric structures.

On the other hand, the second fraction obtained from the reaction gave a single sharp signal in the MALDI-tof MS corresponding to 3374.89 m/z. This obtained mass have a difference with our expected product **95** of 226 m/z that can match the substitution of two fluorine atoms for two molecules of octanol used as solvent (see figure 87). The same type of side reaction was observed previously in the formation of the porphyrin triad (scheme 67). ^{1}H-NMR analysis of the sample obtained also shows broad signals making the analysis very difficult. Finally, not enough material was obtained with this methodology to perform other analysis. The same reaction was attempted using a bigger scale but only traces of the compound were obtained being the polymeric mixture the main fraction obtained in all attempts.

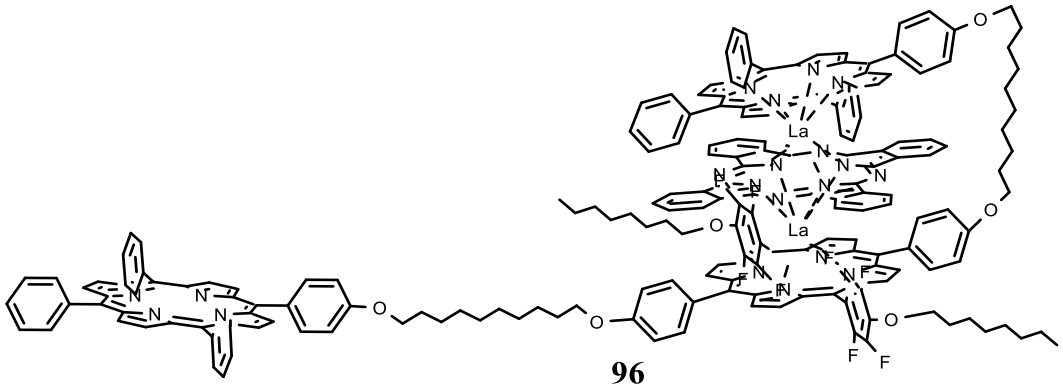

96

Figure 87. Representation of the structure of complex **96** with mass of 3374.89 m/z.

The same procedure was then performed using the non-fluorinated triad **73** as starting material, maintaining the rest of the conditions identical (scheme 72). This was attempted in order to eliminate the possibility of reaction of the fluorine atoms of this complex. Only a test reaction could be attempted using this methodology as only few milligrams of porphyrin triad **73** were available.

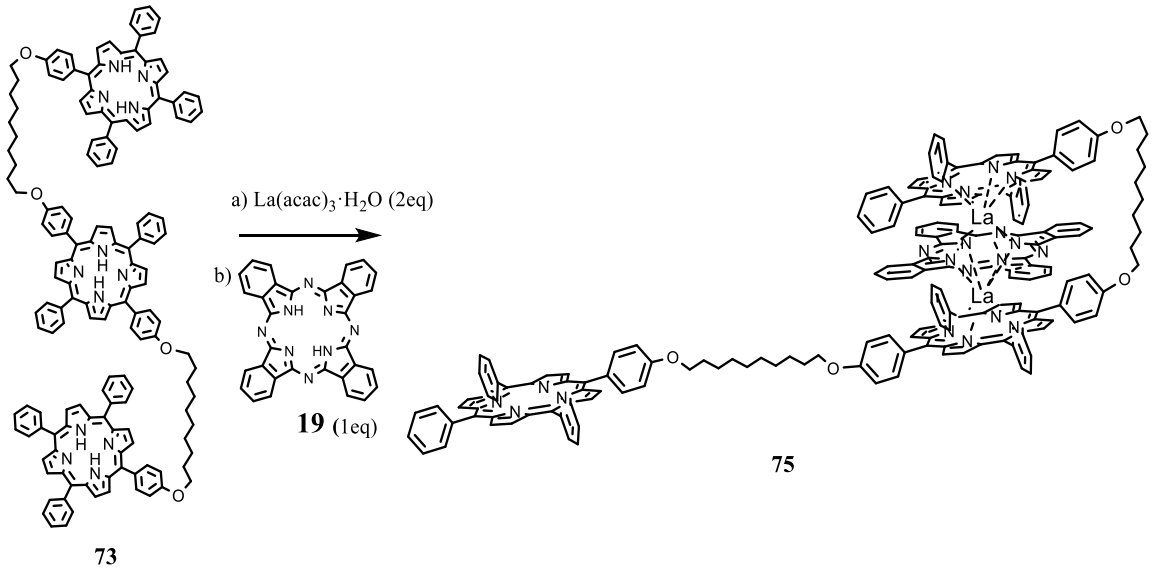

Scheme 72. Representation of the synthesis of complex **75**.

After a stoichiometric reaction between porphyrin triad **73** and lanthanum acetylacetonate hydrate for 8 h, phthalocyanine **19** was added and the mixture refluxed overnight. The crude mixture was precipitated with MeOH and a few drops of distilled water to recover a purple solid that was purified by column chromatography on silica gel. Two fractions were then collected after the column: the first main brown fraction and a small second purple fraction. Both fractions were analysed by MALDI-tof MS and only one peak corresponding to the expected product **75** of 2973.53 m/z was observed in both of them.

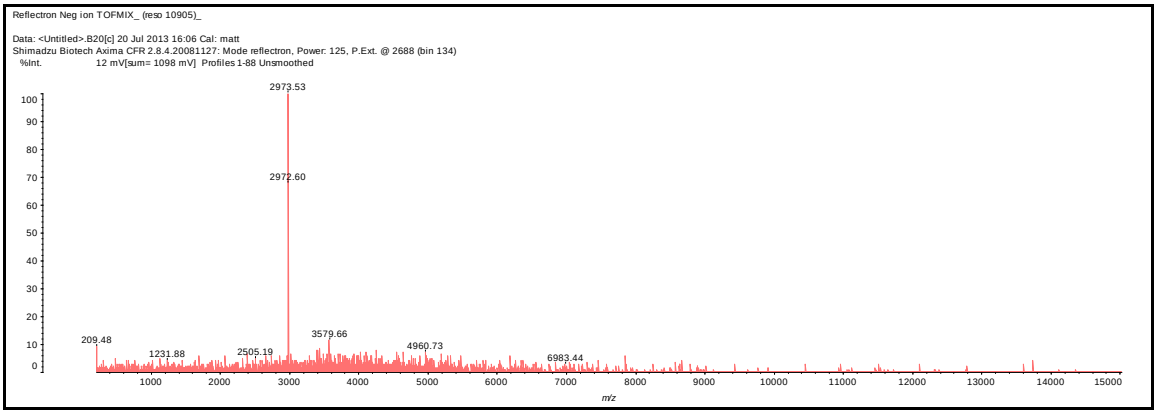

Figure 88. MALDI-tof MS obtained for the formation of extended triple decker **75**.

Then, ^{1}H-NMR spectra was processed for both fractions. The ^{1}H-NMR spectrum of the second spot corresponded to unreacted starting material with some impurities. On the other hand, the first brown fraction resembled much more to the expected spectra for extended triple decker **75** as it could be observed from comparison between previously synthesised triple decker **50** (from porphyrin C_{10} dyad **45**) and the obtained product **75**.

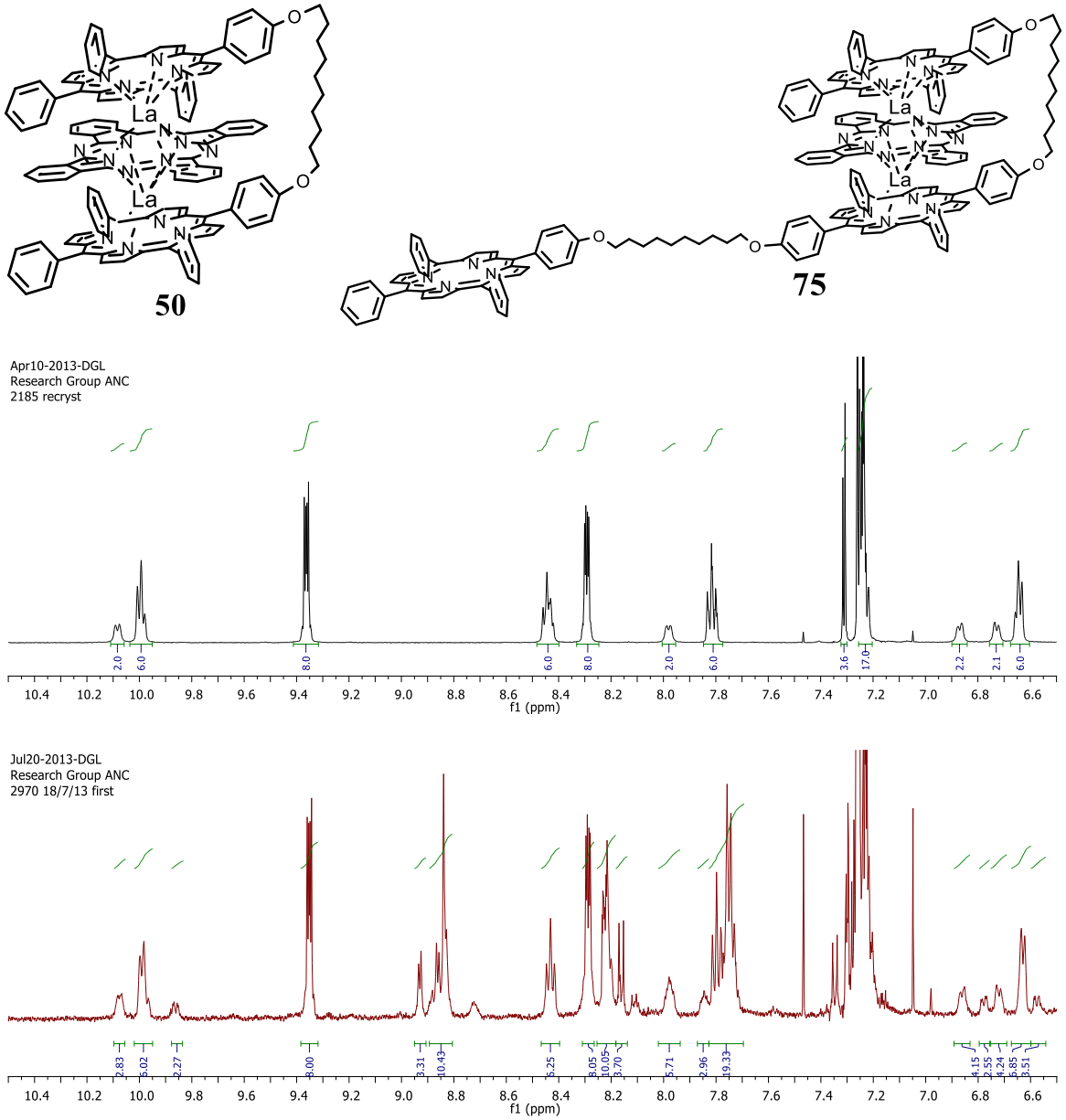

Figure 89. Comparison between triple decker **50** and the product **75**.

A much more complicated spectrum was expected for product **75** as in this case, the obtained complex has much lower symmetry due to the extra porphyrin. However there were

a few factors in the ^{1}H-NMR spectrum that were very typical of the formation of triple deckers and were observed in all previous triple decker analogues:

- The appearance of the phthalocyanine peaks (around 9.35 and 8.3 ppm) in the spectra is a first indication that the phthalocyanine was successfully inserted into the complex. This also appeared in the same range as simpler triple decker **50** (above).
- The splitting observed at around 10 ppm is very typical for this type of complex and they should correspond to the internal *ortho*- protons of the phenyl groups of the porphyrins that are forming the triple decker as previously analysed for other triple deckers.[80]
- The same type of splitting can be also observed in the region of 6.7 ppm for the peaks corresponding to the external *meta*- phenyl protons of the porphyrins. This also is in coherence with the above spectra for the normal triple decker.
- Finally peaks corresponding to the free porphyrin could also be observed in the region of 8.9 ppm but unlike the previous signals typical of triple deckers, this could not be differentiated from the starting material. On the other hand, starting material was not observed on the MALDI-tof MS, therefore these signals should correspond the free porphyrin of the product **75**.

Unfortunately, analytically pure material could not be obtained for the product due to the small amount of material that was recovered from the reaction. For this reason, successful analytical data from the complex could not be obtained. On the other hand, the analysis performed for the fraction obtained from the column is in accordance with the presence of the expected product as previously analysed.

4.5.2. Conclusions

The synthesis of *trans*-porphyrins has proven to be difficult due to the instability of some dipyrromethanes that are needed as precursors. The synthesis of several dipyrromethanes was attempted in order to establish the best possible synthetic route for the synthesis of *trans*-porphyrins. Even with stable dipyrromethanes such as **77** or **78**, other problems appeared during the synthesis when scrambling processes are present. Finally, some *trans*-porphyrins were obtained in big scale using pentafluorophenyl dipyrromethane **90** as starting material. This allowed the synthesis of porphyrin triad **94** in big scale. On the other hand, another porphyrin triad **73** could also be obtained from *trans*-porphyrin **80** but with a low yield due to a very difficult purification.

Once porphyrin triads **73** and **94** were synthesised, a first standard procedure for the formation of triple deckers was attempted using this porphyrin triads as templates. Various problems were encountered such as addition of solvent molecules to the product and appearance of other undesired side products. On the other hand, extended porphyrin triple decker **75** could be observed using porphyrin triad **73** as starting material. With the data collected so far, it was proven that some more complex structures can be obtained in a controlled manner. The methodology developed during this work was successful but the synthesis still need optimisation and other porphyrin triads need to be further studied in order to overcome the various problems observed.

5.1. General methods

Physical measurements

^{1}H NMR spectra were recorded either at 400 MHz on a Varian 400 spectrometer, or at 500 MHz in a Bruker 500. Signals are quoted in ppm as δ downfield from tetramethylsilane (δ 0.00) as internal standard, or using residual solvent as reference. ^{13}C NMR spectra were recorded at 100.5 or 126 MHz on the same spectrometers. The nucleus and operating frequency are indicated for each set of data and coupling constants J given in Hertz. The spectra were recorded at room temperature unless otherwise stated.

Infrared spectra were recorded on a Perkin-Elmer 1720X FT-IR spectrophotometer as neat liquid films or Nujol mulls for solid materials. UV-vis Spectra were taken on a Hitachi U-3000-X spectrometer in solvent as stated.

Mass spectra were recorded on a Shimadzu Axima-CFR MALDI-tof spectrometer by direct sample deposition or using *trans*-2-[3-(4-t-butyl-phenyl)-2-methyl-2-propenylidene]malononitrile (DCTB) as matrix for the analysis when specified.

TLC was carried out on a Merck aluminium backed silica gel 60 F254 coated plates, and the compounds were visualised by viewing under UV light at 254 nm or 366 nm.

Column chromatography was performed at ambient temperature using Fluka or Merck silica gel 60 (70-230 mesh) at ambient pressure or occasionally at moderate pressure. Solvent ratios are given as v/v.

Melting points are uncorrected and recorded using a Kofler hot-stage melting point apparatus with a digiton model 2751-K display.

Reagents, Solvents and Reaction Conditions

Unless otherwise stated, all chemicals were obtained from commercial sources and were used without purification.

Nitrogen gas used is oxygen free. Petroleum ether is light petroleum (B.p. 40-60 ˚C). Dried solvents, THF and diethyl ether, were freshly distilled from sodium and benzophenone when especified. Other solvents were SLR-grade and used without drying, unless otherwise stated.

Water refers to distilled water. Brine is a saturated aqueous solution of sodium chloride. Organic layers were dried over anhydrous magnesium sulphate. Evaporation of solvent was carried out on a Büchi rotary evaporator at reduced pressure.

Temperatures quoted in the reaction conditions are the temperatures of the reaction cooling or heating baths.

5.2. Synthetic procedures

5,10,15,20-Tetraphenylporphyrins, general procedure 1:

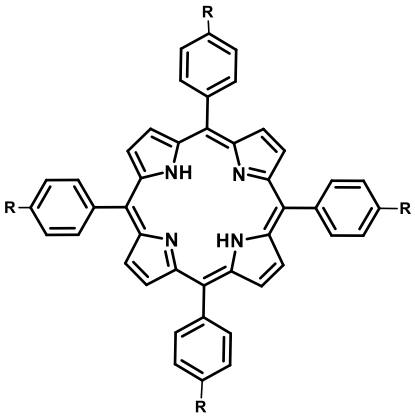

For the synthesis of symmetrical porphyrins, a modified version of the synthesis developed by Adler was followed.[42] The corresponding aldehyde (0.1mol) was dissolved in propionic acid (250 ml) and left to reflux, to this, freshly distilled pyrrole (0.1 mol) was added dropwise and the mixture reacted for 30 min opened to air. Then, the reaction mixture was cooled down to room temperature and left precipitating overnight in the fridge, then MeOH was added to the mixture (200 ml), filtered and further washed with MeOH to obtain purple crystalline solids of the product.

Tetraphenylporphyrin[42] (TPP) 3

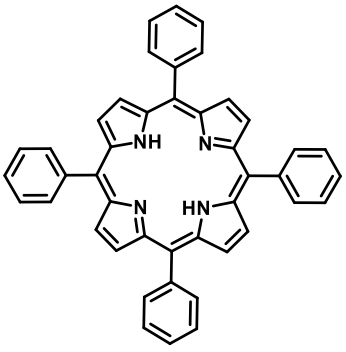

3

The title compound was obtained following the general procedure 1 reacting benzaldehyde (8.48 g, 80 mmol) and pyrrole (5.36 g, 80 mmol) in propionic acid (200 ml).

The title compound was obtained as a purple solid (2.21 g, 18 %). m.p. >350 ˚C. ^{1}H NMR (500 MHz, $CDCl_3$) δ 8.77 (s, 8H), 8.15 (dd, *J* = 7.7, 1.5 Hz, 8H), 7.72 – 7.65 (m, 12H), -2.85 (s, 2H). ^{13}C NMR (126 MHz, $CDCl_3$) δ 142.31, 134.71, 127.85, 126.83, 120.28. MS (MALDI-tof): m/z = 614.22 [M^+]. UV-vis (DCM)/nm: 417, 515, 550, 590, 648. IR (KBr, cm^{-1}): 2833, 1604, 1505, 1460, 1437, 1348, 1287, 1245, 1172, 1105, 1033, 980, 964.

Tetra-*p*-bromophenylporphyrin[131] (TBrPP) 11

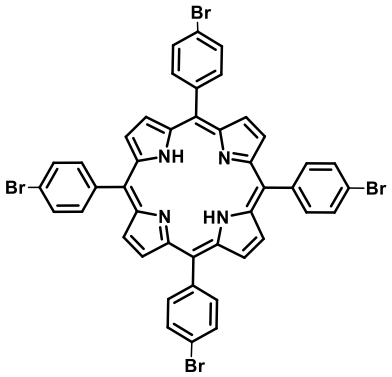

11

The title compound was obtained following the general procedure 1 reacting 4-bromobenzaldehyde (14.8 g, 80 mmol) and pyrrole (5.36 g, 80 mmol) in propionic acid (200 ml). The title compound was obtained as a purple solid after recrystallization from DCM/MeOH (2.96 g, 16 %). m.p. >350 ˚C. ^{1}H NMR (500 MHz, $CDCl_3$) δ 8.84 (s, 8H), 8.07 (d, *J* = 8.5 Hz, 8H), 7.90 (d, *J* = 8.5 Hz, 8H), -2.87 (s, 2H). ^{13}C NMR (126 MHz, $CDCl_3$) δ 140.97, 135.98, 130.14, 122.79, 119.14. MS (MALDI-tof): m/z = 930.8 [M^+]. IR (KBr, cm^{-1}): 3062, 190.6, 1556, 1474, 1390, 1348, 1266, 1211, 1176, 1069, 1011, 964.

Tetra-*p*-methoxyphenylporphyrin[131] (T(OMe)PP) 12

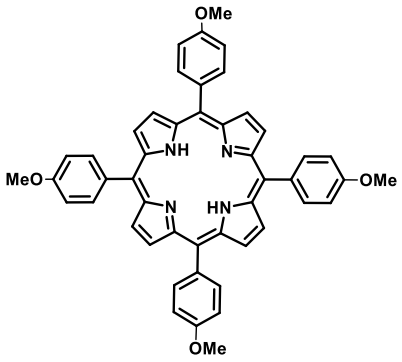

12

The title compound was obtained following the general procedure 1 reacting *p*-methoxybenzaldehyde (14.8 g, 80 mmol) and pyrrole (5.36 g, 80 mmol) in propionic acid (200 ml). The title compound was obtained as a purple solid (2.47 g, 17 %). m.p. >350 ˚C. ^{1}H NMR (500 MHz, $CDCl_3$) δ 8.86 (s, 8H) H_{β}; 8.13 (d, J = 8.5 Hz, 8H) H_{oPh}; 7.29 (d, J = 8.5 Hz, 8H) H_{mPh}; 4.10 (s, 12H) -O-CH_3; -2.75 (s, 2H) -N*H*. ^{13}C NMR (126 MHz, $CDCl_3$) δ 159.52, 158.96, 135.74, 134.79, 119.87, 112.33, 77.36, 55.73. MS (MALDI-tof): m/z = 733.92 [M^+]. IR (KBr, cm^{-1}): 2833, 1604, 1505, 1460, 1437, 1348, 1287, 1245, 1172, 1105, 1033, 980, 964.

***p*-(6'-Bromohexanoxy)benzaldehyde[132] 10**

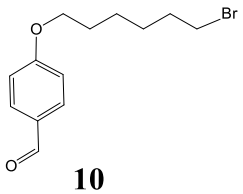

10

4-hydroxybenzaldehyde (3 g, 24 mmol) was mixed with 1,6-dibromohexane (14.9 g, 61.4 mmol) and dissolved in 200 ml of acetone, and 5 g of potassium carbonate were added. The mixture was then left refluxing overnight. After 20 h refluxing, it was filtered and the solids washed with DCM. The solvents were removed and the white solid obtained was purified using silica column chromatography using DCM:Pet ether (1:1 v/v) as eluent. Then the fraction containing the product was precipitated with hexanes in ice to yield white solids (4.29 g, 61 %). m.p.: 40.5-41.6 °C. ^{1}H NMR (500 MHz, $CDCl_3$) δ 9.88 (s, 1H) C*H*O, 7.83

(d, *J* = 8.8 Hz, 2H) $\underline{H}_{oPh}$, 6.99 (d, *J* = 8.7 Hz, 2H) $\underline{H}_{mPh}$, 4.05 (t, *J* = 6.4 Hz, 2H) O-C$\underline{H}_2$, 3.43 (t, *J* = 6.7 Hz, 2H) Br-C$\underline{H}_2$, 1.91 (p, *J* = 6.8 Hz, 2H) -C$\underline{H}_2$-, 1.84 (p, *J* = 6.8 Hz, 2H) -C$\underline{H}_2$-, 1.54 – 1.50 (m, 4H) -C$\underline{H}_2$-. ^{13}C NMR (126 MHz, $CDCl_3$): δ 191.00, 164.27, 132.16, 129.93, 114.86, 68.25, 33.91, 32.73, 29.02, 27.99, 25.36.

p-(10'-Bromodecanoxy)benzaldehyde[133] 84

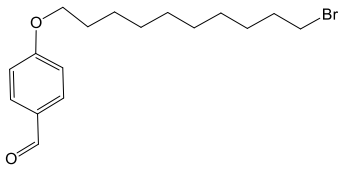

84

4-hydroxybenzaldehyde (2 g, 16 mmol) was mixed with 1,10-dibromohexane (12.3 g, 40.1 mmol) and dissolved in 200 ml of acetone, then 5 g of potassium carbonate were added. The mixture was left refluxing overnight. After 20 h refluxing, it was filtered and the solids washed with DCM. The solvents were removed and the white solid obtained was purified using silica column chromatography using DCM:Pet ether (1:1 v/v) as eluent. Then the first fraction containing the product was precipitated with hexanes in ice to yield white solids (4.56 g, 82 %). m.p.: 29.5-30.3 °C. ^{1}H NMR (500 MHz, $CDCl_3$) δ 9.88 (s, 1H), 7.82 (d, *J* = 8.8 Hz, 2H), 6.99 (d, *J* = 8.7 Hz, 2H), 4.04 (t, *J* = 6.5 Hz, 2H), 3.41 (t, *J* = 6.9 Hz, 2H), 1.95 – 1.66 (m, 4H), 1.51 – 1.40 (m, 4H), 1.39 – 1.27 (m, 8H). ^{13}C NMR (126 MHz, $CDCl_3$) δ: 190.96, 164.40, 132.13, 129.91, 114.89, 68.54, 34.17, 32.94, 29.54, 29.48, 29.41, 29.19, 28.87, 28.28, 26.08.

Tetrakis-4-(6'-bromohexanoxy)phenylporphyrin[134] 13

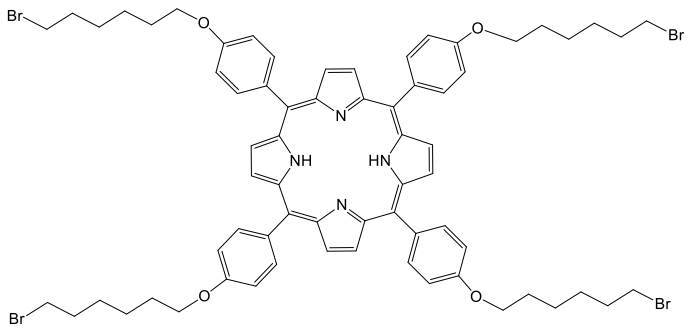

13

Using general procedure 1,[42] *p*-(6'-bromohexanoxy)benzaldehyde **10** (5 g, 17.5 mmol) and freshly distilled pyrrole (1.2 ml, 1.16 g, 17.5 mmol) refluxed in propionic acid for 30 min. After work up, purple crystals of the pure product were obtained (0.653 g, 11 %). ^{1}H NMR (500 MHz, $CDCl_3$) δ 8.86 (s, 8H) $\underline{H_{\beta}}$; 8.11 (d, *J* = 8.5 Hz, 8H) $\underline{H_{oPh}}$; 7.27 (d, *J* = 8.5 Hz, 8H) $\underline{H_{mPh}}$; 4.26 (t, *J* = 6.3 Hz, 8H) -O-C$\underline{H_2}$-$(CH_2)_2$-, 3.51 (t, *J* = 6.8 Hz, 8H) Br-C$\underline{H_2}$-$(CH_2)_2$-; 2.01 (q, 6.6 Hz, 16H) -O-CH_2-(C$\underline{H_2}$)$_2$-; 1.72 – 1.62 (m, 16H) Br-CH_2-(C$\underline{H_2}$)$_2$-; -2.76 (s, 2H) N*H*. ^{13}C NMR (126 MHz, $CDCl_3$) δ 159.52, 158.96, 147.61, 135.74, 134.79, 119.87, 112.33, 68.33, 34.09, 32.88, 29.50, 28.23, 26.25. MS (MALDI-tof): m/z = 1331.23 [M^+]. IR (KBr, cm^{-1}): 2930, 2853, 1605, 1572, 1507, 1465, 1428, 1389, 1350, 1282, 1243, 1174, 1107, 1048, 980, 964, 802.

Following a different methodology, tetra-*p*-hydroxyphenylporphyrin **15** (0.33 g, 0.486 mmol), 1,6-dibromohexane (1.5 ml, 2.34 g, 9.72 mmol) and potassium carbonate (1.62 g, 11.8 mmol) were dissolved in 20 ml of MEK and refluxed overnight. After 20 h, the reaction was cooled down and precipitated with MeOH, after filtration, the crude solids were separated by column chromatography using DCM:Pet. ether (1:1 v/v) with 1% Et_3N as eluent to recover the product as a purple solid (1.85 g, 59 %).

Tetra-p-hydroxyphenylporphyrin[84] (T(OH)PP) 15

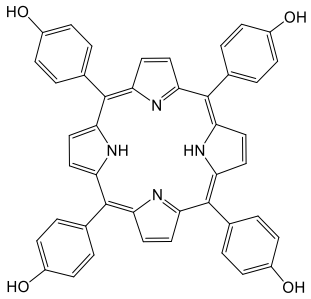

15

Tetrakis-*p*-methoxyphenylporphyrin **12** (1 g, 1.36 mmol) was dissolved in DCM (30 ml) and stirred. Then, BBr_3 (32.6 ml of 1 M solution in DCM, 32.6 mmol)) was added dropwise and the reaction left stirring overnight. After quenching the reaction with MeOH and neutralising it with triethylamine, the reaction turned from green to dark red colour. The crude was concentrated and redissolved in ethyl acetate. Water was then added and the mixture extracted several times with ethyl acetate, dried with $MgSO_4$, filtered and concentrated to obtain the title product (0.77 g, 83 %) with spectroscopic data in full accordance with the literature.[84] ^{1}H NMR (500 MHz, Acetone) δ 8.93 (s, 8H) H_β; 8.07 (d, J = 6.5 Hz, 8H) H_{oPh}; 7.30 (d, J = 6.5 Hz, 8H) H_{mPh}; 2.63 (s (br), 4H) -O*H*, -2.70 (s, 2H) N*H*. MS (MALDI-tof): m/z = 679.33 [M^+]. IR (KBr, cm^{-1}): 3330 (br), 1614, 1514, 1249, 1181, 803.

5-*p*-hydroxyphenyl-10,15,20-triphenylporphyrin[83] (TPP-OH) 34

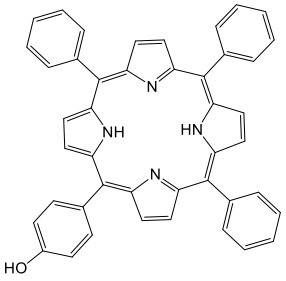

34

A modified version of the procedure developed by Adler[42] was followed using a mixture of aldehydes. Both *p*-hydroxybenzaldehyde (3.05 g, 25 mmol) and benzaldehyde (7.96 g, 75 mmol) where dissolved in propionic acid (200 ml) and left to reflux. To the

refluxing mixture, freshly distilled pyrrole (6.94 ml, 6.71 g, 100 mmol) was added dropwise and the mixture was refluxed for 30 min. After cooling down to room temperature, the crude mixture was precipitated selectively with MeOH (150 ml) and after suction filtration, a purple solid was obtained. The crude solids were purified by column chromatography (maximum 6 cm high) using DCM:Pet ether (1:1) as eluent to collect a first purple fraction corresponding to TPP **3**. Then, when no more purple solution eluted, the solvent was changed to 100 % DCM to recover the product TPP-OH (0.812 g, 5 %). m.p. >350 ˚C. ^{1}H NMR (500 MHz, $CDCl_3$): δ 8.88 (m, 2H) and 8.84 (m, 6H) H_β; 8.215 (d, *J* = 10 Hz, 6H), 8.08 (d, *J* = 10 Hz, 2H) for H_{oPh}; 7.77 (m, 9H) and 7.21 (d, *J* = 10 Hz, 2H) H_{pPh} and H_{mPh}; 5.18 (s, br, 1H) –OH; -2.77 (s, 2H) –NH. ^{13}C NMR (500 MHz, $CDCl_3$) δ 155.55, 142.35, 135.85, 134.88, 134.71, 127.85, 126.83, 120.24, 120.16, 120.00, 113.82. MS (MALDI-tof): m/z = 631.54 [M^+].

(Tetraphenylporphyrin)indium chloride[65] (TPP-InCl) 16

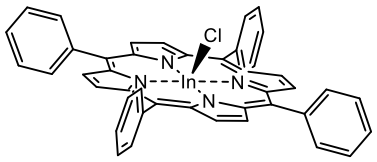

16

According to the method developed by Butchler,[65] metal free TPP **3** (1.62 g, 2.13 mmol) and $InCl_3$ (0.94 g, 4.26 mmol) were dissolved in acetic acid (200 ml) and the mixture left refluxing overnight. The resultant reaction mixture was cooled and evaporated to obtain brown solids, which were dissolved in DCM and subjected to flash chromatography on silica gel using DCM/Pet. Ether (2/3) as eluent. A purple solids of **16** were isolated (1.28 g, 83 %). ^{1}H NMR (500 MHz, $CDCl_3$) δ 9.00 (s, 8H) H_β; 8.33 – 8.28 (m, 4H) H_{oPh}; 8.04 (d, *J* = 7.5 Hz, 4H) $H_{o'Ph}$; 7.77 – 7.73 (m, 8H) H_{mPh};, 7.71 – 7.64 (m, 4H) H_{pPh}. ^{13}C NMR (500 MHz, $CDCl_3$) δ 149.62, 141.88, 135.24, 134.41, 132.94, 128.17, 127.04, 126.88, 121.91. MS (MALDI-tof): m/z = 727.22 [M^+]. IR (KBr, cm^{-1}): 3059, 1596, 1474, 1439, 1338, 1205, 1176, 1069, 1010.

(Tetra-*p*-bromophenylporphyrin)indium chloride[66] (TBrPP-InCl) 21

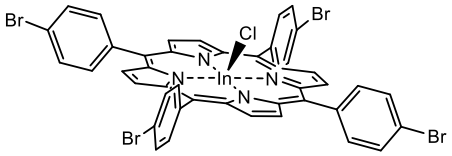

21

The indium insertion method developed by Butchler was followed.[65] TBrPP **11** (50 mg, 0.05 mmol) and $InCl_3$ (22.1 mg, 0.10 mmol) were dissolved in acetic acid (200 ml) and the mixture left refluxing for 48 h. The resultant crude mixture was dried to obtain brown solids, which were dissolved in DCM and subjected to flash chromatography on silica gel using DCM/MeOH (2:3 v/v) as eluent. Compound **21** was isolated as a purple solid (35 mg, 65 %). ^{1}H NMR (500 MHz, $CDCl_3$) δ 8.84 (s, 8H) H_β; 8.07 (dt, *J* = 8.5, 2.5 Hz, 8H) H_{oPh}; 7.90 (dt, *J* = 8.5, 2.5 Hz, 8H) H_{mPh}. ^{13}C NMR (500 MHz, $CDCl_3$) δ 140.97, 135.98, 130.14, 122.79, 119.14, 77.36. MS (MALDI-tof): m/z = 1078.12 [M^+]. IR (KBr, cm^{-1}): 2923, 2853, 1723, 1586, 1473, 1391, 1208, 1072, 1007, 966.

(Tetra-*p*-hydroxiphenylporphyrin)indium chloride[65] (TOHPP-InCl) 18

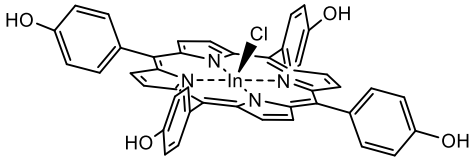

18

The indium insertion method developed by Butchler was followed.[65] TOHPP **15** (0.6 g, 0.9 mmol) and $InCl_3$ (0.39 g, 1.8 mmol) were dissolved in acetic acid (200 ml) and the mixture left refluxing for 48 h. The resultant crude mixture was dried to obtain green solids, which were dissolved in MeOH and neutralised with triethylamine and then subjected to flash chromatography on silica gel using MeOH/Pet ether (2:3 v/v) as eluent. Purple solids of **18** were isolated (0.12 mg, 16 % yield). m.p >350 ˚C. ^{1}H NMR (500 MHz, Acetone) δ 9.13 (d, *J* = 24.2 Hz, 8H), 8.89 (s, 4H), 8.11 (s, 4H), 8.03 (d, *J* = 7.0 Hz, 4H), 8.00 (d, *J* = 7.0 Hz, 4H), 7.27 (s, 4H), -2.73 (s, 2H). MS (MALDI-tof): m/z = 826.32 [M^+].

(Tetraphenylporphyrin)ruthenium carbonmonoxyde, ethanol complex[70]

TPPRu(CO)(EtOH) 24

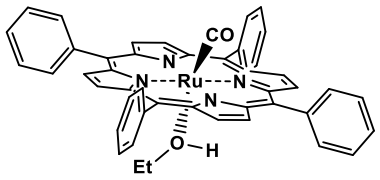

24

A modified method for the insertion of ruthenium into porphyrins developed by Collman was followed.[70] To a solution of ruthenium dodecacarbonyl (31 mg, 0.05 mmol) in toluene 10 ml under Ar atmosphere, TPP **3** was added (30 mg, 0.05 mmol) and left refluxing overnight. Then, the reaction was cooled down and EtOH (100 ml) added to the mixture and left stirring again overnight, then filtered and the liquid fraction concentrated and separated by column chromatography in alumina (neutral) using DCM:EtOH (99:1 v/v) mixture as eluent. The dark red band collected and concentrated and recrystallized from the mixture of DCM-hexane to recover the pure product (22.3 mg, 58 % yield). ^{1}H NMR (500 MHz, $CDCl_3$) δ 8.69 (s, 8H) H_β; 8.22 (d, *J* = 6.5 Hz, 4H) H_{oPh}; 8.13 (d, *J* = 6.5 Hz, 4H) $H_{o'Ph}$; 7.74 (m, 12H) H_{mPh} and H_{pPh}; 0.75 (s, 1H). –O*H*; 0.34 (s(br), 2H) -CH_2; -0.51 (s(br), 3H) -CH_3. MS (MALDI-tof): m/z = 714.23 [M^+-(EtOH)-(CO)]. UV-vis (DCM)/nm: 411, 528. IR (KBr, cm^{-1}): 2962, 2161, 2042, 1949(CO), 1596, 1440, 1351, 1260, 1176, 1069, 1008, 796, 753, 718, 704, 418

(Tetraphenylporphyrin)ruthenium carbonmonoxyde, pyridine[135] TPPRu(CO)(py) 25

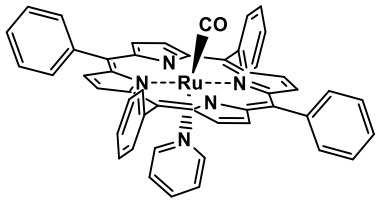

25

To a solution of ruthenium dodecacarbonyl (31 mg, 0.05 mmol) in toluene 10 ml under argon, TPP **3** was added (30 mg, 0.05 mmol) and left refluxing overnight. Then, the reaction was cooled down and EtOH (100 ml) added to the mixture and left stirring again overnight, then filtered and the liquid fraction concentrated and separated by column chromatography in alumina (neutral) using DCM:EtOH (99:1 v/v) mixture as eluent. The dark red band collected and redissolved in 10 ml of DCM, to this, an excess of pyridine (10 ml) was added and left stirring for 30 min. The solvents were distilled under pressure to collect the desired complex as a purple solid (23 mg, 57 %). ^{1}H NMR (500 MHz, $CDCl_3$) δ 8.61 (s, 8H) H_{β}; 8.25 – 8.20 (m, 4H) H_{oPh}; 8.05 (d, *J* = 7.4 Hz, 4H) $H_{o'Ph}$; 7.72 (p, *J* = 4.0 Hz, 8H) H_{mPh}; 7.66 (m, 4H) H_{pPh}; 6.08 (tt, *J* = 7.5, 1.5 Hz, 1H) $H_{p\mathrm{Py}}$; 5.20 (td, J=7.5 Hz, 2H) $H_{m\mathrm{Py}}$; 1.55 (dd, *J* = 6.6, 1.5 Hz, 2H) $H_{o\mathrm{Py}}$. (MALDI-tof): m/z = 714.23 [M^+-(py)-(CO)] and 791.92 [M^+-(CO)]. UV-vis (DCM)/nm: 412, 532. IR (KBr, cm^{-1}): 2962, 1971(CO), 1597, 1529, 1442, 1360, 1305, 1260, 1070, 1007.

Zinc metallated porphyrins, general procedure 2:

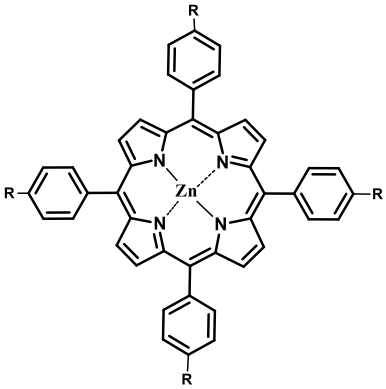

In a general synthetic procedure for the zinc insertion into porphyrins,[85] the porphyrin is going to be refluxed in acetone in the presence of zinc acetate for 30 to 60 min. After completion, the solvent was evaporated and the crude extracted with DCM/H_2O, dried over $MgSO_4$ and concentrated to collect the pure product.

Zinc 5-*p*-hydroxyphenyl-10,15,20-triphenylporphyrin[136] ZnTPPOH 39

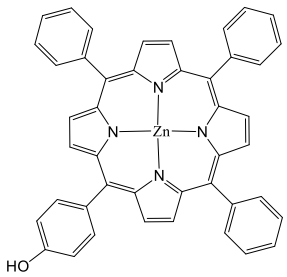

39

Following general procedure 2, TPP-OH **34** (1 g, 1.58 mmol) and zinc acetate (0.3 g, 1.63 mmol) were refluxed in 300 ml of acetone. Then concentrated, redissolved in DCM (100 ml) and extracted with water (2 x 100 ml) and brine (100 ml) to recover the product as a light purple solid (1.05 g, 96 %). ^{1}H NMR (500 MHz, $CDCl_3$) δ 8.99 (d, J = 4.6 Hz, 2H) and 8.96 (d, J = 4.7 Hz, 2H) $H_{\beta'}$ and 8.95 (s, 4H) H_{β}; 8.23 (dd, J = 7.5, 1.5 Hz, 6H) H_{oPh}; 8.08 (dd, 2H) $H_{oPh'}$; 7.82 – 7.72 (m, 9H) H_{mPh} and H_{pPh}; 7.20 (dd, 2H) H_{mPh}; 5.04 (s, br, 1H) -O*H*. ^{13}C NMR (126 MHz, $CDCl_3$) δ 155.55, 142.35, 135.85, 134.88, 134.71, 127.85, 126.83, 120.24, 120.16, 120.00, 113.82. (MALDI-tof): m/z = 693.21 [M^+]. IR (KBr, cm^{-1}): 3382 (br), 2957, 1648, 1598, 1485, 1440, 1339, 1269, 1170, 1069, 1003, 995, 880.

Zinc Tetrakis-5,10,15,20-(*p*-(6'-bromohexanoxy)phenyl)porphyrin 18

ZnT(OC$_6$Br)$_4$PP 40

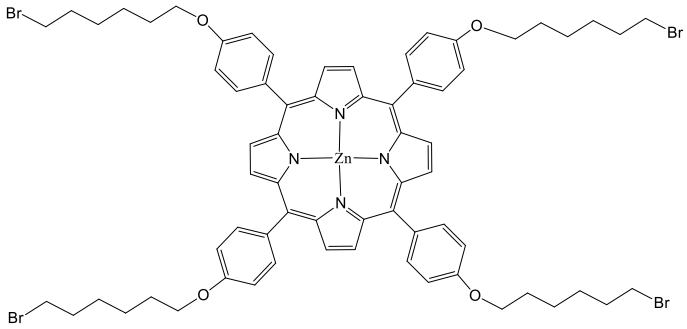

40

Free porphyrin **13** (725 mg, 0.54 mmol) was metallated using a modified version of procedure 2 by heating it and zinc acetate (120 mg, 0.65 mmol) in 60 ml of refluxing mixture of DCM:acetone (2:1) for 90 min. Then, 100 ml of water were added, extracted, filtered and recrystallized from DCM:MeOH to obtain light-purple crystals (751 mg, 99 %). ^{1}H NMR (500 MHz, $CDCl_3$): δ 8.97 (s, 8H) H_β; 8.11 (d, 8H, J=8.0Hz) H_{oPh}; 7.27 (d, 8H, J=8.0Hz) H_{mPh}; 4.27 (t, 8H, J=6.5Hz) O-CH_2; 3.51 (t, 8H, J=6.5Hz) Br-CH_2; 2.01 (m, 16H) -CH_2-; 1.67 (m, 16H) -CH_2-. ^{13}C NMR (126 MHz, $CDCl_3$) δ 159.52, 158.96, 147.61, 135.74, 134.79, 119.87, 112.33, 68.33, 34.09, 32.88, 29.50, 28.23, 26.25. MS (MALDI-tof): m/z = 1395.19 [M^+]. IR (KBr, cm^{-1}): 2932, 2855, 1606, 1525, 1508, 1493, 1461, 1338, 1244, 1174, 1107, 1068, 998, 847, 804.

Dysprosium porphyrin acetylacetonate[75] 28

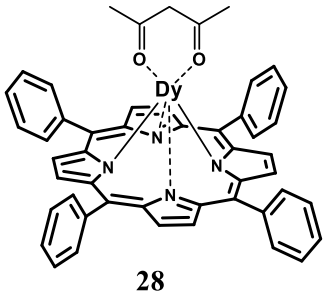

28

A modified procedure of the synthesis of half sandwich complexes developed by Jiang J. was followed.[60] In this case, TPP **3** (61.4 mg, 0.1 mmol) was mixed with dysprosium acetylacetonate (55.2 mg, 0.1 mmol) and refluxed in 4 ml of octanol for 5 h. The reaction completion was checked by UV-vis and then, 60 ml of pet. ether were added to the mixture and the resultant solids collected by vacuum filtration. The resultant purple solid was subjected to column chromatography in neutral alumina using DCM:pet. ether (1:1) and the second light-pink fraction collected. After concentration and recrystallisation in DCM:MeOH, the half sandwich complex was isolated (16.3 mg, 21 %). MALDI-tof: 776.31 m/z [M^+-(acac)]. UV-vis (DCM)/nm: 416, 553.

Dysprosium porphyrinatephthalocyanate double decker 30

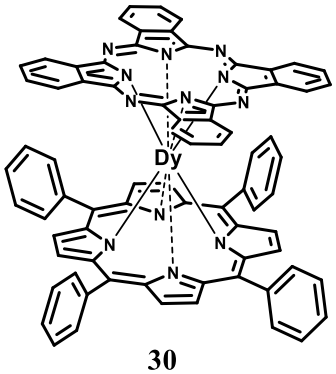

30

For the synthesis of **30**, a modified method for the synthesis of double decker developed by Jiang, J. et al. was followed.[60] In this case, TPP **3** (122.8 mg, 0.2 mmol) was mixed with dysprosium acetylacetonate (110.36 mg, 0.24 mmol) and the mixture refluxed in octanol (5 ml) for 6 h. Then, the reaction was cooled enough to stop the reflux and phthalonitrile (150 mg, 1.2 mmol) and DBU (0.1 ml) were added to the reaction mixture and

refluxed overnight. MeOH was then added to the mixture and the resultant precipitate formed was collected using vacuum filtration. The dark solids obtained were purified by column chromatography in neutral alumina using DCM as eluent and the first brown fraction containing the title compound was collected and concentrated. Analytically pure product was then obtained after recrystallization in DCM:MeOH (27.4 mg, 17 %). MALDI-tof: 1287.94 m/z [M^+] UV-vis (DCM)/nm: 337, 418, 598, 749. (^{1}H NMR and ^{13}C NMR could not be performed due to its magnetic properties).

Lanthanum porphyrin acetylacetonate[75] 31

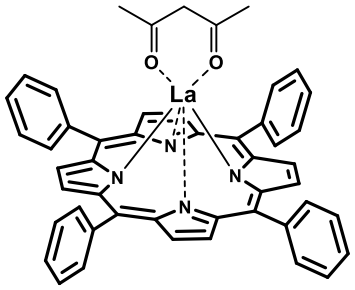

31

A modified procedure for the synthesis of SAT porphyrin complexes was performed.[60] In this case, metal free TPP **3** (122.4 mg, 0.2 mmol) was refluxed in 4 ml of octanol for 5 h in the presence of lanthanum acetylacetonate hydrate (104.69 mg, 0.24 mmol). The reaction completion was checked by UV-vis and then, 20 ml of pet. ether were added to the mixture and the crude left precipitating overnight. The resultant solid was added to 20 ml of DCM, filtered and concentrated to recover the pure metallated complex. (32.5 mg, 19 %). MALDI-tof: 776.31 m/z [M^+-(acac)]. IR (KBr, cm^{-1}): 2924, 1534, 1472, 1437, 1193, 1073, 975.

Lanthanum porphyrinatephthalocyanate double decker[53] 32

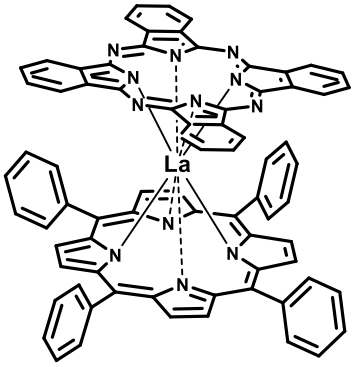

32

According to Jiang's procedure,[60] TPP **3** (122 mg, 0.2 mmol), phthalonitrile (150 mg, 1.2 mmol) and lanthanum acetylacetonate hydrate (104 mg, 0.24 mmol) were mixed together in 4 ml of octanol. Then, 0.1 ml of DBU was added to the mixture and everything refluxed for 18 h. After cooling down the mixture, pet. ether was added (20 ml) and the resultant black solids were recovered by filtration. The solids obtained were subjected to column chromatography over silica gel using DCM:pet. ether (1:1 v/v) as eluent. The resultant green fractions obtained were collected and further separated in silica gel using THF:pet. ether (3:10 v/v). The last green fraction was collected, concentrated and recrystallized from DCM/MeOH mixture to give the title compound as a pure green solid (177.5 mg, 70 %). MALDI-tof: 1265.60 m/z [M^+]. ^{1}H NMR (500 MHz, DMSO) δ 9.11 – 9.06 (m, 8H), 8.21 – 8.17 (m, 8H), 8.00 (s, 8H), 7.68 – 7.59 (m, 8H), 7.42 – 7.25 (m, 8H), 6.91 (d, *J* = 7.0 Hz, 4H). ^{13}C NMR (126 MHz, $CDCl_3$) δ 151.54, 139.32, 128.10, 124.95, 34.43, 30.47. UV-vis, (DCM)/nm(log ε): 343(4.8), 419(4.8), 624(4.3). IR (KBr, cm^{-1}): 2957, 2869, 1667, 1646, 1483, 1457, 1390, 1364, 1330, 1246, 1161, 1057, 980, 882.

Lanthanum functionalised double decker 42

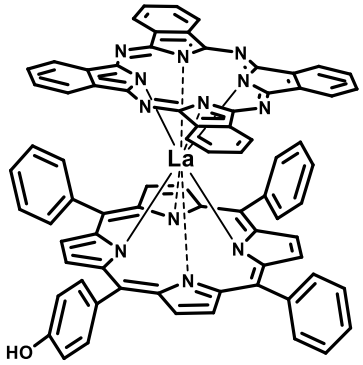

42

The modified procedure for the synthesis of double deckers[60] was followed. TPP-OH **34** (126 mg, 0.2 mmol), phthalonitrile (150 mg, 1.2 mmol) and lanthanum acetylacetonate hydrate (104 mg, 0.24 mmol) were mixed together in 4 ml of octanol. Then, 0.1 ml of DBU was added to the mixture and everything refluxed for 18 h. After cooling down the mixture, pet. ether was added (20 ml) and the resultant black solids were recovered by filtration. The solids obtained were subjected to column chromatography over silica gel using DCM:Pet. ether (1:1 v/v) as eluent and the fraction containing the desired double decker (checked by MALDI-tof MS) further purified in silica gel chromatography using THF:Pet. ether (3:10 v/v) as eluent. Double decker **42** was obtained pure as green solids after recrystallisation (183.6 mg, 72 %). MS MALDI-tof: 1280.66 m/z [M^+]. ^{1}H NMR (500 MHz, DMSO) δ 9.12 (dd, *J* = 5.4, 3.0 Hz, 8H), 8.22 (dd, *J* = 5.6, 2.7 Hz, 8H), 8.13 – 8.10 (m, *J* = 4.2 Hz, 4H), 8.02 (d, *J* = 4.1 Hz, 4H), 7.71 – 7.65 (m, 8H), 7.42 – 7.37 (m, 8H), 7.12 (s, 3H). ^{13}C NMR (126 MHz, DMSO) δ 151.54, 139.32, 128.10, 124.95, 34.43, 30.47. UV-vis, (DCM)/nm(log ε): 337(4.5), 419(4.8), 608(3.9), 747(3.7). IR (KBr, cm^{-1}): 3384.9, 2957, 1669, 1645, 1469, 1434, 1159, 1057.

Multiporphyrin array 36 (M_a = Zn, M_b = H,H)

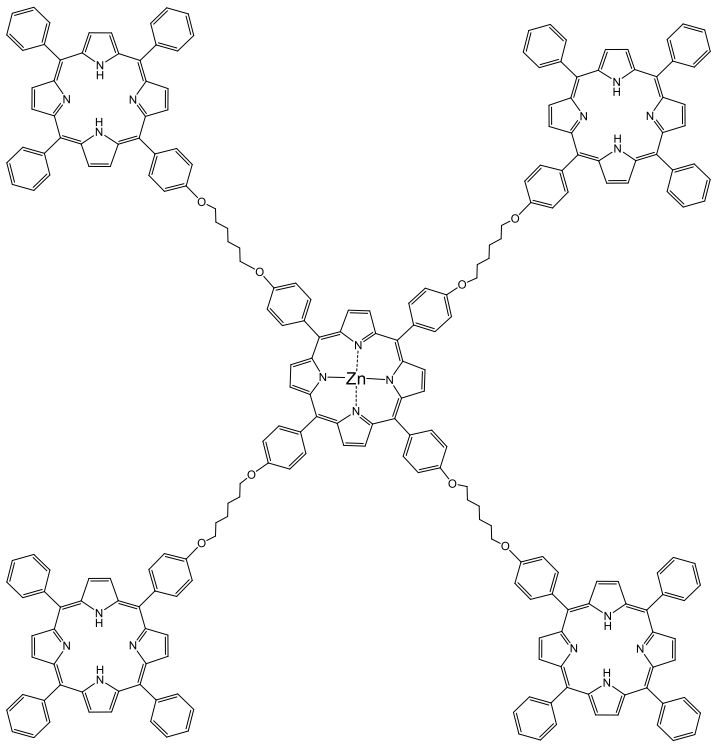

36

Zinc porphyrin **40** (370 mg, 0.265 mmol) and TPP-OH **34** (1 g, 1.58 mmol) were dissolved in 100 ml DMF and left stirring at 80º C for 6 days. The reaction was then cooled down, concentrated until approximately 20 ml and precipitated with water and filtered. The resulting solids were then loaded into a silica gel column and separated using DCM:Pet ether (1:1 v/v), the contents of the first fraction where then recrystallized in DCM:MeOH to obtain the pure title compound (420 mg, 44 %). m.p.: 297-300 °C. MS (MALDI-tof): m/z = 3594.84 $[M^+ + (H^+)_2]$. UV-vis, (DCM)/nm(log ε): 415(5.6), 518(4.2), 551(4.1), 591(3.8), 646(3.6). ^{1}H NMR (500 MHz, $CDCl_3$) δ 9.01 (s, 8H) $H_{\beta\text{-}central}$, 8.90 (d, J = 4.5 Hz, 8H) $H_{\beta\text{-}per}$, 8.83 (s, 24H) $H_{\beta\text{-}per}$, 8.24 – 8.17 (m, 24H) H_{oPh}, 8.16 – 8.09 (m, 16H) $H_{oPh'}$, 7.78 – 7.67 (m, 36H) H_{mPh} and H_{pPh}, 7.33 – 7.26 (m, 16H) $H_{mPh'}$, 4.37 – 4.23 (m, 16H)) -O-CH_2-, 2.08 (s, 16H) -CH_2-, 1.81 (s, 16H) -CH_2-, -2.77 (s, 8H) -N*H*. IR (KBr, cm^{-1}): 2936, 1604, 1506, 1243, 1174, 995. (^{13}C NMR spectra could not be processed due to precipitation of the material in the NMR solvent for high concentrations).

Multiporphyrin array 35 (M_a = H,H, M_b = Zn)

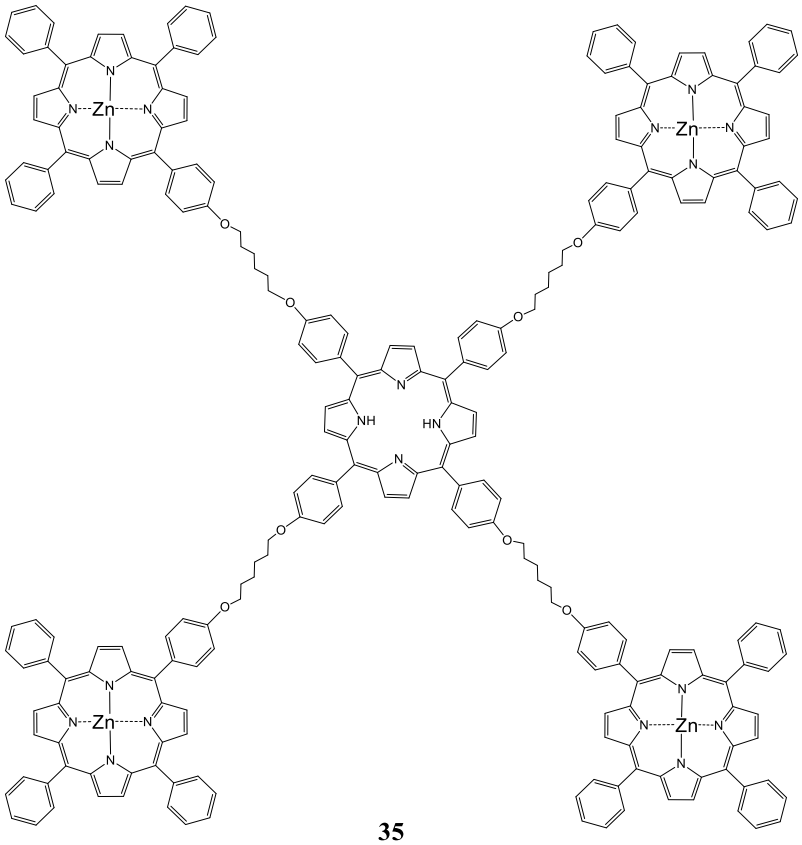

35

Metal free porphyrin **13** (0.317 g, 0.24 mmol), ZnTPP-OH **39** (0.8 g, 1.14 mmol) and potassium carbonate (1.12 g, 8.1 mmol) were heated in DMF (60 ml) at 60º C for 5 days. Then water was added to the crude and filtered off, the crude was eluted through a short silica pad using THF and all impurities removed, then the mixture of compound **35** and silica was mixed with DCM and gravity filtered. The resultant purple solution was then precipitated with MeOH and the purple solid collected (0.287 g, 26 %). ^{1}H NMR (400 MHz, $CDCl_3$) δ 9.00 (d, *J* = 4.5 Hz, 8H) and 8.93 (d, *J* = 4.5 Hz, 8H) $H_{\beta'per}$; 8.93 (s, 16H) $H_{\beta\text{-}per}$; 8.89 (s, 8H) $H_{\beta\text{-}central}$; 8.20 (dd, *J* = 8.7, 3.3 Hz, 24H) H_{oPh}; 8.12 (dd, *J* = 8.0, 5.9 Hz, 16H) $H_{oPh'}$; 7.76 – 7.67 (m, 36H) H_{mPh} and H_{pPh}; 7.31 – 7.22 (m, 16H) $H_{mPh'}$; 4.25 (m, 16H) -O-CH_2-; 2.05 (d, *J* = 5.8 Hz, 16H) -CH_2-; 1.78 (s, 16H) -CH_2-; -2.73 (s, 2H) -N*H*. m.p. 203-205 °C. MS (MALDI-tof): m/z =3787.58 [M^++(H^+)$_4$]. UV-vis, (DCM)/nm(log ε): 420(4.8), 549(3.7), 587(3.4). IR (KBr, cm^{-1}): 2936, 1604, 1506, 1339, 1243, 1174, 994. (^{13}C NMR spectra could not be processed due to precipitation of the material in the NMR solvent for high concentrations).

Multiporporphyrin array 37 (M_a = Ru, M_b = Zn)

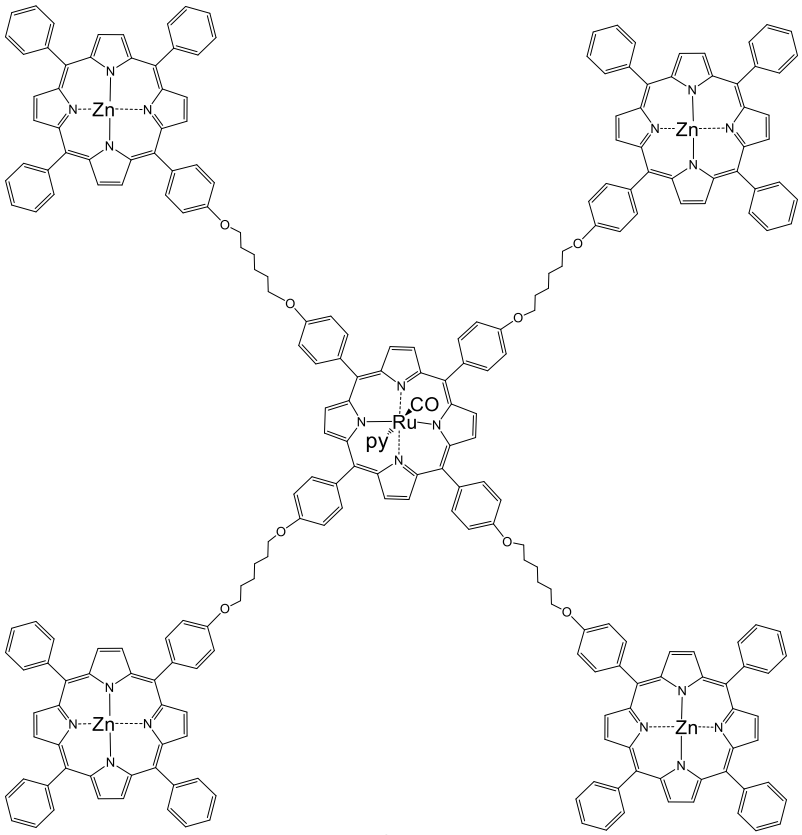

37

Multiporphyrin array **35** (20 mg, 5.28x10^{-3} mmol) and ruthenium dodecacarbonate were dissolved in 5 ml of toluene and left refluxing overnight. After 20 h refluxing, the crude was poured over 100 ml of ethanol and filtered. Then washed with MeOH to recover a purple solid that was mixed in an excess of pyridine and left stirring for 4 h. Then, the crude was concentrated to dryness to obtain multiporphyrin array **37** as a light purple solid (18.8 mg, 89 %). ^{1}H NMR (400 MHz, $CDCl_3$) H_β δ 9.00 (d, J = 4.7 Hz, 8H) H_β, 8.93 (d, J = 4.5 Hz, 24H) H_β, 8.74 (s, 8H) H_{oPh}, 8.23 – 8.17 (m, 24H), 8.13 (d, J = 8.4 Hz, 16H) $H_{oPh'}$, 7.76 – 7.68 (m, 36H) H_{mPh} and H_{pPh}, 7.28 (dd, J = 5.6, 4.6 Hz, 16H) $H_{mPh'}$, 4.28 (d, J = 6.4 Hz, 16H) -O-CH_2-, 3.57 (s) H_{py}, 2.05 (d, J = 7.3 Hz, 16H) -CH_2-, 1.80 (s, 16H) -CH_2-, 1.15 (s, 60H) H_{py}. UV-vis, (DCM)/nm(log ε): 416(5.6), 421(5.5), 548(4.3). IR (KBr, cm^{-1}): υ_{co} = 1941.31. (^{13}C NMR spectra could not be processed due to precipitation of the material in the NMR solvent for high concentrations).

Multiporporphyrin array 38 (M_a = Zn, M_b = Ru)

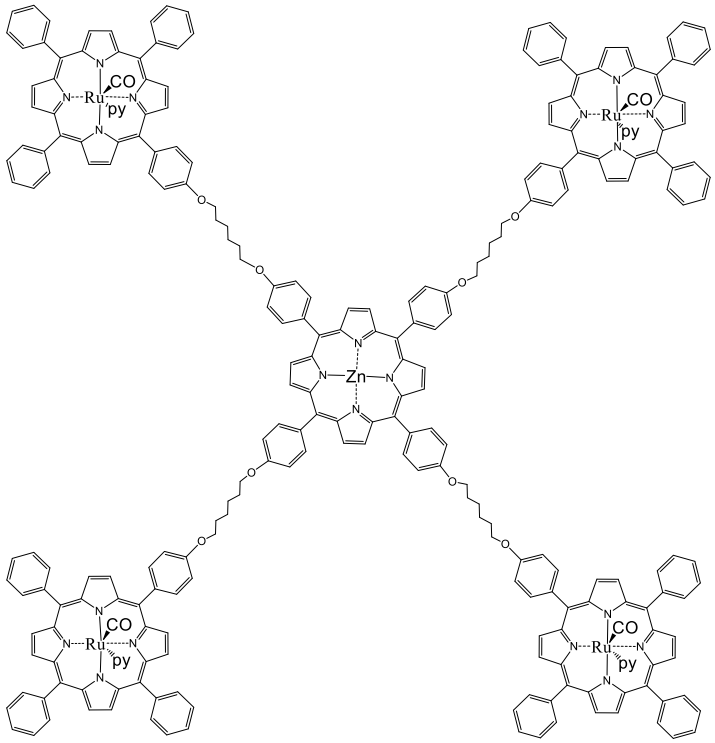

38

Multiporphyrin array **36** (53 mg, 1.47×10^{-5} mol) was mixed with ruthenium dodecacarbonyl (11.3 mg, 1.77×10^{-5} mol) and dissolved in 2 ml of toluene. The mixture was left refluxing for 48 h. Then, 2 ml of pyridine were added and the mixture left stirring at rt. for 4 h. The crude was then precipitated with MeOH and filtered and after recrystallization with DCM:pet ether, the pure product was obtained (12 mg, 20 %). MS (MALDI-tof): m/z = 4585.06 ($[M]^+$+$(py)_2$). UV-vis, (DCM)/nm(log ε): 404(4.8), 420(4.9), 537(3.9). IR: υ_{co} = 1949.75 cm^{-1} (full characterisation could not be obtained due to decomposition of the material during recrystallisation).

5-(10'-bromodecanoxyphenyl)-10,15,20-triphenylporphyrin[137] (TPP-OC$_{10}$Br) 47

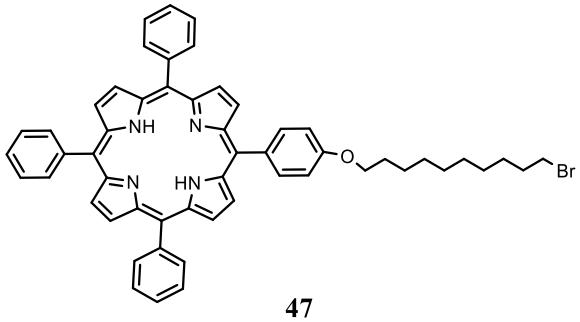

47

TPP-OH **34** (100 mg, 0.16 mmol, 1 eq) and 1,10-dibromodecane (57 mg, 0.19 mmol, 1.2 eq) were dissolved in 25 ml of acetone. K_2CO_3 (55 mg, 0.39 mmol, 2.5 eq) were then added and the mixture refluxed for 24 h. The crude mixture was then precipitated with 50 ml of distilled water and filtered. The solids obtained were washed with MeOH to recover a purple solid. After column chromatography of the solid over silica gel using THF:pet ether (1:3 v/v) as eluent and a recrystallization from DCM/MeOH, the title compound was obtained pure (57 mg, 42 %). ^{1}H NMR (500 MHz, $CDCl_3$) δ 8.89 (d, *J* = 4.5 Hz, 2H) and 8.84 (s, 6H) H_β; 8.22 (m, 6H) and 8.12 (dd, J = 2 Hz, J = 6.5 Hz, 2H) H_{oPh}; 7.77 (m, 9H) and 7.28 (dd, *J* = 2 Hz, *J* = 6.5 Hz, 2H) H_{pPh} and H_{mPh}; 4.25 (t, *J* = 7 Hz, 2H) -O-CH_2-; 3.44 (t, *J* = 7 Hz, 2H) -CH_2-Br; 2.03 – 1.95 (m, 2H)-CH_2-; 1.90 (m, 2H)-CH_2-; 1.63 (m, 2H)-CH_2-; -2.75 (s, 2H) -N*H*. ^{13}C NMR (500 MHz, $CDCl_3$) δ 159.02, 142.26, 135.63, 134.58, 134.35, 127.70, 126.69, 120.07, 112.76, 68.33, 34.09, 32.88, 29.56, 29.53, 29.50, 29.46, 28.83, 28.23, 26.25. MS (MALDI-tof): m/z = 851.33 [M^+]. IR (KBr, cm^{-1}): 2926, 2854, 1594, 1507, 1471, 1440, 1350, 1284, 1246, 1175, 1001, 980, 965, 845.

Porphyrin C_{10} dyad 45 (TPP-O-$(CH_2)_{10}$-O-TPP)

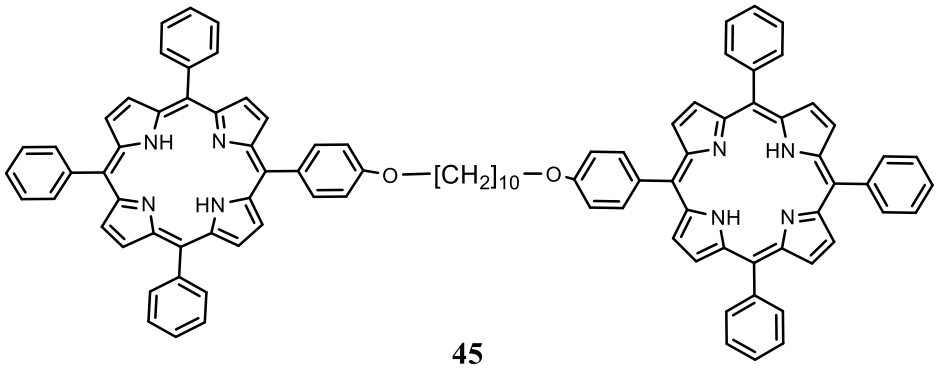

45

A mixture of 1,10-dibromodecane (47.6 mg, 0.16 mmol) and TPP-OH **34** (200 mg, 0.32 mmol) was dissolved in acetone (40 ml), then an excess of K_2CO_3 (220 mg, 1.5 mmol) was added and the mixture left refluxing for 48 h. Then the mixture was precipitated with MeOH and two slow recrystallisations from the DCM:MeOH mixture yielded the pure product as a purple solid (127 mg, 57 %). m.p. > 350 °C. ^{1}H NMR (500 MHz, $CDCl_3$): δ 8.89 (d, *J* = 4.5 Hz, 4H) and 8.83 (d, *J* = 4.5 Hz, 12H) H_β; 8.21 (dd, *J* = 7, <2 Hz, 12H) H_{oPh}; 8.12 (dd, *J* = 7, <2 Hz, 4H) $H_{oPh'}$; 7.79 – 7.70 (m, 18H) H_{mPh} and H_{pPh}; 7.29 (dd, *J* = 7, <2 Hz, 4H) $H_{mPh'}$; 4.28 (t, *J* = 6.5 Hz, 4H) O-CH_2-CH_2-; 2.07 – 1.99 (m, 4H) O-CH_2-CH_2-; 1.72 – 1.65 (m, 4H) -CH_2-; 1.53 (s, 8H) -CH_2-; -2.76 (s, 4H) N*H*. ^{13}C NMR (500 MHz, $CDCl_3$): δ 159.18, 142.38, 135.77, 134.70, 134.48, 127.82, 126.81, 125.68, 120.35, 120.20, 120.07, 112.90, 77.41, 77.16, 76.91, 68.51, 30.48, 29.83, 29.74, 26.45. MS (MALDI-tof): m/z = 1399.61 [M^+]. UV-vis, (DCM)/nm(log ε): 418(5.3), 514(3.9), 551(3.7), 593(3.5), 649(3.7). IR (KBr, cm^{-1}):2928, 2858, 1600, 1514, 1471, 1442, 1349, 1246, 965.

Porphyrin C_{12} dyad 46 (TPP-O-$(CH_2)_{12}$-O-TPP)

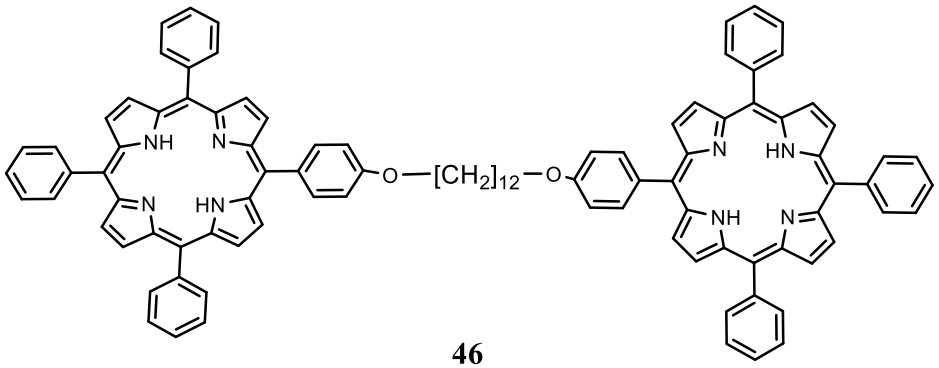

46

A mixture of 1,12-dibromododecane (45.3 mg, 0.138 mmol) and TPP-OH **34** (200 mg, 0.317 mmol) was dissolved in MEK (10 ml), then an excess of K_2CO_3 (220 mg, 1.58 mmol) and a catalytic amount of potassium iodide (6 mg, 0.036 mmol) were added to the mixture and everything refluxing for 48 h. Then the mixture was precipitated with MeOH and separated by column chromatography using THF:pet ether (3:7 v/v) as eluent to yield the pure product as a purple solid (75 mg, 38 %). m.p. 312-315 °C. ^{1}H NMR (400 MHz, $CDCl_3$) δ 8.89 (d, *J* = 4.5 Hz, 4H) and 8.84 (d, *J* = 4.5 Hz, 12H) H_β; 8.21 (dd, *J* = 8.5; <2 Hz, 12H) H_{oPh}; 8.11 (d, *J* = 8.5 Hz, 4H) $H_{oPh'}$; 7.80 – 7.71 (m, 18H) H_{mPh} and H_{pPh}; 7.28 (d, *J* = 8.5 Hz, 4H) $H_{mPh'}$; 4.26 (t, *J* = 6.4 Hz, 4H) -O-CH_2-; 2.05 – 1.89 (m, 4H) -CH_2-; 1.71 – 1.61 (m, 4H); 1.53 (s, 12H) -CH_2-; -2.76 (s, 4H) N*H*. ^{13}C NMR (126 MHz, $CDCl_3$) δ 158.92, 142.13, 135.52, 134.45, 134.23, 127.57, 126.56, 125.42, 120.10, 119.95, 119.82, 112.65, 77.16, 76.91, 76.65, 68.25, 30.22, 29.57, 29.49, 26.19. MS (MALDI-tof): m/z = 1428.65 [M^+]. UV-vis, (DCM)/nm(log ε): 418(5.1), 515(3.8), 550(3.5), 591(3.3), 647(3.6). IR (KBr, cm^{-1}): 2956, 2931, 2869, 1599, 1471, 1440, 1363, 1245, 1175, 1071, 1001, 980, 966.

Metal free phthalocyanine[138] 19

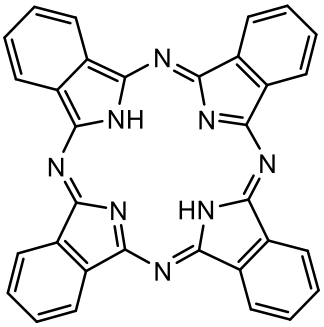

19

Following a general procedure using lithium as a template,[139] a solution of phthalonitrile (0.5 g, 4 mmol) in 1-pentanol (6 ml) was heated to 120 °C, and then lithium (28 mg, 4 mmol) was added to this solution and the reaction was continued for 1 h. Then, acetic acid was added (10 ml) and refluxed for 1 h. After that, the reaction mixture was cooled down to room temperature, methanol (100 ml) was added to precipitate the product and the dark blue solid of the pure phthalocyanine collected by vacuum filtration (210.7 mg, 41 %).

As an alternative method, the corresponding phthalonitrile can be also reacted with DBU as catalyst to form the desired phthalocyanine.[140] This method was performed by refluxing phthalonitrile (0.5 g, 4 mmol) in pentan-1-ol in the presence of DBU for 3 h under inert atmosphere. After cooling, the solution was poured over methanol and the dark blue precipitate collected by vacuum filtration and washed with MeOH to obtain the pure free phthalocyanine (185.0 mg, 36 %). MALDI-tof: m/z = 514.22 [M^+]. Due to high insolubility in organic solvents further characterisation was not possible.

1,2-dibromo-4,5-dimethoxybenzene 97[98]

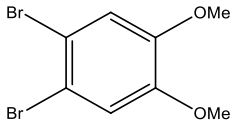

1,2-Dimethoxybenzene (16.14 g, 117 mmol) and iodine (0.63 g, 2.5 mmol) were added to dichloromethane (315 ml) with stirring on an ice bath. Bromine (15 ml, 46.8 g, 296 mmol) was added at a rate of roughly one drop a second. The mixture changed from purple to yellow-brown through the course of the reaction. After addition of the Br_2 was complete, the reaction was stirred an additional 3 hours. Volatiles were removed under vacuum and the resulting solid was dissolved in hot isopropanol (315 ml). The solution was cooled (-20 ˚C) for 24 h. The resulting solid was isolated by filtration and dried under vacuum to produce colourless needles (34.43 g, 99 %).m.p. 91 ˚C. ^{1}H NMR (400 MHz, $CDCl_3$) δ 7.05 (s, 2H), 3.85 (s, 6H). ^{13}C NMR (101 MHz, $CDCl_3$) δ 149.04, 116.09, 114.92, 56.42.

1-Octyl magnesium iodide 98[141]

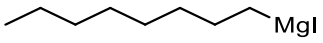

Magnesium turnings (6.05 g, 0.25 mol) were added to distilled Et_2O (25 ml) under an inert atmosphere and heated to reflux. After 10 min of reflux, a single crystal of iodine was added together with 1-Iodooctane (30.0 ml, 40 g, 0.17 mol) in Et_2O (25 ml) in a dropwise manner using an addition funnel. The mixture was left refluxing for 1 h after the complete addition of the alkyl halide. The mixture was left to cool and used immediately for the Kumada coupling reaction. The resulting Grignard reagent was obtained as a viscous grey liquid and the concentration was assumed to result from a 95 % conversion (50 ml, 3.32 M).

4,5-Dioctyl-1,2-dimethoxybenzene 99[98]

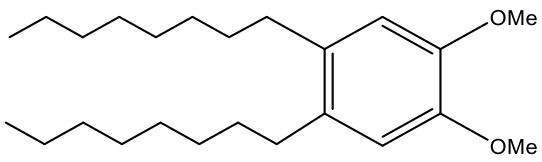

4,5-dibromoveratrole (10.0 g, 0.0338 mol) and 1,1'-bis(diphenylphosphino)ferrocenepalladium(II) dichloride $Pd(dppf)Cl_2$ (1.24 g, 1.69 mmol, 5 %) were added to dry Et_2O (5 ml) in a round bottom flask under Ar atmosphere. A solution of n-octylmagnesium iodide in diethyl ether (50 ml, 3.32 M, 0.169 mol) was added to the solid mixture via syringe at rt. Upon addition the reaction changes colour to dark green and then mustard yellow. This was then left to stir for a further 30 min after which it was set to reflux for 18 h. The resulting reaction was a dark, black mixture that upon cooling becomes viscous. The crude mixture was quenched in water and the remaining catalyst filtered off under vacuum. The recovered filtrate was washed with dilute HCl (2x25 ml), brine, and extracted with pet ether. The organics were then dried (Na_2SO_4) and the solvent removed under reduced pressure. The resulting title compound was purified by column chromatography over silica gel using pet ether as eluent to give the pure product as a light orange oil (5,7 g, 47 %). ^{1}H NMR (400 MHz, $CDCl_3$) δ 6.67 (s, 2H) H_{Ar}, 3.86 (s, 6H) -O-C$\underline{H}_3$, 2.60 – 2.50 (m, 4H) -(C$\underline{H}_2$)$_7$-CH_3, 1.63 – 1.52 (m, 4H) -(C$\underline{H}_2$)$_7$-CH_3, 1.43 – 1.26 (m, 20H) -(C$\underline{H}_2$)$_7$-CH_3, 0.93 – 0.89 (m, 6H) -(CH_2)-C$\underline{H}_3$. ^{13}C NMR (101 MHz, $CDCl_3$) δ 146.87, 132.68, 112.70, 55.94, 32.53, 31.98, 31.79, 29.83, 29.61, 29.38, 22.75, 14.15.

4,5-Dioctyl-1,2-dihydroxybenzene 100[98]

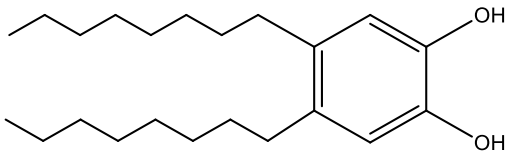

4,5 dioctyl-1,2-dimethoxybenzene (5.7 g, 0.016 mol) was dissolved in a mixture of hydrobromic acid and glacial acetic acid (200 ml, 1:1 v/v) to give an emulsion and left refluxing for 18 h under normal atmosphere. The mixture turned dark brown in colour and was left to cool to room temperature. After cooling, the product was washed with water (3x50 ml), brine and extracted with DCM. The organics were dried (Na_2SO_4) and the solvent removed under reduced pressure to give the pure product as a dark brown oil (4.78 g, 91 %). ^{1}H NMR (400 MHz, $CDCl_3$) δ 6.66 (s, 2H) H_{Ar}, 4.98 (s, 2H) -O<u>H</u>, 2.52 – 2.42 (m, 4H) -(C<u>H</u>$_2$)$_7$-CH_3, 1.56 – 1.47 (m, 4H) -(C<u>H</u>$_2$)$_7$-CH_3, 1.39 – 1.23 (m, 20H) -(C<u>H</u>$_2$)$_7$-CH_3, 0.93 – 0.85 (m, 6H) -$(CH_2)_7$-C<u>H</u>$_3$.

4,5-Dioctyl(1,2-ditrifluoromethanesulfonyloxy)benzene 101[98]

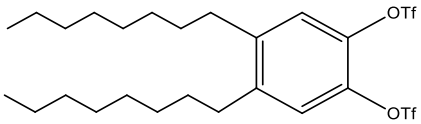

4,5-Dioctyl-1,2-dihydroxybenzene (4,5 g, 0.0134 mol) and lutidine (4.64 ml, 4.30 g, 0.040 mol) were dissolved in 100 ml of distilled DCM. The mixture was cooled to -78 ºC and trifluoromethanesulfonic anhydride (11.25 ml, 18.86 g, 0.067 mol) was added dropwise via syringe under an inert atmosphere. After the addition, the light brown solution was left to warm to room temperature and stirred overnight. The crude product was washed with water (2x50 ml), brine and extracted with DCM. The organics were dried (Na_2SO_4) and filtered. The solvent was removed and loaded onto a short silica gel column and eluted in hexane and a single fluorescent band was isolated from a brown\black baseline. The title compound was recovered as a clear oil (5.62 g, 70 %). ^{1}H NMR (400 MHz, $CDCl_3$) δ 7.20 (s, 2H), 2.62 (d, J = 8 Hz, 4H), 1.63 – 1.53 (m, 4H), 1.43 – 1.22 (m, 20H), 0.93 – 0.85 (m, 6H). ^{13}C NMR (101 MHz, $CDCl_3$) δ 143.29, 137.96, 123.70, 118.77 (q, J = 320.8 Hz, C_{OTf}), 32.44, 31.98, 30.67, 29.62, 29.52, 29.34, 22.80, 14.20.

4,5-Dioctylphthalonitrile 102[98]

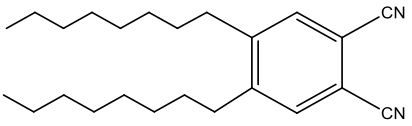

To a solution of bis(dibenzylideneacetone)palladium (0.343 g, 0.37 mmol, 4 mol %) and Pd(dppf)Cl_2 (0.832 g, 1.5 mmol, 16 mol %) in anhydrous DMF (18 ml) at rt, 4,5 dioctyl(1,2-ditrifluoromethanesulfonyloxy)benzene (5.62 g, 9.39 mmol) was added under argon atmosphere via syringe. The reaction mixture was stirred and heated until the temperature stabilised at 62 ºC. Once the temperature was obtained, zinc cyanide (1.32 g, 11.26 mmol) was added in 12 equal additions over a period of two hours. After the addition, the reaction was left stirring and heating at 62 ºC for a further 18 h. The resulting mixture was quenched in water and the excess cyanide and spent catalyst filtered off using vacuum filtration. The filtrate was washed with water, brine and extracted with DCM. The organics were dried (Na_2SO_4) and filtered. The solvent was evaporated to give a bright yellow oil. The resultant oil was purified by column chromatography over silica gel (1:3 v/v DCM:Pet ether) to give the product as a yellow oil (1.54 g, 47 %). ^{1}H NMR (400 MHz, $CDCl_3$) δ 7.55 (s, 2H), 2.67 (t, *J* = 9.5 Hz, 4H), 1.71 – 1.49 (m, 4H), 1.42 – 1.23 (m, 20H), 0.88 (t, *J* = 7.0 Hz, 6H). ^{13}C NMR (101 MHz, $CDCl_3$): 147.5, 134.1, 115.9, 112.9, 32.7, 31.9, 30.5, 29.6, 29.5, 29.3, 22.8, 21.2.

Metal free 2,3,9,10,16,17,23,24-octakis(octyl)phthalocyanine[98] 55

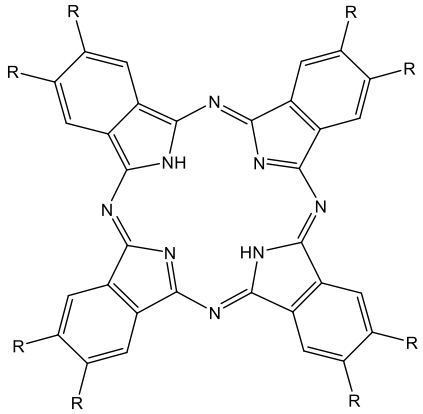

$R=C_8H_{17}$

55

4,5-Dioctylphthalonitrile (0.7 g, 2.19 mmol) was added to a 1 necked round bottom flask and dissolved in pentanol (6 ml), to this, DBU (0.5 ml, 10 % mol) was added and the mixture left to reflux for 3 h at 140 ºC. After cooling down to room temperature, MeOH (20 ml) were added and the resulting mixture filtered under suction. The product was obtained as a blue solid (92 mg, 12 %). MS (MALDI-tof): m/z = 1412.67 [M^+]. UV-vis, (DCM)/nm(log ε): 344(4.8), 671(4.9), 705(4.9). ^{1}H NMR (400 MHz, $CDCl_3$) δ 9.4 (8H, s), 3.3–3.25 (16H, m) 2.3–2.25 (32H, m), 1.63–1.58 (64H, m), 1.4–1.35 (24H, m), 0.32 (2H, s). IR (KBr, cm^{-1}): 2955, 2919, 2851, 1467, 1324, 1149, 1015.

Metal-free 1,4,8,11,15,18,22,25-octakis(octyl)phthalocyanine[98] 56

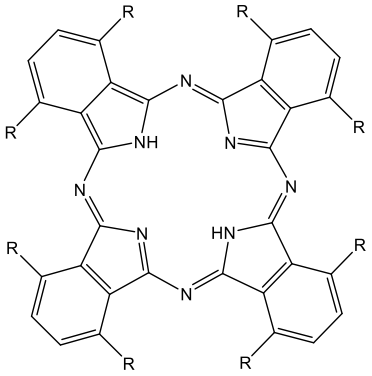

$R=C_8H_{17}$

56

4,6-dioctylphthalonitrile (0.7 g, 2.19 mmol) was added to a 1 necked round bottom flask and dissolved in pentanol (6 ml), to this, DBU (0.5 ml, 10 % mol) was added and the mixture left to reflux for 3 h. After cooling down to room temperature, MeOH (20 ml) was added and the resulting mixture filtered under suction and washed with MeOH. The product was obtained as a green solid (101 mg, 15 %). ^{1}H NMR (400 MHz, $CDCl_3$) δ 7.87 (s, 8H) Ar*H*, 4.44 (d, *J* = 6.9 Hz, 16H) -C*H*$_2$-, 2.08 (dt, *J* = 15.3, 7.7 Hz, 16H) -C*H*$_2$-, 1.60 – 1.51 (m, 16H) -C*H*$_2$-, 1.36 – 1.29 (m, 16H) -C*H*$_2$-, 1.27 – 1.15 (m, 54H) -C*H*$_2$-, 0.79 (t, *J* = 6.9 Hz, 24H) -C*H*$_3$, 0.04 (s, 2H) N*H*. MS (MALDI-tof): m/z = 1412.67 [M^+]. UV-vis, (DCM)/nm(log ε): 354(4.7), 701(5.0), 728(5.1). IR (KBr, cm^{-1}): 2952, 2921, 2851, 1466, 1327, 1148, 1026, 874.

Metal-free 2,3,9,10,16,17,23,24-octakis(dimethyldioxolane)phthalocyanine[142] 65

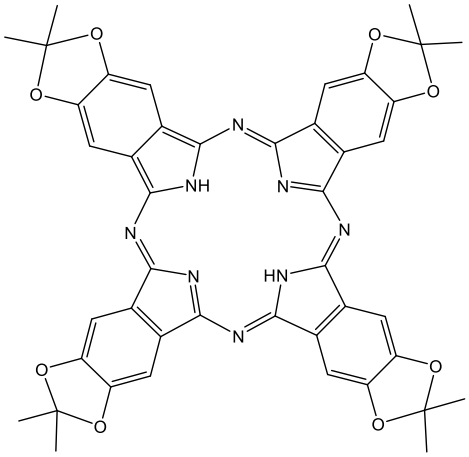

65

4,5-dimethyldioxolanephthalonitrile **66** (0.37 g, 18.5 mmol) was added to a 1 necked round bottom flask and dissolved in pentanol (8 ml), to this, DBU (0.3 ml, 10 % mol) was added and the mixture left to reflux for 3 h. After cooling down to room temperature, MeOH (30 ml) was added and the resulting precipitate containing phthalocyanine **65** filtered off. The product was obtained as a dark-blue solid (80 mg, 22 %). ^{1}H NMR (500 MHz, $CDCl_3$) δ 8.51 (s, 8H), 1.53 (s, 24H). MS (MALDI-tof): m/z = 802.69 [M^+]. UV-vis, (DCM)/nm(log ε): 347(4.1), 691(4.2), 652(4.1). IR (KBr, cm^{-1}): 2991, 1490, 1476, 1450, 1412, 1377, 1334, 1280, 1220, 1074, 1026, 982, 852.

Closed triple decker dyad 50

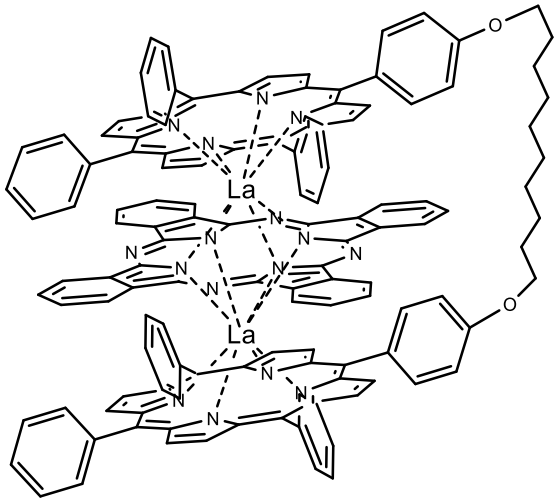

50

C_{10} porphyrin dyad **45** (200 mg, 0.143 mmol) was mixed with lanthanum(III) acetylacetonate hydrate (125 mg, 0.286 mmol) in a 25 ml round bottom flask and dissolved in 15 ml of octanol. The mixture was set up to reflux at 200 ºC under Ar for 16 h and after complete metallation being checked by UV-Vis, free phthalocyanine **19** was then added and everything left refluxing overnight under inert atmosphere. After 18 h, the solvent was removed by distillation under reduced pressure and the crude recrystallised from DCM:MeOH. The resulting solids were then separated by column chromatography through silica gel using DCM:pet ether (6:4 v/v) as eluent and the first brown fraction containing the title product was collected as dark brown solids (268 mg, 86 %). ^{1}H NMR (500 MHz, $CDCl_3$) δ 10.08 (d, *J* = 7.2 Hz, 2H) $H_{oiPh'}$; 9.99 (t, *J* = 7 Hz, 6H) H_{oiPh}; 9.36 (dd, *J* = 5, 3 Hz, 8H) H_{pC}; 8.48 – 8.40 (m, 6H) H_{ooPh}; 8.29 (dd, *J* = 5, 3 Hz, 8H) H_{pC}; 7.98 (d, *J* = 6.5 Hz, 2H) $H_{ooPh'}$; 7.86 – 7.77 (m, 6H) H_{miPh}; 7.31 (d, *J* = 4 Hz, 4H) H_{β}; 7.26 – 7.21 (m, 18H) H_{β}, H_{miPh} and H_{pPh} ; 6.87 (d, *J* = 6.0 Hz, 2H) $H_{miPh'}$; 6.73 (d, *J* = 7Hz, 2H) $H_{moPh'}$; 6.64 (t, *J* = 7 Hz, 6H) H_{moPh}; 4.59 (t, *J* = 7 Hz, 4H) -O-CH_2- ; 2.33 – 2.23 (m, 4H) -CH_2-; 1.92 (m, 8H) -CH_2- ; 1.81 (s, 4H) -CH_2-. ^{13}C NMR (126 MHz, $CDCl_3$) δ 158.74, 153.70, 148.23, 147.88, 143.14, 136.74, 133.57, 133.43, 130.19, 128.57, 128.46, 127.74, 127.25, 125.97, 125.93, 123.60, 120.22, 120.12, 110.26, 29.62, 29.39, 28.75, 26.76, 15.81. MS (MALDI-tof): m/z = 2186.05 [M^+]. UV-vis, (DCM)/nm(log ε): 360(4.8), 419(5.2), 485(2.7), 550(2.5), 605(2.6). IR (KBr, cm^{-1}): 3053, 2928, 2855, 1606, 1513, 1469, 1439, 1406, 1330, 1288, 1243, 1198, 1177, 1116, 1003, 984, 880.

Closed triple decker dyad 72

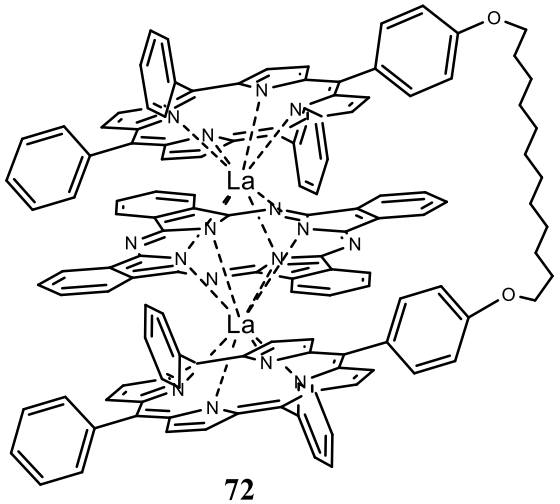

72

C_{12} porphyrin dyad **46** (10 mg, $7x10^{-3}$ mmol) was mixed with lanthanum(III) acetylacetonate hydrate (6.4 mg, $14.7x10^{-3}$ mmol) in a 10 ml round bottom flask and dissolved in 5 ml of octanol. The mixture was set up to reflux at 200 ºC under Ar for 6 h and after complete metallation being checked by UV-Vis, The free phthalocyanine (3.6 mg, $7x10^{-3}$ mmol) was then added and everything left refluxing overnight under inert atmosphere. After 18 h, the solvent was removed by distillation under reduced pressure and the crude was purified by column chromatography over silica gel using DCM: Pet ether (1:1 v/v) as eluent. The fraction containing the product was then recrystallised from DCM:MeOH to yield the title product as dark brown solids (9.6 mg, 62 %). ^{1}H NMR (500 MHz, $CDCl_3$) δ 9.91 (t, *J* = 7.0 Hz, 6H) H_{oiPh}; 9.86 (d, *J* = 6.5 Hz, 2H) $H_{oiPh'}$; 9.37 (dd, *J* = 5.5, 3 Hz, 8H) H_{pC}; 8.42 (t, *J* = 7 Hz, 6H) H_{ooPh}; 8.30 (dd, *J* = 5.5, 3 Hz, 8H) H_{pC}; 7.97 (d, *J* = 6 Hz, 2H) $H_{ooPh'}$; 7.81 (t, *J* = 7.5 Hz, 6H) H_{miPh}; 7.31 (d, *J* = 4.5 Hz, 4H) H_{β}; 7.25 – 7.19 (m, 18H) H_{β}, H_{miPh} and H_{pPh} ; 6.80 (d, *J* = 6 Hz, 2H) $H_{miPh'}$; 6.62 (d, *J* = 7 Hz, 8H) $H_{moPh'}$ and H_{moPh}; 4.46 (t, *J* = 6.5 Hz, 4H) -O-CH_2- ; 2.21 – 2.12 (m, 4H) -CH_2-; 1.96 – 1.86 (m, 4H) -CH_2-; 1.79 (m, 4H) -CH_2-; 1.73 (s, 8H) -CH_2-. ^{13}C NMR (101 MHz, $CDCl_3$) δ 153.71, 148.28, 147.95, 147.92, 147.90, 143.12, 143.08, 136.77, 133.63, 133.43, 130.20, 128.66, 128.59, 128.50, 127.23, 125.93, 123.66, 120.24, 30.03, 29.85, 29.41, 27.00, 26.71, 1.17.MS (MALDI-tof): m/z = 2215.01 [M^+]. UV-vis, (DCM)/nm(log ε): 363(4.7), 421(5.1), 480(2.3), 553(2.1), 611(2.5).

Open bis-triple decker 53

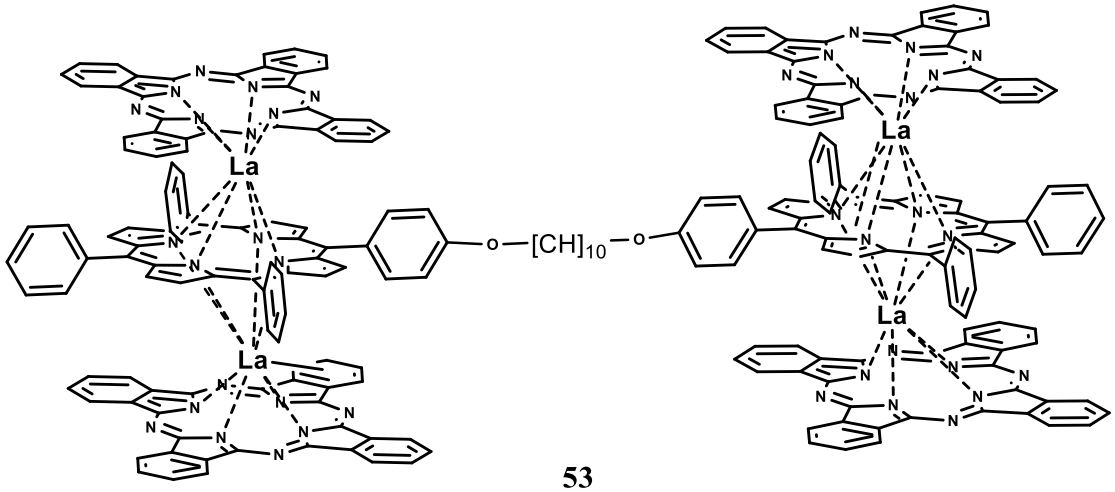

53

C_{10} porphyrin dyad **45** (25 mg, 17.9x10^{-3} mmol) was mixed with lanthanum(III) acetylacetonate hydrate (32.7 mg, 76.0x10^{-3} mmol) in a 25 ml round bottom flask and dissolved in 10 ml of octanol. The mixture was set up to reflux at 200 ºC under Ar overnight and then, an excess of free phthalocyanine **19** (92 mg, 179.0x10^{-3} mmol) was added and everything left refluxing overnight under inert atmosphere. After 16 h, the reaction was cooled down and precipitated with pet ether. The resulting green solids were then separated by column chromatography through silica gel using DCM as eluent and the green fraction containing the title product was collected as dark green solids (24.9 mg, 34 %). ^{1}H NMR (400 MHz, $CDCl_3$) δ 10.01 (d, *J* = 7.0 Hz, 12H) H_{Arpor}; 9.91 (d, *J* = 8.0 Hz, 5H) H_{Arpor}; 8.82 (dd, *J* = 5.5, 3 Hz) H_{ArpC}; 8.41 (t, *J* = 7.5 Hz, 13H) H_{Arpor}; 8.23 – 8.14 (m, 9H) H_{Arpor}; 8.03 – 7.93 (m, 9H) H_{Arpor}; 7.84 (dd, *J* = 5.5, 3 Hz, 32H) H_{ArpC}; 7.76 (d, *J* = 4.4 Hz, 3H) H_{Arpor}; 7.70 (d, *J* = 7.8 Hz, 14H) H_{Arpor}; 4.81 (t, *J* = 6.5 Hz, 4H) -O-CH_2-; 2.45 (m, 4H) -CH_2-; 2.10 (m, 4H) -CH_2-, 1.93 (m, 4H) -CH_2-; 1.83 (m, 8H) -CH_2-. MS (MALDI-tof): m/z = 4002.84 [M$^+$]. UV-vis, (DCM)/nm(log ε): 347(5.4), 417(2.9), 669(4.6), 705(4.7). IR (KBr, cm^{-1}): 2961, 2917, 2849, 1645, 1463, 1261, 1093, 1020, 879. (^{13}C NMR spectra could not be obtained for this compound due to the absence of peaks in the processed spectrum because of the low amount obtained).

Closed triple decker 64

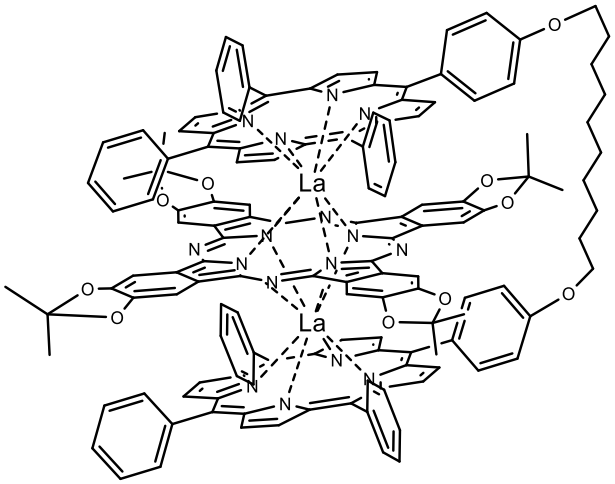

64

C_{10} porphyrin dyad **45** (30 mg, 0.021 mmol) was mixed with lanthanum(III) acetylacetonate hydrate (19.26 mg, 0.044 mmol) in a 5 ml round bottom flask and dissolved in 3 ml of octanol. The mixture was set up to reflux at 200 ºC under Ar for 6 h. and after complete metallation being checked by UV-Vis, the free phthalocyanine **65** (16 mg, 0.021 mmol) was then added and everything left refluxing overnight under inert atmosphere. After 18 h., the solvent was removed by distillation under reduced pressure and the crude washed and filtered with MeOH. The resulting brown solids where then separated by column chromatography through silica gel using EtOAc:Pet ether (1:4 v/v) as eluent and the first brown fraction containing the title product was collected as dark brown solids (34.4 mg, 76 %). ^{1}H NMR (500 MHz, d-toluene) δ 10.41 (d, *J* = 8.5 Hz, 2H) $H_{oiPh'}$; 10.30 (d, *J* = 7.0 Hz, 4H) H_{oiPh}; 10.25 (d, *J* = 7.0 Hz, 2H) $H_{oiPh'}$; 9.04 (s, 2H) H_{pC}; 9.02 (s, 2H) H_{pC}; 9.02 (s, 2H) H_{pC}; 8.99 (s, 2H) H_{pC}; 8.41 (t, *J* = 7.5 Hz, 6H) H_{ooPh}; 8.19 (d, *J* = 8.5 Hz, 2H) $H_{ooPh'}$; 7.80 (d, *J* = 4.5 Hz, 4H) H_{β}; 7.69 (d, *J* = 4.5 Hz, 4H) H_{β}; 7.67 – 7.64 (m, 8H) H_{β}; 7.60 (t, *J* = 7.5 Hz, 6H) H_{pPh}; 7.06 (d, *J* = 7.5 Hz, 6H) H_{miPh}; 6.92 (m, 2H) $H_{miPh'}$; 6.86 (m, 2H) $H_{moPh'}$; 6.77 (d, *J* = 6.5 Hz, 6H) H_{moPh}; 4.25 (t, *J* = 7.0 Hz, 4H) -O-CH_2-; 2.21 (dt, *J* = 4.5, 2.0 Hz, 2H) -CH_2-; 2.13 – 2.11 (m, 2H) -CH_2-; 2.11 – 2.09 (m, 2H) -CH_2- (hidden under solvent); 2.04 (dd, *J* = 4.5, 2.0 Hz, 2H) -CH_2-; 1.95 (dt, *J* = 4.5, 2.0 Hz, 2H) -CH_2-; 1.64 (s, 12H) C-(CH_3)$_2$; 1.60 (s, 12H) C-(CH_3)$_2$; 1.58 (s, 6H) -CH_2-. ^{13}C NMR (126 MHz, CD_2Cl_2) δ 151.57, 148.06, 134.00, 128.95, 128.87, 128.76, 127.74, 126.49, 126.44, 120.61, 120.55, 30.26, 30.24, 29.83, 29.13, 26.50, 26.43. MS (MALDI-tof): m/z = 2503.72 [M^+]. UV-vis, (DCM)/nm(log ε): 369(4.4), 419(4.8), 556(3.5), 602(3.5). IR (KBr, cm^{-1}): 2965, 2920, 2851, 1605, 1471, 1396, 1261, 1066, 982, 862.

Closed triple decker 57

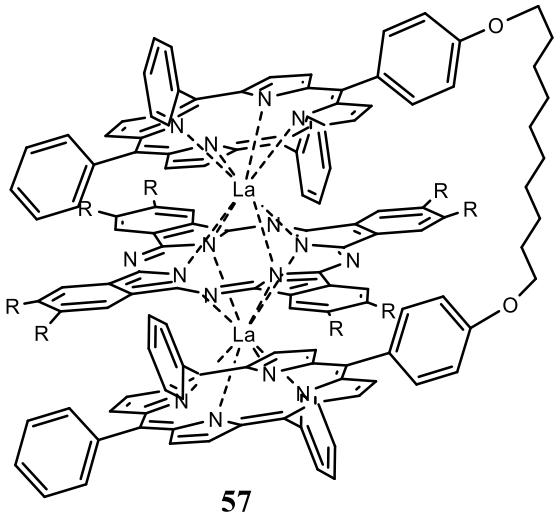

57

R=C_8H_{17}

C_{10} dyad **45** (9.9 mg, 7.1x10^{-3} mmol) was mixed with lanthanum(III) acetylacetonate hydrate (6.5 mg, 14.9x10^{-3} mmol) in a 10 ml round bottom flask and dissolved in 5 ml of octanol. The mixture was set up to reflux at 200 ºC under Ar for 6 h and after complete metallation (checked by UV-vis), free phthalocyanine **55** (10 mg, 7.08x10^{-3} mmol) was added and everything left refluxing overnight under inert atmosphere. After 16 h, the solvent was removed by distillation under reduced pressure to obtain green solids, that were separated by column chromatography using DCM:Pet ether (1:1 v/v) to obtain triple decker **57** (18.4 mg, 83 %). ^{1}H NMR (500 MHz, CD_2Cl_2) δ 10.01 (t, *J* = 7.0 Hz, 8H) $H_{oiPh'}$, 9.12 (s, 2H) H_{ArpC}, 9.11 (s, 2H) H_{ArpC}, 9.10 (s, 2H) H_{ArpC}, 9.07 (s, 2H) H_{ArpC}, 8.44 (dd, *J* = 9.0, 5.3 Hz, 6H) H_{ooPh}, 7.98 (d, *J* = 6.0 Hz, 2H) $H_{ooPh'}$, 7.81 (t, *J* = 8.0 Hz, 6H) H_{miPh}, 7.40 – 7.15 (m, 22H) H_{β}, H_{miPh} and H_{pPh}, 6.87 (d, *J* = 6.0 Hz, 2H) $H_{miPh'}$, 6.80 (d, *J* = 8.0 Hz, 2H) $H_{moPh'}$, 6.75 (t, *J* = 6.0 Hz, 6H) H_{moPh}, 4.53 (t, *J* = 7.0 Hz, 4H) -O-CH_2-, 3.43 – 3.26 (m, 16H) -CH_2-$_{Pc}$, 2.25 (t, *J* = 7.0 Hz, 4H) -CH_2-$_{por}$, 2.18 – 2.02 (m, 16H) -CH_2-$_{Pc}$, 1.97 – 1.77 (m, 27H) -CH_2-, 1.74 – 1.63 (m, 16H) -CH_2-$_{Pc}$, 1.38 – 1.19 (m, 38H) -CH_2-, 1.10 – 1.00 (m, 19H), 0.96 (t, *J* = 7.0 Hz, 6H), 0.87 (t, *J* = 7.0 Hz, 10H). MS (MALDI-tof): m/z = 3086.15 [M$^+$]. UV-vis, (DCM)/nm(log ε): 365(5.5), 421(5.7), 497(3.8), 610(3.6). IR (KBr, cm^{-1}): 2958, 2924, 2854, 1610, 1514, 1466, 1323, 1243, 1078, 984. (^{13}C NMR spectra could not be obtained due to slow decomposition in the NMR solvent)

Dipyrromethanes, general procedure 3

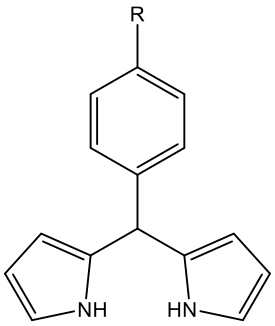

The various dipyrromethanes were obtained following a modified general method developed by Lindsey for the synthesis of dipyrromethanes.[119] Pyrrole (25 eq) and the corresponding aldehyde (1.0 eq) were added to a dry round-bottomed flask and degassed with a stream of Ar for 5 min. TFA (0.10 eq) was then added, and the solution was stirred under Ar at room temperature for 5 min and then quenched with 0.1 M NaOH. Ethyl acetate was then added. The organic phase was washed with water and dried (Na_2SO_4), and the solvent removed under vacuum to afford an orange oil. Column chromatography followed by crystallization give the pure dipyrromethane as a crystalline solid as compared with literature data.[119,125]

5-Phenyldipyrromethane[119] 76

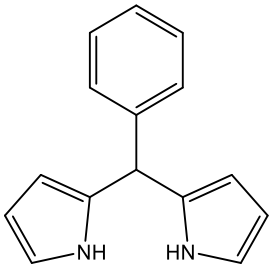

76

The general procedure 3 was followed reacting benzaldehyde (1.53 g, 1.5 ml, 14.4 mmol) and freshly distilled pyrrole (24.1 g, 25 ml, 360 mmol). The dipyrromethane **76** was obtained after the column chromatography in 1:1 DCM:Pet ether. To obtain the dipyrromethane as an analytically pure solid it had to be further purified via kugelrohr distillation. After the distillation, the product was obtained as a white crystalline solid

(0.42 g, 13 %). m.p.: 101-104 °C (lit[119] = 100-101 °C). ^{1}H NMR (500 MHz, $CDCl_3$) δ 7.83 (s(br), 2H), 7.18 - 7.32 (m, 5H), 6.64 (d, J = 2.6, 2H), 6.15 (d, J = 2.6, 2H), 5.89 (s, 2H), 5.43 (s, 1H).

5-(*p*-hydroxyphenyl)dipyrromethane[119] 78

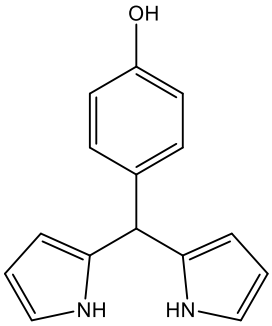

78

The general procedure 3 was followed reacting 4-hydroxybenzaldehyde (1.76 g, 14.4 mmol) and freshly distilled pyrrole (24.1 g, 25 ml, 360 mmol). The resultant crude was purified using 19:1 DCM/EtOAc as eluent for the column chromatography followed by crystallisation in hexane to yield the pure product as pale pink solids (2.12 g, 62 %). m.p.: 126 °C ^{1}H NMR (500 MHz, $CDCl_3$) δ 7.92 (s(br), 2H) N*H*, 7.08 (d, *J* = 8.5 Hz, 2H) H_{oPh}, 6.76 (d, *J* = 8.5 Hz, 2H) H_{mPh}, 6.70 (td, *J* = 2.5, 1.5 Hz, 2H) H_{pyrr}, 6.16 (q, *J* = 2.5 Hz, 2H) H_{pyrr}, 5.94 – 5.88 (m, 1H) H_{pyrr}, 5.42 (s, 1H) H_{met}, 4.67 (s, 1H) H_{OH}. ^{13}C NMR (126 MHz, $CDCl_3$) δ 154.56, 134.55, 132.94, 129.76, 117.30, 115.56, 108.56, 107.22, 43.29. IR (KBr, cm^{-1}): 3411 (br), 3119, 1613, 1556, 1512, 1436, 1260, 1095, 844.

5-(*p*-methoxyphenyl)dipyrromethane[119] 77

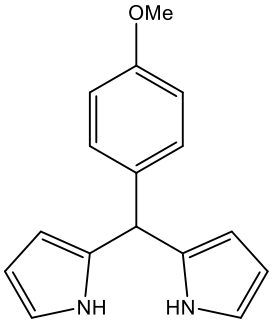

77

The general procedure 3 was followed reacting 4-methoxybenzaldehyde (1.96 g, 1.75 ml, 14.4 mmol) and freshly distilled pyrrole (24.1 g, 25 ml, 360 mmol). The resultant crude was purified using DCM/Pet ether (1:1 v/v) as eluent for the column chromatography followed by crystallization in EtO_2:Hexane to yield the pure product as white solids (2.1 g, 58 %). m.p.: 98 °C. ^{1}H NMR (500 MHz, $CDCl_3$) δ 7.90 (s(br), 2H) N*H*, 7.14 (d, *J* = 8.5 Hz, 2H) H_{oPh}, 6.86 (d, *J* = 8.5 Hz, 2H) H_{mPh}, 6.69 (dd, *J* = 4.5, 2.5 Hz, 2H) H_{pyrr}, 6.16 (dd, *J* = 6, 2.5 Hz, 2H) H_{pyrr}, 5.94 – 5.89 (m, 2H) H_{pyrr}, 5.43 (s, 1H) C*H*, 3.80 (s, 3H) –CH_3. ^{13}C NMR (126 MHz, $CDCl_3$) δ 158.69, 134.33, 132.99, 129.53, 117.24, 114.14, 108.55, 107.19, 55.44, 43.28. IR (KBr, cm^{-1}): 3099, 3000, 2956, 2934, 2836, 2906, 1583, 1608, 1560, 1509, 1464, 1441, 1425, 1400, 1324, 1302, 1247, 1176, 1114, 1091, 1028, 970, 885, 841.

Pentafluorophenyldipyrromethane[119] 90

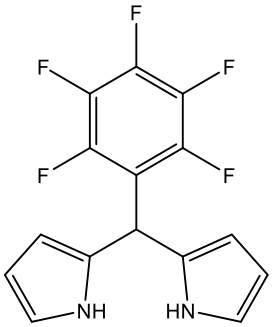

90

General procedure 3 was followed reacting pentafluorobenzaldehyde (2.82 g, 1.78 ml, 14.4 mmol) and freshly distilled pyrrole (24.1 g, 25 ml, 360 mmol). The resultant crude was purified using DCM/pet. ether (1:1 v/v) as eluent for the column chromatography

followed by kugelrohr distillation to yield the pure product as orange crystals (2.29 g, 51 %). m.p.: 129-130 °C. ^{1}H NMR ($CDCl_3$) δ 8.15 (s(br), 2H) N*H*, 6.73 (m, 2H) H_{pyrr}, 6.16 (q, J = 3 Hz, 2H) H_{pyrr}, 6.12 – 5.92 (m, 2H) H_{pyrr}, 5.90 (s, 1H) C*H*. ^{13}C NMR (126 MHz, $CDCl_3$) δ 33.0, 107.6, 108.6, 118.1, 128.1.

Trans-5,15-bis(pentafluorophenyl)-10,20-bis(*p*-methoxyphenyl)porphyrin[143] 91

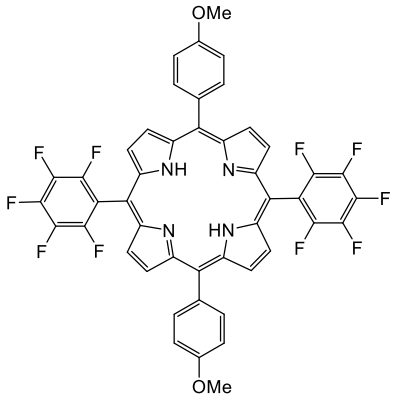

91

Pentafluorophenyldipyrromethane **90** (2.31 g, 7.4 mmol) and *p*-methoxybenzaldehyde (1.00 g, 0.9 ml, 7.4 mmol) were dissolved in 500 ml of DCM and the mixture stirred. To the mixture, TFA (0.1 eq) was added and everything stirred for 30 min. Then, DDQ (1 eq) was added and the mixture stirred for 60 min. The crude was then filtered through an alumina pad (7.5 cm diameter) and eluted with further DCM. The solvent was then evaporated to obtain a black solid that was then redissolved in toluene and DDQ was added and refluxed for 1 h to oxidize any remaining chlorine. The mixture was then cooled down and filtered through another alumina pad (4 cm diameter) and DCM added until no more purple solution was eluted. The solvent was then evaporated and the resulting purple solid was recrystallized from DCM/MeOH to obtain bright purple crystals of **91** (0.49 g, 16 %). m.p.: > 350 °C. ^{1}H NMR (500 MHz, $CDCl_3$) δ 8.90 (d, *J* = 4.7 Hz, 4H) H_{β}, 8.71 (d, *J* = 4.6 Hz, 4H) H_{β}, 8.04 (d, *J* = 9.0 Hz, 4H) H_{oPh}, 7.23 (d, *J* = 9.0 Hz, 4H) H_{mPh}, 4.03 (s, 6H) –CH_3, -2.88 (s, 2H) N*H*. ^{19}F NMR (500 MHz, $CDCl_3$) δ -136.78 (dd, *J* = 24.0, 8.3 Hz), -152.46 (t, *J* = 20.8 Hz), -162.05 (td, *J* = 24.0, 8.3 Hz). ^{13}C NMR (126 MHz, $CDCl_3$) δ 159.88, 135.82, 133.70, 129.19, 128.38, 125.45, 121.43, 116.70, 112.61, 102.14, 55.76. MS (MALDI-tof): m/z = 854.84 [M^+].

Trans-5,15-bis(pentafluorophenyl)-10,20-bis(_p_-hydroxyphenyl)porphyrin 92

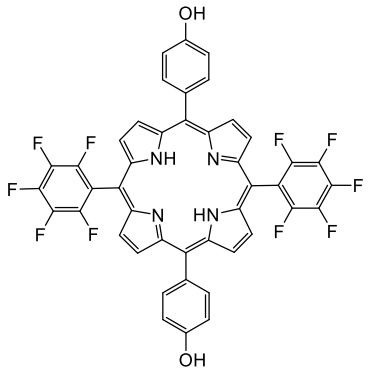

92

Trans-porphyrin **90** (200 mg, 0.23 mmol) was refluxed in a mixture of HBr/HOAc (1:1 v/v) for 24 h. Then, after cooling down the mixture, the crude was poured over a solution of $NaHCO_3$ and filtered off. The solids were then collected with MeOH and triethylamine was added until the solution turned purple. The resultant solids from the evaporation of the solvent where then separated by column chromatography in DCM:Pet ether (1:1 v/v) and the last spot containing the pure product was collected (73.5 mg, 38 %). m.p. > 350 °C. ^{1}H NMR (500 MHz, Acetone) δ 9.13 (s, 4H) H_{β}, 9.01 (d, J = 4.5 Hz, 4H) H_{β}, 8.96 (s, 2H) -O*H*, 8.06 (d, J = 8.5 Hz, 4H) H_{oPh}, 7.27 (d, J = 8.5 Hz, 4H) H_{mPh}. ^{19}F NMR (500 MHz, Acetone) δ -140.12 (dd, J = 24.0, 8.0 Hz), -156.04 (t, J = 20.5 Hz), -164.89 (td, J = 24.0, 8.0 Hz). ^{13}C NMR (126 MHz, Acetone) δ 158.83, 136.77, 133.19, 122.73, 117.28, 115.01, 103.11, 68.16, 26.26. MS (MALDI-tof): m/z = 827.42 [M^+].

T*rans*-porphyrin 93

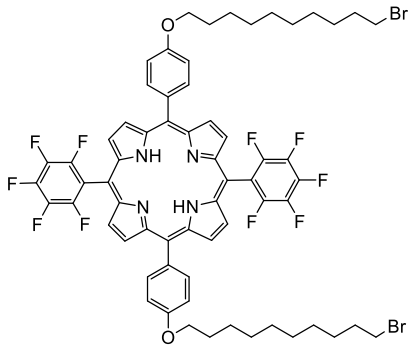

93

An impure sample of pentafluorophenyl dipyrromethane **93** (3 g, 9.6 mmol) purified by column chromatography and *p*-(10'-bromodecanoxy)benzaldehyde **84** (2 g, 5.86 mmol) were dissolved in 500 ml of DCM and cooled to 0 ˚C in an ice bath. The mixture was stirred and protected from light and TFA was added (1.2 ml). After stirring for 30 min, 1.5 g of DDQ were added to the mixture and the reaction continued for 60 min. The crude mixture was passed through an alumina pad (7.5 cm of diameter) and washed with DCM until pale brown solution came out. The collected washings were concentrated and the solids redissolved in 100 ml of toluene, 0.7 g of DDQ were added and everything refluxed for 1 h to oxidise any remaining chlorine. The resulting solution was passed through an alumina pad (3 cm of diameter) and washed with DCM. The liquids collected were then concentrated to approximately 50 ml and 50 ml MeOH were added and left crystallising for 1 h. The resultant precipitate was filtered off and separated by silica gel chromatography using DCM:pet. ether (1:1 v/v) as eluent followed by recrystallisation from DCM/MeOH to yield purple crystals of the product (0.66 g, 18 %). m.p.: 224-225 °C. ^{1}H NMR (500 MHz, $CDCl_3$) δ 8.99 (d, *J* = 4.5 Hz, 4H) H_β, 8.78 (d, *J* = 4.5 Hz, 4H) H_β, 8.11 (d, *J* = 8.5 Hz, 4H) H_{oPh}, 7.30 (d, *J* = 8.5 Hz, 4H) H_{mPh}, 4.26 (t, *J* = 6.5 Hz, 4H) -O-CH_2-, 3.44 (dd, *J* = 8.5, 5.0 Hz, 4H) -CH_2-, 2.03 – 1.96 (m, 4H) -CH_2-, 1.94 – 1.87 (m, 4H) -CH_2-, 1.69 – 1.60 (m, 4H) -CH_2-, -2.81 (s, 2H) N*H*. ^{19}F NMR (500 MHz, $CDCl_3$) δ -136.79 (dd, *J* = 24.5, 8.0 Hz), -152.50 (t, *J* = 20.5 Hz), -162.08 (m). ^{13}C NMR (126 MHz, $CDCl_3$) δ 159.46, 135.84, 113.11, 68.52, 34.22, 33.01, 29.69, 29.64, 29.63, 29.59, 28.96, 28.36, 26.38. MS (MALDI-tof): m/z = 1265.76 [M^+].

Trans-5,15-diphenyl-10,20-di-_p_-hydroxyphenylporphyrin[144] 80

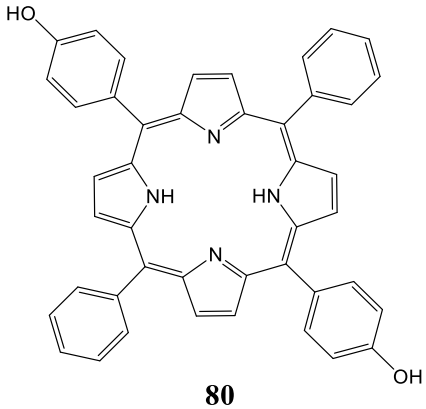

80

For the synthesis of **80**, a modified version of the methodology provided by Adler was performed with a statistical mixture of aldehydes. To do so, benzaldehyde (5.3 g, 50 mmol) and *p*-hydroxybenzaldehyde (6.1 g, 50 mmol) were dissolved in propionic acid (250 ml). When the mixture reached reflux, freshly distilled pyrrole (6.5 g, 6.7 ml, 0.1 mol) was added dropwise to the reaction mixture. When the addition was completed, the reaction was further refluxed for 30 min. Then, the mixture was allowed to cool at rt. and then 250 ml of MeOH were added to the mixture and everything left precipitating overnight. Then, the mixture was filtered and washed with MeOH to recover the statistical mixture of porphyrins. The mixture of *cis*/*trans* isomers were previously separated from the complex mixture of porphyrins using THF/pet ether (1:3 v/v) as eluent.

The isomers of TPP-$(OH)_2$ **80** and **87** were then separated using silica gel chromatography. THF:toluene:pet ether (1:2:2 v/v) mixture was used as eluent allowing partial separation of the isomers. The title compound was obtained as an analytically pure purple crystalline solid (0.1 g, 1 %). ^{1}H NMR (500 MHz, $CDCl_3$) δ 8.87 (d, *J* = 4.5 Hz, 4H) Hβ, 8.84 (d, *J* = 4.5 Hz, 4H) Hβ, 8.21 (dd, *J* = 8.0, 1.5 Hz, 4H) H_{oPh}, 8.08 (d, *J* = 8.5 Hz, 4H) $H_{oPh'}$, 7.81 – 7.73 (m, 6H) H_{mPh} and H_{pPh}, 7.21 (d, *J* = 8.5 Hz, 4H) H_{mPh}, 5.10 (s, 2H) O*H*, -2.77 (s, 2H) N*H*. MS (MALDI-tof): m/z = 648.07 [M^+]. IR (KBr, cm^{-1}): 3327(br), 2956, 2924, 2872, 1608, 1514, 1471, 1349, 1231, 1170, 966. (^{13}C NMR could not be obtained due to the low amount of material obtained).

Cis-5,10-diphenyl-15,20-bis-_p_-hydroxyphenylporphyrin 87

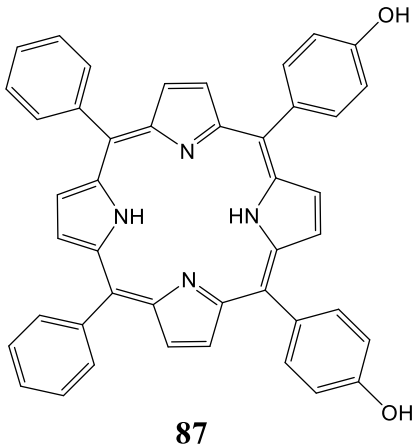

87

Cis-porphyrin **87** was synthesised along with the *trans*-isomer **80**. The isomers of TPP-$(OH)_2$ **80** and **87** were then separated using silica gel chromatography. THF:toluene:pet. ether (1:2:2) mixture was used as eluent allowing partial separation of the isomers. The title compound was obtained as a pure purple crystalline solid (0.1 g, 1 %). MS (MALDI-tof): m/z = 648.07 [M^+]. ^{1}H NMR (500 MHz, $CDCl_3$) δ 8.88 (s, 4H) H_β, 8.84 (d, *J* = 3.1 Hz, 4H) H_β, 8.22 (d, *J* = 6.3 Hz, 4H) H_{oPh}, 8.07 (d, *J* = 8.4 Hz, 4H) $H_{oPh'}$, 7.81 – 7.72 (m, 6H) H_{mPh} and H_{pPh}, 7.19 (d, *J* = 8.4 Hz, 4H) $H_{mPh'}$, 5.16 (s, *J* = 69.9 Hz, 2H) O*H*, -2.76 (s, 2H) N*H*. IR (KBr, cm^{-1}): 3325(br), 2957, 2924, 2875, 1606, 1513, 1472, 1231, 966. (^{13}C NMR could not be obtained due to the low amount of material obtained).

5,15-Di(p-10'-bromodecanoxyphenyl)-10,20-diphenylporphyrin 82

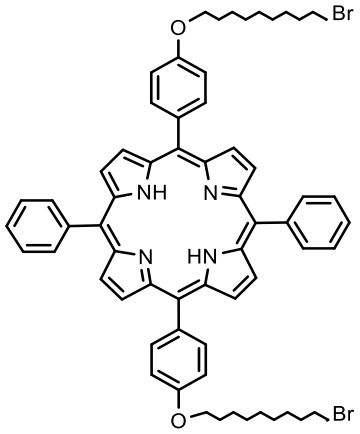

82

A mixture of *trans* porphyrin **80** (78 mg, 120.6 mmol), potassium carbonate (83 mg, 602.8 mmol) and 1,10-dibromodecane (144 mg, 482.2 mmol) in 75 ml acetone overnight. When the reaction was completed, 50 ml of distilled water were added to the mixture and the purple precipitate formed was filtered off. The solids were then separated by silica gel chromatography using DCM/Pet. ether (1:1 v/v) as eluent to recover a first purple band containing the mono-alkylated intermediate. Then the eluent was changed to 100 % DCM and the product collected, concentrated and recrystallised using DCM/Pet ether to obtain the title compound as a purple solid (41.1 mg, 31.5 %). ^{1}H NMR (500 MHz, $CDCl_3$) δ 8.88 (d, *J* = 4.5 Hz, 1H), 8.84 (d, *J* = 4.5 Hz, 1H), 8.22 (d, *J* = 6.5 Hz, 1H), 8.11 (d, *J* = 8.5 Hz, 1H), 7.82 – 7.71 (m, 6H), 7.27 (d, *J* = 8.5 Hz, 1H), 4.25 (t, *J* = 6.5 Hz, 1H), 3.44 (t, *J* = 6.5 Hz, 1H), 2.03 – 1.94 (m, 4H), 1.94 – 1.83 (m, 4H), 1.72 – 1.56 (m, 4H), -2.75 (s, 2H). ^{13}C NMR (126 MHz, $CDCl_3$) δ 159.13, 142.44, 135.76, 134.71, 134.50, 127.81, 126.81, 120.12, 112.88, 77.16, 68.45, 34.22, 33.01, 29.69, 29.65, 29.63, 29.59, 28.96, 28.36, 26.38. MS (MALDI-tof): m/z = 1086.14 [M^+]. IR (KBr, cm^{-1}): 2930, 2853, 1606, 1505, 1465, 1351, 1285, 1245, 1176, 965, 843.

Porphyrin triad 73

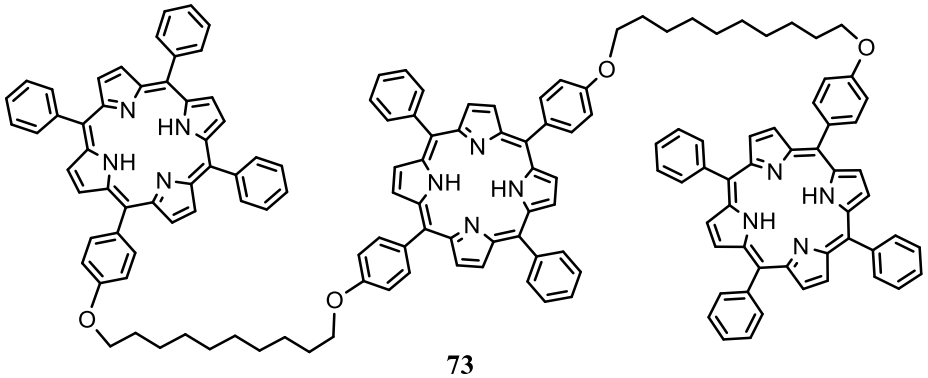

73

Trans-porphyrin **80** (15.0 mg, 0.023 mmol) and alkylated porphyrin **47** (43.5 mg, 0.05 mmol) were dissolved in DMF. Then, potassium carbonate (16 mg, 0.11 mmol) and a catalytic amount of KI (≈1 mg) were added and the mixture heated to 60 ˚C and stirred for 48 h. Then, 20 ml of distilled water were added and the precipitate formed was filtered and washed with MeOH. The purple solid obtained was recrystallized twice from the mixture of DCM:MeOH to recover the pure triad **73** (27.1 mg, 53 %).^{1}H NMR (500 MHz, $CDCl_3$) δ 8.91 – 8.86 (m, 8H), 8.86 – 8.78 (m, 16H), 8.24 – 8.16 (m, *J* = 5.9 Hz, 16H), 8.13 – 8.08 (m, 8H), 7.70 (s, *J* = 7.4 Hz, 24H), 7.31 – 7.27 (m, *J* = 8.4 Hz, 8H), 4.28 (s, 8H), 2.06 – 1.99 (m, 8H), 1.68 (s, 8H), 1.25 (s, 8H), -2.77 (s, 6H). MS (MALDI-tof): m/z = 2186.50 [M^+]. IR (KBr, cm^{-1}): 2919, 2855, 1607, 1510, 1470, 1349, 1244, 1174, 965. (^{13}C NMR could not be obtained due to precipitation of the material in the NMR tube at high concentrations).

Extended triple decker 75

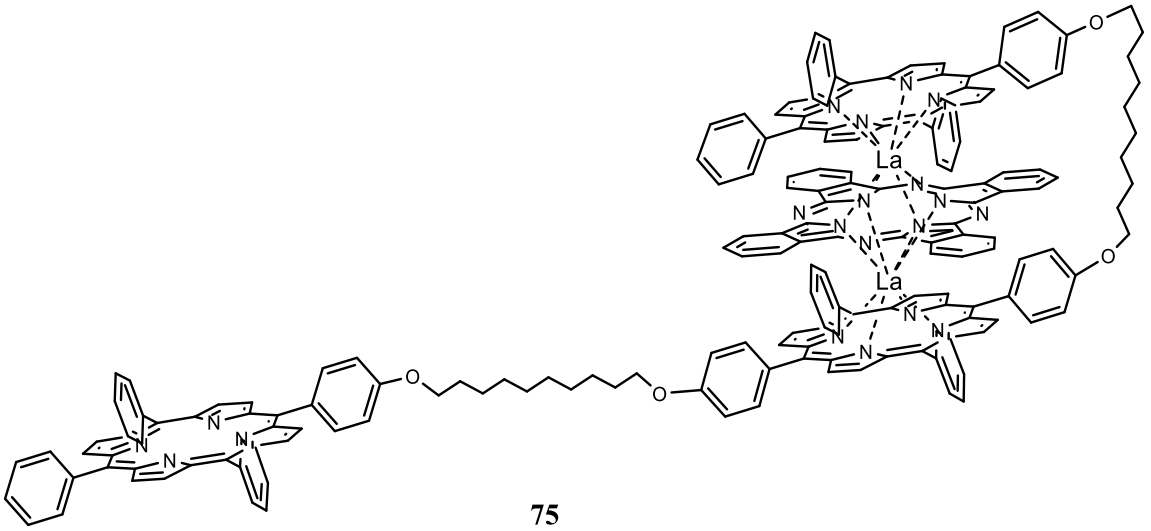

75

Porphyrin triad **73** (15 mg, 6.8×10^{-3} mmol) and lanthanum acetylacetonate hydrate (5.99 mg, 0.013 mmol) were dissolved in 3 ml octanol and refluxed for 8 h. Then, it was cooled down enough to stop the boiling and PcH_2 **19** (3.53 mg, 0.06 mmol) was added to the mixture and subjected to reflux for 18h. When the reaction was completed, the reaction was cooled down to rt. and a mixture of methanol/water 5 ml (10:1 v/v) was added and left precipitating overnight. The resultant solid was filtered off and separated by silica gel column chromatography using THF/Pet ether (2:3 v/v). The pure product was collected as the second brown fraction and further purified by recrystallisation to obtain the pure product (2 mg, <1 %). MS (MALDI-tof): m/z = 2974.69 [M^+]. ^{1}H NMR (500 MHz, $CDCl_3$) δ 10.07 (s, 2H), 9.99 (d, *J* = 7.4 Hz, 4H), 9.87 (s, 2H), 9.35 (dd, *J* = 5.3, 2.9 Hz, 8H), 8.93 (d, *J* = 4.8 Hz, 2H), 8.86 (d, *J* = 4.7 Hz, 2H), 8.84 (s, 6H), 8.43 (t, *J* = 7.6 Hz, 6H), 8.29 (dd, *J* = 5.6, 2.4 Hz, 8H), 8.25 – 8.20 (m, 8H), 8.16 (d, *J* = 8.6 Hz, 2H), 7.98 (s, 4H), 7.77 (ddd, *J* = 13.5, 11.7, 7.0 Hz, 16H), 7.35 (d, *J* = 8.6 Hz, 2H), 7.31 – 7.29 (m, 4H), 7.24 – 7.22 (m, 6H), 6.85 (s, 2H), 6.79 – 6.76 (m, 2H), 6.73 (s, 2H), 6.63 (d, *J* = 6.3 Hz, 4H), 6.57 (s, 2H), 4.65 – 4.54 (m, 8H), 4.41 – 4.30 (m, 8H), 1.91 (s, 8H), 1.80 (s, 8H), 1.62 (s, 8H), -2.74 (s, 2H). (^{13}C NMR could not be obtained due to the low amount of material obtained).

Extended double decker 68

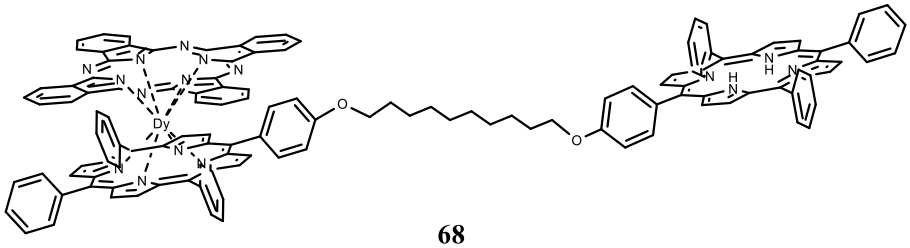

68

For the synthesis of extended double decker **68**, C_{10} dyad **45** (101 mg, 0.072 mmol), $Dy(acac)_3{\cdot}H_2O$ (49.8 mg, 0.11 mmol) and PcH_2 **19** (37.1 mg, 0.072 mmol), were dissolved in 7 ml of octanol and refluxed for 24 h. Then, the solvent was distilled under pressure to obtain dark solids that were purified by silica gel column chromatography using THF/Pet ether using EtOAc/pet. ether (1:1) as eluent and the third brown band collected, concentrated and further separated using DCM/Pet ether (3:2) to collect the last brown fraction. The resultant purple-brown solids were then recrystallised from DCM/MeOH to yield the pure product (51 mg, 34 %). ^{1}H NMR (500 MHz, $CDCl_3$) δ 8.83 – 8.72 (m, 4H), 8.70 (s, 2H), 8.49 (s, 2H), 8.23 (s, 2H), 8.19 – 8.05 (m, 8H), 8.00 (d, *J* = 8.3 Hz, 1H), 7.97 – 7.90 (m, 3H), 7.74 – 7.66 (m, *J* = 7.1 Hz, 3H), 7.65 – 7.58 (m, 2H), 7.35 (d, *J* = 8.0 Hz, 2H), 7.18 (d, *J* = 8.4 Hz, 1H), 6.20 (d, *J* = 8.2 Hz, 2H), 2.88 (d, *J* = 5.8 Hz, 2H), 2.81 (s, 2H), 1.30 (s, 2H), 1.13 (s, 1H), 0.32 (s, 2H), -0.30 (s, 2H), -0.78 (s, 2H), -1.25 (s, 2H), -1.78 (s, 2H), -2.35 (s, 2H), -2.91 (s, 1H), -3.07 (s, 2H), -3.24 (s, 2H), -3.35 (s, 2H), -3.72 (d, *J* = 31.9 Hz, 4H), -18.87 (d, *J* = 105.7 Hz, 1H), -19.00 – -19.15 (m, 1H), -31.50 (s, 1H), -53.74 (s, 1H), -70.46 (s, 1H). MS (MALDI-tof): m/z = 2076.06 [M^+]. (^{1}H NMR and ^{13}C NMR could not be fully analysed due to problems with shifting)

Extended double decker 70

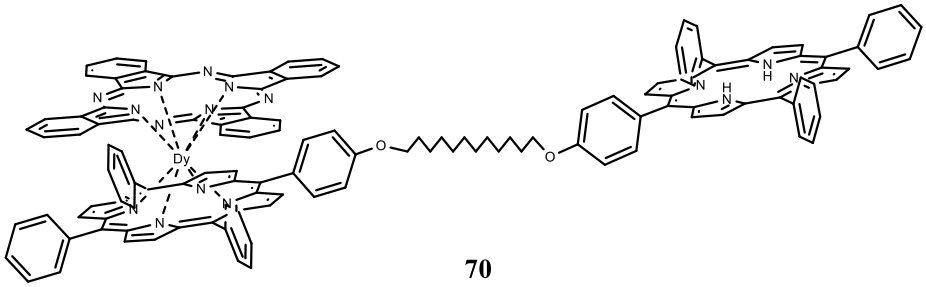

70

For the synthesis of extended double decker **70**, C_{12} dyad **46** (25 mg, 0.017 mmol), $Dy(acac)_3{\cdot}H_2O$ (12.1 mg, 0.022 mmol) and PcH_2 **19** (9.0 mg, 0.017 mmol), were dissolved in 7 ml of octanol and refluxed for 24 h. Then, the solvent was distilled under pressure to obtain dark solids where recrystallized from DCM/hexane. The resultant solid was purified by column chromatography over silica gel using DCM as eluent. The resultant purple fraction was then further separated by gravity percolation column chromatography using EtOAc/Pet ether (1:4) as eluent. The second brown fraction contained the product (11.4 mg, 31 %). MS (MALDI-tof): m/z = 2102.86 [M^+]. Analytically pure material could not be obtained and it was used without further purification at this step).

(1) Ogi, S.; Ikeda, T.; Wakabayashi, R.; Shinkai, S.; Takeuchi, M. *Chem. Eur. J.* **2010**, *16*, 8285.

(2) Andréasson, J.; Straight, S. D.; Bandyopadhyay, S.; Mitchell, R. H.; Moore, T. A.; Moore, A. L.; Gust, D. *Angew. Chem. Int. Ed.* **2007**, *46*, 958.

(3) Sakaue, S.; Fuyuhiro, A.; Fukuda, T.; Ishikawa, N. *Chem. Commun.* **2012**, *48*, 5337.

(4) Saha, S.; Johansson, E.; Flood, A. H.; Tseng, H.-R.; Zink, J. I.; Stoddart, J. F. *Chem. Eur. J.* **2005**, *11*, 6846.

(5) Feynman, R. P. *Engineering and Science* **1960**, *23*, 22.

(6) Ballardini, R.; Balzani, V.; Credi, A.; Gandolfi, M. T.; Venturi, M. *Acc. Chem. Res.* **2001**, *34*, 445.

(7) Balzani, V.; Credi, A.; Venturi, M. *Chem. Eur. J.* **2002**, *8*, 5524.

(8) Planck, M. *The theory of heat radiation*; P. Blakiston's Son & Co: Philadelphia, 1914.

(9) Mauzerall, D. *Phil. Trans. R. Soc. B* **1976**, *273*, 287.

(10) Symposium, C. F. *Chlorophyll Organization and Energy Transfer in Photosynthesis*; John Wiley & Sons: GB, 2009.

(11) Scheuring, S.; Sturgis, J. N. *Science* **2005**, *309*, 484.

(12) Ficken, G. E.; Johns, R. B.; Linstead, R. P. *J. Chem. Soc.* **1956**, 2272.

(13) Smith, A. *Heme, Chlorophyll, and Bilins*; 1200 ed.; Humana Press Inc.: Totowa, NJ/US, 2001.

(14) Maxwell, K.; Johnson, G. N. *J. Exp. Bot.* **2000**, *51*, 659.

(15) Knör, G.; Strasser, A. *Inorg. Chem. Commun.* **2005**, *8*, 471.

(16) Liu, Z.; Yasseri, A. A.; Lindsey, J. S.; Bocian, D. F. *Science* **2003**, *302*, 1543.

(17) Zhao, Z.; Cammidge, A. N.; Hughes, D. L.; Cook, M. J. *Org. Lett.* **2010**, *12*, 5138.

(18) Ferraudi, G. *Phthalocyanines: Properties and Applications*; VCH Publishers: New York, 1989; Vol. 1.

(19) Barrett, P. A.; Dent, C. E.; Linstead, R. P. *J. Chem. Soc.* **1936**, 1719.

(20) Rothemund, P.; Menotti, A. R. *J. Am. Chem. Soc.* **1941**, *63*, 267.

(21) Calvin, M.; Ball, R. H.; Aronoff, S. *J. Am. Chem. Soc.* **1943**, *65*, 2259.

(22) Rothemund, P.; Menotti, A. R. *J. Am. Chem. Soc.* **1948**, *70*, 1808.

(23) de la Torre, G.; Bottari, G.; Sekita, M.; Hausmann, A.; Guldi, D. M.; Torres, T. *Chem. Soc. Rev.* **2013**, *42*, 8049.

(24) Li, L.-L.; Diau, E. W.-G. *Chem. Soc. Rev.* **2013**, *42*, 291.

(25) Hanack, M.; Lang, M. *Adv. Mater.* **1994**, *6*, 819.

(26) Gouterman, M. *J. Chem. Phys* **1959**, *30*, 1139.

(27) Gouterman, M. *J. Mol. Spectrosc.* **1961**, *6*, 138.

(28) Rubio, M.; Roos, B. O.; Serrano-Andrés, L.; Merchán, M. *J. Chem. Phys* **1999**, *110*, 7202.

(29) Rio, Y.; Salome Rodriguez-Morgade, M.; Torres, T. *Org. Biomol. Chem.* **2008**, *6*, 1877.

(30) Zhao, Z.; Cammidge, A. N.; Cook, M. J. *Chem. Commun.* **2009**, 7530.

(31) *J. Am. Chem. Soc.* **2000**, *122*, 3984.

(32) Chen, X.; Thomas, J.; Gangopadhyay, P.; Norwood, R. A.; Peyghambarian, N.; McGrath, D. V. *J. Am. Chem. Soc.* **2009**, *131*, 13840.

(33) Sommerauer, M.; Rager, C.; Hanack, M. *J. Am. Chem. Soc.* **1996**, *118*, 10085.

(34) Aratani, N.; Kim, D.; Osuka, A. *Acc. Chem. Res.* **2009**, *42*, 1922.

(35) Ik Yang, S.; Li, J.; Sun Cho, H.; Kim, D.; Bocian, D. F.; Holten, D.; Lindsey, J. S. *J. Mater. Chem.* **2000**, *10*, 283.

(36) O'Sullivan, M. C.; Sprafke, J. K.; Kondratuk, D. V.; Rinfray, C.; Claridge, T. D. W.; Saywell, A.; Blunt, M. O.; O'Shea, J. N.; Beton, P. H.; Malfois, M.; Anderson, H. L. *Nature* **2011**, *469*, 72.

(37) Heyes, D. J.; Ruban, A. V.; Wilks, H. M.; Hunter, C. N. *Proc. Natl. Acad. Sci.* **2002**, *99*, 11145.

(38) Heyes, D. J.; Heathcote, P.; Rigby, S. E. J.; Palacios, M. A.; van Grondelle, R.; Hunter, C. N. *J. Biol. Chem.* **2006**, *281*, 26847.

(39) Wohrle, D. *Adv. Mater.* **1997**, *9*, 1191.

(40) Cocolios, P.; Guilard, R.; Bayeul, D.; Lecomte, C. *Inorg. Chem.* **1985**, *24*, 2058.

(41) Chen, Y.; Su, W.; Bai, M.; Jiang, J.; Li, X.; Liu, Y.; Wang, L.; Wang, S. *J. Am. Chem. Soc.* **2005**, *127*, 15700.

(42) Adler, A. D.; Longo, F. R.; Finarelli, J. D.; Goldmacher, J.; Assour, J.; Korsakoff, L. *J. Org. Chem.* **1967**, *32*, 476.

(43) Lindsey, J. S. *Acc. Chem. Res.* **2009**, *43*, 300.

(44) Whitten, D. G.; Lopp, I. G.; Wildes, P. D. *J. Am. Chem. Soc.* **1968**, *90*, 7196.

(45) Martirosyan, G. G.; Azizyan, A. S.; Kurtikyan, T. S.; Ford, P. C. *Chem. Commun.* **2004**, 1488.

(46) Kawamura, K.; Igarashi, S.; Yotsuyanagi, T. *Microchimica Acta* **2011**, *172*, 319.

(47) Cammidge, A. N.; Berber, G.; Chambrier, I.; Hough, P. W.; Cook, M. J. *Tetrahedron* **2005**, *61*, 4067.

(48) Biesaga, M.; Pyrzyńska, K.; Trojanowicz, M. *Talanta* **2000**, *51*, 209.

(49) Fleischer, E. B.; Wang, J. H. *J. Am. Chem. Soc.* **1960**, *82*, 3498.

(50) Barkigia, K. M.; Fajer, J.; Adler, A. D.; Williams, G. J. B. *Inorg. Chem.* **1980**, *19*, 2057.

(51) Walker, V. E. J.; Castillo, N.; Matta, C. r. F.; Boyd, R. J. *J. Phys. Chem. A* **2010**, *114*, 10315.

(52) Lu, F.; Sun, X.; Li, R.; Liang, D.; Zhu, P.; Choi, C.-F.; Ng, D. K. P.; Fukuda, T.; Kobayashi, N.; Bai, M.; Ma, C.; Jiang, J. *New J. Chem.* **2004**, *28*, 1116.

(53) Chabach, D.; Tahiri, M.; De Cian, A.; Fischer, J.; Weiss, R.; Bibout, M. E. M. *J. Am. Chem. Soc.* **1995**, *117*, 8548.

(54) Sheng, N.; Yuan, Z.; Wang, J.; Chen, W.; Sun, J.; Bian, Y. *Dyes and Pigm.* **2012**, *95*, 627.

(55) Shirk, J. S.; Lindle, J. R.; Bartoli, F. J.; Boyle, M. E. *J. Phys. Chem.* **1992**, *96*, 5847.

(56) Chow, B. C.; Cohen, I. A. *Bioinorg. Chem.* **1971**, *1*, 57.

(57) Yu, J.; Mathew, S.; Flavel, B. S.; Johnston, M. R.; Shapter, J. G. *J. Am. Chem. Soc.* **2008**, *130*, 8788.

(58) Zhao, Z.; Cammidge, A. N.; Hughes, D. L.; Cook, M. J. *Org. Lett.* **2010**, *12*, 5138.

(59) Birin, K. P.; Gorbunova, Y. G.; Tsivadze, A. Y. *Dalton Trans.* **2012**, *41*, 9672.

(60) Jiang, J.; Choi, M. T. M.; Law, W.-F.; Chen, J.; Ng, D. K. P. *Polyhedron* **1999**, *17*, 3903.

(61) Tabard, A.; Guilard, R.; Kadish, K. M. *Inorg. Chem.* **1986**, *25*, 4277.

(62) Mal"chugina, O. V.; Stuzhin, P. A. *Russ. Chem. Bull.* **2002**, *51*, 2261.

(63) Cocolios, P.; Guilard, R.; Fournari, P. *J. Organomet. Chem.* **1979**, *179*, 311.

(64) Eaton, S. S.; Eaton, G. R. *J. Am. Chem. Soc.* **1975**, *97*, 3660.

(65) Buchler, J. W.; Eikelmann, G.; Puppe, L.; Rohbock, K.; Schneehage, H. H.; Weck, D. *Justus Liebigs Annalen der Chemie* **1971**, *745*, 135.

(66) Lee, Y.-Y.; Chen, J.-H.; Hsieh, H.-Y. *Polyhedron* **2003**, *22*, 1633.

(67) Fleischer, E. B.; Thorp, R.; Venerable, D. *J. Chem. Soc.* **1969**, 475a.

(68) Eaton, S. S.; Eaton, G. R. *Inorg. Chem.* **1977**, *16*, 72.

(69) Rebouças, J. l. S.; Cheu, E. L. S.; Ware, C. J.; James, B. R.; Skov, K. A. *Inorg. Chem.* **2008**, *47*, 7894.

(70) Collman, J. P.; Barnes, C. E.; Brothers, P. J.; Collins, T. J.; Ozawa, T.; Gallucci, J. C.; Ibers, J. A. *J. Am. Chem. Soc.* **1984**, *106*, 5151.

(71) Ogi, S.; Ikeda, T.; Takeuchi, M. *J Inorg. and Organomet. Polym.* **2013**, *23*, 193.

(72) Lux, F.; Dempf, D.; Graw, D. *Angew. Chem.* **1968**, *80*, 792.

(73) Ishikawa, N.; Otsuka, S.; Kaizu, Y. *Angew. Chem. Int. Ed.* **2005**, *44*, 731.

(74) Buchler, J. W.; De Cian, A.; Fischer, J.; Kihn-Botulinski, M.; Paulus, H.; Weiss, R. *J. Am. Chem. Soc.* **1986**, *108*, 3652.

(75) Jiang, J.; Liu, W.; Cheng, K.-L.; Poon, K.-W.; Ng, Dennis K. P. *Eur. J. Inorg. Chem.* **2001**, *2001*, 413.

(76) Kadish, K. M.; Moninot, G.; Hu, Y.; Dubois, D.; Ibnlfassi, A.; Barbe, J. M.; Guilard, R. *J. Am. Chem. Soc.* **1993**, *115*, 8153.

(77) Jiang, J.; Mak, T. C. W.; Ng, D. K. P. *Chem. Ber.* **1996**, *129*, 933.

(78) Jiang, J.; Ng, D. K. P. *Acc. Chem. Res.* **2008**, *42*, 79.

(79) Birin, K. P.; Gorbunova, Y. G.; Tsivadze, A. Y. *Dalton Trans.* **2011**, *40*, 11474.

(80) Birin, K. P.; Gorbunova, Y. G.; Tsivadze, A. Y. *Magn. Reson. Chem.* **2010**, *48*, 505.

(81) Guyon, F.; Pondaven, A.; Guenot, P.; L'Her, M. *Inorg. Chem.* **1994**, *33*, 4787.

(82) D'Urso, A.; Fragala, M. E.; Purrello, R. *Chem. Commun.* **2012**, *48*, 8165.

(83) Little, R. G. *J. Heterocycl. Chem.* **1981**, *18*, 129.

(84) Liu, S.-T.; Reddy, K. V.; Lai, R.-Y. *Tetrahedron* **2007**, *63*, 1821.

(85) Imahori, H.; Hayashi, S.; Hayashi, H.; Oguro, A.; Eu, S.; Umeyama, T.; Matano, Y. *J. Phys. Chem. C* **2009**, *113*, 18406.

(86) Sibrian-Vazquez, M.; Hao, E.; Jensen, T. J.; Vicente, M. G. H. *Bioconjugate Chem.* **2006**, *17*, 928.

(87) Cai, J.-H.; Huang, J.-W.; Yu, H.-C.; Ji, L.-N. *J. Sol-Gel Sci. Technol.* **2011**, *58*, 698.

(88) Birin, K. P.; Gorbunova, Y. G.; Tsivadze, A. Y. *Dalton Trans.* **2011**, *40*, 11539.

(89) Kirin, I. S. M., P. N.; Makashev, Yu. A. *Russ. J. Inorg. Chem.* **1965**, *10*, 1065.

(90) J. W. Buchler, H.-G. K., M. Knoff, K.-L. Lay and S. Pfeifer *Z. Naturforsch, Teil B* **1983**, *38*.

(91) Lachkar, M. D. C., Andre; Fischer, Jean; Weiss, Raymond *New J. Chem.* **1988**, *12*, 729.

(92) Moussavi, M.; De Cian, A.; Fischer, J.; Weiss, R. *Inorg. Chem.* **1986**, *25*, 2107.

(93) Sun, X.; Li, R.; Wang, D.; Dou, J.; Zhu, P.; Lu, F.; Ma, C.; Choi, C.-F.; Cheng, Diana Y. Y.; Ng, Dennis K. P.; Kobayashi, N.; Jiang, J. *Eur. J. Inorg. Chem.* **2004**, *2004*, 3806.

(94) Padmaja, K.; Youngblood, W. J.; Wei, L.; Bocian, D. F.; Lindsey, J. S. *Inorg. Chem.* **2006**, *45*, 5479.

(95) Jiang, J.; Bian, Y.; Furuya, F.; Liu, W.; Choi, M. T. M.; Kobayashi, N.; Li, H.-W.; Yang, Q.; Mak, T. C. W.; Ng, D. K. P. *Chem. Eur. J.* **2001**, *7*, 5059.

(96) Yu. Tsivadze, A.; Birin, K. P.; Gorbunova, Y. G. *J. Porphyrins Phthalocyanines* **2009**, *13*, 283.

(97) McKeown, N. B. *Phthalocyanine Materials. Synthesis, Structure and Function*; 6 ed.; Cambridge University Press: Cambridge, 1998.

(98) Cook, M. J.; Tizzard, G. J.; Cammidge, A. N.; Coles, S. J.; MacDonald, C. J.; Chambrier, I.; Sosa-Vargas, L. X. *J. Porphyrins Phthalocyanines* **2013**, *17*, 511.

(99) Cammidge, A. N.; Tseng, C.-H.; Chambrier, I.; Hughes, D. L.; Cook, M. J. *Tetrahedron Lett.* **2009**, *50*, 5254.

(100) Bo, S.; Tang, D.; Liu, X.; Zhen, Z. *Dyes and Pigments* **2008**, *76*, 35.

(101) Ng, D. K. P.; Jiang, J. *Chem. Soc. Rev.* **1997**, *26*, 433.

(102) Cammidge, A. N.; Cook, M. J.; Hughes, D. L.; Nekelson, F.; Rahman, M. *Chem. Commun.* **2005**, 930.

(103) Gasparro, F. P.; Kolodny, N. H. *J. Chem. Educ.* **1977**, *54*, 258.

(104) Ikeda, M.; Takeuchi, M.; Shinkai, S.; Tani, F.; Naruta, Y. *Bull. Chem. Soc. Jpn.* **2001**, *74*, 739.

(105) Kan, J.; Wang, H.; Sun, W.; Cao, W.; Tao, J.; Jiang, J. *Inorg. Chem.* **2013**, *52*, 8505.

(106) Kurzen, H.; Bovigny, L.; Bulloni, C.; Daul, C. *Chem. Phys. Lett.* **2013**, *574*, 129.

(107) Bertini, I.; Coutsolelos, A.; Dikiy, A.; Luchinat, C.; Spyroulias, G. A.; Troganis, A. *Inorg. Chem.* **1996**, *35*, 6308.

(108) Sweet, L. E.; Roy, L. E.; Meng, F.; Hughbanks, T. *J. Am. Chem. Soc.* **2006**, *128*, 10193.

(109) Lin, X.; Doble, D. M. J.; Blake, A. J.; Harrison, A.; Wilson, C.; Schröder, M. *J. Am. Chem. Soc.* **2003**, *125*, 9476.

(110) Martin, J. L.; Thompson, L. C.; Radonovich, L. J.; Glick, M. D. *J. Am. Chem. Soc.* **1968**, *90*, 4493.

(111) Hinckley, C. C. *J. Am. Chem. Soc.* **1969**, *91*, 5160.

(112) Horrocks, W. D.; Sipe, J. P. *J. Am. Chem. Soc.* **1971**, *93*, 6800.

(113) McCreary, M. D.; Lewis, D. W.; Wernick, D. L.; Whitesides, G. M. *J. Am. Chem. Soc.* **1974**, *96*, 1038.

(114) Wang, H.; Wang, K.; Bian, Y.; Jiang, J.; Kobayashi, N. *Chem. Commun.* **2011**, *47*, 6879.

(115) Wang, H.; Kobayashi, N.; Jiang, J. *Chem. Eur. J.* **2012**, *18*, 1047.

(116) Wang, H.; Qian, K.; Wang, K.; Bian, Y.; Jiang, J.; Gao, S. *Chem. Commun.* **2011**, *47*, 9624.

(117) Shang, H.; Wang, H.; Wang, K.; Kan, J.; Cao, W.; Jiang, J. *Dalton Trans.* **2013**, *42*, 1109.

(118) Littler, B. J.; Ciringh, Y.; Lindsey, J. S. *J. Org. Chem.* **1999**, *64*, 2864.

(119) Littler, B. J.; Miller, M. A.; Hung, C.-H.; Wagner, R. W.; O'Shea, D. F.; Boyle, P. D.; Lindsey, J. S. *J. Org. Chem.* **1999**, *64*, 1391.

(120) Wilson, G. S.; Anderson, H. L. *Synlett* **1996**, *1996*, 1039.

(121) Arsenault, G. P.; Bullock, E.; MacDonald, S. F. *J. Am. Chem. Soc.* **1960**, *82*, 4384.

(122) Barnett, G. H.; Hudson, M. F.; Smith, K. M. *Tetrahedron Lett.* **1973**, *14*, 2887.

(123) Casiraghi, G.; Cornia, M.; Rassu, G.; Del Sante, C.; Spanu, P. *Tetrahedron* **1992**, *48*, 5619.

(124) Casiraghi, G.; Cornia, M.; Zanardi, F.; Rassu, G.; Ragg, E.; Bortolini, R. *J. Org. Chem.* **1994**, *59*, 1801.

(125) Sobral, A. l. J. F. N.; Rebanda, N. G. C. L.; da Silva, M.; Lampreia, S. H.; Ramos Silva, M.; Beja, A. M.; Paixão, J. A.; Rocha Gonsalves, A. M. d. A. *Tetrahedron Lett.* **2003**, *44*, 3971.

(126) Lee, C.-H.; S. Lindsey, J. *Tetrahedron* **1994**, *50*, 11427.

(127) Adonin, N. Y.; Bardin, V. V. *J. Fluorine Chem.* **2013**, *153*, 165.

(128) Cargill, M. R.; Sandford, G.; Tadeusiak, A. J.; Love, G. D.; Hollfelder, N.; Pleis, F.; Nelles, G.; Kilickiran, P. *Liq. Cryst.* **2011**, *38*, 1069.

(129) Chen, Q.-Y.; Li, Z.-T. *J. Chem. Soc., Perkin Trans. 1* **1993**, 1705.

(130) Gryko, D. T.; Wyrostek, D.; Nowak-Król, A.; Abramczyk, K.; Rogacki, M. K. *Synthesis* **2008**, *2008*, 4028.

(131) Sharghi, H.; HassaniNejad, A. *Tetrahedron* **2004**, *60*, 1863.

(132) Jiang, S.; Liu, M.; Cui, Y.; Zou, D.; Wu, Y. *Eur. J. Org. Chem.* **2013**, *2013*, 2591.

(133) Yu, L.; Cao, R.; Yi, W.; Yan, Q.; Chen, Z.; Ma, L.; Peng, W.; Song, H. *Bioorg. Med. Chem. Lett.* **2010**, *20*, 3254.

(134) Xing, C.; Xu, Q.; Tang, H.; Liu, L.; Wang, S. *J. Am. Chem. Soc.* **2009**, *131*, 13117.

(135) Collman, J. P.; Brothers, P. J.; McElwee-White, L.; Rose, E.; Wright, L. J. *J. Am. Chem. Soc.* **1985**, *107*, 4570.

(136) Jin, J.; Dong, Z.; He, J.; Li, R.; Ma, J. *Nanoscale Res Lett* **2009**, *4*, 578.

(137) Wang, D.; Cheng, X.; Shi, Y.; Sun, E.; Tang, X.; Zhuang, C.; Shi, T. *Sol. State Sci.* **2009**, *11*, 195.

(138) Galanin, N. E.; Shaposhnikov, G. P. *Russ. J. Gen. Chem.* **2012**, *82*, 764.

(139) Cook, M. J.; Dunn, A. J.; Howe, S. D.; Thomson, A. J.; Harrison, K. J. *J. Chem. Soc., Perkin Trans. 1* **1988**, 2453.

(140) Idowu, M.; Nyokong, T. *J. Photochem. Photobiol., A* **2008**, *199*, 282.

(141) Vargas, L. X. S., 2011.

(142) Ivanov, A. V.; Svinareva, P. A.; Zhukov, I. V.; Tomilova, L. G.; Zefirov, N. S. *Russ. Chem. Bull.* **2003**, *52*, 1562.

(143) Suzuki, M.; Osuka, A. *Org. Lett.* **2003**, *5*, 3943.

(144) Arimura, T.; Tsuchiya, Y.; Tashiro, M.; Tachiya, M. *J. Photopolym. Sci. Technol.* **2007**, *20*, 533.

Crystallographic data

Table 1. Crystal data and structure refinement details.

Identification code	**2013ncs0805r1a**	
Empirical formula	$C_{130}H_{90}La_2N_{16}O_2$	
Formula weight	2186.00	
Temperature	100(2) K	
Wavelength	0.71075 Å	
Crystal system	Triclinic	
Space group	*P*–1	
Unit cell dimensions	a = **13.4498(9) Å**	α = **84.304(9)°**
	b = **14.5712(10) Å**	β = **70.593(8)°**
	c = **16.0742(11) Å**	γ = **89.1220(10)°**
Volume	2956.0(4) $Å^3$	
Z	1	
Density (calculated)	1.228 Mg / m^3	
Absorption coefficient	0.769 mm^{-1}	
F(000)	1112	
Crystal	Plate; Colourless	
Crystal size	0.06 × 0.04 × 0.01 mm^3	
θ range for data collection	2.644 – 25.017°	
Index ranges	$-15 \le h \le 15$, $-17 \le k \le 17$, $-19 \le l \le 19$	
Reflections collected	42896	
Independent reflections	10369 [R_{int} = 0.1379]	
Completeness to θ = 25.242°	97.0 %	
Absorption correction	Semi–empirical from equivalents	
Max. and min. transmission	1.000 and 0.729	
Refinement method	Full-matrix least-squares on F^2	
Data / restraints / parameters	10369 / 3132 / 1069	
Goodness-of-fit on F^2	1.035	

Final *R* indices [$F^2 > 2\sigma(F^2)$]	*R1* = 0.0853, *wR2* = 0.1820
R indices (all data)	*R1* = 0.1564, *wR2* = 0.2064
Extinction coefficient	n/a
Largest diff. peak and hole	1.216 and –0.966 e $Å^{-3}$

Diffractometer: *Rigaku AFC12* goniometer equipped with an enhanced sensitivity (HG) *Saturn724+* detector mounted at the window of an *FR-E+ SuperBright* molybdenum rotating anode generator with VHF *Varimax* optics (70µm focus). **Cell determination and data collection**: *CrystalClear-SM Expert 3.1 b27 (Rigaku, 2013).* **Data reduction, cell refinement and absorption correction**: *CrystalClear-SM Expert 3.1 b27 (Rigaku, 2013).* **Structure solution**: *SUPERFLIP* (Palatinus, L. & Chapuis, G. (2007). J. Appl. Cryst. 40, 786-790). **Structure refinement**: *SHELXL-2012* (Sheldrick, G.M. (2008). Acta Cryst. A64, 112-122). **Graphics:** *OLEX2* (Dolomanov, O. V., Bourhis, L. J., Gildea, R. J., Howard, J. A. K. & Puschmann, H. (2009). J. Appl. Cryst. 42, 339-341).

Special details:

DELU, SIMU and RIGU restraints applied to whole structure. Selective DFIX restraints applied (see CIF for details). Solvent mask applied (see CIF for details). Full details of restraints applied are listed in CIF

Table 2. Atomic coordinates [$\times 10^4$], equivalent isotropic displacement parameters [$Å^2 \times 10^3$] and site occupancy factors. U_{eq} is defined as one third of the trace of the orthogonalized U^{ij} tensor.

Atom	*x*	*y*	*z*	U_{eq}	*S.o.f.*
La1	1009(1)	4633(1)	605(1)	42(1)	1
N1	2064(6)	5742(5)	1069(5)	55(2)	1
N2	501(6)	4373(5)	2250(4)	52(2)	1
N3	1362(5)	2990(5)	984(4)	47(2)	1
N4	2900(5)	4361(5)	–195(5)	55(2)	1
N5	900(20)	3372(14)	–1426(19)	47(7)	0.65(2)
N6	1100(20)	4960(13)	–1153(15)	41(3)	0.65(2)
N7	1757(19)	6538(13)	–1419(13)	38(5)	0.65(2)
N8	303(12)	6293(9)	–26(9)	37(2)	0.65(2)
C55	1370(20)	4212(14)	–1630(16)	39(4)	0.65(2)
C56	2233(19)	4452(13)	–2455(14)	43(5)	0.65(2)
C57	2771(17)	3953(14)	–3168(13)	56(6)	0.65(2)
C58	3537(17)	4408(14)	–3871(13)	76(7)	0.65(2)
C59	3809(15)	5318(13)	–3867(11)	70(6)	0.65(2)
C60	3297(17)	5823(13)	–3158(12)	57(6)	0.65(2)
C61	2468(15)	5393(12)	–2471(11)	38(5)	0.65(2)
C62	1756(18)	5690(12)	–1642(12)	37(4)	0.65(2)
C63	1100(20)	6815(11)	–672(13)	37(4)	0.65(2)
C64	1085(19)	7756(12)	–430(12)	47(5)	0.65(2)
C65	1642(14)	8576(10)	–871(11)	59(5)	0.65(2)
C66	1352(17)	9363(11)	–479(12)	84(6)	0.65(2)
C67	516(17)	9401(11)	314(13)	92(7)	0.65(2)
C68	–31(15)	8614(10)	767(11)	67(5)	0.65(2)
C69	252(15)	7788(10)	375(11)	50(5)	0.65(2)

C70	–201(17)	6856(11)	628(11)	35(4)	0.65(2)
C1	2921(8)	6235(7)	498(7)	66(2)	1
C2	3025(9)	7087(8)	851(8)	87(3)	1
C3	2246(9)	7081(8)	1622(8)	85(3)	1
C4	1621(8)	6235(7)	1791(6)	65(2)	1
C5	776(8)	5969(6)	2552(6)	60(2)	1
C6	265(7)	5095(6)	2778(5)	52(2)	1
C7	–558(8)	4790(6)	3581(6)	63(2)	1
C8	–793(8)	3899(6)	3572(6)	61(2)	1
C9	–107(7)	3625(6)	2717(5)	47(2)	1
C10	–39(7)	2732(6)	2454(5)	48(2)	1
C11	667(7)	2412(6)	1672(5)	51(2)	1
C12	806(7)	1487(6)	1465(6)	57(2)	1
C13	1589(8)	1499(6)	685(6)	64(3)	1
C14	1954(7)	2433(6)	382(6)	51(2)	1
C15	2809(7)	2722(6)	–388(6)	59(2)	1
C16	3256(7)	3589(6)	–635(6)	58(2)	1
C17	4218(7)	3848(7)	–1357(7)	69(3)	1
C18	4448(7)	4732(7)	–1350(7)	67(3)	1
C19	3633(7)	5073(7)	–609(6)	59(2)	1
C20	3632(7)	5953(7)	–313(7)	69(2)	1
C21	490(50)	6620(40)	3250(30)	65(5)	0.36(2)
C22	–330(40)	7100(30)	3250(20)	76(6)	0.36(2)
C23	–650(40)	7830(30)	3810(30)	81(6)	0.36(2)
C24	–110(40)	7980(40)	4380(30)	83(7)	0.36(2)
C25	750(40)	7400(20)	4340(20)	86(7)	0.36(2)
C26	1090(40)	6720(20)	3750(20)	78(6)	0.36(2)
C27	–726(7)	1959(6)	3087(5)	54(2)	1
C28	–1723(9)	1801(8)	3085(7)	81(3)	1
C29	–2318(10)	1027(8)	3615(8)	91(3)	1

C30	−1888(9)	472(7)	4144(6)	66(2)	1
C31	−944(9)	664(7)	4155(7)	77(3)	1
C32	−355(9)	1412(7)	3640(6)	70(2)	1
C33	3260(20)	1950(20)	−1060(20)	71(5)	0.51(3)
C34	2810(20)	1833(19)	−1708(17)	66(5)	0.51(3)
C35	3130(20)	1109(15)	−2241(17)	79(6)	0.51(3)
C36	3940(20)	550(19)	−2118(19)	91(6)	0.51(3)
C37	4390(20)	670(18)	−1470(20)	92(6)	0.51(3)
C38	4050(20)	1385(18)	−919(19)	84(5)	0.51(3)
C39	4384(17)	6710(20)	−930(30)	68(4)	0.5
C40	4193(13)	7198(12)	−1646(12)	55(4)	0.5
C41	4892(13)	7894(13)	−2190(13)	57(4)	0.5
C42	5768(15)	8113(14)	−1988(14)	61(4)	0.5
C43	5983(16)	7660(18)	−1312(14)	79(5)	0.5
C44	5307(16)	6944(17)	−776(14)	82(5)	0.5
O1	6390(10)	8834(10)	−2538(9)	78(3)	0.5
O2	−2421(11)	−332(9)	4699(8)	72(3)	0.5
C45	7268(15)	9090(15)	−2365(14)	74(5)	0.5
C46	7806(15)	9922(14)	−3019(15)	76(5)	0.5
C47	7369(16)	10754(14)	−2967(13)	70(4)	0.5
C48	6822(17)	11063(13)	−3564(13)	69(4)	0.5
C49	6362(19)	12086(15)	−3589(15)	85(5)	0.5
C50	6000(20)	12337(15)	−4353(16)	87(5)	0.5
C51	5023(17)	11895(14)	−4372(13)	73(5)	0.5
C52	4647(19)	11936(15)	−5143(14)	83(5)	0.5
C53	3741(19)	11556(14)	−5180(14)	81(5)	0.5
C54	3394(16)	10608(13)	−4652(13)	68(5)	0.5
N5A	1100(40)	3410(20)	−1390(30)	29(6)	0.35(2)
N6A	1150(40)	5010(20)	−1110(30)	42(3)	0.35(2)

N7A	1870(40)	6570(20)	–1290(20)	36(7)	0.35(2)
N8A	380(20)	6294(16)	89(16)	37(2)	0.35(2)
C55A	1480(50)	4280(30)	–1600(30)	43(6)	0.35(2)
C56A	2400(40)	4530(20)	–2370(30)	42(7)	0.35(2)
C57A	3020(30)	4050(20)	–3070(30)	54(9)	0.35(2)
C58A	3850(30)	4520(30)	–3700(20)	64(9)	0.35(2)
C59A	4100(30)	5410(30)	–3630(20)	73(9)	0.35(2)
C60A	3480(30)	5930(20)	–2970(20)	56(9)	0.35(2)
C61A	2650(30)	5450(20)	–2320(20)	40(7)	0.35(2)
C62A	1860(40)	5740(20)	–1520(20)	41(6)	0.35(2)
C63A	1180(40)	6820(20)	–540(30)	37(6)	0.35(2)
C64A	1190(40)	7750(20)	–280(30)	50(7)	0.35(2)
C65A	1960(20)	8478(17)	–611(18)	49(7)	0.35(2)
C66A	1830(30)	9196(18)	–120(20)	72(8)	0.35(2)
C67A	1060(30)	9180(20)	710(20)	84(9)	0.35(2)
C68A	370(30)	8440(19)	1100(20)	71(8)	0.35(2)
C69A	440(30)	7719(19)	570(20)	53(8)	0.35(2)
C70A	–110(40)	6830(20)	770(30)	45(7)	0.35(2)
C33A	3400(30)	1960(20)	–845(19)	63(5)	0.49(3)
C34A	3100(30)	1684(19)	–1552(19)	61(5)	0.49(3)
C35A	3570(30)	930(20)	–2019(17)	71(5)	0.49(3)
C36A	4300(30)	450(20)	–1790(20)	87(6)	0.49(3)
C37A	4630(20)	697(18)	–1050(20)	86(6)	0.49(3)
C38A	4170(20)	1480(20)	–570(20)	81(6)	0.49(3)
C21A	310(30)	6680(20)	3202(19)	58(4)	0.64(2)
C22A	–216(17)	7476(13)	2985(14)	66(4)	0.64(2)
C23A	–590(20)	8132(16)	3577(14)	77(5)	0.64(2)
C24A	–514(18)	8021(19)	4406(17)	72(5)	0.64(2)
C25A	–10(20)	7269(14)	4640(13)	83(5)	0.64(2)
C26A	387(19)	6589(13)	4067(12)	73(5)	0.64(2)

C39A	4506(18)	6590(20)	–810(30)	78(5)	0.5
C40A	4264(17)	7388(16)	–1235(19)	98(7)	0.5
C41A	5072(18)	8015(16)	–1760(20)	105(7)	0.5
C42A	6103(19)	7770(20)	–1920(20)	101(7)	0.5
C43A	6327(15)	7032(17)	–1463(15)	82(5)	0.5
C44A	5558(15)	6372(16)	–966(14)	76(5)	0.5

Table 3. Bond lengths [Å] and angles [°].

La1–N1	2.488(7)
La1–N2	2.493(6)
La1–N3	2.491(7)
La1–N4	2.486(7)
La1–N6^{i}	2.75(3)
La1–N6	2.78(3)
La1–N8^{i}	2.686(12)
La1–N8	2.804(14)
La1–N6A^{i}	2.80(6)
La1–N6A	2.70(6)
La1–N8A^{i}	2.89(2)
La1–N8A	2.69(2)
N1–C1	1.371(11)
N1–C4	1.383(11)
N2–C6	1.385(10)
N2–C9	1.370(10)
N3–C11	1.399(10)
N3–C14	1.361(10)
N4–C16	1.382(11)
N4–C19	1.396(11)

N5–C55	1.344(12)
N5–C70^{i}	1.33(3)
N6–La1^{i}	2.75(3)
N6–C55	1.369(11)
N6–C62	1.389(12)
N7–C62	1.320(12)
N7–C63	1.331(11)
N8–La1^{i}	2.686(12)
N8–C63	1.388(11)
N8–C70	1.384(11)
C55–C56	1.458(12)
C56–C57	1.400(12)
C56–C61	1.408(14)
C57–H57	0.9500
C57–C58	1.370(15)
C58–H58	0.9500
C58–C59	1.382(17)
C59–H59	0.9500
C59–C60	1.394(15)
C60–H60	0.9500
C60–C61	1.386(13)
C61–C62	1.461(12)
C63–C64	1.460(13)
C64–C65	1.414(15)
C64–C69	1.407(14)
C65–H65	0.9500
C65–C66	1.353(15)
C66–H66	0.9500
C66–C67	1.397(16)

C67–H67	0.9500
C67–C68	1.375(16)
C68–H68	0.9500
C68–C69	1.401(15)
C69–C70	1.461(14)
C70–N5^{i}	1.33(3)
C1–C2	1.442(13)
C1–C20	1.431(13)
C2–H2	0.9500
C2–C3	1.331(14)
C3–H3	0.9500
C3–C4	1.454(13)
C4–C5	1.390(13)
C5–C6	1.412(12)
C5–C21	1.495(19)
C5–C21A	1.520(15)
C6–C7	1.429(12)
C7–H7	0.9500
C7–C8	1.343(12)
C8–H8	0.9500
C8–C9	1.469(11)
C9–C10	1.400(11)
C10–C11	1.417(11)
C10–C27	1.529(12)
C11–C12	1.414(11)
C12–H12	0.9500
C12–C13	1.342(12)
C13–H13	0.9500
C13–C14	1.436(12)

C14–C15	1.413(11)
C15–C16	1.372(12)
C15–C33	1.61(3)
C15–C33A	1.46(3)
C16–C17	1.448(12)
C17–H17	0.9500
C17–C18	1.330(13)
C18–H18	0.9500
C18–C19	1.449(12)
C19–C20	1.412(13)
C20–C39	1.541(15)
C20–C39A	1.469(15)
C21–C22	1.29(6)
C21–C26	1.34(6)
C22–H22	0.9500
C22–C23	1.44(5)
C23–H23	0.9500
C23–C24	1.37(7)
C24–H24	0.9500
C24–C25	1.41(6)
C25–H25	0.9500
C25–C26	1.41(4)
C26–H26	0.9500
C27–C28	1.365(14)
C27–C32	1.348(13)
C28–H28	0.9500
C28–C29	1.422(14)
C29–H29	0.9500
C29–C30	1.375(15)

C30–H30	0.9500
C30–C31	1.310(14)
C30–O2	1.440(15)
C31–H31	0.9500
C31–C32	1.383(13)
C32–H32	0.9500
C33–C34	1.396(10)
C33–C38	1.398(10)
C34–H34	0.9500
C34–C35	1.397(10)
C35–H35	0.9500
C35–C36	1.396(10)
C36–H36	0.9500
C36–C37	1.399(10)
C37–H37	0.9500
C37–C38	1.403(10)
C38–H38	0.9500
C39–C40	1.39(2)
C39–C44	1.39(2)
C40–H40	0.9500
C40–C41	1.408(18)
C41–H41	0.9500
C41–C42	1.37(2)
C42–C43	1.33(3)
C42–O1	1.39(2)
C43–H43	0.9500
C43–C44	1.41(2)
C44–H44	0.9500
O1–C45	1.36(2)

O2–C54^{i}	1.40(2)
C45–H45A	0.9900
C45–H45B	0.9900
C45–C46	1.54(3)
C46–H46A	0.9900
C46–H46B	0.9900
C46–C47	1.34(3)
C47–H47A	0.9900
C47–H47B	0.9900
C47–C48	1.43(3)
C48–H48A	0.9900
C48–H48B	0.9900
C48–C49	1.61(3)
C49–H49A	0.9900
C49–H49B	0.9900
C49–C50	1.47(3)
C50–H50A	0.9900
C50–H50B	0.9900
C50–C51	1.49(3)
C51–H51A	0.9900
C51–H51B	0.9900
C51–C52	1.48(3)
C52–H52A	0.9900
C52–H52B	0.9900
C52–C53	1.37(3)
C53–H53A	0.9900
C53–H53B	0.9900
C53–C54	1.54(3)
C54–O2^{i}	1.40(2)

C54–H54A	0.9900
C54–H54B	0.9900
N5A–C55A	1.341(16)
N5A–C70A^{i}	1.40(5)
N6A–La1^{i}	2.80(6)
N6A–C55A	1.371(15)
N6A–C62A	1.385(16)
N7A–C62A	1.318(16)
N7A–C63A	1.326(15)
N8A–La1^{i}	2.89(2)
N8A–C63A	1.385(16)
N8A–C70A	1.380(16)
C55A–C56A	1.457(16)
C56A–C57A	1.403(17)
C56A–C61A	1.403(17)
C57A–H57A	0.9500
C57A–C58A	1.367(19)
C58A–H58A	0.9500
C58A–C59A	1.38(2)
C59A–H59A	0.9500
C59A–C60A	1.390(19)
C60A–H60A	0.9500
C60A–C61A	1.391(17)
C61A–C62A	1.458(16)
C63A–C64A	1.458(16)
C64A–C65A	1.42(2)
C64A–C69A	1.402(18)
C65A–H65A	0.9500
C65A–C66A	1.348(19)

C66A–H66A	0.9500
C66A–C67A	1.40(2)
C67A–H67A	0.9500
C67A–C68A	1.38(2)
C68A–H68A	0.9500
C68A–C69A	1.394(19)
C69A–C70A	1.459(18)
C70A–N5A^{i}	1.40(5)
C33A–C34A	1.42(3)
C33A–C38A	1.41(3)
C34A–H34A	0.9500
C34A–C35A	1.41(3)
C35A–H35A	0.9500
C35A–C36A	1.33(4)
C36A–H36A	0.9500
C36A–C37A	1.47(4)
C37A–H37A	0.9500
C37A–C38A	1.45(3)
C38A–H38A	0.9500
C21A–C22A	1.42(3)
C21A–C26A	1.42(3)
C22A–H22A	0.9500
C22A–C23A	1.39(2)
C23A–H23A	0.9500
C23A–C24A	1.36(3)
C24A–H24A	0.9500
C24A–C25A	1.37(3)
C25A–H25A	0.9500
C25A–C26A	1.40(2)

C26A–H26A	0.9500
C39A–C40A	1.37(2)
C39A–C44A	1.39(3)
C40A–H40A	0.9500
C40A–C41A	1.41(2)
C41A–H41A	0.9500
C41A–C42A	1.38(3)
C42A–H42A	0.9500
C42A–C43A	1.32(3)
C43A–H43A	0.9500
C43A–C44A	1.40(2)
C44A–H44A	0.9500
N1–La1–N2	72.8(2)
N1–La1–N3	113.3(2)
N1–La1–N6	114.5(4)
N1–La1–N6^{i}	112.1(4)
N1–La1–N8	80.6(3)
N1–La1–N8^{i}	169.7(3)
N1–La1–N6A^{i}	114.8(7)
N1–La1–N6A	112.0(8)
N1–La1–N8A^{i}	167.5(5)
N1–La1–N8A	76.5(5)
N2–La1–N6	167.4(6)
N2–La1–N6^{i}	77.5(6)
N2–La1–N8^{i}	110.8(3)
N2–La1–N8	114.5(3)
N2–La1–N6A^{i}	79.2(12)
N2–La1–N6A	168.5(12)
N2–La1–N8A	111.3(5)

N2–La1–N8A^{i}	113.2(5)
N3–La1–N2	72.7(2)
N3–La1–N6^{i}	113.5(4)
N3–La1–N6	111.4(4)
N3–La1–N8	166.0(3)
N3–La1–N8^{i}	76.9(3)
N3–La1–N6A^{i}	112.1(8)
N3–La1–N6A	113.0(8)
N3–La1–N8A	170.2(5)
N3–La1–N8A^{i}	79.1(5)
N4–La1–N1	72.6(2)
N4–La1–N2	114.1(2)
N4–La1–N3	72.4(2)
N4–La1–N6^{i}	168.4(6)
N4–La1–N6	78.4(6)
N4–La1–N8	112.7(4)
N4–La1–N8^{i}	113.1(4)
N4–La1–N6A	77.4(12)
N4–La1–N6A^{i}	166.7(11)
N4–La1–N8A^{i}	112.6(6)
N4–La1–N8A	112.4(6)
N6^{i}–La1–N6	90.0(4)
N6^{i}–La1–N8	59.2(6)
N6–La1–N8	59.0(5)
N8^{i}–La1–N6^{i}	60.7(5)
N8^{i}–La1–N6	60.3(6)
N8^{i}–La1–N8	89.2(4)
N6A–La1–N6A^{i}	89.4(8)
N6A–La1–N8A^{i}	60.1(11)

N6A^{i}–La1–N8A^{i}	57.9(9)
N8A–La1–N6A	61.4(9)
N8A–La1–N6A^{i}	61.2(11)
N8A–La1–N8A^{i}	91.1(6)
C1–N1–La1	124.2(6)
C1–N1–C4	108.0(7)
C4–N1–La1	121.9(6)
C6–N2–La1	121.9(5)
C9–N2–La1	121.2(5)
C9–N2–C6	107.9(7)
C11–N3–La1	124.0(5)
C14–N3–La1	123.8(5)
C14–N3–C11	106.6(7)
C16–N4–La1	123.5(6)
C16–N4–C19	107.2(7)
C19–N4–La1	123.1(6)
C70^{i}–N5–C55	120.4(18)
La1^{i}–N6–La1	90.0(4)
C55–N6–La1^{i}	115(2)
C55–N6–La1	115(2)
C55–N6–C62	107.2(9)
C62–N6–La1	115.3(17)
C62–N6–La1^{i}	114.0(18)
C62–N7–C63	123.5(11)
La1^{i}–N8–La1	90.8(4)
C63–N8–La1^{i}	116.0(12)
C63–N8–La1	113.5(13)
C70–N8–La1	114.2(11)
C70–N8–La1^{i}	114.1(11)

C70–N8–C63	107.7(9)
N5–C55–N6	127.3(11)
N5–C55–C56	122.1(11)
N6–C55–C56	110.5(9)
C57–C56–C55	133.0(11)
C57–C56–C61	120.7(10)
C61–C56–C55	106.3(8)
C56–C57–H57	121.1
C58–C57–C56	117.9(12)
C58–C57–H57	121.1
C57–C58–H58	119.3
C57–C58–C59	121.5(11)
C59–C58–H58	119.3
C58–C59–H59	119.2
C58–C59–C60	121.6(11)
C60–C59–H59	119.2
C59–C60–H60	121.2
C61–C60–C59	117.5(12)
C61–C60–H60	121.2
C56–C61–C62	106.0(9)
C60–C61–C56	120.5(10)
C60–C61–C62	133.3(10)
N6–C62–C61	110.0(9)
N7–C62–N6	126.7(10)
N7–C62–C61	123.3(10)
N7–C63–N8	127.0(10)
N7–C63–C64	123.6(10)
N8–C63–C64	109.4(9)
C65–C64–C63	133.3(10)

C69–C64–C63	106.7(9)
C69–C64–C65	119.6(11)
C64–C65–H65	121.3
C66–C65–C64	117.4(11)
C66–C65–H65	121.3
C65–C66–H66	118.4
C65–C66–C67	123.1(13)
C67–C66–H66	118.4
C66–C67–H67	119.6
C68–C67–C66	120.9(12)
C68–C67–H67	119.6
C67–C68–H68	121.4
C67–C68–C69	117.1(11)
C69–C68–H68	121.4
C64–C69–C70	106.4(9)
C68–C69–C64	121.7(11)
C68–C69–C70	131.9(11)
$N5^{i}$–C70–N8	129.0(14)
$N5^{i}$–C70–C69	120.8(13)
N8–C70–C69	109.7(9)
N1–C1–C2	109.5(9)
N1–C1–C20	126.2(8)
C20–C1–C2	124.3(9)
C1–C2–H2	126.9
C3–C2–C1	106.3(9)
C3–C2–H2	126.9
C2–C3–H3	125.1
C2–C3–C4	109.8(9)
C4–C3–H3	125.1

N1–C4–C3	106.4(8)
N1–C4–C5	127.6(8)
C5–C4–C3	125.9(9)
C4–C5–C6	126.1(8)
C4–C5–C21	117(3)
C4–C5–C21A	118.8(17)
C6–C5–C21	117(3)
C6–C5–C21A	115.0(17)
N2–C6–C5	125.0(8)
N2–C6–C7	108.0(8)
C5–C6–C7	127.0(8)
C6–C7–H7	125.3
C8–C7–C6	109.4(8)
C8–C7–H7	125.3
C7–C8–H8	126.9
C7–C8–C9	106.1(8)
C9–C8–H8	126.9
N2–C9–C8	108.5(7)
N2–C9–C10	126.0(7)
C10–C9–C8	125.4(8)
C9–C10–C11	127.8(8)
C9–C10–C27	119.1(7)
C11–C10–C27	112.9(7)
N3–C11–C10	123.6(7)
N3–C11–C12	109.5(7)
C12–C11–C10	126.9(8)
C11–C12–H12	126.7
C13–C12–C11	106.6(8)
C13–C12–H12	126.7

C12–C13–H13	125.5
C12–C13–C14	109.0(8)
C14–C13–H13	125.5
N3–C14–C13	108.2(7)
N3–C14–C15	125.8(8)
C15–C14–C13	125.9(8)
C14–C15–C33	115.5(15)
C14–C15–C33A	114.1(15)
C16–C15–C14	127.1(8)
C16–C15–C33	117.4(15)
C16–C15–C33A	117.4(15)
N4–C16–C17	107.7(8)
C15–C16–N4	125.6(8)
C15–C16–C17	126.5(8)
C16–C17–H17	125.3
C18–C17–C16	109.4(9)
C18–C17–H17	125.3
C17–C18–H18	126.5
C17–C18–C19	107.1(9)
C19–C18–H18	126.5
N4–C19–C18	108.6(8)
N4–C19–C20	125.8(8)
C20–C19–C18	125.4(9)
C1–C20–C39	116(2)
C1–C20–C39A	117(2)
C19–C20–C1	125.2(8)
C19–C20–C39	119(2)
C19–C20–C39A	118(2)
C22–C21–C5	112(4)

C22–C21–C26	127(3)
C26–C21–C5	121(4)
C21–C22–H22	120.3
C21–C22–C23	119(4)
C23–C22–H22	120.3
C22–C23–H23	120.2
C24–C23–C22	120(4)
C24–C23–H23	120.2
C23–C24–H24	122.1
C23–C24–C25	116(4)
C25–C24–H24	122.1
C24–C25–H25	117.9
C26–C25–C24	124(4)
C26–C25–H25	117.9
C21–C26–C25	114(3)
C21–C26–H26	123.0
C25–C26–H26	123.0
C28–C27–C10	120.1(9)
C32–C27–C10	120.9(9)
C32–C27–C28	119.0(9)
C27–C28–H28	120.2
C27–C28–C29	119.6(10)
C29–C28–H28	120.2
C28–C29–H29	120.5
C30–C29–C28	119.0(11)
C30–C29–H29	120.5
C29–C30–H30	120.1
C29–C30–O2	123.3(12)
C31–C30–C29	119.7(11)

C31–C30–H30	120.1
C31–C30–O2	117.0(11)
C30–C31–H31	119.1
C30–C31–C32	121.9(11)
C32–C31–H31	119.1
C27–C32–C31	120.7(10)
C27–C32–H32	119.7
C31–C32–H32	119.7
C34–C33–C15	119.4(18)
C34–C33–C38	123(2)
C38–C33–C15	117.3(17)
C33–C34–H34	120.3
C33–C34–C35	120(2)
C35–C34–H34	120.2
C34–C35–H35	121.1
C36–C35–C34	118(3)
C36–C35–H35	121.1
C35–C36–H36	118.8
C35–C36–C37	122(3)
C37–C36–H36	118.8
C36–C37–H37	120.0
C36–C37–C38	120(2)
C38–C37–H37	120.0
C33–C38–C37	117(2)
C33–C38–H38	121.5
C37–C38–H38	121.5
C40–C39–C20	123.2(17)
C40–C39–C44	116.6(14)
C44–C39–C20	120.2(18)

C39–C40–H40	119.1
C39–C40–C41	121.8(16)
C41–C40–H40	119.1
C40–C41–H41	120.5
C42–C41–C40	118.9(18)
C42–C41–H41	120.5
C41–C42–O1	115.1(18)
C43–C42–C41	121.1(17)
C43–C42–O1	123.8(18)
C42–C43–H43	119.7
C42–C43–C44	120.6(18)
C44–C43–H43	119.7
C39–C44–C43	120.9(18)
C39–C44–H44	119.5
C43–C44–H44	119.5
C45–O1–C42	117.8(16)
$C54^{i}$–O2–C30	118.8(14)
O1–C45–H45A	109.8
O1–C45–H45B	109.8
O1–C45–C46	109.2(18)
H45A–C45–H45B	108.3
C46–C45–H45A	109.8
C46–C45–H45B	109.8
C45–C46–H46A	107.0
C45–C46–H46B	107.0
H46A–C46–H46B	106.7
C47–C46–C45	121.3(18)
C47–C46–H46A	107.0
C47–C46–H46B	107.0

C46–C47–H47A	107.5
C46–C47–H47B	107.5
C46–C47–C48	119.4(19)
H47A–C47–H47B	107.0
C48–C47–H47A	107.5
C48–C47–H47B	107.5
C47–C48–H48A	106.9
C47–C48–H48B	106.9
C47–C48–C49	121.8(17)
H48A–C48–H48B	106.7
C49–C48–H48A	106.9
C49–C48–H48B	106.9
C48–C49–H49A	108.8
C48–C49–H49B	108.8
H49A–C49–H49B	107.7
C50–C49–C48	113.8(17)
C50–C49–H49A	108.8
C50–C49–H49B	108.8
C49–C50–H50A	107.6
C49–C50–H50B	107.6
C49–C50–C51	119(2)
H50A–C50–H50B	107.1
C51–C50–H50A	107.6
C51–C50–H50B	107.6
C50–C51–H51A	105.8
C50–C51–H51B	105.8
H51A–C51–H51B	106.2
C52–C51–C50	126.1(19)
C52–C51–H51A	105.8

C52–C51–H51B	105.8
C51–C52–H52A	105.4
C51–C52–H52B	105.4
H52A–C52–H52B	106.0
C53–C52–C51	127.7(19)
C53–C52–H52A	105.4
C53–C52–H52B	105.4
C52–C53–H53A	108.2
C52–C53–H53B	108.2
C52–C53–C54	116(2)
H53A–C53–H53B	107.3
C54–C53–H53A	108.2
C54–C53–H53B	108.2
$O2^{i}$–C54–C53	110.4(18)
$O2^{i}$–C54–H54A	109.6
$O2^{i}$–C54–H54B	109.6
C53–C54–H54A	109.6
C53–C54–H54B	109.6
H54A–C54–H54B	108.1
C55A–N5A–$C70A^{i}$	123(3)
La1–N6A–$La1^{i}$	90.6(8)
C55A–N6A–La1	113(4)
C55A–N6A–$La1^{i}$	115(4)
C55A–N6A–C62A	107.0(14)
C62A–N6A–$La1^{i}$	119(3)
C62A–N6A–La1	112(4)
C62A–N7A–C63A	121.6(17)
La1–N8A–$La1^{i}$	88.9(6)
C63A–N8A–$La1^{i}$	115(2)

C63A–N8A–La1	114(2)
C70A–N8A–La1^{i}	115(2)
C70A–N8A–La1	115(2)
C70A–N8A–C63A	108.1(14)
N5A–C55A–N6A	127.3(19)
N5A–C55A–C56A	121.7(19)
N6A–C55A–C56A	110.7(14)
C57A–C56A–C55A	133.4(17)
C61A–C56A–C55A	106.0(13)
C61A–C56A–C57A	120.5(15)
C56A–C57A–H57A	121.3
C58A–C57A–C56A	117.4(18)
C58A–C57A–H57A	121.3
C57A–C58A–H58A	119.2
C57A–C58A–C59A	121.5(18)
C59A–C58A–H58A	119.2
C58A–C59A–H59A	118.8
C58A–C59A–C60A	122.5(19)
C60A–C59A–H59A	118.8
C59A–C60A–H60A	122.0
C61A–C60A–C59A	115.9(18)
C61A–C60A–H60A	122.0
C56A–C61A–C62A	106.4(13)
C60A–C61A–C56A	121.6(15)
C60A–C61A–C62A	131.9(17)
N6A–C62A–C61A	109.9(13)
N7A–C62A–N6A	128.5(17)
N7A–C62A–C61A	121.5(17)
N7A–C63A–N8A	128.3(17)

N7A–C63A–C64A	121.4(17)
N8A–C63A–C64A	110.3(13)
C65A–C64A–C63A	131(2)
C69A–C64A–C63A	104.6(13)
C69A–C64A–C65A	121.5(19)
C64A–C65A–H65A	121.7
C66A–C65A–C64A	116.6(17)
C66A–C65A–H65A	121.7
C65A–C66A–H66A	119.4
C65A–C66A–C67A	121.1(19)
C67A–C66A–H66A	119.4
C66A–C67A–H67A	118.2
C68A–C67A–C66A	123.6(19)
C68A–C67A–H67A	118.2
C67A–C68A–H68A	122.1
C67A–C68A–C69A	115.8(18)
C69A–C68A–H68A	122.1
C64A–C69A–C70A	108.4(14)
C68A–C69A–C64A	120.8(17)
C68A–C69A–C70A	130.7(18)
$N5A^{i}$–C70A–C69A	128(3)
N8A–C70A–$N5A^{i}$	122(3)
N8A–C70A–C69A	108.1(14)
C34A–C33A–C15	117(2)
C34A–C33A–C38A	120(2)
C38A–C33A–C15	123(2)
C33A–C34A–H34A	118.9
C35A–C34A–C33A	122(2)
C35A–C34A–H34A	118.9

C34A–C35A–H35A	120.1
C36A–C35A–C34A	120(2)
C36A–C35A–H35A	120.1
C35A–C36A–H36A	119.6
C35A–C36A–C37A	121(2)
C37A–C36A–H36A	119.6
C36A–C37A–H37A	119.9
C38A–C37A–C36A	120(2)
C38A–C37A–H37A	119.9
C33A–C38A–H38A	121.7
C37A–C38A–C33A	117(2)
C37A–C38A–H38A	121.7
C22A–C21A–C5	122.8(19)
C26A–C21A–C5	121(2)
C26A–C21A–C22A	115.7(14)
C21A–C22A–H22A	119.3
C23A–C22A–C21A	121.5(16)
C23A–C22A–H22A	119.3
C22A–C23A–H23A	119.3
C24A–C23A–C22A	121.3(19)
C24A–C23A–H23A	119.3
C23A–C24A–H24A	120.4
C23A–C24A–C25A	119(2)
C25A–C24A–H24A	120.4
C24A–C25A–H25A	119.2
C24A–C25A–C26A	121.5(17)
C26A–C25A–H25A	119.2
C21A–C26A–H26A	119.7
C25A–C26A–C21A	120.6(17)

C25A–C26A–H26A	119.7
C40A–C39A–C20	117.3(17)
C40A–C39A–C44A	119.5(16)
C44A–C39A–C20	123(2)
C39A–C40A–H40A	119.9
C39A–C40A–C41A	120.2(19)
C41A–C40A–H40A	119.9
C40A–C41A–H41A	120.7
C42A–C41A–C40A	119(2)
C42A–C41A–H41A	120.7
C41A–C42A–H42A	120.0
C43A–C42A–C41A	120(2)
C43A–C42A–H42A	120.0
C42A–C43A–H43A	118.9
C42A–C43A–C44A	122.2(19)
C44A–C43A–H43A	118.9
C39A–C44A–C43A	117.7(19)
C39A–C44A–H44A	121.2
C43A–C44A–H44A	121.2

Symmetry transformations used to generate equivalent atoms:

(i) –x,–y+1,–z

Table 4. Anisotropic displacement parameters [$Å^2 \times 10^3$]. The anisotropic displacement factor exponent takes the form: $-2\pi^2[h^2a^{*2}U^{11} + \cdots + 2\ h\ k\ a^*\ b^*\ U^{12}\ ]$.

Atom	U^{11}	U^{22}	U^{33}	U^{23}	U^{13}	U^{12}
La1	43(1)	43(1)	33(1)	–7(1)	–4(1)	–8(1)

N1	60(4)	54(4)	52(3)	–6(3)	–20(3)	–13(3)
N2	66(4)	50(3)	35(3)	–5(2)	–12(3)	–8(3)
N3	45(4)	47(3)	42(3)	–8(2)	–5(3)	1(3)
N4	42(3)	57(3)	56(4)	–3(3)	–4(3)	–7(3)
N5	45(12)	46(5)	37(9)	–13(5)	6(8)	–12(6)
N6	43(5)	41(4)	29(4)	–8(3)	3(3)	–11(4)
N7	38(7)	45(5)	27(6)	–8(4)	–5(5)	–14(4)
N8	38(3)	40(3)	27(4)	–9(2)	–4(2)	–8(2)
C55	37(8)	44(5)	30(4)	–10(4)	1(5)	–9(4)
C56	43(9)	47(5)	31(5)	–10(4)	2(6)	–15(5)
C57	52(11)	59(6)	40(6)	–22(5)	15(7)	–23(6)
C58	76(12)	69(7)	48(8)	–28(6)	33(8)	–34(7)
C59	74(10)	69(7)	40(7)	–22(6)	23(7)	–34(7)
C60	64(9)	54(6)	34(7)	–9(5)	11(7)	–28(6)
C61	37(7)	47(5)	25(5)	–10(4)	–2(5)	–16(4)
C62	39(7)	42(4)	26(5)	–7(3)	–5(5)	–12(4)
C63	38(7)	42(4)	28(6)	–7(3)	–6(5)	–11(4)
C64	53(8)	46(4)	38(7)	–14(4)	–7(6)	–15(4)
C65	72(9)	51(5)	44(7)	–10(5)	–4(6)	–25(6)
C66	110(11)	55(6)	57(9)	–17(6)	15(8)	–35(7)
C67	118(12)	54(6)	69(9)	–26(6)	24(8)	–34(6)
C68	83(10)	52(5)	49(8)	–20(5)	7(7)	–22(5)
C69	62(8)	46(4)	38(7)	–14(4)	–7(6)	–16(5)
C70	39(6)	45(4)	23(6)	–10(4)	–14(5)	–6(4)
C1	63(5)	62(5)	70(4)	–8(4)	–16(3)	–21(4)
C2	86(6)	76(5)	86(6)	–19(5)	–6(5)	–42(5)
C3	95(7)	72(5)	78(6)	–22(4)	–12(5)	–33(5)
C4	77(5)	61(5)	56(4)	–17(3)	–18(3)	–17(4)
C5	82(5)	54(4)	47(4)	–11(3)	–22(3)	–10(3)

C6	69(5)	50(3)	37(4)	–9(3)	–16(3)	0(3)
C7	85(6)	57(4)	40(4)	–11(3)	–11(4)	–3(4)
C8	75(6)	58(4)	38(4)	–10(3)	–3(4)	–2(4)
C9	53(5)	55(3)	33(3)	–6(3)	–11(3)	–3(3)
C10	50(4)	52(4)	38(4)	–6(3)	–8(3)	–2(3)
C11	54(4)	51(4)	40(3)	–7(3)	–6(3)	–4(3)
C12	64(5)	49(4)	48(4)	–5(3)	–3(4)	–2(4)
C13	77(6)	47(4)	50(4)	–8(3)	3(4)	0(4)
C14	45(4)	50(4)	49(4)	–8(3)	–2(3)	2(3)
C15	50(4)	53(4)	58(4)	–6(3)	4(3)	5(3)
C16	49(4)	56(3)	56(5)	–3(3)	1(4)	1(3)
C17	54(5)	66(5)	64(5)	3(4)	5(4)	–2(4)
C18	48(5)	69(5)	68(5)	6(4)	1(4)	–5(4)
C19	43(4)	66(4)	60(5)	1(3)	–7(3)	–12(3)
C20	55(4)	70(4)	74(5)	–5(3)	–10(3)	–17(3)
C21	99(10)	50(8)	45(7)	–7(7)	–21(6)	–10(7)
C22	107(10)	71(11)	50(11)	–14(9)	–25(9)	3(9)
C23	116(12)	74(12)	57(12)	–19(9)	–31(10)	10(10)
C24	120(14)	76(12)	55(11)	–17(9)	–31(10)	3(11)
C25	123(13)	81(11)	64(11)	–25(9)	–40(11)	5(11)
C26	111(12)	71(11)	59(10)	–18(9)	–35(9)	–3(10)
C27	65(4)	50(4)	36(4)	–8(3)	–3(3)	–1(3)
C28	70(5)	84(6)	76(6)	24(5)	–16(4)	–17(4)
C29	79(6)	98(7)	83(7)	26(5)	–16(5)	–25(5)
C30	80(5)	63(5)	38(5)	–1(4)	1(4)	–11(4)
C31	94(6)	73(6)	57(6)	13(4)	–19(5)	–16(5)
C32	84(6)	66(5)	54(5)	11(4)	–21(4)	–12(4)
C33	69(9)	61(7)	58(8)	–9(6)	12(6)	6(6)
C34	70(11)	47(9)	53(8)	–3(7)	14(7)	1(7)

C35	99(13)	53(10)	66(10)	–9(8)	–1(9)	19(8)
C36	110(13)	69(11)	73(11)	–9(9)	–6(9)	33(9)
C37	103(11)	82(9)	70(12)	–13(9)	0(9)	30(8)
C38	82(10)	81(9)	66(11)	–12(8)	7(8)	22(7)
C39	50(7)	76(8)	75(7)	1(6)	–19(5)	–20(6)
C40	38(7)	61(8)	57(8)	–15(6)	–1(5)	–4(6)
C41	42(6)	64(8)	59(8)	–11(6)	–7(6)	–8(6)
C42	36(7)	68(8)	72(8)	–7(7)	–7(6)	–8(6)
C43	56(8)	88(10)	93(9)	12(8)	–29(7)	–31(7)
C44	60(7)	91(10)	95(9)	15(8)	–31(7)	–30(7)
O1	56(6)	89(7)	74(7)	1(6)	–4(5)	–28(5)
O2	85(8)	70(7)	48(7)	–1(5)	–6(6)	–15(6)
C45	56(8)	77(8)	75(10)	1(7)	–4(7)	–25(7)
C46	52(8)	65(7)	92(11)	3(7)	0(7)	–24(6)
C47	75(11)	70(8)	54(9)	–13(7)	–5(8)	–15(7)
C48	77(11)	68(8)	54(9)	–23(7)	–5(8)	–5(8)
C49	99(12)	72(9)	80(10)	–21(8)	–21(9)	–2(8)
C50	110(11)	64(10)	86(11)	–14(8)	–29(9)	–6(8)
C51	99(10)	56(10)	56(9)	–27(8)	–8(8)	0(8)
C52	107(11)	68(11)	63(9)	9(8)	–16(8)	–40(9)
C53	108(11)	57(9)	68(10)	–2(8)	–14(9)	–36(8)
C54	65(11)	58(9)	65(11)	–8(8)	2(9)	–19(8)
N5A	29(13)	43(7)	19(10)	–10(6)	–11(8)	0(7)
N6A	44(7)	43(6)	31(4)	–10(4)	1(4)	–8(5)
N7A	35(10)	43(6)	26(8)	–3(5)	–6(8)	–6(6)
N8A	38(3)	40(3)	27(4)	–9(2)	–4(2)	–8(2)
C55A	43(10)	45(6)	33(6)	–11(5)	1(7)	–7(6)
C56A	40(11)	50(7)	31(8)	–11(5)	–1(8)	–8(6)
C57A	50(14)	58(9)	42(9)	–22(7)	6(10)	–12(8)

C58A	59(13)	69(10)	46(11)	–28(8)	15(10)	–21(9)
C59A	69(13)	71(10)	53(12)	–28(9)	21(11)	–28(9)
C60A	60(12)	62(9)	32(11)	–18(7)	8(10)	–22(8)
C61A	39(10)	48(7)	30(8)	–9(6)	–5(8)	–8(6)
C62A	43(10)	44(6)	29(6)	–6(4)	–2(7)	–8(6)
C63A	37(9)	41(5)	29(7)	–6(4)	–4(7)	–6(5)
C64A	58(11)	43(6)	41(9)	–10(6)	–4(8)	–9(6)
C65A	56(11)	41(7)	43(10)	–6(7)	–5(8)	–8(7)
C66A	86(14)	51(9)	55(11)	–17(8)	13(9)	–26(9)
C67A	101(15)	58(9)	61(11)	–26(8)	22(10)	–34(9)
C68A	88(14)	57(8)	50(10)	–21(8)	9(9)	–27(9)
C69A	64(12)	46(6)	42(9)	–13(6)	–3(9)	–12(7)
C70A	51(11)	43(6)	34(8)	–12(6)	–2(8)	–5(5)
C33A	62(8)	54(6)	50(8)	–2(6)	12(6)	6(6)
C34A	66(11)	46(9)	46(8)	0(7)	12(7)	3(7)
C35A	85(12)	56(9)	50(9)	–8(7)	9(8)	15(8)
C36A	102(13)	77(10)	64(12)	–17(9)	–4(9)	34(9)
C37A	93(11)	82(10)	63(12)	–13(8)	–1(9)	34(8)
C38A	82(10)	83(9)	64(11)	–16(8)	–4(8)	27(8)
C21A	81(10)	50(6)	48(5)	–13(5)	–25(5)	–8(6)
C22A	103(10)	55(7)	52(7)	–22(6)	–39(7)	5(7)
C23A	115(11)	71(9)	60(7)	–29(6)	–44(8)	16(9)
C24A	100(13)	77(8)	56(7)	–35(6)	–41(8)	25(9)
C25A	120(13)	87(8)	54(7)	–34(6)	–41(8)	35(9)
C26A	105(12)	73(8)	53(6)	–27(5)	–37(7)	26(8)
C39A	59(6)	79(7)	86(10)	–3(6)	–12(6)	–25(5)
C40A	66(7)	92(9)	116(13)	18(9)	–10(8)	–23(7)
C41A	70(8)	92(9)	128(14)	20(10)	–9(8)	–26(7)
C42A	69(8)	99(10)	114(12)	12(10)	–9(8)	–25(8)

C43A	62(7)	85(10)	90(11)	–9(9)	–13(7)	–27(7)
C44A	61(6)	82(9)	79(10)	–12(8)	–12(6)	–23(6)

Table 5. Hydrogen coordinates [$\times 10^4$] and isotropic displacement parameters [$Å^2 \times 10^3$].

Atom	*x*	*y*	*z*	U_{eq}	*S.o.f.*
H57	2610	3320	–3164	68	0.65(2)
H58	3890	4091	–4373	91	0.65(2)
H59	4357	5607	–4359	84	0.65(2)
H60	3509	6439	–3145	68	0.65(2)
H65	2199	8574	–1420	71	0.65(2)
H66	1734	9916	–757	100	0.65(2)
H67	323	9978	544	111	0.65(2)
H68	–577	8629	1321	81	0.65(2)
H2	3545	7559	585	104	1
H3	2118	7557	2006	102	1
H7	–889	5160	4048	75	1
H8	–1300	3522	4028	73	1
H12	420	961	1810	69	1
H13	1858	974	381	76	1
H17	4622	3450	–1772	82	1
H18	5036	5074	–1754	81	1
H22	–711	6968	2870	91	0.36(2)
H23	–1223	8204	3793	97	0.36(2)
H24	–316	8439	4784	99	0.36(2)
H25	1133	7485	4732	103	0.36(2)
H26	1700	6359	3709	93	0.36(2)
H28	–2017	2205	2730	97	1

H29	–3003	897	3604	110	1
H30	–2273	–50	4501	79	0.5
H31	–656	280	4527	93	1
H32	319	1542	3676	84	1
H34	2283	2242	–1788	79	0.51(3)
H35	2819	1001	–2672	95	0.51(3)
H36	4184	70	–2491	109	0.51(3)
H37	4921	267	–1395	110	0.51(3)
H38	4347	1481	–474	101	0.51(3)
H40	3575	7056	–1774	66	0.5
H41	4758	8206	–2689	69	0.5
H43	6598	7819	–1188	95	0.5
H44	5482	6615	–304	98	0.5
H45A	7761	8569	–2430	89	0.5
H45B	7068	9255	–1749	89	0.5
H46A	8516	9996	–2973	91	0.5
H46B	7911	9751	–3623	91	0.5
H47A	7935	11214	–3043	84	0.5
H47B	6868	10768	–2357	84	0.5
H48A	6222	10628	–3448	83	0.5
H48B	7306	10988	–4169	83	0.5
H49A	5762	12136	–3037	102	0.5
H49B	6915	12534	–3604	102	0.5
H50A	6583	12202	–4894	105	0.5
H50B	5908	13013	–4395	105	0.5
H51A	5073	11231	–4191	88	0.5
H51B	4441	12134	–3887	88	0.5
H52A	4622	12601	–5333	100	0.5
H52B	5226	11683	–5620	100	0.5

H53A	3832	11497	–5809	98	0.5
H53B	3162	11993	–4963	98	0.5
H54A	3932	10146	–4896	82	0.5
H54B	3332	10643	–4025	82	0.5
H57A	2875	3420	–3102	65	0.35(2)
H58A	4256	4219	–4201	77	0.35(2)
H59A	4727	5692	–4052	88	0.35(2)
H60A	3616	6564	–2966	67	0.35(2)
H65A	2528	8460	–1151	59	0.35(2)
H66A	2285	9724	–342	86	0.35(2)
H67A	996	9699	1036	101	0.35(2)
H68A	–127	8426	1678	86	0.35(2)
H34A	2570	2013	–1715	73	0.49(3)
H35A	3365	770	–2496	86	0.49(3)
H36A	4622	–49	–2108	104	0.49(3)
H37A	5140	339	–880	103	0.49(3)
H38A	4384	1662	–106	97	0.49(3)
H22A	–309	7562	2422	79	0.64(2)
H23A	–910	8670	3402	92	0.64(2)
H24A	–809	8460	4816	87	0.64(2)
H25A	83	7208	5205	99	0.64(2)
H26A	711	6062	4256	88	0.64(2)
H40A	3550	7516	–1175	118	0.5
H41A	4906	8597	–1998	126	0.5
H42A	6655	8120	–2351	121	0.5
H43A	7034	6950	–1475	98	0.5
H44A	5748	5792	–742	92	0.5

Table 6. Torsion angles [°].

La1–N1–C1–C2	151.9(7)
La1–N1–C1–C20	–29.7(14)
La1–N1–C4–C3	–152.7(7)
La1–N1–C4–C5	30.0(14)
La1–N2–C6–C5	–36.6(12)
La1–N2–C6–C7	144.4(6)
La1–N2–C9–C8	–145.5(6)
La1–N2–C9–C10	38.6(11)
La1–N3–C11–C10	–29.7(11)
La1–N3–C11–C12	151.5(6)
La1–N3–C14–C13	–151.9(6)
La1–N3–C14–C15	30.5(12)
La1–N4–C16–C15	–32.9(13)
La1–N4–C16–C17	151.0(6)
La1–N4–C19–C18	–150.9(6)
La1–N4–C19–C20	34.1(13)
La1–N6–C55–N5	54(5)
La1^{i}–N6–C55–N5	–48(5)
La1^{i}–N6–C55–C56	129(2)
La1–N6–C55–C56	–129(2)
La1^{i}–N6–C62–N7	51(4)
La1–N6–C62–N7	–51(4)
La1^{i}–N6–C62–C61	–128.4(17)
La1–N6–C62–C61	129.5(17)
La1^{i}–N8–C63–N7	–50(3)
La1–N8–C63–N7	53(3)
La1^{i}–N8–C63–C64	128.2(18)

La1–N8–C63–C64	–128.6(19)
La1–N8–C70–N5^{i}	–43(3)
La1^{i}–N8–C70–N5^{i}	60(3)
La1^{i}–N8–C70–C69	–127.7(15)
La1–N8–C70–C69	129.7(15)
La1–N6A–C55A–N5A	48(9)
La1^{i}–N6A–C55A–N5A	–54(9)
La1–N6A–C55A–C56A	–125(5)
La1^{i}–N6A–C55A–C56A	132(5)
La1–N6A–C62A–N7A	–55(8)
La1^{i}–N6A–C62A–N7A	48(8)
La1–N6A–C62A–C61A	126(4)
La1^{i}–N6A–C62A–C61A	–131(3)
La1–N8A–C63A–N7A	49(7)
La1^{i}–N8A–C63A–N7A	–51(7)
La1–N8A–C63A–C64A	–131(4)
La1^{i}–N8A–C63A–C64A	128(4)
La1^{i}–N8A–C70A–N5A^{i}	33(6)
La1–N8A–C70A–N5A^{i}	–69(6)
La1–N8A–C70A–C69A	126(3)
La1^{i}–N8A–C70A–C69A	–133(3)
N1–C1–C2–C3	0.9(14)
N1–C1–C20–C19	–7.4(18)
N1–C1–C20–C39	167.4(12)
N1–C1–C20–C39A	–179.3(13)
N1–C4–C5–C6	6.8(18)
N1–C4–C5–C21	177(3)
N1–C4–C5–C21A	–170.6(14)
N2–C6–C7–C8	2.8(11)

N2–C9–C10–C11	1.0(15)
N2–C9–C10–C27	175.7(8)
N3–C11–C12–C13	1.9(11)
N3–C14–C15–C16	5.9(17)
N3–C14–C15–C33	–171.2(13)
N3–C14–C15–C33A	171.5(15)
N4–C16–C17–C18	1.0(12)
N4–C19–C20–C1	4.8(17)
N4–C19–C20–C39	–169.8(12)
N4–C19–C20–C39A	176.7(14)
N5–C55–C56–C57	–1(6)
N5–C55–C56–C61	176(3)
N6–C55–C56–C57	–178(3)
N6–C55–C56–C61	–1(4)
N7–C63–C64–C65	4(5)
N7–C63–C64–C69	177(3)
N8–C63–C64–C65	–174(3)
N8–C63–C64–C69	–1(3)
C55–N6–C62–N7	180(3)
C55–N6–C62–C61	0(4)
C55–C56–C57–C58	178(3)
C55–C56–C61–C60	177(3)
C55–C56–C61–C62	1(3)
C56–C57–C58–C59	3(3)
C56–C61–C62–N6	–1(3)
C56–C61–C62–N7	179(3)
C57–C56–C61–C60	–6(4)
C57–C56–C61–C62	179(3)
C57–C58–C59–C60	–2(3)

C58–C59–C60–C61	–3(3)
C59–C60–C61–C56	6(3)
C59–C60–C61–C62	–180(3)
C60–C61–C62–N6	–176(3)
C60–C61–C62–N7	5(4)
C61–C56–C57–C58	1(4)
C62–N6–C55–N5	–176(4)
C62–N6–C55–C56	1(4)
C62–N7–C63–N8	–1(5)
C62–N7–C63–C64	–179(3)
C63–N7–C62–N6	–1(5)
C63–N7–C62–C61	179(3)
C63–N8–C70–N5^{i}	–170(3)
C63–N8–C70–C69	3(3)
C63–C64–C65–C66	173(3)
C63–C64–C69–C68	–175(2)
C63–C64–C69–C70	2(3)
C64–C65–C66–C67	–2(3)
C64–C69–C70–N5^{i}	170(3)
C64–C69–C70–N8	–3(3)
C65–C64–C69–C68	–1(4)
C65–C64–C69–C70	176(2)
C65–C66–C67–C68	3(4)
C66–C67–C68–C69	–3(3)
C67–C68–C69–C64	2(3)
C67–C68–C69–C70	–175(2)
C68–C69–C70–N5^{i}	–13(4)
C68–C69–C70–N8	174(2)
C69–C64–C65–C66	1(3)

C70^{i}–N5–C55–N6	–11(6)
C70^{i}–N5–C55–C56	172(4)
C70–N8–C63–N7	–179(3)
C70–N8–C63–C64	–1(3)
C1–N1–C4–C3	1.2(11)
C1–N1–C4–C5	–176.0(10)
C1–C2–C3–C4	–0.1(15)
C1–C20–C39–C40	–98(4)
C1–C20–C39–C44	82(4)
C1–C20–C39A–C40A	–72(4)
C1–C20–C39A–C44A	117(4)
C2–C1–C20–C19	170.8(11)
C2–C1–C20–C39	–14.5(18)
C2–C1–C20–C39A	–1.2(19)
C2–C3–C4–N1	–0.7(14)
C2–C3–C4–C5	176.6(11)
C3–C4–C5–C6	–170.0(10)
C3–C4–C5–C21	1(3)
C3–C4–C5–C21A	12.6(19)
C4–N1–C1–C2	–1.3(12)
C4–N1–C1–C20	177.0(10)
C4–C5–C6–N2	–3.1(16)
C4–C5–C6–C7	175.7(10)
C4–C5–C21–C22	102(5)
C4–C5–C21–C26	–73(6)
C4–C5–C21A–C22A	65(3)
C4–C5–C21A–C26A	–113(3)
C5–C6–C7–C8	–176.2(9)
C5–C21–C22–C23	–173(4)

C5–C21–C26–C25	176(4)
C5–C21A–C22A–C23A	–177(2)
C5–C21A–C26A–C25A	177(2)
C6–N2–C9–C8	2.3(10)
C6–N2–C9–C10	–173.6(9)
C6–C5–C21–C22	–87(5)
C6–C5–C21–C26	99(6)
C6–C5–C21A–C22A	–112(3)
C6–C5–C21A–C26A	69(3)
C6–C7–C8–C9	–1.4(11)
C7–C8–C9–N2	–0.6(11)
C7–C8–C9–C10	175.4(9)
C8–C9–C10–C11	–174.3(9)
C8–C9–C10–C27	0.4(14)
C9–N2–C6–C5	175.9(9)
C9–N2–C6–C7	–3.1(10)
C9–C10–C11–N3	–6.4(15)
C9–C10–C11–C12	172.2(9)
C9–C10–C27–C28	87.5(11)
C9–C10–C27–C32	–94.0(11)
C10–C11–C12–C13	–176.8(9)
C10–C27–C28–C29	174.1(9)
C10–C27–C32–C31	–174.3(8)
C11–N3–C14–C13	2.5(10)
C11–N3–C14–C15	–175.1(9)
C11–C10–C27–C28	–97.1(10)
C11–C10–C27–C32	81.4(10)
C11–C12–C13–C14	–0.4(12)
C12–C13–C14–N3	–1.4(11)

C12–C13–C14–C15	176.3(10)
C13–C14–C15–C16	–171.3(10)
C13–C14–C15–C33	11.6(17)
C13–C14–C15–C33A	–5.7(19)
C14–N3–C11–C10	176.1(8)
C14–N3–C11–C12	–2.7(10)
C14–C15–C16–N4	–4.5(17)
C14–C15–C16–C17	170.8(10)
C14–C15–C33–C34	87(3)
C14–C15–C33–C38	–89(3)
C14–C15–C33A–C34A	95(2)
C14–C15–C33A–C38A	–81(3)
C15–C16–C17–C18	–175.0(10)
C15–C33–C34–C35	–174(3)
C15–C33–C38–C37	175(3)
C15–C33A–C34A–C35A	–177(3)
C15–C33A–C38A–C37A	175(3)
C16–N4–C19–C18	2.1(10)
C16–N4–C19–C20	–172.9(10)
C16–C15–C33–C34	–90(3)
C16–C15–C33–C38	94(3)
C16–C15–C33A–C34A	–98(2)
C16–C15–C33A–C38A	86(3)
C16–C17–C18–C19	0.3(12)
C17–C18–C19–N4	–1.5(12)
C17–C18–C19–C20	173.5(10)
C18–C19–C20–C1	–169.3(10)
C18–C19–C20–C39	16.0(17)
C18–C19–C20–C39A	2.5(19)

C19–N4–C16–C15	174.1(10)
C19–N4–C16–C17	–1.9(10)
C19–C20–C39–C40	77(4)
C19–C20–C39–C44	–103(4)
C19–C20–C39A–C40A	115(4)
C19–C20–C39A–C44A	–56(4)
C20–C1–C2–C3	–177.5(11)
C20–C39–C40–C41	179(3)
C20–C39–C44–C43	–178(3)
C20–C39A–C40A–C41A	–177(3)
C20–C39A–C44A–C43A	179(3)
C21–C5–C6–N2	–174(3)
C21–C5–C6–C7	5(3)
C21–C5–C21A–C22A	147(26)
C21–C5–C21A–C26A	–32(21)
C21–C22–C23–C24	–3(7)
C22–C21–C26–C25	2(9)
C22–C23–C24–C25	2(7)
C23–C24–C25–C26	1(7)
C24–C25–C26–C21	–3(7)
C26–C21–C22–C23	1(10)
C27–C10–C11–N3	178.7(8)
C27–C10–C11–C12	–2.8(13)
C27–C28–C29–C30	2.2(17)
C28–C27–C32–C31	4.2(15)
C28–C29–C30–C31	0.3(17)
C28–C29–C30–O2	–179.4(10)
C29–C30–C31–C32	–0.6(17)
C29–C30–O2–C54^{i}	5.0(19)

C30–C31–C32–C27	–1.7(16)
C31–C30–O2–C54^{i}	–174.7(13)
C32–C27–C28–C29	–4.4(16)
C33–C15–C16–N4	172.5(13)
C33–C15–C16–C17	–12.2(18)
C33–C15–C33A–C34A	–4(8)
C33–C15–C33A–C38A	–180(12)
C33–C34–C35–C36	–2(4)
C34–C33–C38–C37	0(4)
C34–C35–C36–C37	2(4)
C35–C36–C37–C38	–1(4)
C36–C37–C38–C33	0(4)
C38–C33–C34–C35	1(4)
C39–C20–C39A–C40A	17(16)
C39–C20–C39A–C44A	–155(23)
C39–C40–C41–C42	–2(4)
C40–C39–C44–C43	2(5)
C40–C41–C42–C43	2(3)
C40–C41–C42–O1	–177.4(16)
C41–C42–C43–C44	–1(4)
C41–C42–O1–C45	179.4(19)
C42–C43–C44–C39	–2(4)
C42–O1–C45–C46	–177.3(17)
C43–C42–O1–C45	0(3)
C44–C39–C40–C41	0(5)
O1–C42–C43–C44	179(2)
O1–C45–C46–C47	70(3)
O2–C30–C31–C32	179.1(10)
C45–C46–C47–C48	–101(3)

C46–C47–C48–C49	–174.9(19)
C47–C48–C49–C50	169(2)
C48–C49–C50–C51	72(3)
C49–C50–C51–C52	–169(2)
C50–C51–C52–C53	–178(2)
C51–C52–C53–C54	–37(3)
C52–C53–C54–O2^{i}	175.9(19)
N5A–C55A–C56A–C57A	6(12)
N5A–C55A–C56A–C61A	–172(6)
N6A–C55A–C56A–C57A	–180(7)
N6A–C55A–C56A–C61A	2(8)
N7A–C63A–C64A–C65A	–13(10)
N7A–C63A–C64A–C69A	–174(6)
N8A–C63A–C64A–C65A	167(6)
N8A–C63A–C64A–C69A	6(6)
C55A–N6A–C62A–N7A	–179(7)
C55A–N6A–C62A–C61A	2(8)
C55A–C56A–C57A–C58A	180(7)
C55A–C56A–C61A–C60A	–178(5)
C55A–C56A–C61A–C62A	–1(6)
C56A–C57A–C58A–C59A	4(7)
C56A–C61A–C62A–N6A	–1(6)
C56A–C61A–C62A–N7A	–180(5)
C57A–C56A–C61A–C60A	3(8)
C57A–C56A–C61A–C62A	–180(5)
C57A–C58A–C59A–C60A	–7(7)
C58A–C59A–C60A–C61A	7(6)
C59A–C60A–C61A–C56A	–5(7)
C59A–C60A–C61A–C62A	178(5)

C60A–C61A–C62A–N6A	177(6)
C60A–C61A–C62A–N7A	–2(9)
C61A–C56A–C57A–C58A	–2(8)
C62A–N6A–C55A–N5A	172(7)
C62A–N6A–C55A–C56A	–2(9)
C62A–N7A–C63A–N8A	0(10)
C62A–N7A–C63A–C64A	–180(6)
C63A–N7A–C62A–N6A	4(10)
C63A–N7A–C62A–C61A	–177(6)
C63A–N8A–C70A–N5A^{i}	163(6)
C63A–N8A–C70A–C69A	–2(6)
C63A–C64A–C65A–C66A	–167(6)
C63A–C64A–C69A–C68A	168(5)
C63A–C64A–C69A–C70A	–7(6)
C64A–C65A–C66A–C67A	6(6)
C64A–C69A–C70A–N5A^{i}	–158(6)
C64A–C69A–C70A–N8A	6(6)
C65A–C64A–C69A–C68A	5(8)
C65A–C64A–C69A–C70A	–171(5)
C65A–C66A–C67A–C68A	0(6)
C66A–C67A–C68A–C69A	–4(6)
C67A–C68A–C69A–C64A	1(7)
C67A–C68A–C69A–C70A	176(5)
C68A–C69A–C70A–N5A^{i}	26(10)
C68A–C69A–C70A–N8A	–169(5)
C69A–C64A–C65A–C66A	–9(7)
C70A^{i}–N5A–C55A–N6A	21(11)
C70A^{i}–N5A–C55A–C56A	–166(7)
C70A–N8A–C63A–N7A	178(6)

C70A–N8A–C63A–C64A	–2(6)
C33A–C15–C16–N4	–169.8(16)
C33A–C15–C16–C17	6(2)
C33A–C15–C33–C34	176(11)
C33A–C15–C33–C38	0(7)
C33A–C34A–C35A–C36A	1(4)
C34A–C33A–C38A–C37A	0(4)
C34A–C35A–C36A–C37A	0(4)
C35A–C36A–C37A–C38A	–2(4)
C36A–C37A–C38A–C33A	2(4)
C38A–C33A–C34A–C35A	–1(4)
C21A–C5–C6–N2	174.4(13)
C21A–C5–C6–C7	–6.8(17)
C21A–C5–C21–C22	–3(19)
C21A–C5–C21–C26	–177(29)
C21A–C22A–C23A–C24A	–3(4)
C22A–C21A–C26A–C25A	–2(4)
C22A–C23A–C24A–C25A	3(4)
C23A–C24A–C25A–C26A	–3(4)
C24A–C25A–C26A–C21A	3(4)
C26A–C21A–C22A–C23A	2(4)
C39A–C20–C39–C40	165(23)
C39A–C20–C39–C44	–15(16)
C39A–C40A–C41A–C42A	7(5)
C40A–C39A–C44A–C43A	8(6)
C40A–C41A–C42A–C43A	–12(5)
C41A–C42A–C43A–C44A	15(5)
C42A–C43A–C44A–C39A	–13(4)
C44A–C39A–C40A–C41A	–6(6)

Symmetry transformations used to generate equivalent atoms:

(i) –x,–y+1,–z